Characterization by imaging and high-density electrophysiology of substrates and ventricular arrhythmias

Benjamin Berte

CHARACTERIZATION BY IMAGING AND HIGH-DENSITY ELECTROPHYSIOLOGY OF SUBSTRATES AND VENTRICULAR ARRHYTHMIAS.

BERTE BENJAMIN, MD

Membres du Jury

Mr. Le Professeur Olivier BERNUS, Président

Mr. le Professeur Christian DE CHILLOU, Rapporteur

Mr. le Docteur Philippe MAURY, Rapporteur

Mr. le Professeur Mattias DUYTSCHAEVER, Examinateur

Mr. le Docteur Rémi DUBOIS, Examinateur

Mr. le Professeur Pierre JAIS, Directeur de Thèse

université de BORDEAUX

THÈSE PRÉSENTÉE
POUR OBTENIR LE GRADE DE

DOCTEUR DE

L'UNIVERSITÉ DE BORDEAUX

Ecole doctorale: Science de la Vie et de la Santé.
Option: Bio-imagerie

Par Benjamin BERTE
Né le 18 juillet 1980 à Anvers, Belgique

Characterization by imaging and high-density electrophysiology of substrates and ventricular arrhythmias.

Présentée et soutenue publiquement le 4 septembre 2015

Membres du Jury

Mr. Le Professeur Olivier BERNUS, Président

Mr. le Professeur Christian DE CHILLOU, Rapporteur

Mr. le Docteur Philippe MAURY, Rapporteur

Mr. le Professeur Mattias DUYTSCHAEVER, Examinateur

Mr. le Docteur Rémi DUBOIS, Examinateur

Mr. le Professeur Pierre JAIS, Directeur de Thèse

Table of Contents

List of abbreviations

ICM	ischaemic cardiomyopathy
NICM	non-ischaemic cardiomyopathy
ARVC	arrhythmogenic right ventricular cardiomyopathy
ICD	intracardiac cardioverter device
EGM	electrogram
LAVA	local abnormal ventricular activity
HANA	high amplitude normal activity
EPI	epicardial
ENDO	endocardial
pt	patient
MRI	magnetic resonance imaging
MDCT	multidetector computed tomography
PPI	post-pacing interval
TCL	tachycardia cycle length
VT	ventricular tachycardia
RV	right ventricle
LV	left ventricle
EAM	electro-anatomical mapping
EF	ejection fraction
ICE	intravascular ultrasound

List of scientific publications related to the thesis

PUBLISHED PAPERS

1.**Epicardial only mapping and ablation of ventricular tachycardia: a case series.**

Berte B, Yamashita S, Sacher F, Cochet H, Hooks D, Aljefairi N, Amraoui S, Denis A, Derval N, Hocini M, Haïssaguerre M, Jaïs P. Europace. 2015 Apr 2. pii: euv072.

2.**Noninvasive mapping of ventricular arrhythmias.**

Shah AJ, Lim HS, Yamashita S, Zellerhoff S, **Berte B**, Mahida S, Hooks D, Aljefairi N, Derval N, Denis A, Sacher F, Jais P, Dubois R, Hocini M, Haissaguerre M. Card Electrophysiol Clin. 2015 Mar;7(1):99-107. doi: 10.1016/j.ccep.2014.11.014. Epub 2014 Dec 24. Review.

3. **Role of high-resolution image integration to visualize left phrenic nerve and coronary arteries during epicardial ventricular tachycardia ablation.**

Yamashita S, Sacher F, Mahida S, **Berte B**, Lim HS, Komatsu Y, Amraoui S, Denis A, Derval N, Laurent F, Montaudon M, Hocini M, Haïssaguerre M, Jaïs P, Cochet H. Circ Arrhythm Electrophysiol. 2015 Apr;8(2):371-80. doi: 10.1161/CIRCEP.114.002420. Epub 2015 Feb 21.

4. **New strategies for ventricular tachycardia and ventricular fibrillation ablation.**

Hooks DA, **Berte B**, Yamashita S, Mahida S, Sellal JM, Aljefairi N, Frontera A, Derval N, Denis A, Hocini M, Haïssaguerre M, Jaïs P, Sacher F. Expert Rev Cardiovasc Ther. 2015 Mar;13(3):263-76. doi: 10.1586/14779072.2015.1009039. Epub 2015 Feb 10.

5. **Substrate Mapping and Ablation for Ventricular Tachycardia: The LAVA Approach.**

Sacher F, Lim HS, Derval N, Denis A, **Berte B**, Yamashita S, Hocini M, Haissaguerre M, Jaïs P. J Cardiovasc Electrophysiol. 2015 Apr;26(4):464-71. doi: 10.1111/jce.12565. Epub 2014 Dec 2.

6. **Postmyocarditis ventricular tachycardia in patients with epicardial-only scar: a specific entity requiring a specific approach.**

Berte B, Sacher F, Cochet H, Mahida S, Yamashita S, Lim H, Denis A, Derval N, Hocini M, Haïssaguerre M, Jaïs P. J Cardiovasc Electrophysiol. 2015 Jan;26(1):42-50. doi: 10.1111/jce.12555. Epub 2014 Nov 5.

7. **Impact of septal radiofrequency ventricular tachycardia ablation: insights from magnetic resonance imaging.**

Berte B, Sacher F, Mahida S, Yamashita S, Lim HS, Denis A, Derval N, Hocini M, Haïssaguerre M, Cochet H, Jaïs P. Circulation. 2014 Aug 19;130(8):716-8. doi: 10.1161/CIRCULATIONAHA.114.010175.

8. **Safety and prevention of complications during percutaneous epicardial access for the ablation of cardiac arrhythmias.**

Lim HS, Sacher F, Cochet H, **Berte B**, Yamashita S, Mahida S, Zellerhoff S, Komatsu Y, Denis A, Derval N, Hocini M, Haïssaguerre M, Jaïs P. Heart Rhythm. 2014 Sep;11(9):1658-65. doi: 10.1016/j.hrthm.2014.05.041. Epub 2014 Jun 5. Review. No abstract available.

SUBMITTED PAPERS

9. **Irrigated needle ablation creates larger and more transmural ventricular lesions compared to standard unipolar ablation in an ovine model.**

Benjamin Berte MD[1,2]; Hubert Cochet MD, PhD[1,2]; Julie Magat MD, PhD[2]; Jérôme Naulin[2]; Frédéric Sacher MD, PhD[1,2]; Daniele Ghidoli[3]; Xavier Pillois PhD[1]; Frédéric Casassus MD[1]; Seigo Yamashita MD, PhD[1]; Saagar Mahida MD, PhD[1]; Nicolas Derval MD[1]; Mélèze Hocini MD[1,2]; Bruno Quesson PhD[2]; Olivier Bernus PhD[2]; Rukshen Weerasooriya MD, PhD[4]; Michel Haïssaguerre MD[1,2]; Pierre Jaïs MD, PhD[1,2]. Submitted to Circ AEP.

10. **VT Recurrence after VT ablation in Non-Ischaemic Cardiomyopathy: Incomplete Ablation or Disease Progression? A Multicentric European Study.**

B Berte[1], F Sacher[1], J Venlet[2], D Andreu[3], S Mahida[1], B Aldhoon[4], T De Potter[5], A Sarkozy[7], R Tavernier[6], A Marius[8], M Hocini[1], M Haïssageurre[1], T Deneke[9], J Kautzner[4], A Berruezo[3], H Cochet[1], K Zeppenfeld[2], P Jaïs[1]. Submitted to JCE.

11. **Impact of electrode type on mapping of scar-related VT.**

B Berte, MD; J Relan, PhD; F Sacher, MD, PhD; X Pillois, MD, PhD; A Appetiti, S Yamashita, MD, PhD; S Mahida, MD, PhD; F Casassus, MD; D Hooks, MD, PhD; J-M Sellal, MD; S Amraoui, MD; A Denis, MD; N Derval, MD; H Cochet, MD, PhD; M Hocini, MD; M Haïssaguerre, MD, PhD; R Weerasooriya, MD, PhD; P Jaïs, MD, PhD. Accepted in JCE.

12. **Characterization of the Left-sided Substrate in Arrhythmogenic Right Ventricular Cardiomyopathy**

Benjamin Berte, Sana Amraoui, Arnaud Denis, Seigo Yamashita, Yuki Komatsu, Xavier Pillois, Frédéric Sacher, Sagar Mahida, Jean-Yves Wielandts, Jean-Marc Sellal, Antonio Frontera, Nora Al Jefairi, Nicolas Derval, Michel Montaudon, François Laurent, Mélèze Hocini, Michel Haïssaguerre, Pierre Jaïs, Hubert Cochet. Submitted to Circ AEP.

List of oral presentations, posters, book chapters related to the thesis

EP BOOK CHAPTER

Daoud & Kalbfleisch / Color Atlas and Synopsis of Electrophysiology 2015.

Mapping & Ablation of Ventricular Tachycardia: Local Abnormal Ventricular Activity. **B Berte**, F Sacher, P Jaïs

PRESENTATIONS:

2015 **Gulf EP symposium Dubai:**

Lecture on non-invasive mapping with the CardioInsight system

Poster presentations at **HRS Boston**:

1. VT Recurrence After VT Ablation in Non-Ischaemic Cardiomyopathy: Incomplete Ablation or Disease Progression? A Multicentric European Study. **B Berte**, F Sacher, J Venlet, D Andreu, B Aldhoon, T De Potter, A Sarkozy, R Tavernier, N Derval, M Hocini, M Haïssageurre, J Kautzner, A Berruezo, K Zeppenfeld, P Jaïs

2. Irrigated Needle Ablation Creates Larger and More Transmural Ventricular Lesions Compared to Standard Unipolar Ablation in an Ovine Model. **B Berte**, H Cochet, J Magat, F Sacher, X Pillois, D Ghidoli, J Naulin, N Derval, M Hocini, B Quesson, O Bernus, M Haïssaguerre, P Jaïs

2014 Poster presentations at **ISCAT Paris**:

1. Ventricular Tachycardia Ablation using an end point of non-inducibility and EP substrate elimination: predictors for multiple

procedures and impact on safety. **B Berte**, F Sacher , S Yamashita, S Mahida, H Lim, M Hocini, M Haïssaguerre, P Jaïs. **ISCAT AWARD BEST POSTER.**

Oral presentation at **HRS San Fransisco**:

1. Lessons from redo VT ablation: safety and efficacy. **B Berte**, F Sacher , S Yamashita, S Mahida, H Lim, M Hocini, M Haïssaguerre, P Jaïs. Chair W Stevenson.

Poster presentations at **HRS San Fransisco**:

1. An Intramural Focus of a Septal Ventricular Tachycardia: Pitfalls and Solutions. **Benjamin Berte**, MD, Frederic Sacher, MD, Hubert Cochet, MD, Saagar N. Mahida, MBChB, Seigo Yamashita, MD, Han S. Lim, MBBS, Arnaud Denis, MD, Nicolas Derval, MD, Meleze Hocini, MD, Michel Haissaguerre, PhD, Pierre Jais, MD. Haut-L'évêque/CHU Bordeaux, Bordeaux, France

2. New Non-Invasive Mapping of Ventricular Tachycardia: a Feasibility Pilot-Study. **Benjamin Berte**, MD, valentin meillet, Eng., Remi Dubois, Eng., Hubert Cochet, MD, Frederic Sacher, MD, Carole Pomier, Saagar N. Mahida, MBChB, Seigo Yamashita, MD, Han S. Lim, MBBS, Arnaud Denis, MD, Sana Amraoui, MD, Nicolas Derval, MD, Meleze Hocini, MD, Michel Haissaguerre, PhD and Pierre Jais, MD. Haut-L'évêque/CHU Bordeaux, Bordeaux, France, LYRIC

3. Non-Ischemic Cardiomyopathy with Subepicardial Scar: a Specific Entity Requiring a Specific Approach. **Benjamin Berte**, MD, Frederic Sacher, MD, Hubert Cochet, MD, Saagar N. Mahida, MBChB, Seigo Yamashita, MD, Han S. Lim, MBBS, Arnaud Denis, MD, Sana Amraoui, MD, Nicolas Derval, MD, Meleze Hocini, MD, Michel Haissaguerre, PhD and Pierre Jais, MD. Haut-L'évêque/CHU Bordeaux, Bordeaux, France

Oral presentation at **BHRM Brussels**:

1. Lessons from redo VT ablation: safety and efficacy. **B Berte**, F Sacher , S Yamashita, S Mahida, H Lim, M Hocini, M Haïssaguerre,

P Jaïs. Haut-L'évêque/CHU Bordeaux, Bordeaux, France **MEHDA AWARD BEST ABSTRACT**

Poster presentations at **BHRM Brussels**:

1. An intramural focus of a septal ventricular tachycardia: insights from MRI. **B. Berte**, F. Sacher, H. Cochet, S. Mahida, S. Yamashita, H. Lim, A. Denis, N. Derval, M. Hocini, M. Haïssaguerre, P. Jaïs - CHU de Bordeaux, Hôpital de Haut-Lévêque, F

2. Non-ischaemic cardiomyopathy with subepicardial scar: a specific entity requiring a specific approach. **B. Berte**, F. Sacher, H. Cochet, S. Mahida, S. Yamashita, H. Lim, A. Denis, N. Derval, M. Hocini, M. Haïssaguerre, P. Jaïs - CHU de Bordeaux, Hôpital de Haut-Lévêque, F

3. New non-invasive mapping of ventricular arrhythmia: a feasibility pilot-study. **B. Berte**, V. Meillet, R. Dubois, H. Cochet, F. Sacher, C. Pomier, S. Yamashita, A. Denis, N. Derval, M. Hocini, M. Haïssaguerre, P. Jaïs - LIRYC Institute, CardioInsight Inc, CHU de Bordeaux, Hôpital de Haut-Lévêque, F

4. LAVA distribution is predictable and differs by VT substrate. **B. Berte**, H. Cochet, M. Hakkinen, N. Derval, F. Sacher, M. Hocini, S. Yamashita, H. Lim, S. Mahida, A. Denis, S. Amraoui, M. Haissaguerre, P. Jaïs - LIRYC Institute, CHU de Bordeaux, Hôpital de Haut-Lévêque, F

5. LAVA does not always fall within the scar border zone in non-ischemic VT substrates. **B. Berte**, J. Relan, H. Cochet, M. Hanninen, F. Sacher, M. Hocini, S. Yamashita, A. Denis, N. Derval, M. Hocini, M. Haissaguerre, P. Jaïs - LIRYC Institute, CHU de Bordeaux, Hôpital de Haut-Lévêque, F

Acknowledgements

Mr le Pr Jaïs, directeur de thèse, vous me faites l'honneur de faire parti de mon jury de thèse. Je tiens à vous exprimer le profond respect que j'ai pour vous. Je vous remercie infiniment pour votre patience... et pour l'enseignement complet que vous m'avez dispensé au cours de ces deux dernières années. Vous m'avez inculqué la rigueur "japonaise", et je vous en suis reconnaissant. J'éspère avoir été à la hauteur.

Mr le Dr Olivier Bernus, président du Jury, directeur du LYRIC, vous me faites l'honneur de juger cette thèse et je vous en remercie.

Mr le Pr Christian De Chillou, rapporteur, je vous remercie d'avoir accépté de faire parti de mon jury de thèse. Vous êtes un modèle en rythmologie et j'admire votre côté gentleman au quotidien.

Mr le Dr Philippe Maury, rapporteur, permettez-moi de vous exprimer le profond respect que j'ai pour vous. Je vous remercie encore pour votre disponibilité...notamment pendant la présentation de mi-thèse par téléconférence.

Mr le Pr Mattias Duytschaever, examinateur, même si j'écrivais une page de remerciements, cela ne suffirait pas. Merci d'avoir suscité en moi cette réelle passion pour la rythmologie, et d'avoir toujours répondu à ma soif d'apprendre et de m'améliorer au quotidien. Merci pour tes grandes qualités humaines et ton soutien dans tous mes projets personnels et professionnels. Merci pour tout.

Mr le Dr Rémi Dubois, examinateur, je te remercie infiniment pour tout. Ce fut un réel plaisir de pouvoir discuter et travailler ensemble. J'ai eu de la chance de pouvoir croiser ta route, et le LYRIC aussi.

Michel Haïssaguerre, vous m'avez fait l'immense honneur de m'accepter dans votre service pendant ces deux dernières années et je vous en suis infiniment reconnaissant. C'est un rêve pour tous les rythmologues, de pouvoir travailler à vos

côtés, et je vous suis très reconnaissant de m'avoir permis de le réaliser. Vous êtes l'Homme universel, cet homme passioné qui écrit un NEJM tout en freudonnant une opérette et en bricolant.

Mélèze Hocini, j'ai une profonde admiration pour vous. Vous êtes un modèle d'excellence. Votre puissance et bataille contre le féminisme de pitié m'a ému.

Nicolas Derval, tu es la source d'énergie de ce service et aussi le seul à apprécier mon humour (mauvais gout?). Tu m'es d'un grand soutien pour retrouver "ma banane".

Fred Sacher, tu as largement contribué à ma formation pour l'ablation de TV et je t'en suis très reconnaissant. Attention avec les belges et leur bière...

Arnaud Denis, merci pour ton humeur jovial et candide.

Les fellows, pour le temps qu'ils m'ont accordé. Particulièrement Saagar pour sa rigueur japonnaise dans l'écriture des articles, et Seigo, pour son flegme anglais. J'ai une profonde amitié pour vous.

Don Huberto, c'est un réel plaisir de travailler à tes côtés. Merci pour ta rigueur. Ton enthousiasme pour la médecine, en tant que radiologue, m'a surpis! Il ne te reste plus qu'à jouer au golf pour devenir le radiologue idéal!

A l'équipe du LYRIC et de la PTIB, Olivier, Rémi, Virginie, Delphine, Julie, c'était un immense plaisir de travailler avec vous. A mes yeux, vous excellez dans le domaine de la recherche française et mondiale. Votre passion pour la recherche est contagieuse.

Les infirmières, pour votre flexibilité et votre aide. L'électrophysiologie est un travail d'équipe et sans vous il n'y aurait pas de réussite.

Christoph Scharf, le MacGyver du monde de l'electrophysiology, merci pour ta confiance et l'opportunité de continuer mon chemin à tes côtés. Ton enthousiasme et energie positive sont enrichissants. Je nous souhaite un bon futur ensemble.

Ma famille, surtout mon grand-père, pour m'avoir guidé dans mon adolescence. Malheureusement, tu n'es plus là, mais je pense à toi lorsque j'écris cette thèse.

Mes amis, merci pour leur sincérité et leur amitié. C'est important dans la vie et je vous en suis sincerement reconnaissant.

et pour conclure:

Isabelle, mon amour, mon manager, tu me donnes envie d'être meilleur (donne moi encore un peu de temps...!). Merci pour ton aide, ton amour et ta patience avec moi.

Mon enfant, mon souffle de vie, Charles, j'ai écrit ma thèse à partir de la première echo et je la défendrai quelques semaines après ta naissance. On pourra dire que vous êtes naît ensemble!

Résumé

L'ablation par radiofréquence constitue un des traitements des tachycardies ventriculaires, en association avec les drogues anti-arrhythmiques et l'implantation d'un défibrillateur. L'objectif principal de cette thèse est de mieux comprendre le substrat arrhythmogène non seulement à l'aide d'imagerie cardiaque (IRM et scanner) de haute résolution et de cartographie de haute densité, en utilisant des catheters multipolaires. Cela nous permettra d'analyzer la relation structure-fonction. Nous avons étudié cette relation sur différents types de substrats (ICM, NICM, DAVD, et myocardites). Nous avons ainsi prouvé la supériorité de la cartographie de haute densité obtenue à partir de cathéters multipolaires, comparativement au données recueillies par l'imagerie, dans l'identification de la cicatrice arythmogène et la detection des LAVA.

La deuxième partie de cette thèse concerne l'étude du substrat arythmogène épicardique. Nous avons ainsi décrit la technique de cartographie par voie percutanée antérieure, puis démontré l'efficacité des procédures uniquement avec abord épicardique. La segmentation du nerf phrénique et des artères coronaires ont permis de diminuer le taux de complications théoriquement liés à cet abord. Nous avons poursuivi ce travail avec l'analyze des sites d'intérêt de l'ablation des TV: les LAVA. Après une description de l'a stratégie d'élimination des LAVA, nous avons tenté de trouver des prédicteurs permettant de localiser les sites de LAVA, à partir des données d'imagerie. Quand l'imagerie montre une cicatrice intraseptale ou intramurale, les LAVA ne peuvent pas être enregistré avec la cartographie et des alternative technique d'ablation sont nécessaires comme une ablation bipolaire, l'alcoolisation intra coronaire et l'ablation avec l'aiguille irrigée.

Le dernier chapitre est une revue sur le futur de l'imagerie, de la cartographie et de l'ablation des tachycardies ventriculaires. Une meilleure compréhension du substrat

arythmogène pourrait améliorer l'efficacité et la sécurité des ablations de tachycardie ventriculaire.

Mots de clés :

IRM - scanner - LAVA - cartographie de haute densité - ICM - DAVD - myocardites - NICM - épicardique - substrat intramural

Titre :

Characterisation avec de l'imagerie et électrophysiologie de haute densité de substrats et arythmies ventriculaires.

Summary

Radiofrequency (RF) catheter ablation is an effective treatment strategy for scar-related ventricular tachycardia (VT), resistant to anti-arrhythmic drugs and intracardiac defibrillator (ICD) placement. The goal of this thesis was to better understand and characterize the arrhythmogenic VT substrate in different cardiomyopathic processes: ischaemic cardiomyopathy (ICM), non-ischaemic cardiomyopathy (NICM), arrhythmogenic right ventricular cardiomyopathy (ARVC) and myocarditis. For this purpose, we combined high resolution imaging including different modalities and high resolution electrical maping to better understand the structure-function relationship. We focussed on multiple different aspects of VT ablation as outlined below.

The first part of this thesis focuses on the role of multipolar mapping catheters and imaging to analyze their structural and functional relationship. We demonstrated superiority of high density mapping with multipolar mapping on conventional mapping in detection of scar, channels, local abnormal ventricular activity (LAVA) and sensitivity for near field signals.

The second part of this thesis focuses on ablation of epicardial VT substrate. We demonstrated the efficacy and safety of epicardial only procedures in a highly selected population. We used imaging to have access to the exact anatomy of the heart, to image the substrate but also to increase the safety of ablation procedures by imaging the phrenic nerve and the coronary artery system.

The third part of this thesis focuses on analysis of the mapping and ablation of potential targets for scar-related VT ablation. Within this context, we identified predictors of interesting ablation (LAVA) sites based on preprocedural imaging. We also analyzed the role of alternative strategies such as bipolar ablation, ethanol ablation and irrigated needle ablation to ablate intramural and intraseptal substrate,

often resistant ablation targets. Overall, we demonstrate that novel imaging, mapping and ablation techniques potentially improve the outcome of VT ablation.

Key words:

MRI - MDCT - LAVA - high density mapping - ICM - ARVC - myocarditis - NICM - epicardial mapping - intramural substrate.

I. INTRODUCTION

A. History

Over the past two decades, ventricular tachycardia (VT) ablation for patients with ischaemic (ICM) and non-ischaemic cardiomyopathy (NICM) has emerged as a successful adjunctive therapy to implantable cardioverter defibrillators (ICD) and anti-arrhythmic drug (AAD) therapy. Recurrent ICD shocks are associated with increased morbidity and mortality.[1, 2] While drugs such as amiodarone have been reported to reduce ICD shock burden, in a significant porportion of patients, they are ineffective. Furthermore they do not have any impact on mortality and may be associated with multiple side effects. VT ablation is an important therapeutic intervention in cases with recurrent VT where drugs are either ineffective or poorly tolerated.

The first VT ablations were performed surgically in severely ill post-infarct patients with ventricular aneurysms. Over time, the technique evolved with the development of high energy ablation (fulguration), radiofrequency (RF) ablation and eventually irrigated RF ablation. Scar-related VT most commonly arises due to macro re-entry circuits, but can also be focal. The predominant sites of ventricular scar vary according to the underlying condition: myocardial infarction produces predominantly endocardial scar with various extension into the wall thickness sometimes involving a papillary muscle. Cardiac surgery may favour incisional re-entry while arrhythmogenic right ventricular cardiomyopathy (ARVC) has a

substrate that begins and predominates epicardially. This is also true for myocarditis or Chagas disease, again with various transmural extensions. In patients with sarcoidosis, the basal septum is the most commonly affected site. The purkinje network may also be responsible for ventricular arrhythmias, usually in ischemic scars as these cells may survive the myocardial infarction and may trigger VF, or in idiopathic VF.

Previously, VT ablation strategies were based primarily on activation and entrainment mapping, with the endpoint of non-inducibility of VT.[3] These approaches were associated with a number of limitations, most importantly the dependence of the induction of clinically relevant and tolerated VT. Additional issues included failure to consistently induce VT and questionable relevance of induced VT morphologies. As a consequence, VT ablation was mainly performed in a highly selected patient population.

To overcome the aforementioned limitations, substrate-based ablation strategies have been developed. One of the first studies to provide the ground for targeting the substrate came from De Bakker *et al* describing the scar related VT circuits related to surviving bundles associated with zig-zag course resulting in slow conduction (Figure 1).[4] It has subsequently emerged that the substrate initially described in myocardial infarction is in fact responsible for scar related re-entrant VTs occurring in other conditions.

As discussed above, the arrhythmogenic substrate in patients with scar-related VT may be endocardial, epicardial and/or intramural. Epicardial and in particular, intramural VT substrate maybe difficult to access using endocardal approaches. An

important development in this context was the percutaneous puncture technique, first reported by Sosa *et al,* which allowed for epicardial mapping and ablation. Given the scar distribution, this technique has proved particularly useful in NICM.[5]

In recent years, with the emergence of novel strategies and technologies, the role of VT ablation has expanded resulting in safer, more efficient VT ablation procedures. The possibility to ablate in sinus rhythm also contributed to to the expansion of the technique to a broader patient's population. With the expansion of heart failure population and an increased number of ICD implantations, the demand for VT ablation is also increasing. In 2013, a number of 434 new implants per million were reported in the US, a number three times higher then the mean European implantation rate. The ICD implant rate is expected to rise over the coming years. Many of these patients will be or become candidate for VT ablation.

B. Mechanisms of VT

There are three main mechanisms for ventricular tachycardia: abnormal automaticity, triggered activity and macro-reentry. These mechanisms are discussed in more detail in the following section.

Automaticity

Automaticity (spontaneous phase 4 activity) is a normal characteristic of Purkinje fibers. Normal Purkinje cells may function as ancillary pacemakers in patients with compromised function of the cardiac conduction system. Damaged Purkinje fibers

can create isolated PVC's or VT due to Na- and/or Ca- dependent *enhanced normal* automaticity. Overdrive stimulation is a typical characteristic that can help to identify the mechanism of tachycardia. Other ventricular cells do normally not express automaticity, but *abnormal* automaticity (depolarization-induced) can be observed from damaged ventricular cells (and damaged Purkinje cells) due to a less negative membrane resting potential.

Figure 1. Automaticity. (adapted from Clinical Arrhythmology and Electrophysiology 2009. A companion to Braunwald's Heart Disease)

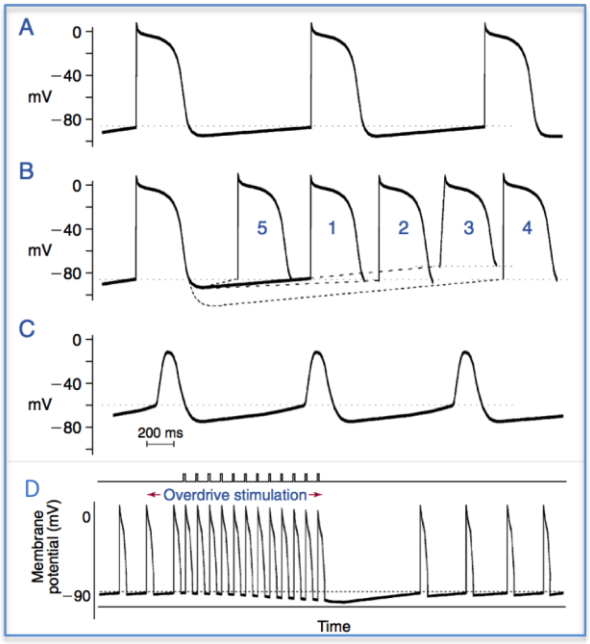

A, Normal His-Purkinje (HP) system action potential (AP). **B,** Rate modulation: (1) by slowing the rate of phase 4 depolarization (2), increasing threshold potential (3), starting from a more negative resting membrane potential (4), all of which slow discharge rate, or by increasing rate of phase 4 depolarization (5), yielding a faster discharge rate. **C,** Abnormal automaticity with change in AP contour (resembling sinus nodal cell) when resting membrane potential is less negative, inactivating most Na-channels. **D,** Overdrive suppression: A spontaneously firing HP cell is paced more rapidly, lowering the membrane potential. After pacing is stopped, spontaneous depolarization takes longer than usual and gradually resumes baseline rate.

Triggered activity

Triggered activity may be due to early or delayed afterdepolarizations. Afterdepolarizations arises as a consequence of oscillations in the membrane potential. Examples of VT arising as a consequence of triggered activity include Torsade de Pointes, polymorphic VT, stretch during heart failure and outflow tract tachycardia.

Figure 2. Triggered activity (adapted from Clinical Arrhythmology and Electrophysiology 2009. A companion to Braunwald's Heart Disease)

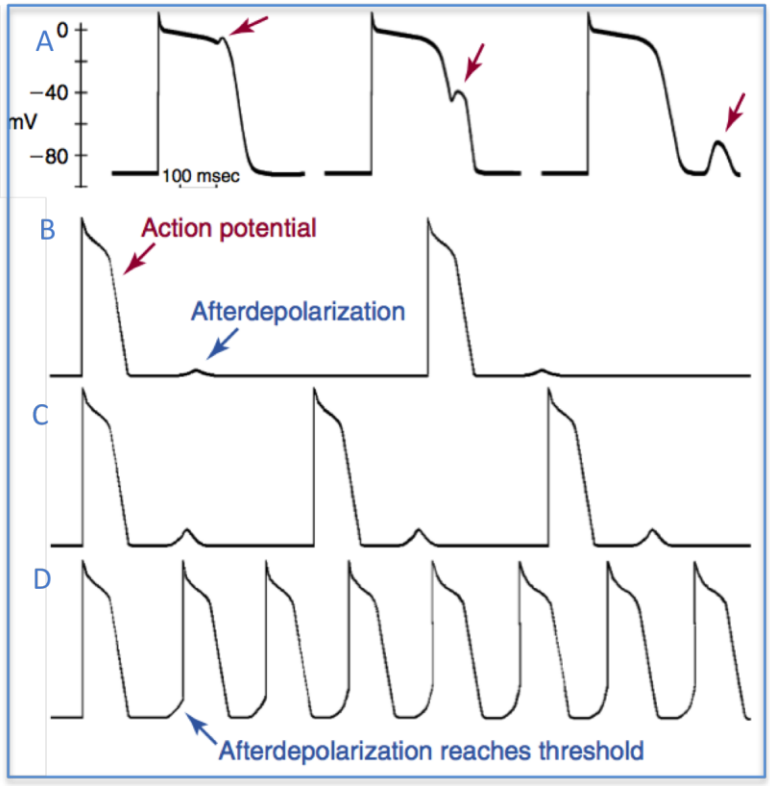

A, Examples of His Purkinje APs with early phase 2 (first arrow), delayed phase 3 (second arrow) and delayed phase 4 (third arrow) after depolarization. **B,** The DAD is seen following the AP at slow rates. **C,** At faster rates, the DAD occurs slightly earlier and increases in amplitude. **D,** At still more rapid rates, the DAD occurs even earlier and eventually reaches threshold, resulting in sustained firing.

Reentry

The majority of scar related VT arises due to macro reentry. Three conditions are essential for a re-entry to occur: 1.) unidirectional block, 2.) at least two conducting pathways/ channels, and 3.) a region of slow conduction. Sufficient conduction slowing is needed to create an excitable gap. Slow conduction is caused by a zigzag conduction inside the scar, due to fibrosis, islands of surviving tissue and myocyte separation as presented in Figure 3.[4]

Figure 3. Zig-zag conduction in the infarct region.[4, 6]

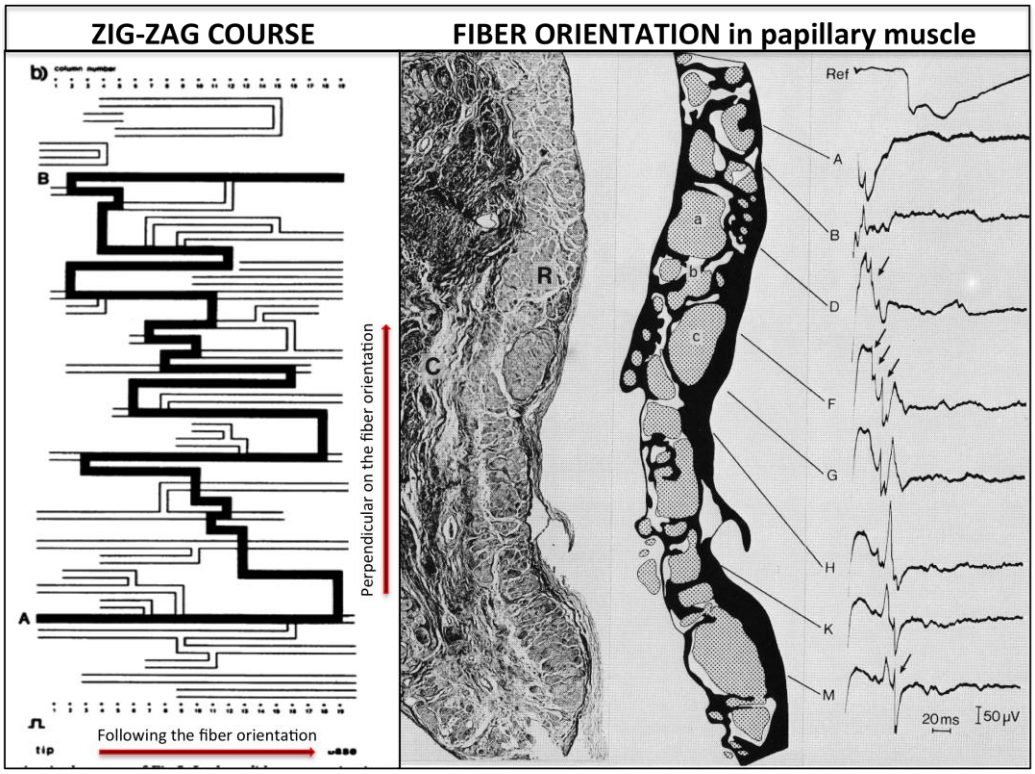

Left side: schematic representation of the electrical propagation inside the scar. Normal conduction along the fiber orientation (horizontal), but severely delayed conduction in the transversal (vertical) orientation. Right side: perpendicular slice on the fiber orientation of a pappillary muscle.

C. Scar formation: the histological substrate

Scar formation and maturation

The majority of ventricular scar is related to myocardial ischemia, presenting as a wave-like necrosis, starting from the endocardium and progressing towards the epicardium. This coagulative necrosis creates an inflammatory response and fibrotic healing of the scar, a process that takes three or more months. Within the scar, bundles of surviving myocytes with damaged intracellular connections (Connexin 43), electrically inactive regions, fibrosis (elastin and collagen), calcification and fat can be found. Animal experiments demonstrated changes in myocyte morphology and length in the scar border zone. Damaged cells have altered electrophysiological properties (cf below: the functional substrate).

Scar remodeling

Fibroblasts do not only serve as matrix-producing reparative cells, but exhibit a wide range of functions in inflammatory and immune responses, angiogenesis and neoplasia. Considering their abundance, their crucial role in cardiac inflammation and repair, and their involvement in myocardial dysfunction and arrhythmogenesis, cardiac fibroblasts may be key therapeutic targets in cardiac remodeling (Figure 4). Tissue heterogeneity and damaged sympathetic nerve innervations or autonomic reinnervations can create abberant conduction.[7, 8] Scar remodeling is an important mediator for the development of late ventricular arrhythmias, often seen years after the myocardial infarction.[9] These findings explain the efficacy of betablockers, renal

denervation and ganglion stellatum blockade in the treatment of ventricular tachycardia.[10]

Figure 4. Scar remodeling.[11]

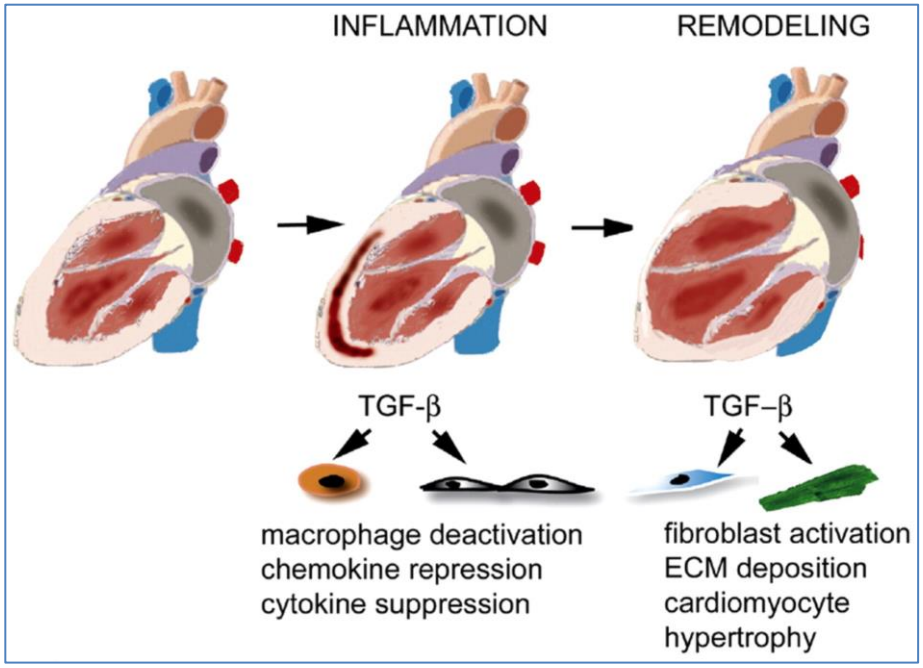

Role of TGF-β signaling in infarct healing and post-infarction remodeling. MI triggers an inflammatory reaction that ultimately results in formation of a scar. Infarct healing is associated with alterations in the geometric characteristics of the ventricle: dilation and hypertrophy, these changes are termed ventricular remodeling. In the early phases of infarct healing TGF-β may be important in resolution of the inflammatory response by deactivating macrophages and by suppressing endothelial cell chemokine and cytokine synthesis. At a later stage, TGF-β activates fibrogenic pathways by inducing extracellular matrix deposition and may contribute to the pathogenesis of LV remodeling by promoting fibrosis and hypertrophy of the non-infarcted myocardium.

D. Electrograms related to scar: the functional substrate

Electroanatomcal mapping (EAM) is critical for characterization of the arrhythmogenic substrate in patients with scar-related VT. In addition to voltage-based scar mapping, abnormal signals –suitable as specific ablation targets– can be mapped and annotated on an EAM map. The abnormal signals are generated by surviving bundles of myocardium within fibrotic scar and are the channels providing the slow enough conduction to sustain re-entry.[6] The concept of late potential ablation was introduced a decade ago, twenty years after surgical resection of aneurysms associated with the disappearance of these electrical signals.[12-14, 15]

Low voltage EGM

The amplitude of an EGM depends on multiple factors: The recording electrode size, the interelectrode distance (for bipolar voltage measurement), the catheter tip orientation, the contact force, the wall thickness, the presence of scar and the distance from the recording area to the scar location.

Marchlinski *et al* [16] analyzed the ventricular endocardium of 6 healthy individuals with an ablation catheter and found that 95% of all LV electrograms were >1.55mV and therefore defined a bipolar voltage <1.5mV as low voltage and arbitrarly defined dense scar as <0.5mV. Later, a low voltage threshold of <1mV for epicardial bipolar low voltage was defined by Cano *et al.* [17]

Furthermore, dense or focal scar will present different voltage characteristics. Piers *et al* previously demonstrated that a rim of only 2mm of healthy myocardial tissue above a zone of scar can be sufficient to show a normal bipolar voltage EGM at the recorded site.[18] Epicardial fat can mimick a low voltage area.[17, 19]

During bipolar voltage recording, a small electrode size and a small interelectrode distance are more sensitive for near field recording. Unipolar voltage recording is useful to investigate the entire wall in order to analyze wall thickness and detect intramural or epicardial scar. Specific voltage thresholds that are used to define scar and normal myocarium are further defined in the section on substrate mapping.

Fragmented signal

EGM fragmentation maybe a representation of myocyte dissaray (due to scar and fibrosis) or complex transmural conduction (e.g. in ARVC) It is recognized as an indicator of slow conduction.[20] Fragmented signals are frequently found inside scar.[21]

Figure 5. Different examples of LAVA and fragmented EGM.[22]

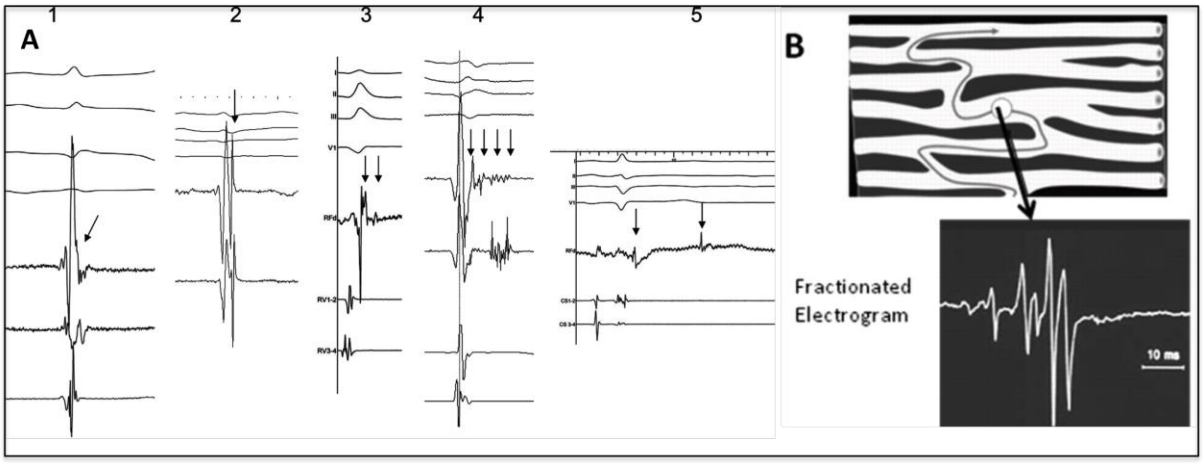

A.Five examples of LAVA (arrows): 1. a LAVA signal buried inside the terminal QRS complex, 2. a normal voltage LAVA just behind the far field QRS, 3. a double potential LAVA, 4. a fragmented LAVA of long duration and 5. a very late double component LAVA. **B.** Zig-zag conduction resulting in a fragmented EGM signal. *Adapted from ref.* [20]

Double potentials

The presence of double potentials may indicate an area of (local or linear) block. Therefore double potentials are also often found in scar regions. De Chillou *et al* described the critical VT isthmus in ICM as bounded by 2 approximately parallel conduction barriers that consisted of a line of double potentials, a scar area, or the mitral valve annulus.[23]

Late potentials and Local Abnormal Ventricular Activity

Nogami *et al* introduced the concept of abnormal potential ablation in ARVC patients with late potential (LP) elimination as endpoint.[24] In a subsequent study, Jais *et al* demonstrated that abnormal potentials including late activities could also be eliminated in scar related VT with ischemic or non ischemic substrate.[22] Bogun *et al* also targeted late potentials and demonstrated favourable results.[25] The idea of LAVA-based ablation gained prominence following a number of recent studies (cf Table 5).[26]

In their report in a large series of ICM and NICM patients, Jaïs *et al* further defined local abnormal ventricular potentials (LAVA) which are characterized by their sharpness (high dV/dt) and poor electrical coupling. LAVA may be unmasked by pacing maneuvers (Table 2) and can be tagged on the substrate map as they may

represent ablation target sites.[22] They are visible in sinus rhythm (SR) and during VT. This term is used by the authors since these potentials are not always late and may in fact be buried in the farfield ventricular potential. LAVA characteristics in Table 1 and LAVA are shown in Figure 5.

Table 1. LAVA characteristics.

Characteristics	LAVA signal	Healthy myocardium
Amplitude (peak-to-peak)(mV)	>90% of LAVA <1.5mV bipolar Amplitude epicardial often > endocardial LAVA (median 0.37mV vs 0.11mV) [22]	>1.5mV bipolar (caveat epicardial fat mapping of >2.8mm thickness)
Slope (dV/dT)	Higher dV/dt (cfr PV potential) than farfield signal	Lower dV/dt than local LAVA High dV/dt if rising from normal conduction system (His, RBB, LBB, healthy Purkinje)
Lateness according to QRS onset (till end of signal)(ms)	>99% of LAVA occur between QRS onset and 200ms after QRS Early at septal sites (43% after QRS complex) and late at lateral (81% after QRS complex) and epicardial sites (epi vs endo: 91% vs 66% after QRS complex (figure 1) Very late (>200ms) within dense scar (76%)	Inside the QRS
Number of peaks (n) / fragmentation	Double potentials /split signal More fragmented deeply inside dense scar	One signal without fragmentation
Duration (ms)	Single sharp potential of short duration can be abnormal >95ms is pathologic and sign of slow conduction	<95ms
Consistency	Consecutive beats with same activation (exluding PVC and fusion beats)	Consecutive beats with same activation
Electrical coupling	Poorly coupled (delay in sinus rhythm, different responses to pacing, cfr lower)	Normal coupling

Table 2. Pacing maneuvers to unmask LAVA.

Pacing site/maneuver	farfield signal versus nearfield (LAVA) signal
RV apex pacing	Unmasked LAVA with delay of local signal Changed or reversed activation (QRS-LAVA towards LAVA-QRS) Variable degree of conduction block (2:1 or more or disappearance) Particularly useful to unmask early septal LAVA and differentiate from healthy conduction system
Extrastimulus pacing	Increased local delay or block
Local pacing (or ectopics) **Fixed amplitude or decreasing output**	Same possibilities as above Loss of farfield capture can result in changes in Stim-QRS delay and QRS morphology of the paced beats Within dense scar, local capture can unmask previously hidden LAVA activity
Pacing at endo/epi facing sites	Different activation sequences Change in conduction delays
Spontaneous PVC	Reversed activation or local delay

E. Imaging of scar: the structural substrate

Imaging techniques used for image integration

The role of pre-procedural delayed-enhancement (DE) MRI and delayed-enhancement multidetector (MD) CT imaging has expanded significantly in recent years. Pre-procedural imaging results in better scar delineation. MRI and MDCT modalities provide valuable information regarding the potential need for an epicardial approach during the first procedure. Of note, however, these imaging techniques are not used routinely. Further, there is currently a lack of data from large prospective randomized controlled trials on the impact of additional imaging on the prognosis after VT ablation.

MRI imaging

Pre-procedural late gadolinium enhancement MRI has become the gold standard imaging modality for the assessment of scar and has better resolution than EAM

systems.[27,28] However a major current limitation of the technique is that it is limited to patients who do not have an ICD. Wideband MRI imaging seems useful to overcome this limitation by a significant decrease in the amount of box and lead artefacts.[29] MRI provides valuable information about the amount of scar and grey zone, scar transmurality, heterogeneity and location and is able to visualize intramural and epicardial scar.[30] The ability to detect and localize scar in both ICM and NICM with DE-MRI has recently been published in a large trial. The VT origin could be identified within a hyperenhanced LV scar region in 96% of cases.[31]

MDCT imaging

In ICD patients, information on scar characteristics can be obtained by secondary wall thinning in the scar region with the use of MDCT, which offers high spatial and temporal resolution.[32] Intra-myocardial hypodensity and subepicardial "scalloping" give additional information on hypoperfusion and (fibro-) fatty replacement.[33] Delayed enhancement MDCT is an emerging but still experimental technique to visualize scar. MDCT also allows segmentation of the coronary arteries, phrenic nerve, coronary sinus, epicardial fat, ventricular calcification, fibrofatty replacement and anatomical channels of relatively preserved wall thickness.[34]

Ultrasound imaging

Pre-procedural ultrasound imaging can visualize an intracardiac thrombus, quantify ejection fraction and delineate possible left ventricular aneurysm. Endocardial and epicardial scar can be visualized with peri-procedural ICE-imaging.[35, 36] In addition,

ICE-imaging can help to perform a safer transseptal puncture, offer fast anatomical mapping, when integrated in an EAM system, can provide real-time information on catheter contact and orientation (e.g. VT originating from a papillary muscle) and can help to prevent potential steam pop.[37]

At CHU Bordeaux, we have developed the MUSIC software (CHU Bordeaux, LYRIC, INRIA) to create personalized models, able to display all these preprocedural information into a 3D-model with structural and functional information, and exported as meshes which can be integrated in the electro-anatomical mapping systems to understand the individual patients' disease and to guide the approach and ablation. The MUSIC platform is presented schematicaly in Figure 6 and an example is given in Figure 7.

Figure 6. The MUSIC platform.

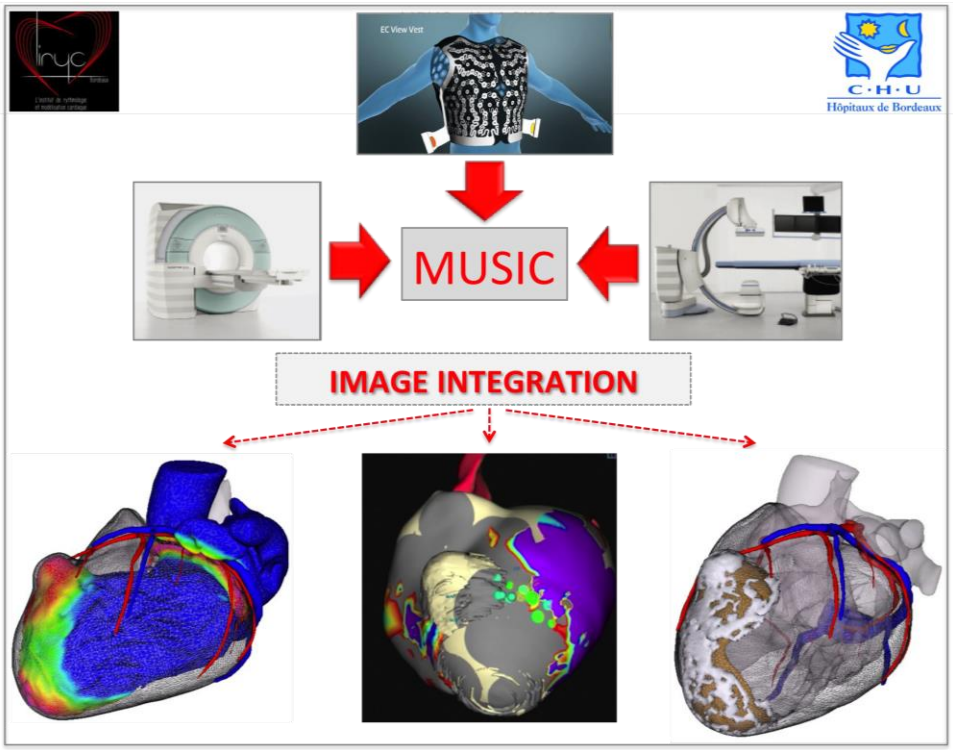

All preprocudural acquired information from MDCT, DE-MRI, body surface mapping etc is included in the MUSIC platform. Different 3D-meshes are made and exported as .vtk or DIF- model: color-coded wall thicness maps, scar and border zone maps etc. These meshes are included in the EAM system to guide the ablation procedure.

Figure 7. Example of preprocedural imaging and integration into the EAM system.

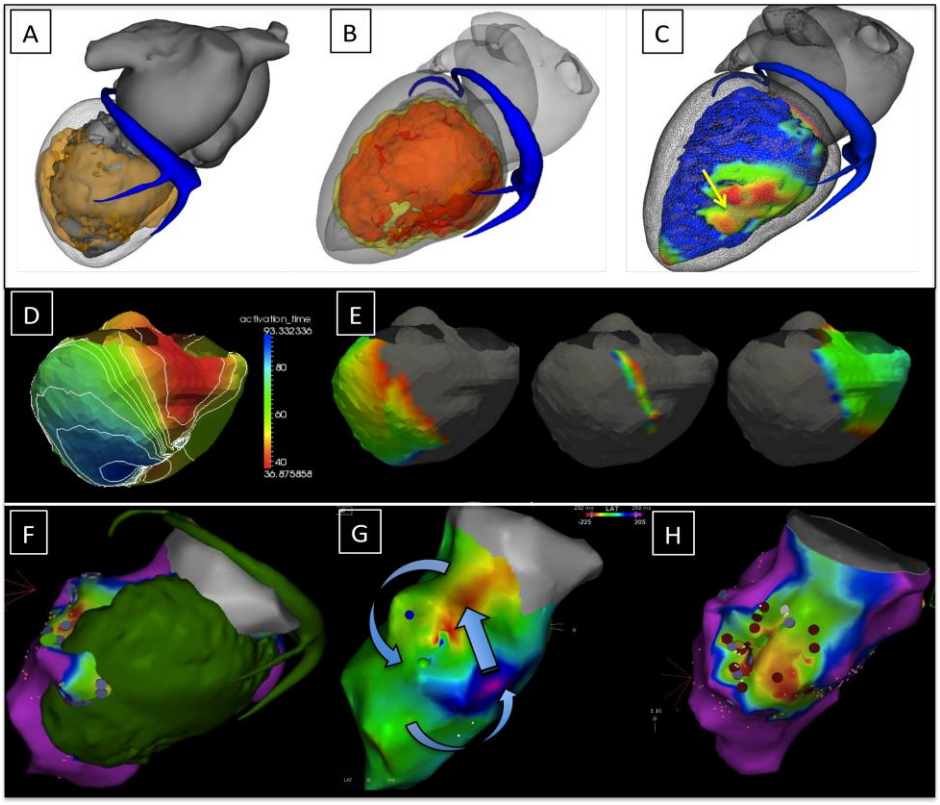

Pt with a previous myocardial infarction. **A.** Inferior scar on DE-MRI, **B.** Wall thinning on MDCT and **C.** Color-coded wall thickness map. All are integrated in the EAM system using the MUSIC platform. **D.** Activation map with body surface ECG mapping in SR. Crowding of isochrones gives impression of a zone of slow conduction and therefore scar. **E.** Phase mapping during VT using body surface mapping. Figure-of-eight activation with impression of the isthmus in the middle figure. **F.** Image integration into the EAM system with merge of MDCT/MRI model with DE scar visualisation and an endocardial bipolar voltage map. **G.** Activation map during VT correlates with the body surface mapping data. **H.** A good correlation between scar on MRI and low voltage on EAM is observed. LAVA points are tagged in purple and ablation points in red. Mid-diastolic LAVA are tagged in green.

F. Mapping of VT

VT ablation is based on the identification of the VT circuit and more specifically, the area of slow conduction within the circuit. This critical part of the circuit is usually protected from the surrounding myocardium by zones of block and is amenable to mapping during VT. Entrainment mapping has proved very effective in determining the entrance, isthmus and exit of the slow conduction zone. The isthmus is usually considered the best and most vulnerable part of the circuit. While this strategy has proven to be very effective, it is entirely relying on VT inducibility and tolerance. Substrate-based mapping and pace-mapping represent important complementary/alternative techniques for VT ablation. Substrate-based approaches are particularly valuable in patients with non-inducible, unstable, or unmappable VT.

General considerations

The 12-lead ECG acquired during VT provides some indication on the exit site in addition to chamber information (LV vs RV), and the possibility of an epicardial exit. Low QRS voltage, widened and fragmented QRS are ECG signs of scar. An endocardial only approach is most widely used for index procedures. Both retrograde aortic and transseptal approaches can be used and are complementary. The transseptal approach may be preferred in patients with significant peripheral vascular disease. Combined endocardial/epicardial ablation is commonly performed in ARVC. An epicardial approach is also commonely considered after a failed endocardial procedure particularly in NICM but also in ICM, particularly in presence of an epicardial scar.

Mapping systems

EAM systems offer non-fluoroscopic catheter localisation, display local EGM characteristics and integrate electro-anatomical information on 3D maps. Anatomical acquisition can be performed by point-by-point or fast anatomical mapping with bipolar or multipolar catheters. The CARTO® 3 system (Biosense Webster) has a magnetic and impedance-based localization of the catheters. The Ensite™ Velocity™ system (St Jude Medical) is entirely impedance based.

A recent study looked at localisation precision and accuracy of the CARTO® 3 system and Ensite™ Velocity™ system in a phantom model. The CARTO® 3 system had a better accuracy (EAM map compared to the real anatomy) and a significantly better localisation precision than the Ensite™ Velocity™ system.[38, 39] Recently, a new magnetic-based mapping system is available (the Rhythmia™ Medical system) which uses a 64 mini-electrodes multipolar mapping catheter (Orion™) and creates fast and accurate high-density maps. However, it is unclear if submillimetric accuracy is clinically relevant and all current systems share the same major limitation: patient's motion results in map shift and all acquired maps become useless. In addition, respiratory motion is incompletely corrected for, not to mention the cardiac motion, which is not corrected at all. A comparison between the 3 mapping systems is included in Table 3.

Table 3. Comparison between electro-anatomical mapping systems.

EAM mapping system	CARTO® 3	ENSITE™ VELOCITY™	RHYTHMIA™ MEDICAL
Basic principle	5-50 μT magnetic field 100 kHz current through patches	5.6 kHz current through patches	160-880μT magnetic field 13 kHz current through patches
Location principle	magnetic and impedance based	impedance based + magnetic based with Mediguide™ possible	magnetic and impedance based
Locator pad	under table	no locator pad	under table
Accuracy	<5mm (3 magnetic coils) inside tip of NAV catheters	accuracy not given	<1mm for Orion™ <2mm for other catheters
Patches	3 front patches	3 front patches	aVL, aVr, aVF, V1,V3,V6 front patches
Reference patch	3 back patches	1 reference patch	1 back patch
Closed or open system	closed for mapping (NAV)/ablation open for other catheters	open for all catheters	closed for Orion™ catheter open for other catheters
Motion compensation	yes	yes	yes
Shift compensation	yes, automatic based on 3 patches	yes, if stable catheter reference or reference patch	no, indicates shift and manual compensation is needed
Additional EP system	no need	no need	no need
Image integration	possible	possible	possible
Issues	epicardial mapping with PentaRay® sometimes less accurate	needs field scaling not as accurate as magnetic based systems	epicardial mapping also collects pts on outer shell
Multipolar mapping	PentaRay® NAV catheter	Ensite™ Array™ Livewire™catheter =suboptimal mapping	IntellaMap Orion™catheter
Points labeling	easy labeling	possible	possible
PVC mapping	PASO™ module for PVC/ VT	simultaneous different PVC maps	PVC mapping
Extra features	Visitag™ module Contact force visualisation UniView™ reduces fluoroscopy	Array™ non-contact mapping Mediguide™ offers better field scaling	fast high density mapping with accurate automatic mapping
Robotic navigation	compatible with EPOCH™ and Amigo™ system	NA	NA
Reference for activation mapping	different possibilities	different possibilities	max amplitude (bipolar signal) or max neg dV/dt (unipolar signal)

Pace-mapping

Unexcitable scar is identified on the EAM map with unipolar stimulation at >10mA and 2ms. Pace-mapping is performed to localize the exit site of the VT usually defined as ≥11/12 match. It is usually identified at the borderzone while pacing deeper inside the scar usually identifies the isthmus region associated with long stim-QRS duration (>40-70ms) due to slow conduction,[40] bounded by unexcitable scar.[41-43]

Multiple scar exit sites (MES, all ≥10/12 match with VT) from the scar can be seen when performing pace-mapping (10mA, 2ms) at an abnormal EGM site, presenting with ≥2 pace-map morphologies (<10/12 match) at same pace-map drive train (400-600ms).[44] Improved freedom from recurrent VT is seen following ablation at these sites. Pace-map induction (PMI) of VT without extra stimulus has also been reported to predict succesful ablation sites for VT termination.[44] Another recently developed technique is the use of high density pace-mapping to visualize the critical isthmus (orientation and length). The technique involves making a detailed colour-coded pace-map. Exit sites characteristically have perfect pace-maps while entrance sites have the worst pace-maps and abrupt changes in pace-map match indicate the isthmus.[41]

Activation and entrainment mapping

After the completion of an anatomical map and substrate map in SR, VT inducibility is tested and if inducible and tolerated, activation mapping with entrainment mapping can be performed with bipolar or multipolar contact mapping, ideally mapping the whole VT cycle length.[45,46] Mid-diastolic potentials, which may indicate the isthmus, and presystolic potentials, which may indicate the exit site can be annotated on the EAM map.

Good ablation sites have identical stim-QRS and EGM-QRS time, a short PPI-TCL (<30ms) and show concealed entrainment.[47] Focal scar related VT is uncommon. It is ideally mapped as earliest activation (EGM onset >40ms before QRS onset), a

good pace-map (≥11/12 pace-map match) and a unipolar QS pattern. Entrainment pacing is illustrated schematically in Figure 8.

Figure 8. Entrainment of VT: algorithm to define the position of a pacing site regarding the VT circuit.

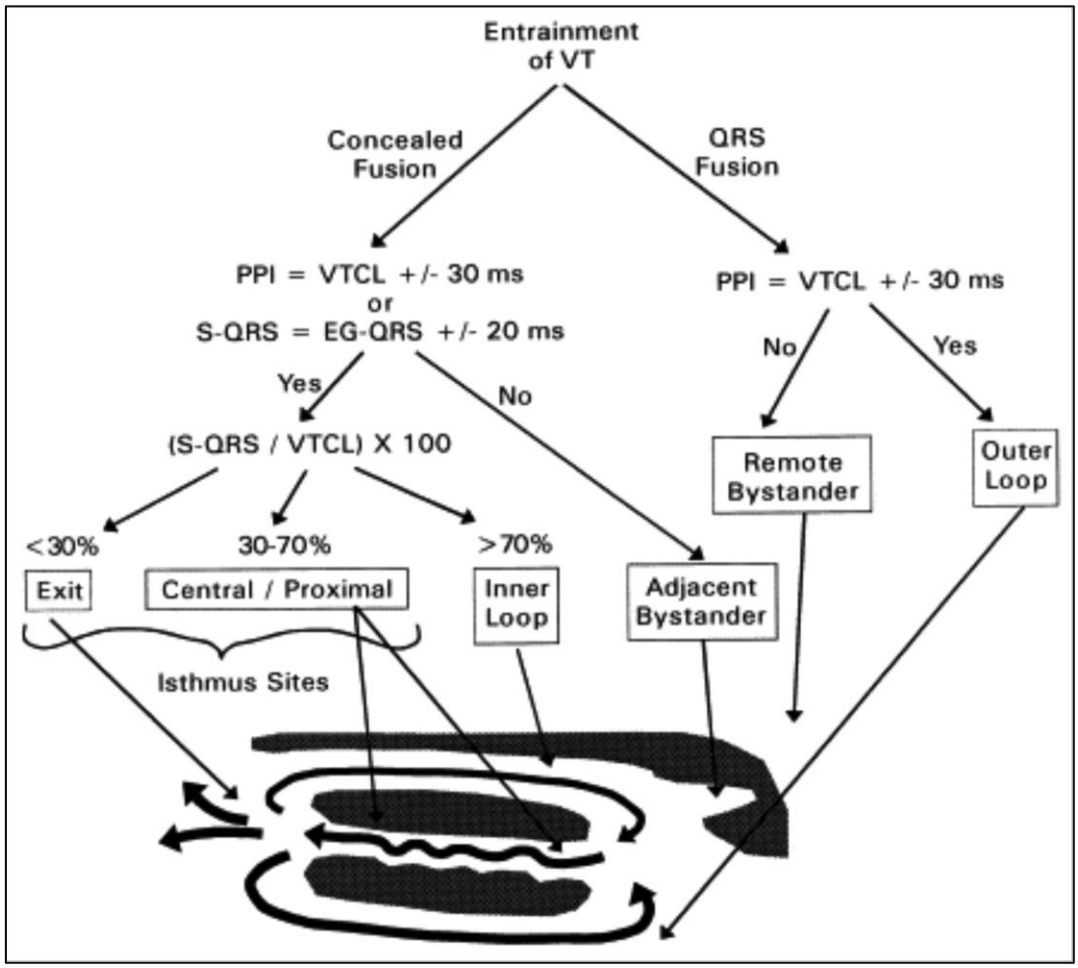

Substrate mapping

Different mapping strategies can be used to identify scar, VT circuit, critical isthmus and ablation targets. Endocardial substrate mapping can be performed with automatic voltage maps with the following bipolar endocardial threshold described by Marchlinski *et al* and widely used: dense scar <0.5mV, border zone 0.5-1.5mV

and normal voltage >1.5mV. As mentioned above, they analyzed the ventricular endocardium of 6 healthy individuals with an ablation catheter and found that 95% of all LV electrograms were >1.55mV and therefore defined a bipolar voltage <1.5mV as low voltage and arbitrarly defined dense scar as <0.5mV. We hypothesize that dedicated multipolar mapping catheters will give different threshold values, although this still has to be investigated. For epicardial mapping, a low voltage threshold <1mV is used with inclusion of abnormal -late, split and wide potentials >80ms.[48-50] Unipolar low voltage thresholds to identify scar are <5.5mV in the RV and <8.3mV in the LV. Unipolar voltages provide information over a wider field and are therefore valuable for predicting the presence of intramural or epicardial scar.[51] The presence of intramural septal scar - suggested by unipolar low voltage - can further be identified by pacing manoeuvres from the basal RV. Septal scar is characterised by, delayed transmural conduction time (>40ms) and fractionated, late, split, and wide (>95ms) bipolar EGMs.[52-54] Epicardial substrate mapping is more challenging due to the presence of epicardial fat which can mimic low voltage areas. Epicardial fat is howeber not associated with delayed and fragmented signals.[17, 19] Unipolar voltage mapping seems more reliable and a unipolar low epicardial voltage threshold <7.95mV has been suggested.[19, 51, 55, 56] Table 4 illustrates different substrate mapping strategies.

Table 4. Different thresholds for substrate mapping.

	Marchlinski *et al*	Cano *et al*	Zeppenfeld *et al*
Normal endocardium	>1.5mV bipolar >8.27mV unipolar LV >5.5mV unipolar RV	>1.5mV bipolar	>1.5mV bipolar
Abnormal epicardium	<1mV bipolar	<1mV bipolar + split, late or wide potentials (>80ms duration)	<1.81mV bipolar <7.95mV unipolar if fat ≥2.8mm: + split, late or wide potentials
Border zone	<0.5mV–1.5mV bipolar	<0.5mV–1.5mV bipolar	<0.5mV–1.5mV bipolar
Dense scar	<0.5mV bipolar	<0.5mV bipolar	<0.5mV bipolar

In all these studies a 3.5mm (Navistar Thermocool) or a 4mm (Navistar) distal tip ablation catheter, not dedicated for mapping (both Biosense Webster) was used.

G. Ablation methods

In most centers, ablation is performed using RF energy with an irrigated bipolar ablation catheter in the unipolar mode. A steerable sheath and contact force measurement may increase the efficacy of performing adequate ablation lesions.[57] While this 'conventional' approach is effective in most VT patients, in a subset of patients, the arrhythmogenic substrate maybe challenging to ablate. As a result, novel ablation techniques have been developed. Examples inlcude alcohol ablation, bipolar ablation and irrigated needle ablation. A high power unipolar ablation (up to 70 watts) increases the risk of complications such as steam pop. A promising new device designed to make deeper intra- and transmural lesions is the irrigated extendable retractable needle catheter (Biosense Webster).[58] Bipolar ablation between the distal tips of two irrigated ablation catheters (ideally visualized on the EAM

system) on adjacent sites (between endocardial and epicardial or between LV and RV septum) is shown to be effective for intraseptal AT and VT in both animal and human studies.[59] Selective intracoronary ethanol ablation is effective in creating deep intramural lesions.[60, 61] Figure 9 illustrates examples of different ablation methods for intraseptal or intramural scar. The injection of collagenase is an effective novel method to homogenize the scar and may open the way towards bio-enzymatic ablation of arrhythmogenic tissue.[62]

Figure 9. Different ablation strategies for intramural or septal scar.

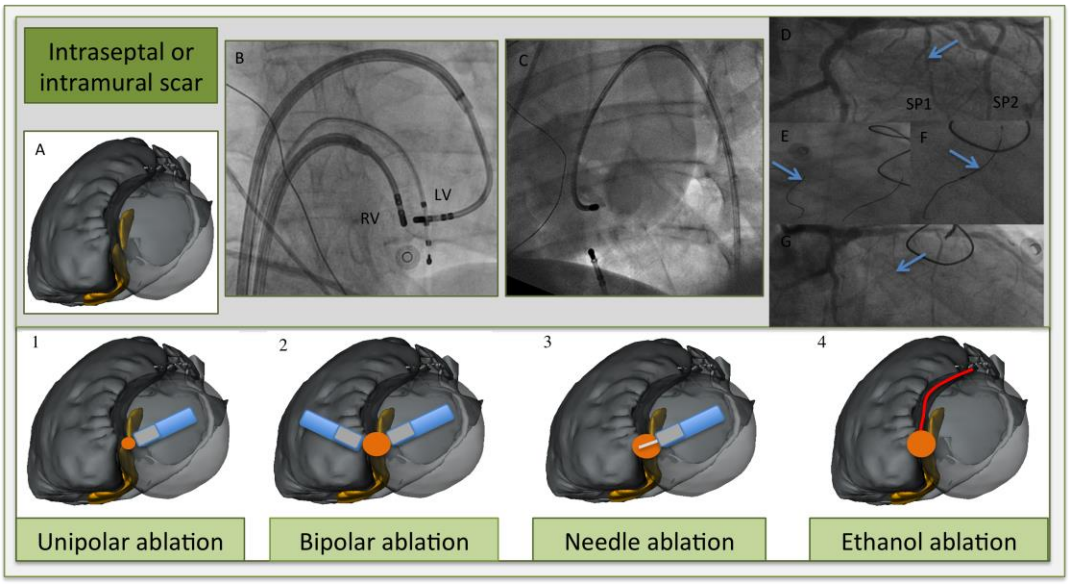

A. Illustration of merged MDCT /MRI segmentation with post-ablation non-transmural scar regions (in yellow) on both sites of the septum (LAO view). Ablation catheters (blue), tip (grey), needle (white), ablation target (red dot), expected ablation lesion (orange dot), first septal perforator (SP1) in red.

1. *High output ablation* (till 70W) gives a slightly larger lesion, however often not transmural and the risk for steam pop or catheter perforation increases.

2. *Bipolar ablation.* Two ablation catheters at opposing septum sites (**B.** AP view, 2 ablation catheters in steerable sheaths and a RV apex catheter for pacing purposes).

3. *Irrigated needle catheter at LV septum*. Needle extended (7-9mm) inside the septum with staining of contrast (**C.** fluoroscopic image with contrast staining at another basolateral site. Needle catheter in steerable sheath, quadripolar catheter in CS and RV apex. Dual chamber ICD leads © image).

4. *Selective coronary ethanol injection*. [cf fluoroscopic sequence: **D.** Coronary angiogram shows septal perforators, with as target the first septal perforator (arrow) **E.** Guidewire cannulation of first (arrow) and second septal perforator. **F.** Balloon occlusion (arrow) with iced saline injection and later 1.5ml ethanol injection because of VT termination. **G.** Occlusion of the first septal perforator (arrow)].

H. Ablation strategy

If feasible, VT is commonly induced and ablation commenced during tolerated VT, followed by activation mapping and entrainment mapping of the complete VT circuit. After VT termination, multiple substrate-based ablation strategies can be used. These include encircling of the scar, linear lesions across voltage channels or across exit sites, linear isthmus ablation to achieve bidirectional block, scar homogenization or scar modification by complete LAVA elimination. Not uncommonly, combinations of the above are used.[16, 22, 63-66] An overview of different strategies are schematicaly explained in Figure 10.

In ICM with secondary wall thinning, it may be of interest to preserve safety to perform endocardial ablation first, in an attempt to eliminate epicardial LAVA thereby limiting epicardial ablation.[67]

Figure 10. Different ablation techniques for scar-related VT ablation.

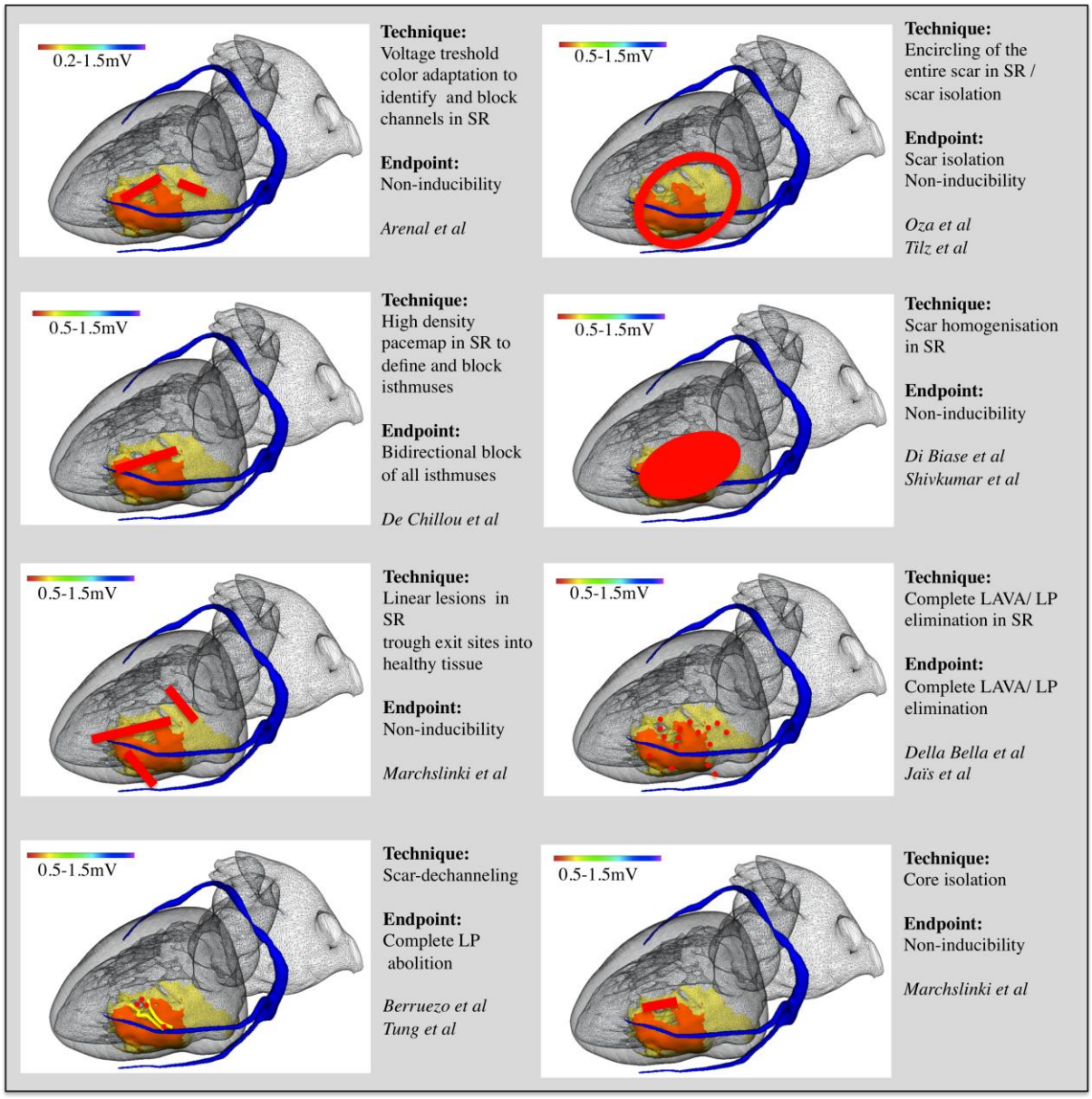

Epicardial ablation

Most centres perform epicardial ablation after a failed endocardial procedure or in cases with epicardial scar on DE-MRI or other imaging studies.[68-70] The 12-lead ECG of the clinical VT may also indicate an epicardial origin.[71, 72] This approach is usually relatively easy but may be complicated in presence of prior cardiac surgery or

pericarditis. A blunt dissection of pericardial adhesions may still be considered using the steerable ablation catheter but the risk for complications is then significantly increased.[73] Alternatively, a surgical subxyphoidal approach has also been proposed in the EP lab.[74]

Epicardial ablation is more challenging because of complications associated with access, the presence of epicardial fat, and potential damage to coronary arteries and the phrenic nerve or extracardiac structures.[75, 76] Epicardial fat has been reported to limit ablation efficacy.[19] Currently, most operators do not ablate if the distance to the coronary artery is 5 mm or less. However, the long term histological impact of ablating in close proximity to the coronary arteries is not known.[77, 78] Phrenic nerve paralysis can be avoided by infusion of saline,air insufflation or balloon insufflation into the pericardial space (with close monitoring for signs of cardiac tamponade).[79, 80] Pre-procedural phrenic nerve and coronary MDCT segmentation and peri-procedural image integration, phrenic nerve pace-mapping at high output (with tagging of phrenic capture sites on the EAM map) and coronary angiogram can help to minimise complications.[19, 34, 81] Post-procedural corticoids to avoid the formation of adhesions can also be given after epicardial ablation.[82]

Endpoints

Different endpoints can be used for VT ablation, however it is important to note that there is currently no consensus in the guidelines.[1] Potential endpoints include elimination of all inducible VT[45], elimination of all clinical (and slower) VT, isthmus block confirmed by pace-mapping[83, 84], scar homogenisation into unexcitable scar[64],

complete scar isolation[65] and elimination of all LAVA in addition to non-inducibility[85-87]. A combined endpoint of non-inducibility of clinical VT (and slower)[88] and complete LAVA elimination have been demonstrated to predict reduced recurrence of future VT.[22, 89, 90] There is no reported extra benefit of ablating all inducible VT that are faster than the clinical VT.

Both non-inducibility and complete LAVA or late potential (LP) elimination are associated with improved outcome.[85,22] The combined endpoint of non-inducibility and complete LAVA or LP elimination has significantly lower recurrence of VT and mortality than complete LP elimination or non-inducibility alone (16% vs 46% and 4% vs 42% respectively; both $p<0.01$) in ICM patients with an ICD.[91] Consensus on ablation endpoints is needed in order to compare efficacy of different techniques. An overview of different endpoints is illustrated in Table 5.

Table 5. Different endpoints used for VT ablation procedures.

	N of patients	Non-inducibility of any VT	Non-inducibility of clinical or slower VT	Inducibility of VT	Complete LAVA / LP elimination	Non-inducibility and LAVA / LP elimination	Recurrence of VT	Death	Follow-up in months
Frankel et al JACC 2012	200pts ICM+NICM	29.5% (A)		24.5% (B) other VT - 12% (C) clinical VT			<30(A) vs 65(B) vs 85(C)% (A vs B: p 0.001 and B vs C: p 0.01)	3(A) vs 21(B) vs 24(C)%	>12 months
Jaïs et al Circ 2012	70pts ICM+NICM			32% any VT	70.1%		Overal 46%	Overal 19%	22(14,27) months
Vergara et al JCE 2012	64pts ICM+NICM	71.4% (A)			84% (B) complete 26% (C) incomplete		Overal 20% 9.5(B) vs 75(C) %: p<0.0001	Overall 22%	13±4 months
Piers et al Circ AEP 2013	45pts NICM	38% (A)	38% (B)	24% (C) clinical VT			Overall 53% 18(A) vs 77(B) : p<0.001 vs 73(C)%	Overal 13%	25±15 months
Della Bella et al Circ 2013	528pts ICM+NICM (VT unit)	77% (A)		10.6% (C) clinical VT - 12% (B) other VT			Overall 34% 28.6(A) vs 39.6(B) : p<0.001 vs 66.7(C)%	Overall 15.6% 8.4(A) vs 18.5(B) : p<0.001 vs 22(C)%	26(13,46) months
Silberbauer et al Circ AEP 2014	160pts ICM	41% (A)		59% (C) any VT	80% (D)	47% (E)	Overall 32% 16.4(E) vs 46.0(A) vs 47.4(C) % : p<0.01	Overall 16.4% 6.6(A) vs 42.1(C) :p<0.01 4.1(E) vs 42.1(C) : p<0.001 vs 22(A)%	18 months
Komatsu et al	195pts ICM+NICM	68% (A)		32% (B) clinical VT 16% (C) any VT	62% (D) complete 38% (E) incomplete	49% NI+LAVA (F) 64% NI-LAVA (G) 12% I - LAVA (H)	Overal 41% 28(D) vs 63(E) :p<0.001 32(A) vs 61(C) :p<0.001	Overal 28% 16(D) vs 49(E) - 20(A) vs 46(C) - 15(F) vs 34(G) vs 46(H) : all p<0.001	23 (7,38) months
Dinov et al (HELP-VT) Circ 2014	227pts ICM+NICM	66.7% in NICM and 77.4% in ICM		33.3% in NICM and 22.6% in ICM			Overal NICM: 77% and ICM: 57%	NICM: 12.7% and ICM: 7.9% : p 0.3	NICM:20(16,36) months ICM: 27(16,37) months

References

1. Zipes DP, Camm AJ, Borggrefe M, et al. ACC/AHA/ESC 2006 guidelines for management of patients with ventricular arrhythmias and the prevention of sudden cardiac death--executive summary: A report of the American College of Cardiology/American Heart Association Task Force and the European Society of Cardiology Committee for Practice Guidelines (Writing Committee to Develop Guidelines for Management of Patients with Ventricular Arrhythmias and the Prevention of Sudden Cardiac Death) Developed in collaboration with the European Heart Rhythm Association and the Heart Rhythm Society. European heart journal 2006;27:2099-140.
2. Aliot EM, Stevenson WG, Almendral-Garrote JM, et al. EHRA/HRS Expert Consensus on Catheter Ablation of Ventricular Arrhythmias: developed in a partnership with the European Heart Rhythm Association (EHRA), a Registered Branch of the European Society of Cardiology (ESC), and the Heart Rhythm Society (HRS); in collaboration with the American College of Cardiology (ACC) and the American Heart Association (AHA). Heart rhythm : the official journal of the Heart Rhythm Society 2009;6:886-933.
3. Ellison KE, Friedman PL, Ganz LI, Stevenson WG. Entrainment mapping and radiofrequency catheter ablation of ventricular tachycardia in right ventricular dysplasia. Journal of the American College of Cardiology 1998;32:724-8.
4. de Bakker JM, van Capelle FJ, Janse MJ, et al. Slow conduction in the infarcted human heart. 'Zigzag' course of activation. Circulation 1993;88:915-26.
5. Sosa E, Scanavacca M, d'Avila A, Pilleggi F. A new technique to perform epicardial mapping in the electrophysiology laboratory. Journal of cardiovascular electrophysiology 1996;7:531-6.
6. de Bakker JM, van Capelle FJ, Janse MJ, et al. Reentry as a cause of ventricular tachycardia in patients with chronic ischemic heart disease: electrophysiologic and anatomic correlation. Circulation 1988;77:589-606.
7. Chen PS, Chen LS, Cao JM, Sharifi B, Karagueuzian HS, Fishbein MC. Sympathetic nerve sprouting, electrical remodeling and the mechanisms of sudden cardiac death. Cardiovascular research 2001;50:409-16.
8. Cao JM, Fishbein MC, Han JB, et al. Relationship between regional cardiac hyperinnervation and ventricular arrhythmia. Circulation 2000;101:1960-9.
9. Sacher F, Tedrow UB, Field ME, et al. Ventricular tachycardia ablation: evolution of patients and procedures over 8 years. Circulation Arrhythmia and electrophysiology 2008;1:153-61.
10. Nademanee K, Taylor R, Bailey WE, Rieders DE, Kosar EM. Treating electrical storm : sympathetic blockade versus advanced cardiac life support-guided therapy. Circulation 2000;102:742-7.
11. Wiener I, Mindich B, Pitchon R. Determinants of ventricular tachycardia in patients with ventricular aneurysms: results of intraoperative epicardial and endocardial mapping. Circulation 1982;65:856-61.
12. Miller JM, Tyson GS, Hargrove WC, 3rd, Vassallo JA, Rosenthal ME, Josephson ME. Effect of subendocardial resection on sinus rhythm endocardial electrogram abnormalities. Circulation 1995;91:2385-91.

13. Harada T, Stevenson WG, Kocovic DZ, Friedman PL. Catheter ablation of ventricular tachycardia after myocardial infarction: relation of endocardial sinus rhythm late potentials to the reentry circuit. Journal of the American College of Cardiology 1997;30:1015-23.
14. Arenal A, Glez-Torrecilla E, Ortiz M, et al. Ablation of electrograms with an isolated, delayed component as treatment of unmappable monomorphic ventricular tachycardias in patients with structural heart disease. Journal of the American College of Cardiology 2003;41:81-92.
15. Piers SRD, Tao Q, van Huls van Taxis CFB, Schalij MJ, van der Geest RJ, Zeppenfeld K. Contrast-Enhanced MRI-Derived Scar Patterns and Associated Ventricular Tachycardias in Nonischemic Cardiomyopathy: Implications for the Ablation Strategy. Circulation Arrhythmia and electrophysiology 2013.
16. Cano O, Hutchinson M, Lin D, et al. Electroanatomic substrate and ablation outcome for suspected epicardial ventricular tachycardia in left ventricular nonischemic cardiomyopathy. Journal of the American College of Cardiology 2009;54:799-808.
17. Piers SR, van Huls van Taxis CF, Tao Q, et al. Epicardial substrate mapping for ventricular tachycardia ablation in patients with non-ischaemic cardiomyopathy: a new algorithm to differentiate between scar and viable myocardium developed by simultaneous integration of computed tomography and contrast-enhanced magnetic resonance imaging. European heart journal 2013;34:586-96.
18. Callans DJ, Ren JF, Michele J, Marchlinski FE, Dillon SM. Electroanatomic left ventricular mapping in the porcine model of healed anterior myocardial infarction. Correlation with intracardiac echocardiography and pathological analysis. Circulation 1999;100:1744-50.
19. Gardner PI, Ursell PC, Fenoglio JJ, Jr., Wit AL. Electrophysiologic and anatomic basis for fractionated electrograms recorded from healed myocardial infarcts. Circulation 1985;72:596-611.
20. Jais P, Maury P, Khairy P, et al. Elimination of local abnormal ventricular activities: a new end point for substrate modification in patients with scar-related ventricular tachycardia. Circulation 2012;125:2184-96.
21. Nogami A, Sugiyasu A, Tada H, et al. Changes in the isolated delayed component as an endpoint of catheter ablation in arrhythmogenic right ventricular cardiomyopathy: predictor for long-term success. Journal of cardiovascular electrophysiology 2008;19:681-8.
22. Vergara P, Trevisi N, Ricco A, et al. Late potentials abolition as an additional technique for reduction of arrhythmia recurrence in scar related ventricular tachycardia ablation. Journal of cardiovascular electrophysiology 2012;23:621-7.
23. Kim RJ, Wu E, Rafael A, et al. The use of contrast-enhanced magnetic resonance imaging to identify reversible myocardial dysfunction. The New England journal of medicine 2000;343:1445-53.
24. Wijnmaalen AP, van der Geest RJ, van Huls van Taxis CF, et al. Head-to-head comparison of contrast-enhanced magnetic resonance imaging and electroanatomical voltage mapping to assess post-infarct scar characteristics in patients with ventricular tachycardias: real-time image integration and reversed registration. European heart journal 2011;32:104-14.

25. Ranjan R, McGann CJ, Jeong EK, et al. Wideband late gadolinium enhanced magnetic resonance imaging for imaging myocardial scar without image artefacts induced by implantable cardioverter-defibrillator: a feasibility study at 3 T. Europace : European pacing, arrhythmias, and cardiac electrophysiology : journal of the working groups on cardiac pacing, arrhythmias, and cardiac cellular electrophysiology of the European Society of Cardiology 2014.
26. Desjardins B, Crawford T, Good E, et al. Infarct architecture and characteristics on delayed enhanced magnetic resonance imaging and electroanatomic mapping in patients with postinfarction ventricular arrhythmia. Heart rhythm : the official journal of the Heart Rhythm Society 2009;6:644-51.
27. Andreu D, Ortiz-Perez JT, Boussy T, et al. Usefulness of contrast-enhanced cardiac magnetic resonance in identifying the ventricular arrhythmia substrate and the approach needed for ablation. European heart journal 2014;35:1316-26.
28. Komatsu Y, Cochet H, Jadidi A, et al. Regional myocardial wall thinning at multidetector computed tomography correlates to arrhythmogenic substrate in postinfarction ventricular tachycardia: assessment of structural and electrical substrate. Circulation Arrhythmia and electrophysiology 2013;6:342-50.
29. Tian J, Jeudy J, Smith MF, et al. Three-dimensional contrast-enhanced multidetector CT for anatomic, dynamic, and perfusion characterization of abnormal myocardium to guide ventricular tachycardia ablations. Circulation Arrhythmia and electrophysiology 2010;3:496-504.
30. Komatsu Y, Sacher F, Cochet H, Jais P. Multimodality imaging to improve the safety and efficacy of epicardial ablation of scar-related ventricular tachycardia. Journal of cardiovascular electrophysiology 2013;24:1426-7.
31. Bala R, Ren JF, Hutchinson MD, et al. Assessing epicardial substrate using intracardiac echocardiography during VT ablation. Circulation Arrhythmia and electrophysiology 2011;4:667-73.
32. Bunch TJ, Weiss JP, Crandall BG, et al. Image integration using intracardiac ultrasound and 3D reconstruction for scar mapping and ablation of ventricular tachycardia. Journal of cardiovascular electrophysiology 2010;21:678-84.
33. Yokoyama K, Nakagawa H, Shah DC, et al. Novel contact force sensor incorporated in irrigated radiofrequency ablation catheter predicts lesion size and incidence of steam pop and thrombus. Circulation Arrhythmia and electrophysiology 2008;1:354-62.
34. Bourier F, Fahrig R, Wang P, et al. Accuracy assessment of catheter guidance technology in electrophysiology procedures: a comparison of a new 3D-based fluoroscopy navigation system to current electroanatomic mapping systems. Journal of cardiovascular electrophysiology 2014;25:74-83.
35. Kapa S, Asirvatham SJ. You can't know where you're going until you know where you've been: the clinical relevance of differences in accurate assessment of catheter location with mapping technologies. Journal of cardiovascular electrophysiology 2014;25:84-6.
36. Brunckhorst CB, Stevenson WG, Soejima K, et al. Relationship of slow conduction detected by pace-mapping to ventricular tachycardia re-entry circuit sites after infarction. Journal of the American College of Cardiology 2003;41:802-9.

37. de Chillou C, Groben L, Magnin-Poull I, et al. Localizing the Critical Isthmus of Post-Infarct Ventricular Tachycardia: The Value of Pace Mapping during Sinus Rhythm. Heart rhythm : the official journal of the Heart Rhythm Society 2013.
38. Brunckhorst CB, Delacretaz E, Soejima K, Maisel WH, Friedman PL, Stevenson WG. Identification of the ventricular tachycardia isthmus after infarction by pace mapping. Circulation 2004;110:652-9.
39. Soejima K, Stevenson WG, Maisel WH, Sapp JL, Epstein LM. Electrically unexcitable scar mapping based on pacing threshold for identification of the reentry circuit isthmus: feasibility for guiding ventricular tachycardia ablation. Circulation 2002;106:1678-83.
40. Tung R, Mathuria N, Michowitz Y, et al. Functional pace-mapping responses for identification of targets for catheter ablation of scar-mediated ventricular tachycardia. Circulation Arrhythmia and electrophysiology 2012;5:264-72.
41. Frankel DS, Mountantonakis SE, Zado ES, et al. Noninvasive programmed ventricular stimulation early after ventricular tachycardia ablation to predict risk of late recurrence. Journal of the American College of Cardiology 2012;59:1529-35.
42. Carbucicchio C, Ahmad Raja N, Di Biase L, et al. High-density substrate-guided ventricular tachycardia ablation: role of activation mapping in an attempt to improve procedural effectiveness. Heart rhythm : the official journal of the Heart Rhythm Society 2013;10:1850-8.
43. Stevenson WG, Khan H, Sager P, et al. Identification of reentry circuit sites during catheter mapping and radiofrequency ablation of ventricular tachycardia late after myocardial infarction. Circulation 1993;88:1647-70.
44. Cano O, Hutchinson M, Lin D, et al. Electroanatomic Substrate and Ablation Outcome for Suspected Epicardial Ventricular Tachycardia in Left Ventricular Nonischemic Cardiomyopathy. JAC 2009;54:799-808.
45. Liuba I, Marchlinski FE. The Substrate and Ablation of Ventricular Tachycardia in Patients With Nonischemic Cardiomyopathy. Circulation Journal 2013;77:1957-66.
46. Casella M, Perna F, Dello Russo A, et al. Right ventricular substrate mapping using the Ensite Navx system: Accuracy of high-density voltage map obtained by automatic point acquisition during geometry reconstruction. Heart rhythm : the official journal of the Heart Rhythm Society 2009;6:1598-605.
47. Hutchinson MD, Gerstenfeld EP, Desjardins B, et al. Endocardial unipolar voltage mapping to detect epicardial ventricular tachycardia substrate in patients with nonischemic left ventricular cardiomyopathy. Circulation Arrhythmia and electrophysiology 2011;4:49-55.
48. Haqqani HM, Tschabrunn CM, Tzou WS, et al. Isolated septal substrate for ventricular tachycardia in nonischemic dilated cardiomyopathy: incidence, characterization, and implications. Heart rhythm : the official journal of the Heart Rhythm Society 2011;8:1169-76.
49. Yoshida K, Yokokawa M, Desjardins B, et al. Septal involvement in patients with post-infarction ventricular tachycardia: implications for mapping and radiofrequency ablation. Journal of the American College of Cardiology 2011;58:2491-500.
50. Betensky BP, Kapa S, Desjardins B, et al. Characterization of trans-septal activation during septal pacing: criteria for identification of intramural ventricular

tachycardia substrate in nonischemic cardiomyopathy. Circulation Arrhythmia and electrophysiology 2013;6:1123-30.
51. Polin GM, Haqqani H, Tzou W, et al. Endocardial unipolar voltage mapping to identify epicardial substrate in arrhythmogenic right ventricular cardiomyopathy / dysplasia. HRTHM 2011;8:76-83.
52. Tokuda M, Tedrow UB, Inada K, et al. Direct comparison of adjacent endocardial and epicardial electrograms: implications for substrate mapping. Journal of the American Heart Association 2013;2:e000215.
53. Sacher F, Wright M, Derval N, et al. Endocardial versus epicardial ventricular radiofrequency ablation: utility of in vivo contact force assessment. Circulation Arrhythmia and electrophysiology 2013;6:144-50.
54. Sapp JL, Beeckler C, Pike R, et al. Initial human feasibility of infusion needle catheter ablation for refractory ventricular tachycardia. Circulation 2013;128:2289-95.
55. Koruth JS, Dukkipati S, Miller MA, Neuzil P, d'Avila A, Reddy VY. Bipolar irrigated radiofrequency ablation: a therapeutic option for refractory intramural atrial and ventricular tachycardia circuits. Heart rhythm : the official journal of the Heart Rhythm Society 2012;9:1932-41.
56. Sacher F, Sobieszczyk P, Tedrow U, et al. Transcoronary ethanol ventricular tachycardia ablation in the modern electrophysiology era. Heart rhythm : the official journal of the Heart Rhythm Society 2008;5:62-8.
57. Tokuda M, Sobieszczyk P, Eisenhauer AC, et al. Transcoronary ethanol ablation for recurrent ventricular tachycardia after failed catheter ablation: an update. Circulation Arrhythmia and electrophysiology 2011;4:889-96.
58. Yagishita D, Ajijola OA, Vaseghi M, et al. Electrical homogenization of ventricular scar by application of collagenase: a novel strategy for arrhythmia therapy. Circulation Arrhythmia and electrophysiology 2013;6:776-83.
59. Marchlinski FE, Callans DJ, Gottlieb CD, Zado E. Linear ablation lesions for control of unmappable ventricular tachycardia in patients with ischemic and nonischemic cardiomyopathy. Circulation 2000;101:1288-96.
60. Arruda M, Fahmy T, Armaganijan L, Di Biase L, Patel D, Natale A. Endocardial and epicardial mapping and catheter ablation of post myocardial infarction ventricular tachycardia: A substrate modification approach. Journal of interventional cardiac electrophysiology : an international journal of arrhythmias and pacing 2010;28:137-45.
61. Di Biase L, Santangeli P, Burkhardt DJ, et al. Endo-epicardial homogenization of the scar versus limited substrate ablation for the treatment of electrical storms in patients with ischemic cardiomyopathy. Journal of the American College of Cardiology 2012;60:132-41.
62. Tilz RR, Makimoto H, Lin T, et al. Electrical isolation of a substrate after myocardial infarction: a novel ablation strategy for unmappable ventricular tachycardias--feasibility and clinical outcome. Europace : European pacing, arrhythmias, and cardiac electrophysiology : journal of the working groups on cardiac pacing, arrhythmias, and cardiac cellular electrophysiology of the European Society of Cardiology 2014.

63. Oza S, Wilber DJ. Substrate-based endocardial ablation of postinfarction ventricular tachycardia. Heart rhythm : the official journal of the Heart Rhythm Society 2006;3:607-9.
64. Komatsu Y, Daly M, Sacher F, et al. Endocardial Ablation to Eliminate Epicardial Arrhythmia Substrate in Scar-Related Ventricular Tachycardia. Journal of the American College of Cardiology 2014.
65. Schweikert RA, Saliba WI, Tomassoni G, et al. Percutaneous pericardial instrumentation for endo-epicardial mapping of previously failed ablations. Circulation 2003;108:1329-35.
66. Schmidt B, Chun KR, Baensch D, et al. Catheter ablation for ventricular tachycardia after failed endocardial ablation: epicardial substrate or inappropriate endocardial ablation? Heart rhythm : the official journal of the Heart Rhythm Society 2010;7:1746-52.
67. Mountantonakis SE, Park RE, Frankel DS, et al. Relationship between voltage map "channels" and the location of critical isthmus sites in patients with post-infarction cardiomyopathy and ventricular tachycardia. Journal of the American College of Cardiology 2013;61:2088-95.
68. Valles E, Bazan V, Marchlinski FE. ECG criteria to identify epicardial ventricular tachycardia in nonischemic cardiomyopathy. Circulation Arrhythmia and electrophysiology 2010;3:63-71.
69. Piers SR, Silva Mde R, Kapel GF, Trines SA, Schalij MJ, Zeppenfeld K. Endocardial or epicardial ventricular tachycardia in nonischemic cardiomyopathy? The role of 12-lead ECG criteria in clinical practice. Heart rhythm : the official journal of the Heart Rhythm Society 2014;11:1031-9.
70. Tschabrunn CM, Haqqani HM, Cooper JM, et al. Percutaneous epicardial ventricular tachycardia ablation after noncoronary cardiac surgery or pericarditis. Heart rhythm : the official journal of the Heart Rhythm Society 2013;10:165-9.
71. Soejima K, Couper G, Cooper JM, Sapp JL, Epstein LM, Stevenson WG. Subxiphoid surgical approach for epicardial catheter-based mapping and ablation in patients with prior cardiac surgery or difficult pericardial access. Circulation 2004;110:1197-201.
72. D'Avila A, Thiagalingam A, Ruskin JN, Reddy VY. Combined ventricular endocardial and epicardial substrate mapping using a sonomicrometry-based electroanatomical mapping system. Pacing and clinical electrophysiology : PACE 2007;30:781-6.
73. Lachman N, Syed FF, Habib A, et al. Correlative anatomy for the electrophysiologist, Part I: the pericardial space, oblique sinus, transverse sinus. Journal of cardiovascular electrophysiology 2010;21:1421-6.
74. Stavrakis S, Jackman WM, Nakagawa H, et al. Risk of coronary artery injury with radiofrequency ablation and cryoablation of epicardial posteroseptal accessory pathways within the coronary venous system. Circulation Arrhythmia and electrophysiology 2014;7:113-9.
75. Roberts-Thomson KC, Steven D, Seiler J, et al. Coronary artery injury due to catheter ablation in adults: presentations and outcomes. Circulation 2009;120:1465-73.

76. Buch E, Vaseghi M, Cesario DA, Shivkumar K. A novel method for preventing phrenic nerve injury during catheter ablation. Heart rhythm : the official journal of the Heart Rhythm Society 2007;4:95-8.
77. Fan R, Cano O, Ho SY, et al. Characterization of the phrenic nerve course within the epicardial substrate of patients with nonischemic cardiomyopathy and ventricular tachycardia. Heart rhythm : the official journal of the Heart Rhythm Society 2009;6:59-64.
78. d'Avila A, Neuzil P, Thiagalingam A, et al. Experimental efficacy of pericardial instillation of anti-inflammatory agents during percutaneous epicardial catheter ablation to prevent postprocedure pericarditis. Journal of cardiovascular electrophysiology 2007;18:1178-83.
79. Bala R, Dhruvakumar S, Latif SA, Marchlinski FE. New endpoint for ablation of ventricular tachycardia: change in QRS morphology with pacing at protected isthmus as index of isthmus block. Journal of cardiovascular electrophysiology 2010;21:320-4.
80. de Chillou C, Groben L, Magnin-Poull I, et al. Localizing the critical isthmus of postinfarct ventricular tachycardia: the value of pace-mapping during sinus rhythm. Heart rhythm : the official journal of the Heart Rhythm Society 2014;11:175-81.
81. Piers SR, Leong DP, van Huls van Taxis CF, et al. Outcome of ventricular tachycardia ablation in patients with nonischemic cardiomyopathy: the impact of noninducibility. Circulation Arrhythmia and electrophysiology 2013;6:513-21.
82. Della Bella P, Baratto F, Tsiachris D, et al. Management of ventricular tachycardia in the setting of a dedicated unit for the treatment of complex ventricular arrhythmias: long-term outcome after ablation. Circulation 2013;127:1359-68.
83. Stevenson WG, Tedrow UB. Ablation for ventricular tachycardia during stable sinus rhythm. Circulation 2012;125:2175-7.
84. Tanner H, Hindricks G, Volkmer M, et al. Catheter ablation of recurrent scar-related ventricular tachycardia using electroanatomical mapping and irrigated ablation technology: results of the prospective multicenter Euro-VT-study. Journal of cardiovascular electrophysiology 2010;21:47-53.
85. Dinov B, Fiedler L, Schonbauer R, et al. Outcomes in Catheter Ablation of Ventricular Tachycardia in Dilated Non-Ischemic Cardiomyopathy in Comparison to Ischemic Cardiomyopathy: Results from the Prospective HEart Centre of LeiPzig VT (HELP - VT) Study. Circulation 2013.
86. Tokuda M, Kojodjojo P, Tung S, et al. Acute failure of catheter ablation for ventricular tachycardia due to structural heart disease: causes and significance. Journal of the American Heart Association 2013;2:e000072.
87. Silberbauer J, Oloriz T, Maccabelli G, et al. Non-Inducibility and Late Potential Abolition: A Novel Combined Prognostic Procedural Endpoint for Catheter Ablation of Post-infarction Ventricular Tachycardia. Circulation Arrhythmia and electrophysiology 2014.

II. OBJECTIVES

The aim of this thesis was to further understand the substrate of scar-related VT by the use of imaging (the structural substrate) and high-density mapping (the functional-electrical substrate).

1. The **first part (chapter III)** deals with the **structural-functional relationship** between scar on imaging and substrate mapping for different disease subtypes: First, in a combined animal and human study, a comparison was made between multipolar and conventional mapping using ablation catheters to analyze the impact on substrate mapping in ICM. Specifically, we analyzed point density, amount of channels and LAVA and the sensitivity for far field vs. near field. We also took advantage of high density mapping with the Carto system to try to better understand disease progression in NICM and ARVC patients, using a retrospective multicentre analysis. We then evaluated a specific subset of myocarditis patients with subepicardial only scar where we compared automatic far field mapping by the EAM systems with manual near field LAVA mapping. Finally, the LV scar and arrhythmogenicity of ARVC with biventricular involvement was analyzed by comparing imaging and EP characteristics.

2. The **second part (chapter IV)** discusses the access, mapping and pitfalls of **epicardial mapping** and ablation. The use of epicardial mapping is of value for diagnostic reasons in ARVC, while ablation is performed from the endocardium, can help to complete LAVA elimination in ICM. Furthemore, this is often the only target

for myocarditis patients. Firstly, a review article that describes the epicardial anterior percutaneous puncture technique has been included. Secondly, a case series of patients with only epicardial mapping and ablation was analyzed. The aim of the study was to determine the feasibility and short-term efficacy of such an approach. Finally, a study analyzing the efficacy of detailed segmentation of epicardial anatomical structures as the left phrenic nerve to improve the safety of epicardial mapping and ablation was undertaken.

3. The **third part (chapter V)** focuses on ablation targets and methods for treatment of ventricular arrhythmia. Firstly, a review article on the Bordeaux **LAVA approach** has been included. The three remaining studies focused on **intramural and septal scar** mapping and ablation: One of the studies focuses on animal work comparing irrigated needle lesions and conventional lesions by the use of EAM mapping, high density MRI imaging and histology. Another study is a unique case of sequentional MRI imaging in a patient with recurrent VT in whom bipolar septal ablation was used to ablate an intramural arrhythmogenic focus. Finally, a case report focuses on a patient-tailored approach for intramural ablation.

4. The **last part (chapter VI)** covers the **future perspectives** of VT and VF ablation. We describe the limitations and pitfalls of current strategies and possible improvements and new technologies.

III. Functional - structural relationship of scar in different disease subtypes.

In part I, the structural substrate on imaging and the functional substrate using electro-anatomical mapping is seperately discussed in sections D and E.

In this part, their mutual relationship which will be called "functional-structural relationship" is investigated, for different disease types of scar-related VT: in ischaemic cardiomyopathy (ICM), in non-ischaemic cardiomyopathy (NICM), in myocarditis and finally in arrythmogenic right ventricular cardiomyopathy (ARVC). Examples of this relationship are illustrated in Figure 1.

Figure 1. Structural-functional relationship in ICM, NICM and ARVC.

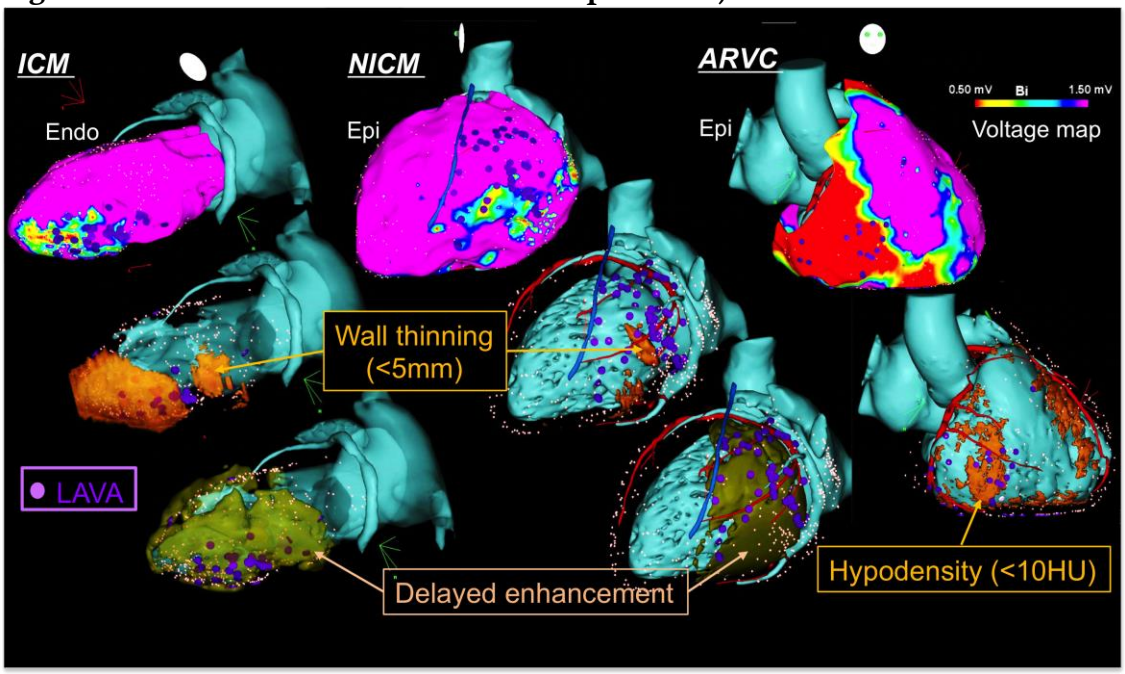

From left to right and top to bottom. Top: EAM bipolar voltage substrate maps created with CARTO3 (Biosense Webster) with low voltage threshold as <1.5mV. Middle: Secondary wall thinning <5mm on MDCT in orange. Bottom: Delayed-enhancement on MRI in brown. LAVA tags in purple and ablation tags in red. Good topical correlation between low voltage, LAVA, wall thinning and scar for all disease subtypes. All 3D-meshes created using the MUSIC platform.

A. *In ICM:* Impact of electrode type on mapping of scar-related VT.

Accepted for publication in JCE in july 2015.

1. Study outline

The majority of patients referred for ablation of scar-related VT have underlying ischaemic cardiomyopathy.[9] Substrate mapping widened the scope of VT ablation since it can be used in unstable and/or non-inducible patients. This approach is however limited by the accuracy and density of the map. In clinical practice, the majority of substrate maps are created with bipolar ablation catheters, which have a larger tip electrode to optimise radiofrequency (RF) efficacy. Most data in literature are analyzed using ablation catheters. A substrate map is made using a point-by-point approach (with or without fast anatomical mapping) and a common fill threshold of <15mm is used for ventricular mapping.

In recent years, a number of different multipolar mapping catheters have been developed (e.g. PentaRay, Biosense Webster and Orion, Boston Scientific). The aim of this study was to investigate the impact of electrode type on mapping of scar-related VT. This was investigated in both animals and humans in a prospective single center comparison of maps created using a multipolar PentaRay catheter (PR mapping) vs. a conventional 3.5mm irrigated Thermocool SF ablation catheter (NAV mapping). We hypothesized that PR mapping would have superior performance in terms of identification of scar and local abnormal ventricular activity (LAVA), due to smaller electrodes and interelectrode distance.

We included 4 sheep and 9 patients with ischaemic cardiomyopathy and mapped using PR and NAV mapping in a random order. A higher point density was found using PR mapping. An electro-anatomical mapping system was used in all (CARTO3, Biosense Webster) and helped to define point pairs as a PR and NAV point found within a 3D-distance of ≤3mm with magnetic accuracy. PR mapping was more sensitive for near field and less sensitive for far field compared to NAV mapping (LAVA amplitude was higher and far field ventricular activity had a lower amplitude). The bipolar scar area was larger using PR mapping. More LAVA and channels were found using PR mapping. An increase of only 2mm interelectrode distance resulted in a significantly higher peak-to-peak voltage recorded at that site.

2. Implications

This study promotes the use of multipolar catheters with small electrode size and interelectrode distance for accurate substrate mapping of scar-related VT for multiple reasons: more LAVA detection and better endpoint definition of complete elimination and a significantly higher point density, still the main limitation of substrate mapping. We hypothesize that the commonly used thresholds for substrate mapping are not suitable (too high) for multipolar mapping and should be reevaluated using DE-MRI scar as gold standard. This is an ungoing work as explained in the last chapter.

3. Manuscript

Impact of electrode type on mapping of scar-related VT.

Authors list: B Berte, MD; J Relan, PhD; F Sacher, MD, PhD; X Pillois, MD, PhD; A Appetiti, S Yamashita, MD, PhD; S Mahida, MD, PhD; F Casassus, MD; D Hooks, MD, PhD; J-M Sellal, MD; S Amraoui, MD; A Denis, MD; N Derval, MD; H Cochet, MD, PhD; M Hocini, MD; M Haïssaguerre, MD, PhD; R Weerasooriya, MD, PhD; P Jaïs, MD, PhD.

Affiliation: Hôpital Cardiologique du Haut-L'évêque, Université de Bordeaux, LIRYC Institute: IHU LIRYC ANR-10-IAHU-04 and Equipex MUSIC ANR-11-EQPX-0030 Bordeaux, France

Running title: Berte *et al.* Mapping of scar-related VT.

Manuscript word count: 3996 words.

Equipex MUSIC ANR-11-EQPX-0030
IHU LIRYC ANR-10-IAHU-04

Conflicts of interest: Dr Berte received an educational EHRA Grant. Drs Jaïs, Haïssaguerre, Hocini, and Sacher have received lecture fees from Biosense Webster and St. Jude Medical. The other authors report no conflicts.

Corresponding author:
Pierre Jaïs, MD
Hôpital Cardiologique du Haut-Lévêque, 33604 Bordeaux-Pessac, France.
Tel: +33 5 57 65 64 71
Fax: +33 5 57 65 65 09
E-mail: pierre.jais@chu-bordeaux.fr

Impact of Electrode Type on Mapping of Scar-Related VT.

Authors list: B Berte, J Relan, F Sacher, X Pillois, A Appetiti, S Yamashita, S Mahida, F Casassus, D Hooks, J-M Sellal, S Amraoui, A Denis, N Derval, H Cochet, M Hocini, M Haïssaguerre, R Weerasooriya, P Jaïs.

Abstract

Background
Substrate-based VT ablation is mostly based on maps acquired with ablation catheters. We hypothesized that multipolar mapping catheters are more effective for identification of scar and local abnormal ventricular activity (LAVA).

Methods and results
Phase1: In a sheep infarction model (two months post-infarction), substrate mapping and LAVA tagging (CARTO®3) was performed, using a Navistar (NAV) vs. a PentaRay (PR) catheter (Biosense Webster). Phase2: Consecutive VT ablation patients from a single center underwent NAV vs. PR mapping. Point pairs were defined as a PR and a NAV point located within a 3D-distance of ≤3mm. Agreement was defined as both points in a pair being manually tagged as normal or LAVA.
Four sheep (4 years, 50±4.8kg) and 9 patients were included (53±14 years, 8 male, 6 ischaemic cardiomyopathy). Mapping density was higher within the scar with PR vs. NAV (3.2 vs. 0.7points/cm^2, p=0.001) with larger bipolar scar area (68±55cm^2 vs. 58±48cm^2, p=0.001). In total, 818 point pairs were analyzed. Using PR, far-field voltages were smaller (PR vs. NAV; bipolar: 1.43±1.84mV vs. 1.64±2.04mV, p=0.001; unipolar; 4.28±3.02mV vs. 4.59±3.67mV, p<0.001). More LAVA were also detected with PR (PR vs. NAV; 126±113 vs. 36±29, p=0.001). When agreement on LAVA was reached (overall: 72%; both LAVA, 40%; both normal, 82%) higher LAVA voltages were recorded on PR (0.48±0.33mV vs. 0.31±0.21mV, p=0.0001).

Conclusion
Multipolar mapping catheters with small electrodes provide more accurate and higher density maps, with a higher sensitivity to near field signals. Agreement between PR and NAV is low.

Word count: 244

Keywords: substrate mapping - VT - multipolar mapping - LAVA - bipolar mapping

Introduction

Substrate-based ablation of ventricular tachycardia (VT) in sinus rhythm is an effective ablation strategy for patients with either non-inducible or hemodynamically poorly tolerated VT.[1, 2] This approach has rendered a greater number of patients amenable to VT ablation.[1, 2] The identification of scar, and hence the arrhythmogenic substrate may be based on bipolar or unipolar voltage mapping, with specific voltage cut-offs used to define normal tissue, scar, and scar border zone.[3, 4] In addition to delineating scar, substrate-based ablation is critically dependent on the identification of local abnormal ventricular activity (LAVA). LAVA signals areas harbouring bundles of surviving tissue inside the scar and at the border zone and present as electrically poorly coupled, low voltage, sharp and fragmented signals.[5-9]

High-density mapping is of critical value for accurate scar visualisation as well as for identification of ablation targets such as LAVA.[10,11] Creation of maps for substrate-based ablation is currently predominantly performed using ablation catheters with bipolar recording from the distal ablation electrode of a typical size of 3.5-4mm tip length, placed at an end-to-end distance of 1 to 2.5mm from the proximal ablation electrode which has a size of 1.3 to 2mm tip length. In addition, contact plays a role in the measured voltage as insufficient catheter contact can artificially produce a low voltage area. It has been demonstrated that type of access, the use of steerable sheaths, and contact force catheters, can help to improve catheter contact.[12] Ablation catheters are designed with a large tip electrode to improve ablation efficacy.[12] However a larger tip electrode may compromise mapping accuracy.

Multipolar catheters with smaller electrodes and shorter interelectrode distances potentially represent more effective tools for high-density mapping for substrate-based ablation. In the present study, we sought to define the efficacy of multipolar mapping catheters by comparing maps obtained with quadripolar ablation catheters to those obtained in the same patients with multipolar small electrode mapping catheters.

Methods

This study is a single centre prospective study conducted at the IHU (Institut Hospitalo-Universitaire) - LIRYC institute (l'Institut de Rythmologie et Modélisation Cardiaque) and CHU (Centre Hopitalier Universitaire) Bordeaux, France.

Mapping in a sheep infarct model

The experimental protocols were conducted in compliance with the Guiding Principles in the Use and Care of Animals published by the National institutes of Health (NIH Publication No. 85-23, Revised 1996). Seven female sheep (age 5 years, 50±4.8 kg) were sedated with an intramuscular injection of 20 mg/kg ketamine hydrochloride and anaesthetized with sodium pentobarbital (10 mg/kg). Slow intravenous infusion of saline maintained hydration throughout the procedure, and anesthesia was maintained using continuous intravenous infusion of ketamine (500 mg/hour) and pentobarbital (150 mg/hour). The trachea was intubated for connection to a respirator (Siemens Servo B, Berlin, Germany). Sheep were then ventilated using room air supplemented with oxygen. An intravenous access was placed in the internal jugular vein for infusion of drugs and fluids. Arterial blood gases were monitored periodically (Radiometer, Copenhagen, Denmark), and ventilatory parameters were adjusted to maintain blood gases within physiological ranges. An ovine myocardial infarction (MI) model was

created by an experienced invasive cardiologist (FC) using selected ethanol injection (1-2cc) in a distal branch of the left anterior descendent artery (LAD).

Two months post-infarct, surviving sheep underwent an identical sedation, analgesia, intubation and ventilation protocol for mapping of the scar using a three-dimensional mapping system (CARTO®3, Biosense Webster). A diagnostic RV catheter (quadripolar catheter, Boston Scientific®) was placed via the femoral vein. The left ventricle (LV) was accessed via a retrograde aortic approach, and a short 7 or 8 Fr sheath was placed in the femoral artery. The default filter settings of CARTO®3 were used for recording of unipolar signals with a high pass filter of 2Hz and a low pass filter of 240Hz. For bipolar signals, a high pass filter of 16Hz and a low pass filter of 500Hz was used.

Separate substrate endocardial maps were created using a conventional 3.5mm ablation catheter (Navi-Star®, Biosense Webster) and a multipolar mapping catheter (PentaRay®, Biosense Webster) in random order creating separate maps. PentaRay (PR) is an irrigated catheter with 5 splines with a total of 20 electrodes, with an electrode size of 1mm. The PentaRay catheter with a 2-6-2 mm spacing was used for the purposes of this study because of the shorter interelectrode distance (2 mm) when used in bipolar mode.

Mapping in humans

Consecutive patients referred for VT ablation were included. Endocardial and/or epicardial substrate maps were made in random order using a standard bipolar 3.5mm catheter (NAV) and a multipolar catheter (PR) using a filling threshold <15. Fill threshold is a parameter on the CARTO system indicating the maximal extrapolation allowed between 2 mapping points. This is a visual method to evaluate mapping density:

by adjusting the fill thresholds one can observe a fully coloured map without grey areas, meaning the fill threshold is below this setting. A fill threshold <15 is commonly used.[25] Antiarrhythmic drugs (AADs) were discontinued 5 half lives before the procedure except for amiodarone. All anticoagulants including warfarin were stopped, if possible, before the procedure with a target INR <2. A LabSystem™ PRO EP Recording System (Boston Scientific) or Sensis (Siemens) was used for signal recording and analysis, a MicroPace system (Boston Scientific) for pacing and a Stockert generator (Biosense Webster) for ablation. Two venous sheaths (one 6 French for the CS catheter and one 7 French sheath for the mapping and ablation catheter) were placed in the groin: one for a CS or RV catheter (quadripolar/decapolar catheter, Boston Scientific®) and one for mapping and ablation (Navi-star® or PentaRay Nav®, Biosense Webster). A 4 or 7 French arterial sheath was used to monitor arterial pressure and for retrograde access for mapping and or ablation.

Access to the pericardial space was gained using a percutaneous anterior subxyphoidal approach and a steerable sheath (small curve or epicardial Agilis™, 8.5 F, St Jude Medical) was placed in the pericardial space. Fast Anatomical Mapping (FAM) was performed with the electro-anatomical mapping (EAM) system (CARTO®3, Biosense Webster) and LAVA points were annotated. Peak-to-peak endocardial and epicardial bipolar voltages were automatically annotated by the EAM system. When a transseptal approach was performed, a steerable sheath (large curve Agilis™, 8.5F, St Jude Medical) was used and an ACT level of >300sec was targeted. The sheath was continuously flushed with heparinized saline.

Analysis of mapping data

A limited mapping time of 30 minutes was used for both PR and NAV mapping. This time was calculated from the moment the mapping catheter entered the left ventricle or pericardial space. If both endocardial and epicardial maps were made, a limited mapping time of 60 minutes was used (30 minutes for each map and method). Mapping was stopped earlier if the patient was hemodynamically unstable or when multiple iatrogenic ventricular ectopics hindered adequate mapping during sinus rhythm. In case of incomplete maps, no further analysis was performed on those maps.

During both phases, mapping density was analyzed using two different methods: First, fill threshold <15 was set to analyse overall density and then it was lowered to <5 to analyse the mapping density in the scar and borderzone region. Secondly, we analyzed all mapping points inside the low voltage area to detect the number of points/cm^2 using the ParaView software (Parallel Vizualization Application, an open-source multi-platform application).

Furthermore, we analyzed the number and the bipolar voltage of local abnormal ventricular activity (LAVA, defined as near field) and the number of conducting voltage channels. Conducting voltage channels were defined as conducting corridors of voltage differences detected by scanning at different voltage thresholds inside the scar area (0.2mV-0.3mV-0.4mV-0.5mV bipolar voltage) of the low voltage tissue (<1.5mV bipolar voltage), with at least one LAVA inside this corridor.

Finally, for further analysis and mapping comparison, raw data from each study were exported and analysed using the ParaView software. All points -sorted by mapping strategy- were projected (NAV on PR points and vice versa) towards the concordant

point with the nearest three-dimensional distance and these points underwent paired analysis.

Paired analysis for each point pair of the bipolar and unipolar amplitude (in mV) of EGM's was performed by comparing mapping points with a maximal three-dimensional distance between point pairs of ≤3mm. The overall peak-to-peak automatically measured bipolar and unipolar voltage was measured for all these point pairs. In addition, analysis was performed for each predefined region on voltage maps: normal voltage (bipolar voltage >1.5mV for the endocardium and >1mV for the epicardium), low voltage (0.5 to 1.5mV for the endocardium and 0.5 to 1mV for the epicardium) and dense scar (<0.5mV).

Agreement between these point pairs was defined by the presence of similar signals as demonstrated by identical manual annotation (normal ventricular signal or LAVA) using PR and NAV. A ventricular signal was annotated as LAVA when presented as electrically poorly coupled, low voltage, sharp and fragmented signals and was annotated as normal if a normal voltage with typical EGM morphology was found. Normal activity was defined as HANA (high amplitude normal ventricular activity).[5-9] A LAVA signal was considered as near field and a HANA signal was considered as far field. Agreement on normal EGM was defined as a detection of a normal EGM using PR and NAV. Agreement on LAVA was defined as a LAVA EGM signal detected by of both catheters. Sensitivity and specificity of the NAV were calculated, using PR as a comparator. If an agreement on LAVA was observed between PR and NAV mapping, the LAVA voltage of these point pairs was manually measured to investigate the ability of both type of catheters to record near field signals.

All automatic bipolar substrate maps made with both NAV and PR were analyzed and manually adapted towards the near field LAVA signal as described recently.[13] The manually adapted maps were then compared using different thresholds (0.5-1.5mV, 0.2-1mV, 0.2-0.8mV, 0.2-0.6mV, 0.2-0.4mV) to visualize scar definition.

In a subanalysis, we investigated other possible factors influencing the EGM recording. Firstly, we measured the effect of larger interelectrode spacing (e.g. conventional bipoles 1-2 vs. larger spaced bipoles 1-3 and 1-4 etc) using PR to detect changes in voltage (far field ventricular voltage) and the ability to detect and locate LAVA (spatial resolution). These bipoles were created after the extraction of the study raw data, the exportation of the selected PentaRay point EGM information and the post-procedural creation of new bipoles using different subtractions of unipolar EGM in Excel (Microsoft). Secondly, we measured the effect of vector orientation using PR by analyzing the EGM signal detected by a conventional bipole along the spline compared to an artificially created perpendicular bipolar across two splines, using the similar method in Excel as described above. These different recordings were made in clear proximity to each other (≤3mm difference).

Ablation in humans

Following the mapping procedure, an induction protocol was performed. In cases where monomorphic VT was inducible and hemodynamically tolerated, ablation was performed during VT at the site of the critical isthmus (based on entrainment maneuvers and timing of the local EGM during tachycardia). LAVA-based ablation approach was performed following termination of VT. In cases in which VT was not

inducible, LAVA ablation was the sole ablation strategy. The LAVA-based ablation approach has previously been described in detail by Jaïs *et al*.[6]

After termination of the ablation procedure, sequential detailed remapping was performed using a PR mapping catheter. We did not remap with the NAV catheter based firstly, on our hypothesis that PR mapping was more sensitive for LAVA detection, and secondly, for practical reasons as it would be too time consuming. Any remaining LAVA identified by PR remapping were ablated to reach the endpoint of complete LAVA elimination and non-inducibility.

Statistical analysis

Continuous variables were expressed as mean ± SD for normally distributed data or median and interquartile range (IQR; 25th–75th percentile) for non-normally distributed data. Categorical data were expressed as counts and percentages. Data were tested for normality by histogram and using the Kolmogorov-Smirnov test. Continuous variables were expressed as mean ± SD and differences between groups were assessed using paired Student t test, or the Wilcoxon signed ranks test when appropriate. All tests with P-values <0.05 were considered statistically significant. Statistical analyses were performed using SPSS Statistics 17.0.

Results

Baseline characteristics.

Phase 1: Myocardial infarction was created in seven female sheep (age 5 years, 50±4.8 kg). Two animals died shortly after the infarction. A further animal died at two months

post-infarct immediately prior to mapping (during induction of anaesthesia). The four surviving animals were included in further analysis. Phase 2: Nine patients with scar-related sustained VT were included (age 53±14 years, 8 male, 6 ischaemic cardiomyopathy). Baseline characteristics are included in Table 1.

Endocardial and epicardial mapping data.

Mapping data are illustrated in Table 2. No epicardial mapping was performed in animals. In humans, 5 patients had incomplete endocardial mapping and 2 patients had no epicardial mapping. As a rule, mapping was interrupted if the patient was hemodynamically unstable or when multiple iatrogenic ventricular ectopics hindered adequate mapping during sinus rhythm as it may happen when the PentaRay catheter is used endocardially. In addition, in patients with NICM, when the substrate was epicardial as demonstrated by imaging, endocardial mapping wasn't systematically considered.

Mapping density.

All values are written as total (mean ± SD / per subject). A total of 8702 (1088±839) endocardial and 11282 (1612±789) epicardial mapping points were recorded using PR. With the NAV catheter 1578 (197±86) endocardial and 1699 (243±48) epicardial mapping points were recorded. Data are shown separately for animals and humans in Tables 2 and 3. Fill threshold of substrate maps was set at 15 to ensure a good substrate analysis. However, we could lower the fill threshold to 5 to better define the border zone in 12/13 maps using PR vs. 0/13 for NAV maps. The density inside the scar was significantly higher using PR (PR vs. NAV; 3.16 points/cm^2 vs. 0.70 points/cm^2, p=0.001).

Scar location and scar area.

The overall low voltage area was significantly larger using PR (PR vs. NAV; 68±55cm^2 vs. 58±48cm^2, p=0.001). More specifically, the epicardial low voltage scar area in humans was larger using PR (PR vs. NAV; 95±72cm^2 vs. 78±66cm^2, p=0.018). There was a trend towards a larger endocardial low voltage area in both animals and patients (PR vs. NAV; animals: 37±3.8cm^2 vs. 33±7.5cm^2, p=0.144; patients; 50±16cm^2 vs. 47±16cm^2, p=0.068). Scar data with both catheters are included in Table 2. Examples are illustrated in Figure 1.

Number of LAVA detected in the scar.

In total, more LAVA (mean 126±113 vs. 36±29, p=0.001) were detected using PR vs. NAV mapping (using PR: 1635 LAVA vs. using NAV: 464 LAVA respectively). Results on LAVA detection are presented in Table 2. Two examples of differences in LAVA detection between PR and NAV for 2 point pairs are presented in Figure 2. Two additional examples are illustrated as supplementary material (Supplementary Figures 1 and 2).

Voltage channels detected within scar.

More voltage-based channels were detected using PR (PR vs. NAV; 2.0±1.8 vs. 0.5±0.8, p=0.017). In the animals, 8 channels were found in 2 animals (50% of animals) using PR mapping and all were missed by NAV mapping. In the humans, 18 channels were identified using PR mapping in 7 patients (78%). Twelve of the 18 aforementioned channels (67%) were missed by NAV mapping. NAV mapping detected 6 channels in 4 patients, which were also detected by PR mapping. NAV mapping did not identify any

channels not detected by PR mapping. Data are presented in Table 2. An example is shown in Figure 1A.

Manually adapted bipolar voltage maps were created in all cases. Using the conventional thresholds (0.5-1.5mV) difference between a PR and NAV map is in the scar area size. When we lowered the thresholds in both animals and patients, channels (cf. above), scar heterogeneity and border zone was better defined with PR than NAV. Three examples are given in Figure 3.

Bipolar and unipolar far field and near field EGM voltage.

In total, 818 endocardial and epicardial point pairs (285 point pairs in 4 animals and 533 point pairs in 9 humans: 63±54 point pairs/map) were found with a distance ≤3mm (mean 2.01±0.62mm) between both points. Overall automatic far field voltage measurements were significantly lower using PR in both bipolar and unipolar mode. Overall voltage data for all point pairs are included in Table 3.

When all 818 point pairs were analyzed for each voltage threshold region: normal tissue and low voltage (border zone and dense scar) there was no bipolar voltage difference (PR vs. NAV; bipolar; 3.29±2.07mV vs. 3.11±2.87mV, p=0.294). However unipolar voltage was lower with PR vs. NAV mapping in normal tissue (PR vs. NAV; 6.49±3.51mV vs. 7.25±4.84mV, p=0.003; n=241). In the border zone of the low voltage area, a significantly lower bipolar and a trend towards lower unipolar voltage was observed with PR (PR vs. NAV; bipolar: 0.92±0.29mV vs. 1.46±1.33mV, p<0.001; unipolar: 4.25±2.46mV vs. 4.42±2.54mV, p=0.156; n=263), Similarly, inside dense scar a significantly lower bipolar and a trend towards lower unipolar voltage was observed

(PR vs. NAV; bipolar: 0.25±0.13mV vs. 0.76±0.86mV respectively, p<0.001 and unipolar: 2.05±0.89mV vs. 2.49±0.99mV respectively, p=0.630; n=298). These data indicating less far field sensing associated with PR mapping.

In 54 point pairs (≤3mm) agreement on LAVA was analyzed between PR and NAV mapping. Manual bipolar LAVA voltage measurement was significantly higher for PR vs. NAV mapping (0.48±0.33mV vs. 0.31±0.21mV respectively, p=0.0001) indicating better near field sensitivity for PR mapping.

Agreement of EGM analysis.

There was an overall agreement of 72% between PR and NAV in terms of EGM analysis. More specifically, the agreement on LAVA was only 40% while agreement on normal EGM was 82%. When using PR as the comparitor, NAV had a sensitivity of 49%, specificity of 77%, positive predictive value of 33%, and negative predictive value of 87%. Results on LAVA agreement and catheter performance are included in Table 4.

Subanalysis of changes in interelectrode distance.

In total, 105 conventional PR bipoles were analyzed. Mean automatic peak-to-peak bipolar EGM voltage increased with increasing inter-electrode distance (bipole 1-2 with a distance of 2mm: 1.1±1.5mV, bipole 1-3 with a distance of 9mm: 1.8±2.0mV and bipole 1-4 with a distance of 12mm: 2.1±2.3mV; p:<0.001) demonstrating increased far field effect. An example is illustrated in Figure 4.

Impact of bipole orientation: along the spline vs. across the splines.

In total, 22 points were analyzed. 18 points were labeled as LAVA along the spline of which 9 (50%) were still seen across the spline while 10 were missed (56%). In 3 points, no LAVA activity was found on the conventional bipoles along the spline but appeared on new bipoles across the splines. An example is illustrated in Figure 5.

Complications and follow-up.

No complications occurred. During phase 1, all animals were sacrificed directly after the procedure. During phase 2, inducibility was not tested in one patient because of hemodynamic instability. Non-inducibility was achieved in 44% of patients. Complete LAVA elimination was achieved in 56% of patients. After a mean follow-up of 10±8months, 30% had recurrence of VT. There were no deaths during follow-up. Endpoint and follow-up data are summarized in Table 5.

Discussion

The aim of this study was to analyze the efficacy of multipolar mapping to identify scar and LAVA in scar-related VT. The main findings of this study are as follows: 1) Mapping with the PentaRay results in higher mapping density and better substrate definition, 2) PentaRay mapping is associated with higher detection of LAVA and voltage channels, 3) mapping with PentaRay reduces far field signal and magnifies the near field component (LAVA) and, 4) the bipolar low voltage area is larger with better scar border zone definition.

Higher mapping density

In a recently published study, Anter *et al* demonstrated a better mapping resolution with PR vs. NAV mapping within areas of low atrial voltage.[14] Based on our findings, the use

of a PentaRay catheter is desirable for high-density mapping and hence more accurate definition of the substrate of scar related VT. This observation is likely to apply to the vast majority of substrate based VT ablation approaches previously described. Liuba *et al* and Riley *et al* used a fill threshold of <20 for ventricular mapping in ARVC and NICM.[15, 16] Currently, a fill threshold of <15 is routinely used for ventricular mapping.[17] With PR mapping, we found a point density of <5 in the scar and in the border zone, which clearly increases the accuracy of the border zone. A better definition of the substrate increases the ablation accuracy and can potentially improve outcome.

Better LAVA detection and endpoint definition.

When a LAVA-based approach is used for VT ablation, it is critical to have the highest sensitivity of LAVA detection.[6] Specifically, improved detection of LAVA is of importance not only to identify ablation targets but also for demonstrating accurate end point assessment such as LAVA elimination.[18, 19] This study demonstrates that the Pentaray catheter is superior for LAVA detection when compared to a conventional ablation catheter. The higher LAVA detection rate is attributable not only due to a higher mapping density but also to a higher bipolar LAVA amplitude, both within the scar and in the border zone. Therefore, even in the presence of a comparable mapping density, mapping with an ablation catheter is predicted to miss some of the LAVA signals due to a lower amplitude. Intuitively, more accurate identification of LAVA would be predicted to improve outcome. Prospective studies are required to determine the impact of better LAVA detection on clinical outcome.

The complete LAVA elimination rate was lower than in the original paper of *Jaïs* et al (56% vs. 70% respectively).[6] We hypothesize this is mainly due to a different patient population: The original LAVA paper consists of mainly (80%) ischaemic

cardiomyopathy (ICM) patients as compared to only (44%) in this paper. NICM patients tend to have more VT recurrence and less complete LAVA elimination than ICM after VT ablation. In addition, no conclusion can be drawn on success rate in only 9 patients.

Better channel detection.

The detection of privileged voltage channels in scar has been demonstrated to be associated with abnormal local potentials and slow conduction critical to VT circuits. Hence these channels are important targets for catheter ablation.[20] The demonstration in our study of superior channel detection with multipolar mapping catheters encourages their use for scar-related VT. Based on our observations, these catheters may be of additional value when using the dechanneling or any substrate based approach for VT ablation.[21]

Impact of interelectrode distance.

A subanalysis demonstrated that larger interelectrode distance with identical electrode size increased the far field bipolar voltage and decreased the spatial resolution of the LAVA detection (LAVA signal visible on multiple bipoles). Of note, an increase of only 3 mm of the interelectrode distance demonstrated a significant increase in far field bipolar voltage. These findings indicate that when using multipolar mapping electrodes, increasing the interelectrode distance to more than 2 mm results in degraded mapping capabilities. On the basis of these findings, we decided to use the PentaRay 2-6-2mm catheter rather than the PentaRay 4-4-4mm catheter in our routine practice. The impact of other multipolar catheters as the IntellaMap Orion™ mapping catheter (Rhythmia Medical, Boston Scientific) and mini-size electrode catheters as the IntellaTip MiFi

catheter (Boston Scientific) has to be investigated in further studies, but we hypothesize similar findings.

In addition to the electrode size and interelectrode distance, this study shows that the orientation of the recording bipole has an impact on LAVA detection and suggest that across the spline bipoles could also be systematically used with the caveat that interelectrode distance may vary and is not controlled with this set up.

New bipolar and unipolar thresholds needed for multipolar substrate mapping?

Previously published data on voltage thresholds for substrate mapping have been obtained using ablation catheters with large electrodes.[23-26] Based on the results of the present study, we do believe that a re-evaluation of the standard voltage thresholds is needed for multipolar mapping and that it should be correlated to DE-MRI or pathological analysis. Larger bipolar near field signal amplitudes were recorded using small electrodes. This could be due to different factors such as noise reduction, bipole orientation and the sharpness of the near field signal. On top of this, difference in inter electrode distance can have a substantial influence. In a recent paper, similar findings of higher near field voltage were found using another multipolar mapping catheter with small-spaced digitally-printed micro electrodes, the Orion catheter: ventricular bipolar voltage thresholds of <2mV are suggested for low voltage and <1mV for scar. In this study, the voltage data were correlated to imaging in a canine model.[27]

Limitations

Firstly, this study suffers from the inherent limitations of a single centre study. Secondly, there is currently no gold standard to detect LAVA activity. We made the assumption that PentaRay mapping performs as the current gold standard and therefore it was defined as the comparitor. We have deliberately chosen the PentaRay mapping as the reference and gold standard. This is arbitrary and could be questioned but in absence of validated gold standard this assumption seams reasonable. Thirdly, LAVA analysis was performed manually. Artificial intelligence algorithms would be desirable to ensure standardization and reproducibility. Mathematical algorithms would be desirable to ensure standardization and reproducibility. In addition, contact force is known to impact the recorded signals but no multipolar mapping catheters are capable of contact force measurement. We therefore used non-contact force ablation catheters for this comparison. Fourthly, a HANA signal was considered as a far field signal to facilitate analysis. It is true that in healthy tissue a HANA signal is a combination of near field and far field signals. Inside the scar or borderzone, this becomes more complex. We defined LAVA signals as near field only and HANA as far field only. The purpose of our definition is to identify pathological near field only signals. Finally, follow-up is relatively short, but the focus of this study is diagnostic and not therapeutic. Comparison of therapeutic decisions based on PR vs NAV data could be of further interest and was not investigated in this study.

Conclusion

PentaRay mapping increases map accuracy for EGM characteristics, map density, channel detection, and LAVA detection. Based on these findings, multipolar mapping would be preferable for accurate substrate assessment. The impact on clinical outcome should be investigated in future studies.

References

[1] Aliot EM, Stevenson WG, Almendral-Garrote JM, Bogun F, Calkins CH, Delacretaz E, Bella PD, Hindricks G, Jais P, Josephson ME, Kautzner J, Kay GN, Kuck KH, Lerman BB, Marchlinski F, Reddy V, Schalij MJ, Schilling R, Soejima K, Wilber D, European Heart Rhythm A, European Society of C, Heart Rhythm S: EHRA/HRS Expert Consensus on Catheter Ablation of Ventricular Arrhythmias: developed in a partnership with the European Heart Rhythm Association (EHRA), a Registered Branch of the European Society of Cardiology (ESC), and the Heart Rhythm Society (HRS); in collaboration with the American College of Cardiology (ACC) and the American Heart Association (AHA). Europace : European pacing, arrhythmias, and cardiac electrophysiology : journal of the working groups on cardiac pacing, arrhythmias, and cardiac cellular electrophysiology of the European Society of Cardiology 2009; 11:771-817.

[2] Natale A, Raviele A, Al-Ahmad A, Alfieri O, Aliot E, Almendral J, Breithardt G, Brugada J, Calkins H, Callans D, Cappato R, Camm JA, Della Bella P, Guiraudon GM, Haissaguerre M, Hindricks G, Ho SY, Kuck KH, Marchlinski F, Packer DL, Prystowsky EN, Reddy VY, Ruskin JN, Scanavacca M, Shivkumar K, Soejima K, Stevenson WJ, Themistoclakis S, Verma A, Wilber D, Venice Chart m: Venice Chart International Consensus document on ventricular tachycardia/ventricular fibrillation ablation. Journal of cardiovascular electrophysiology 2010; 21:339-379.

[3] Cano O, Hutchinson M, Lin D, Garcia F, Zado E, Bala R, Riley M, Cooper J, Dixit S, Gerstenfeld E, Callans D, Marchlinski FE: Electroanatomic substrate and ablation outcome for suspected epicardial ventricular tachycardia in left ventricular nonischemic cardiomyopathy. Journal of the American College of Cardiology 2009; 54:799-808.

[4] Piers SR, van Huls van Taxis CF, Tao Q, van der Geest RJ, Askar SF, Siebelink HM, Schalij MJ, Zeppenfeld K: Epicardial substrate mapping for ventricular tachycardia ablation in patients with non-ischaemic cardiomyopathy: a new algorithm to differentiate between scar and viable myocardium developed by simultaneous integration of computed tomography and contrast-enhanced magnetic resonance imaging. European heart journal 2013; 34:586-596.

[5] de Chillou C, Groben L, Magnin-Poull I, Andronache M, MagdiAbbas M, Zhang N, Abdelaal A, Ammar S, Sellal JM, Schwartz J, Brembilla-Perrot B, Aliot E, Marchlinski FE: Localizing the critical isthmus of postinfarct ventricular tachycardia: the value of pace-mapping during sinus rhythm. Heart rhythm : the official journal of the Heart Rhythm Society 2014; 11:175-181.

[6] Jais P, Maury P, Khairy P, Sacher F, Nault I, Komatsu Y, Hocini M, Forclaz A, Jadidi AS, Weerasooryia R, Shah A, Derval N, Cochet H, Knecht S, Miyazaki S, Linton N, Rivard L, Wright M, Wilton SB, Scherr D, Pascale P, Roten L, Pederson M, Bordachar P, Laurent F, Kim SJ, Ritter P, Clementy J, Haissaguerre M: Elimination of local abnormal ventricular activities: a new end point for substrate modification in patients with scar-related ventricular tachycardia. Circulation 2012; 125:2184-2196.

[7] Berruezo A, Fernández-Armenta J, Mont L, Zeljko H, Andreu D, Herczku C, Boussy T, Tolosana JM, Arbelo E, Brugada J: Combined endocardial and epicardial catheter ablation in arrhythmogenic right ventricular dysplasia incorporating scar dechanneling technique. Circulation Arrhythmia and electrophysiology 2012; 5:111-121.

[8] Marchlinski FE, Callans DJ, Gottlieb CD, Zado E: Linear ablation lesions for control of unmappable ventricular tachycardia in patients with ischemic and nonischemic cardiomyopathy. Circulation 2000; 101:1288-1296.

[9] Di Biase L, Santangeli P, Burkhardt DJ, Bai R, Mohanty P, Carbucicchio C, Dello Russo A, Casella M, Mohanty S, Pump A, Hongo R, Beheiry S, Pelargonio G, Santarelli P, Zucchetti M, Horton R, Sanchez JE, Elayi CS, Lakkireddy D, Tondo C, Natale A: Endo-epicardial homogenization of the scar versus limited substrate ablation for the treatment of electrical storms in patients with ischemic cardiomyopathy. Journal of the American College of Cardiology 2012; 60:132-141.
[10] Della Bella P, Bisceglia C, Tung R: Multielectrode contact mapping to assess scar modification in post-myocardial infarction ventricular tachycardia patients. Europace : European pacing, arrhythmias, and cardiac electrophysiology : journal of the working groups on cardiac pacing, arrhythmias, and cardiac cellular electrophysiology of the European Society of Cardiology 2012; 14 Suppl 2:ii7-ii12.
[11] Santangeli P, Frankel DS, Marchlinski FE: End points for ablation of scar-related ventricular tachycardia. Circulation Arrhythmia and electrophysiology 2014; 7:949-960.
[12] Jesel L, Sacher F, Komatsu Y, Daly M, Zellerhoff S, Lim HS, Derval N, Denis A, Ambri W, Ramoul K, Aurillac V, Hocini M, Haissaguerre M, Jais P: Characterization of Contact Force During Endocardial and Epicardial Ventricular Mapping. Circulation Arrhythmia and electrophysiology 2014; 7(6):1168-73.
[13] Berte B, Sacher F, Cochet H, Mahida S, Yamashita S, Lim H, Denis A, Derval N, Hocini M, Haissaguerre M, Jais P: Postmyocarditis ventricular tachycardia in patients with epicardial-only scar: a specific entity requiring a specific approach. Journal of cardiovascular electrophysiology 2015; 26:42-50.
[14] Anter E, Tschabrunn CM, Josephson ME: High-Resolution Mapping of Scar-Related Atrial Arrhythmias Using Smaller Electrodes with Closer Interelectrode Spacing. Circulation Arrhythmia and electrophysiology 2015; CIRCEP.114.002737. [Epub ahead of print]
[15] Liuba I, Frankel DS, Riley MP, Hutchinson MD, Lin D, Garcia FC, Callans DJ, Supple GE, Dixit S, Bala R, Squara F, Zado ES, Marchlinski FE: Scar Progression in Patients with Nonischemic Cardiomyopathy and Ventricular Arrhythmias: Scar progression in NICM. Heart rhythm : the official journal of the Heart Rhythm Society 2014; 11(5):755-62.
[16] Riley MP, Zado E, Bala R, Callans DJ, Cooper J, Dixit S, Garcia F, Gerstenfeld EP, Hutchinson MD, Lin D, Patel V, Verdino R, Marchlinski FE: Lack of uniform progression of endocardial scar in patients with arrhythmogenic right ventricular dysplasia/cardiomyopathy and ventricular tachycardia. Circulation Arrhythmia and electrophysiology 2010; 3:332-338.
[17] Tian J, Jeudy J, Smith MF, Jimenez A, Yin X, Bruce PA, Lei P, Turgeman A, Abbo A, Shekhar R, Saba M, Shorofsky S, Dickfeld T: Three-dimensional contrast-enhanced multidetector CT for anatomic, dynamic, and perfusion characterization of abnormal myocardium to guide ventricular tachycardia ablations. Circulation Arrhythmia and electrophysiology 2010; 3:496-504.
[18] Tung R, Mathuria NS, Nagel R, Mandapati R, Buch EF, Bradfield JS, Vaseghi M, Boyle NG, Shivkumar K: Impact of local ablation on interconnected channels within ventricular scar: mechanistic implications for substrate modification. Circulation Arrhythmia and electrophysiology 2013; 6:1131-1138.
[19] Komatsu Y, Daly M, Sacher F, Cochet H, Denis A, Derval N, Jesel L, Zellerhoff S, Lim HS, Jadidi A, Nault I, Shah A, Roten L, Pascale P, Scherr D, Aurillac-Lavignolle V, Hocini M, Haissaguerre M, Jais P: Endocardial Ablation to Eliminate Epicardial Arrhythmia Substrate in Scar-Related Ventricular Tachycardia. Journal of the American College of Cardiology 2014; 63(14):1416-26.

[20] Arenal A, del Castillo S, Gonzalez-Torrecilla E, Atienza F, Ortiz M, Jimenez J, Puchol A, Garcia J, Almendral J: Tachycardia-related channel in the scar tissue in patients with sustained monomorphic ventricular tachycardias: influence of the voltage scar definition. Circulation 2004; 110:2568-2574.
[21] Berruezo A, Fernandez-Armenta J, Mont L, Zeljko H, Andreu D, Herczku C, Boussy T, Tolosana JM, Arbelo E, Brugada J: Combined endocardial and epicardial catheter ablation in arrhythmogenic right ventricular dysplasia incorporating scar dechanneling technique. Circulation Arrhythmia and electrophysiology 2012; 5:111-121.
[22] Nayyar S, Wilson L, Ganesan AN, Sullivan T, Kuklik P, Chapman D, Brooks AG, Mahajan R, Baumert M, Young GD, Sanders P, Roberts-Thomson KC: High-density mapping of ventricular scar: a comparison of ventricular tachycardia (VT) supporting channels with channels that do not support VT. Circulation Arrhythmia and electrophysiology 2014; 7:90-98.
[23] Desjardins B, Yokokawa M, Good E, Crawford T, Latchamsetty R, Jongnarangsin K, Ghanbari H, Oral H, Pelosi F, Jr., Chugh A, Morady F, Bogun F: Characteristics of Intramural Scar in Patients with Non-Ischemic Cardiomyopathy and Relation to Intramural Ventricular Arrhythmias. Circulation Arrhythmia and electrophysiology 2013; 6(5):891-7.
[24] Haqqani HM, Tschabrunn CM, Tzou WS, Dixit S, Cooper JM, Riley MP, Lin D, Hutchinson MD, Garcia FC, Bala R, Verdino RJ, Callans DJ, Gerstenfeld EP, Zado ES, Marchlinski FE: Isolated septal substrate for ventricular tachycardia in nonischemic dilated cardiomyopathy: incidence, characterization, and implications. Heart rhythm : the official journal of the Heart Rhythm Society 2011; 8:1169-1176.
[25] Hutchinson MD, Gerstenfeld EP, Desjardins B, Bala R, Riley MP, Garcia FC, Dixit S, Lin D, Tzou WS, Cooper JM, Verdino RJ, Callans DJ, Marchlinski FE: Endocardial unipolar voltage mapping to detect epicardial ventricular tachycardia substrate in patients with nonischemic left ventricular cardiomyopathy. Circulation Arrhythmia and electrophysiology 2011; 4:49-55.
[26] Polin GM, Haqqani H, Tzou W, Hutchinson MD, Garcia FC, Callans DJ, Zado ES, Marchlinski FE: Endocardial unipolar voltage mapping to identify epicardial substrate in arrhythmogenic right ventricular cardiomyopathy/dysplasia. Heart rhythm : the official journal of the Heart Rhythm Society 2011; 8:76-83.
[27] Thajudeen A, Jackman WM, Stewart B, Cokic I, Nakagawa H, Shehata M, Amorn AM, Kali A, Liu E, Harlev D, Bennett N, Dharmakumar R, Chugh SS, Wang X: Correlation of scar in cardiac MRI and high-resolution contact mapping of left ventricle in a chronic infarct model. Pacing and clinical electrophysiology : PACE 2015; 38:663-674.

Table 1. Baseline characteristics.

	N°	years	sex	MDCT	DE-MRI	Disease	Scar location	LVEF (%)	ICD	Betablocker	Amio
Animals	1	4	F		1	ICM	Anteroseptal	40	NA	0	0
	2	4	F		1	ICM	Anteroseptal	35	NA	0	0
	3	4	F		1	ICM	Anteroseptal	40	NA	0	0
	4	4	F		1	ICM	Anteroseptal-apical	30	NA	0	0
		4	**all female**		**4 (100%)**			**36±5**			
Patients	1	59	F	1		DCM	Basal anterolateral	35	1	1	0
	2	25	M	1		ICM	Anterior-apical	30	1	1	0
	3	65	M	1		ICM	Anterior-apical	35	1	1	0
	4	58	M	1		ARVC	RV free wall	55	1	0	0
	5	72	M	1		ICM	Inferior	30	1	1	0
	6	55	M	1	1	MYO	Inferolateral	65	0	1	0
	7	39	F	1	1	ICM	Inferior-apical	44	0	1	0
	8	55	M			DCM	Basal anterior	26	1	0	0
	9	51	M	1		DCM	Basal anterior-inferolateral	35	1	1	0
		53±14	**8 male**	**8 (89%)**	**2 (22%)**			**39±13**	**7 (78%)**	**7**	**0**

Abbreviations: LAVA, local abnormal ventricular activity; PR, PentaRay; NAV, Navi-star; Pt, patient; mm, millimetre; cm, centimetre; N°, number; Endo, endocardial; Epi, epicardial; Amio, amiodarone; NA, not applicable.

Table 2. Substrate mapping data.

	N°	Endo map points PR	Endo map points NAV	Epi map points PR	Epi map points NAV	Endo scar area PR (cm^2)	Endo scar area NAV (cm^2)	Epi scar area PR (cm^2)	Epi scar area NAV (cm^2)	Channel PR	Channel NAV	LAVA PR	LAVA NAV
Animals	1	743	135	NA	NA	40	34	NA	NA	0	0	20	8
	2	966	217	NA	NA	35	31	NA	NA	4	0	16	10
	3	1093	145	NA	NA	33	25	NA	NA	4	0	60	3
	4	2943	132	NA	NA	41	43	NA	NA	0	0	89	19
	Total	**5745**	**629**	**NA**	**NA**	**149**	**133**	**NA**	**NA**	**8**	**0**	**185**	**40**
	Mean	**1436±1015**	**157±40**	**NA**	**NA**	**37±3.8**	**33±7.5**	**NA**	**NA**	**4±0**	**0**	**46±35**	**10±7**
Patients	1	NA	NA	3101	254	NA	NA	231	192	1	0	367	81
	2	1148	141	NA	NA	49	46	NA	NA	0	0	111	33
	3	84	312	1565	200	65	64	39	27	2	0	101	13
	4	NA	NA	883	266	NA	NA	97	90	1	1	82	34
	5	519	151	753	242	58	52	79	46	0	0	63	25
	6	NA	NA	1263	205	NA	NA	28	15	4	0	41	20
	7	1206	345	NA	NA	29	25	NA	NA	2	2	177	79
	8	NA	NA	1808	199	NA	NA	47	35	4	1	161	65
	9	NA	NA	1909	333	NA	NA	143	138	4	2	347	74
	Total	**2957**	**949**	**11282**	**1699**	**201**	**187**	**664**	**543**	**18**	**6**	**1450**	**424**
	Mean	**739±536**	**237±106**	**1612±789**	**243±48**	**50±16**	**47±16**	**95±72**	**78±66**	**2±2**	**1±1**	**161±119**	**47±27**

Abbreviations: LAVA, local abnormal ventricular activity; PR, PentaRay; NAV, Navi-star; Pt, patient; mm, millimetre; cm, centimetre; N°, number; Endo, endocardial; Epi, epicardial; NA, not applicable.

Table 3. Density, distance and voltage data.

	Pt	Density in scar PR (points/cm²)	Density in scar NAV (points/cm²)	Number of point pairs <3mm	Distance between points (mm)	Bipolar voltage PR (mV)	Bipolar voltage NAV (mV)	Unipolar voltage PR (mV)	Unipolar voltage NAV (mV)
Animals	1	3,22	0,25	44	2,27±0,60	0,84±0,70	1,36±1,29	4,49±2,23	4,79±1,78
	2	1,27	0,71	62	1,94±0,66	1,02±1,06	1,09±1,09	2,41±1,03	2,60±1,33
	3	3,44	0,13	88	1,91±0,65	0,88±0,95	1,01±0,96	3,22±1,70	3,66±1,65
	4	1,74	0,56	91	2,07±0,66	1,10±0,97	1,34±1,37	3,06±1,66	3,30±1,77
	Mean	**2.42±1.07**	**0.42±0.27**	**71.25±22.35**	**2.05±0.16**	**0.96±0.12**	**1.2±0.18**	**3.30±0.87**	**3.59±0.91**
Patients	1	1,47	0,64	70	2,01±0,69	1,65±1,99	1,98±2,67	5,69±4,54	5,85±5,03
	2	2,01	1,36	17	2,02±0,52	0,64±0,76	1,95±1,00	1,57±0,63	2,62±0,77
	3	5,32	2,44	18	2,04 0,53	1,07±0,95	1,87±2,40	3,78±2,14	4,64±2,56
	4	5,24	2,47	14	2,37±0,46	1,34±0,91	1,72±1,58	5,01±3,84	6,81±5,34
	5	9,35	1,97	17	2,55±0,59	0,78±1,27	0,83±1,36	3,87±3,44	4,06±3,94
	6	17,6	1,4	17	2,16±0,59	2,28±2,42	2,44±3,23	5,95±2,76	6,14±2,97
	7	12,06	5	182	1,98±0,64	1,64±2,22	1,89±2,48	3,58±2,64	3,72±2,71
	8	3,32	0,6	48	1,95±0,69	2,11±2,69	2,26±3,57	5,16±3,30	5,76±4,37
	9	2,6	0,52	150	2,23±0,61	1,45±1,86	1,96±1,94	6,05±2,88	6,49±5,36
	Mean	**6.55±5.43**	**1.82±1.41**	**59.22±63.88**	**2.15±0.20**	**1.44±0.55**	**1.88±0.45**	**4.52±1.46**	**5.12±1.43**

Abbreviations: LAVA, local abnormal ventricular activity; PR, PentaRay; NAV, Navi-star; Pt, patient; mm, millimetre; mV, milliVolt.

Table 4. Agreement between both catheters.

Sensitivity (PR as comparitor)	49%
Specificity (PR as comparitor)	77%
Positive Predictive Value	33%
Negative Predictive Value	87%
Proportion of overall agreement	72%
Agreement on LAVA	25%
Agreement on HANA (normal)	69%

Abbreviations: LAVA, local abnormal ventricular activity; HANA, High amplitude normal activity; NAV, Navistar; PR, PentaRay**.**

Table 5. Endpoints and follow-up.

Pt	Inducibility	LAVA elimination	Follow-up (months)	Recurrence of VT (months)	Death (months)	Complications
1	not tested	incomplete	16	2	0	0
2	inducible	complete	4	0	0	0
3	not inducible	complete	10	0	0	0
4	not inducible	complete	8	0	0	0
5	inducible	complete	28	0	0	0
6	not inducible	incomplete	8	8	0	0
7	not inducible	complete	3	0	0	0
8	inducible	incomplete	3	3	0	0
9	inducible	incomplete	3	0	0	0

Abbreviations: Pt, patient; LAVA, local abnormal ventricular activity; VT, ventricular tachycardia.

Figure legends.

Figure 1. Comparison of bipolar voltage maps (endocardial: scar <0.5mV; borderzone 0.5-1.5mV; healthy tissue >1.5mV and epicardial: borderzone 0.5-1mV; healthy tissue >1mV) made by NAV vs. PR mapping of animals 2 (in A) and 4 (in B) with an iatrogenic created anteroseptal scar and patient 4 (in C), using the CARTO®3 system. *All images in AP view.* A. LAVA are tagged in pink, the proximal conduction (left-sided His) system in blue and the Purkinje system in yellow. Four voltage and LAVA channels are visible within the scar with PR mapping but none were visible with NAV mapping. B. 3 LAVA channels were visible with PR mapping but none with NAV mapping. Borderzone appears more detailed and smaller using PR mapping. C. Larger scar area and better borderzone definition using PR vs. NAV mapping.

Figure 2. Point pair analysis (≤3mm of distance between a PentaRay and Navistar point) from two examples by manual signal analysis in two different patients (5 and 9). Substrate maps are put at 100% transparence. LAVA using PR (in purple) and NAV (in white) are tagged in different colors on different maps. Distance between to tags is measured using distance measurement tool in the mapping system. A red arrow indicates a clear LAVA visible with PR mapping but barely or not visible with NAV mapping.

Figure 3. Bipolar voltage threshold scanning using NAV vs. PR mapping.

From top to bottom: different bipolar thresholds are used (0.5-1.5mV, 0.2-1mV, 0.2-0.8mV, 0.2-0.6mV, 0.2-0.4mV) after manual reannotation of the maps to the near field LAVA signal. **A**. Patient 4. Epicardial bipolar substrate map using NAV vs. PR. **B.** Animal 2. Endocardial bipolar substrate map using NAV vs. PR. **C**. Animal 4. Endocardial bipolar substrate map using NAV vs. PR. Using the conventional thresholds (first row), less

difference between NAV and PR are seen. In all three examples there is a better resolution using different thresholds with PR. Channels appear and scar heterogeneity can be observed. Borderzone is better defined.

Figure 4. Subanalysis of changes in interelectrode distance.

EGMs of conventional bipoles from a PR catheter position are presented in the first row. Then, from top to bottom, new bipoles were created from the recorded unipolar signals with increasing interelectrode distance. Recordings are presented at 100mm/sec speed and voltage is in microV. In all 4 columns, the peak-to-peak voltage increases with increasing interelectrode distance. Peak-to-peak values between the green lines.

Figure 5. Subanalysis of bipole orientation: along vs. across the splines.

Left side, from top to bottom: the EGM's of 4 newly created bipoles across the splines on the inner electrode circle (yellow circle), schematicly presented in the middle figure. On bipole 20A 4-8, 12-16 and 16-20, the LAVA signal is visible, but at 20A 8-12, one cannot identify the LAVA activity. *Right side, from top to bottom:* PR catheter position at a LAVA site (yellow circle and arrow). Below, the EGMs of 15 conventional bipoles with clear LAVA activity on bipoles 20A 2-3, 3-4, 6-7, 10-11, 11-12, 14-15, 15-16, 18-19 and 19-20. Notice the low bipolar LAVA voltage around 0.11mV and reversal of polarity.

Fig. 1. Comparison of PR versus NAV bipolar substrate maps (in AP view, CARTO 3)

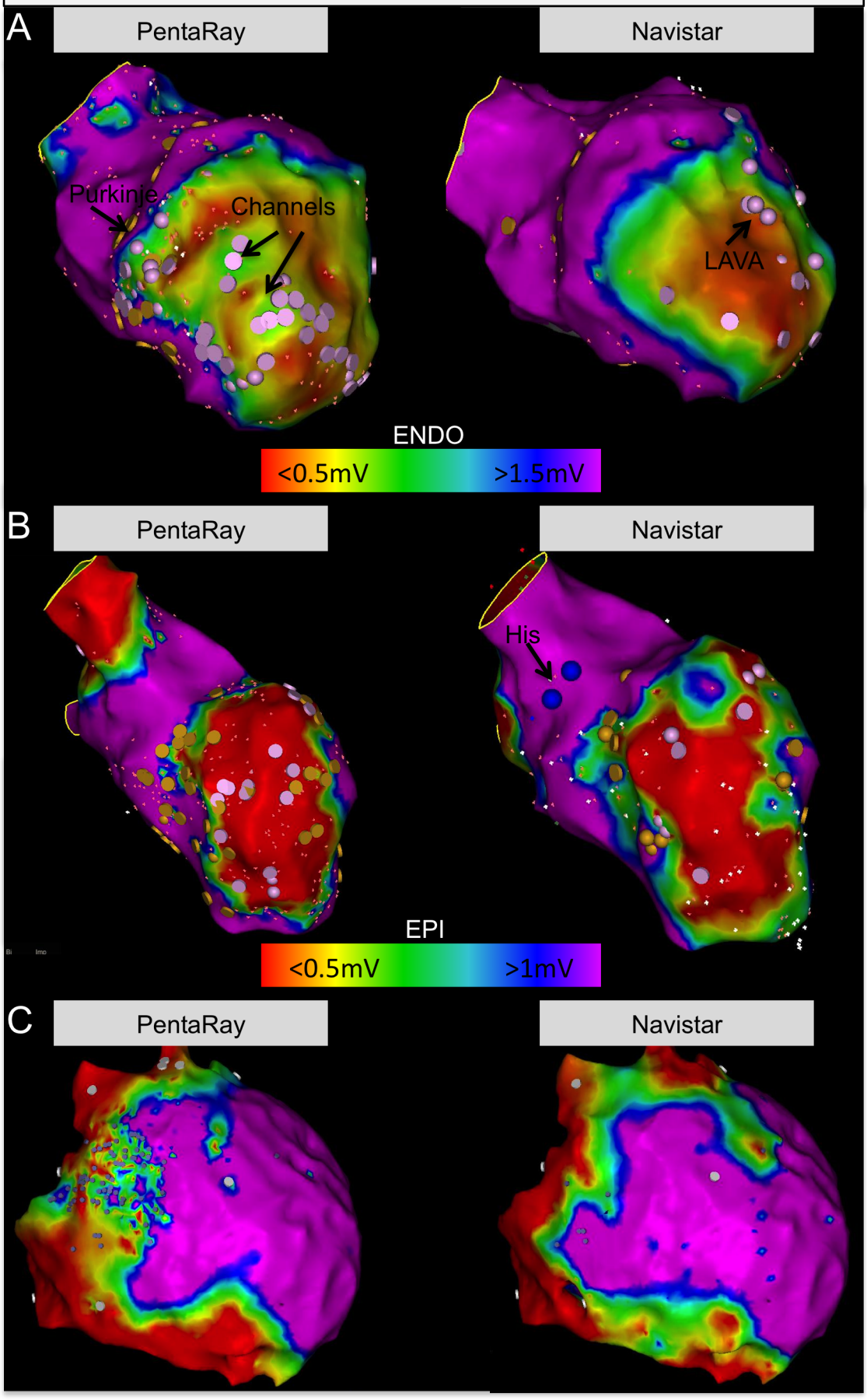

Fig. 2. Examples of 2 point pairs with ≤3mm distance between a Navistar and a PentaRay point.

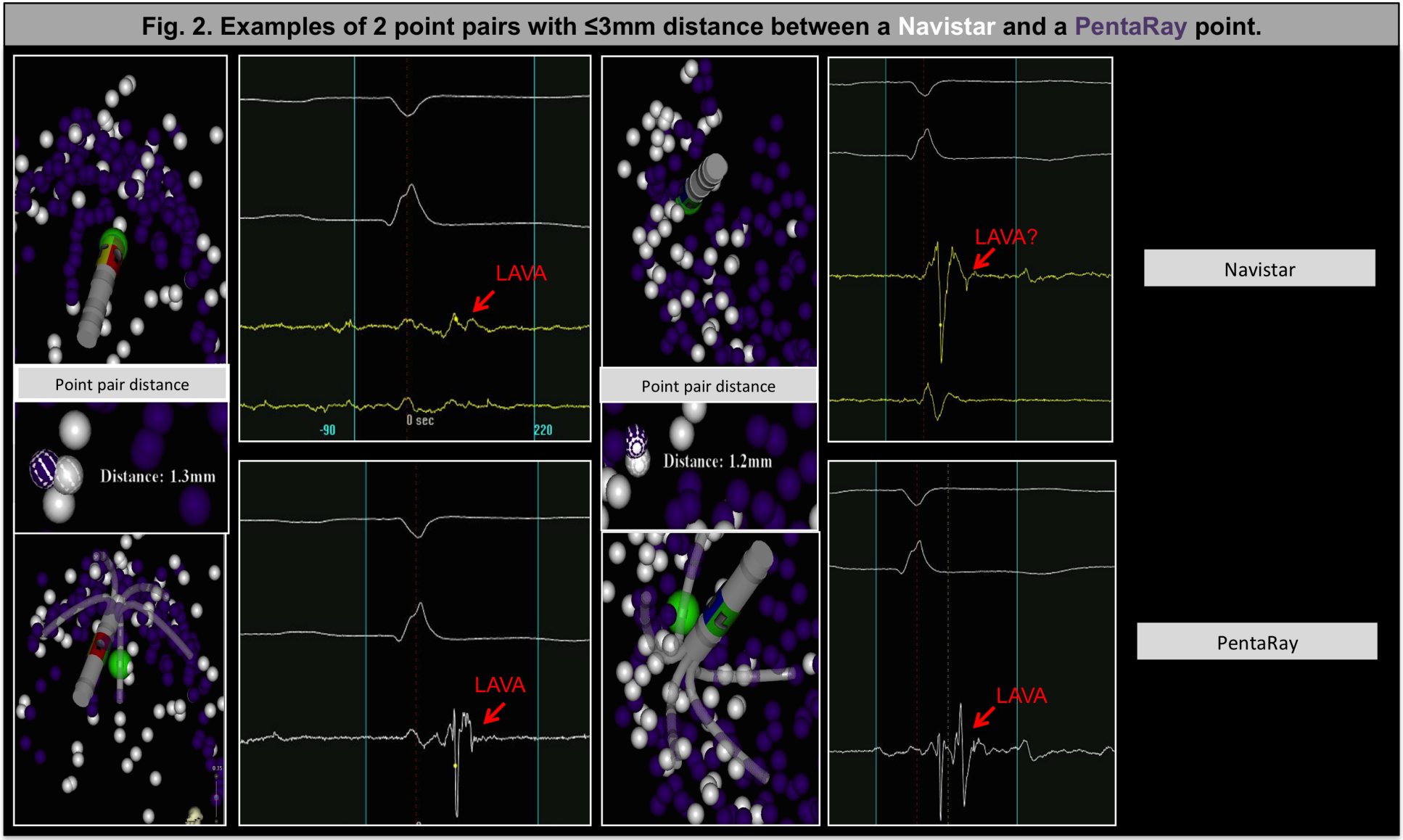

Figure 3. Bipolar voltage threshold scanning using NAV vs. PR.

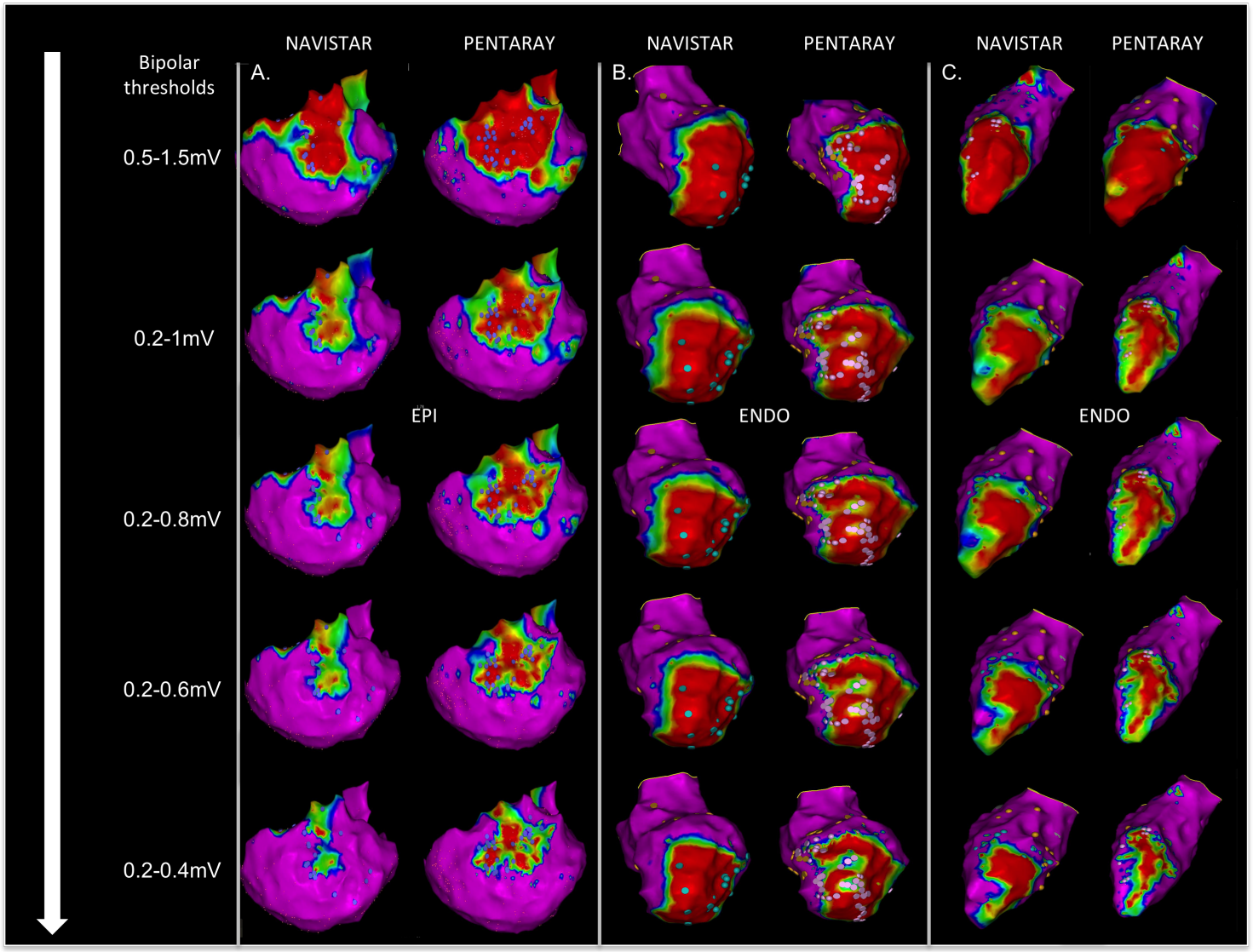

Fig. 4. Example of an identical PentaRay position at a LAVA site with increasing interelectrode spacing

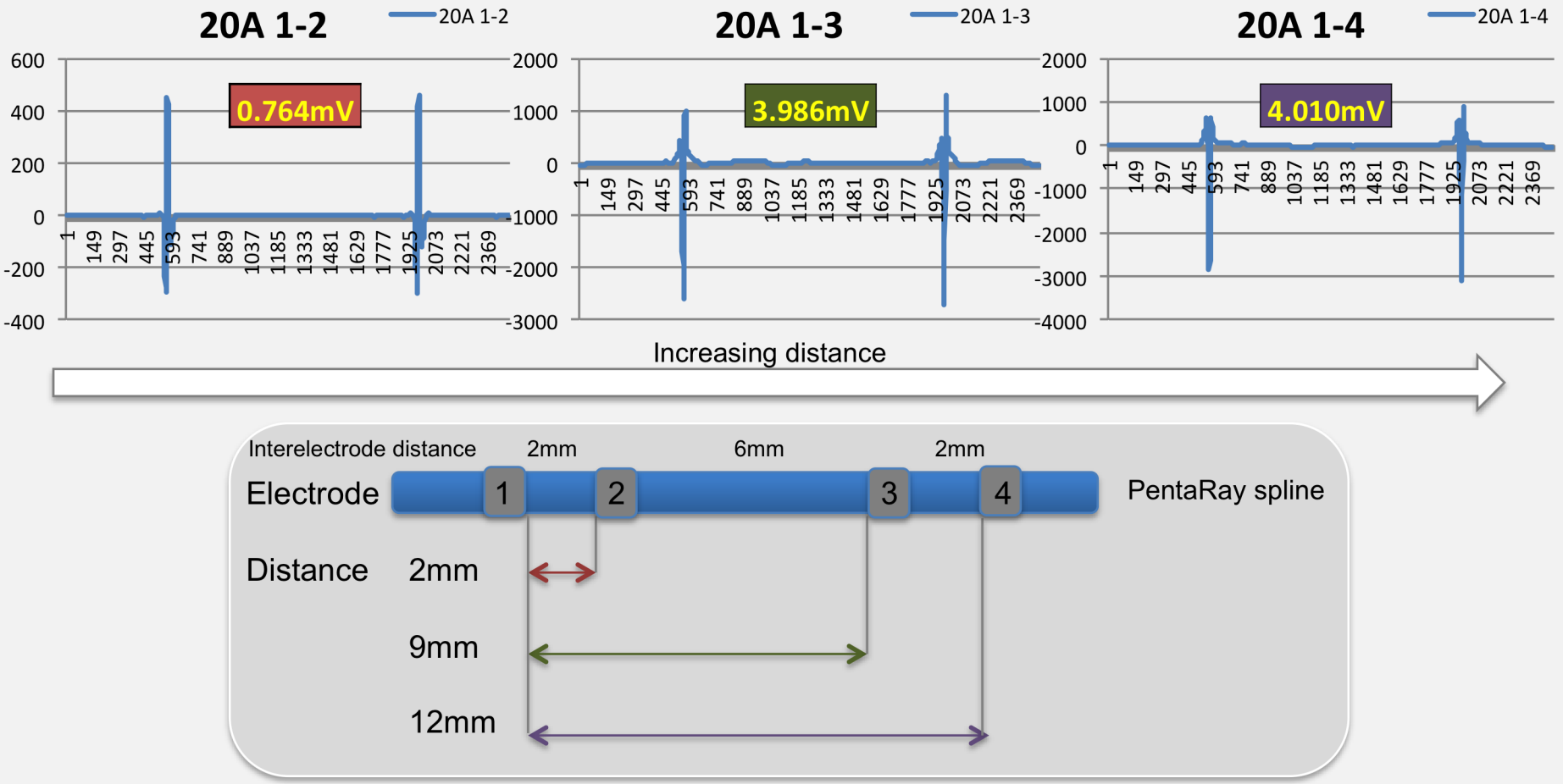

Bipolar signals are calculated postprocessing from the unipolar signals

Fig. 5. Example of a PentaRay catheter at a LAVA site: along vs across the spline.

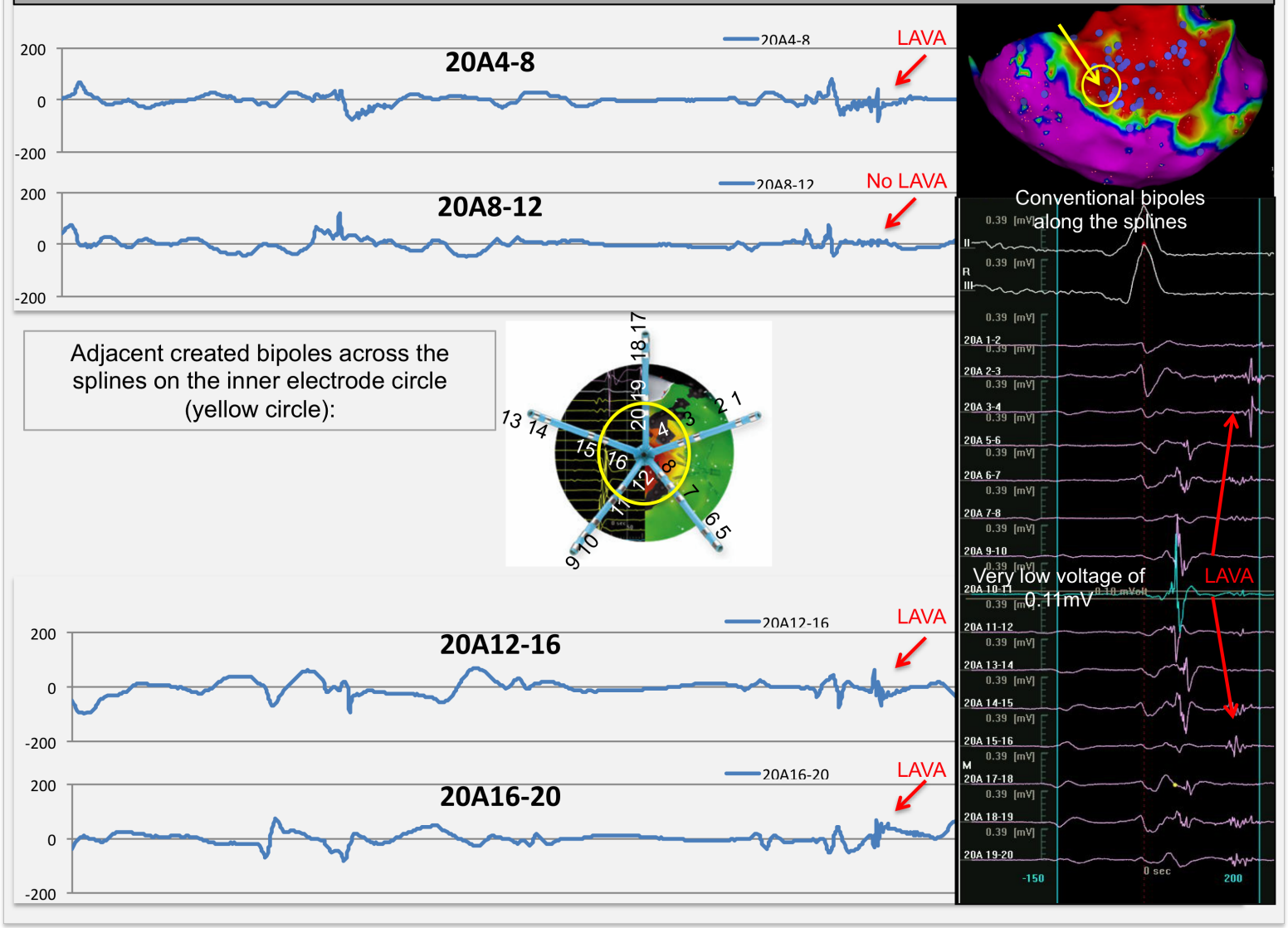

B. In NICM: VT Recurrence after VT ablation in non-ischaemic cardiomyopathy: incomplete ablation or disease progression? A multicentric European study.

Submitted to JCE

1. Study outline

Non-ischaemic cardiomyopathy (NICM) patients referred for scar-related VT ablation often have recurrence of VT. This may be due to multiple factors: scar progression, disease progression, incomplete ablation and endocardial only procedures and lack of catheter stability or contact force around the valves. Our knowledge on this topic is limited to a few small single centre studies, almost exclusively from the Pennsylvania group.[92, 93]

The aim of this retrospective multicenter study was to gather high-quality substrate maps of the same diseased chamber with a minimum interprocedural delay of 12 months to better understand the mechanisms leading to VT recurrences and investigate substrate progression in NICM patients.

In total, 20 patients (7 ARVC patients, 12 NICM patients and 1 myocarditis patient) from nine European centres were included. The mean interprocedural interval was 26±18months. Disease progression was found in the majority (75%) of patients with scar area progression in only half. Epicardial scar area was larger in all and unipolar endocardial scar progression was present in one-third of patients, suggesting intramyocardial or epicardial scar progression. A significant association was found

between ventricular remodeling and scar area progression (in 90%). New VT morphologies were found in 60% of patients. Ablation was performed in previously untouched index scar in 70% of patients, suggesting incomplete ablation at the index procedure.

2. Implications

This is the first multicentric study analyzing the disease progression in NICM patients. We found a progressive disease in both NICM and ARVC, although with significant individual variability. Scar progression is only present in half of the patients. Our data confirm the data of the Pennsylvania group. More epicardial approach and more accurate and extensive index ablation could improve ablation outcome in NICM.

3. Manuscript

VT Recurrence after VT ablation in Non-Ischaemic Cardiomyopathy: Incomplete Ablation or Disease Progression? A Multicentric European Study.

Authors list: B Berte[1], F Sacher[1], J Venlet[2], D Andreu[3], S Mahida[1], B Aldhoon[4], T De Potter[5], A Sarkozy[7], R Tavernier[6], A Marius[8], T Deneke[9], J Kautzner[4], A Berruezo[3], H Cochet[1], K Zeppenfeld[2], P Jaïs[1]

Affiliation:

[1]CHU Bordeaux and LYRIC institute, IHU Bordeaux, France

[2]Leiden University Medical Center, The Netherlands

[3]Thorax Institute, Hospital Clinic, Barcelona, Spain

[4]Institute for Clinical and Experimental Medicine-IKEM, Prague, Czech Republic

[5]OLV Aalst, Belgium

[6]AZ Sint Jan-Bruges, Belgium

[7]UZA Antwerp, Belgium

[8]CHU Nancy, France

[9]Herz- und Gefäss-Klinik, Bad Neustadt, Germany

IHU LIRYC ANR-10-IAHU-04 Equipex MUSIC ANR-11-EQPX-0030

Running title: *Berte et al.* NICM VT ablation.

Conflicts of interest: Dr Berte received an educational EHRA grant.

Dr Jaïs receives consulting fees from Biosense Webster.

Corresponding author:

Pierre Jaïs, MD

Hôpital Cardiologique du Haut-Lévêque, 33604 Bordeaux-Pessac, France.

Tel: +33 5 57 65 64 71; Fax: +33 5 57 65 65 09

E-mail: pierre.jais@chu-bordeaux.fr

word count: 3319 words

ABSTRACT

Aims: Recurrence of ventricular tachycardia (VT) may be observed after VT ablation in non-ischaemic cardiomyopathy (NICM) patients. We analyzed redo NICM cases to determine whether VT recurrences related to incomplete ablation or disease progression.

Methods: In a retrospective multicenter study, NICM patients who underwent repeat VT ablation with 2 qualitative density substrate maps of the same diseased ventricle with an interprocedural delay of ≥12months were included. Disease progression was defined as ≥1 factor: Scar area progression (PROG,+5%), ventricular remodeling [dilatation (DIL,+25ml) or decreased ejection fraction (EF,-5%EF)]. Scar remodeling (REM) was defined as a new VT, without PROG. Incomplete ablation was defined as index VT recurrence or ablation in previously untouched regions inside the index scar without PROG.

Results: In total, 20 patients from 9 centers were included (80% male 55±16 years, 7 ARVC, LVEF 43±14%). Mean interprocedural delay was 26±18 months. The disease progressed in 15 patients (75%) with ventricular remodeling in 14 (70%) [DIL: n=9 patients (45%) and EF decrease: n=9pts (45%)], scar PROG: n=10pts (50%): [bipolar, n=3; unipolar, n=4; combined, n=3]. Scar REM occurred in 4 patients (20%). New VT occurred in 12 patients (60%). Redo ablation sites were located in previously unablated regions inside the index scar in 70% of patients. VT recurrence following the second procedure was seen in 25%. 15% died during a follow-up of 17±17months.

Conclusion: Disease progression is the rule in NICM with recurrent VT. New VTs are often seen but incomplete index ablation is frequent, suggesting the need fore more extensive ablations.

Word count: 249

Keywords: VT ablation - NICM - redo ablation - scar - substrate map

What's new?

- This is the first multicentre study investigating progression of voltage scar area in ARVC.
- In other types of NICM, variable scar progression is observed in a minority of patients presenting for VT ablation.
- Disease progression however is the rule with ventricular dilation and/or reduced ejection fraction.
- Ablation is performed in untouched areas of the index scar in the majority of cases, suggesting more extensive ablation during the first procedure is needed.
- In a large group of patients, different VT morphologies are seen during the redo procedure.

Introduction

Ventricular tachycardia (VT) ablation for non-ischaemic cardiomyopathy (NICM) is challenging and remains associated with poorer outcome when compared to ischaemic cardiomyopathy (ICM).[1-3] A number of factors may contribute to VT recurrence in NICM including scar area progression, scar remodeling, ventricular remodeling, incomplete ablation during the index procedure, lack of epicardial approach, catheter instability etc... Both disease progression and incomplete ablation can result in scar remodeling. To date, studies investigating progression of VT substrate in NICM have been limited to a few small single centre studies.[4, 5]

Whatever the initial myocardial injury, the final histologic outcome is the loss of myocytes and the presence of fibrosis and possibly fat. Fibrosis is detectable as low unipolar and/or bipolar voltage on a substrate map and as delayed enhancement (DE) on DE-magnetic resonance imaging (MRI).[6-10] Epicardial fat can mimic scar by producing low voltage, but in this case, EGM present rather normal properties without fragmentation or long duration.[5, 11, 12]

The aim of this multicenter study was to gather retrospective cases to better understand the mechanisms leading to VT recurrences and investigate substrate progression in NICM patients.

Methods

Patient selection

All non-ischaemic patients referred for a redo VT ablation at participating centers were reviewed. All patients with an interval of <12 months between both procedures, poor substrate maps (fill threshold >15), lack of consecutive endocardial or epicardial maps of the same diseased ventricle were excluded. This study was approved by the Institutional Committee on Human Research at each authors' institution. For uniformity, mapping with the Ensite™ system (St Jude Medical) was excluded and only Carto® (Biosense Webster) maps were considered. NICM was defined as absence of significant coronary artery disease (>60% stenosis), ischaemic cardiomyopathy, significant valvular disease, toxic cardiomyopathy. Reversible cardiomyopathy and sarcoidosis were also excluded.

Substrate mapping

All patients underwent electro anatomical mapping (EAM) with the CARTO® system (XP or 3, Biosense Webster) in sinus rhythm. Mapping was performed with a 3.5mm-tip bipolar catheter (Navistar Thermocool, Biosense Webster) or a multipolar catheter (PentaRay, Biosense Webster). Peak-to-peak voltage measurement was automatically performed with the dedicated software on the CARTO® system. Bipolar electrograms (EGMs) were filtered at 30–500Hz and displayed at 100mm/sec sweep speed. Unipolar EGMs were recorded between the tip electrode and the Wilson central terminal (WCT), filtered at 1–100Hz and displayed at 100mm/sec speed.

Threshold definitions

For uniform analysis, all substrate maps were sent as raw data to the core lab at CHU Bordeaux, France. Thresholds for low voltage were defined as follows: low endocardial bipolar voltage <1.5mV, low endocardial unipolar voltage <5.5mV (RV) and <8.3mV (LV), low epicardial bipolar voltage <1mV and low epicardial unipolar voltage <7.95mV.[13]

Disease progression

Progression of the disease can be due to ventricular remodeling, increase in scar area and evidence for scar remodeling or combinations.

1. Ventricular remodeling

Ventricular volume was measured with the CARTO® algorithm and left ventricular ejection fraction with ultrasound measurements using the Biplane Simpson method. Right ventricular ejection fraction (RVEF=2 x TAPSE) was measured using tricuspid annular plane systolic excursion (TAPSE) using cardiac ultrasound. A significant increase in volume was considered if the volume increased by at least 25 mL, representing >10% change in the mean volume of 242±128mL during the first endocardial ablation.[4, 5] A decrease in EF of ≥5% was seen as significant.

2. Increase in scar area

All scar area measurements were performed using the area measurement algorithm on the CARTO® system by one operator (BB) and repeated >2 weeks after the first measurement. The scar area was measured starting 1cm away from the AV valves. The endocardial measurement difference was <5cm^2 in all patients and mean area surface

was 236±75 cm^2 during the first and 241±87 cm^2 during the second procedure. The epicardial measurement difference was <10cm^2 in all patients with a mean scar surface of 393±74 cm^2 during the first and 400±78 cm^2 during the second procedure. The anticipated 5-cm^2 error in endocardial scar area measurement and 10-cm^2 error in epicardial scar area measurement corresponded to 2.1**%** of the endocardial and 2.5% of the epicardial surface. Therefore, a significant increase in scar area between the 2 procedures was defined as an increase of >5% in the endocardial scar percentage (ie twice the measurement error indexed to the surface area) for both the endocardial and epicardial measurements.[4, 5] Combined scar progression was defined as combined unipolar and bipolar progression. Possible epicardial fat areas on the coronary arteries were not excluded during epicardial measurements. To exclude the effect of ablation, the ablation area in a normal bipolar voltage area during the first procedure was extracted from the measurements during the redo procedure. Increase in low voltage bipolar area corresponding to the ablation site was interpreted as a consequence of ablation.

Scar remodeling

Scar remodeling was defined as VT recurrence with a new 12-lead clinical VT morphology without an increase in scar area. Scar remodeling could be due to insufficient ablation with a changed exit site morphology or due to disease progression itself. We therefore did not include scar remodeling as a definite factor of disease progression and present it separately.

Ablation site analysis

To evaluate if ablation was performed in similar or different sites, the RV endocardium (11 segments), LV endocardium (14 segments) and epicardium (24 segments) were

segmented for a total of 49 ventricular segments. Incomplete ablation was defined as recurrence of the index clinical VT morphology(ies). Additional ablation during the second procedure at previously untouched regions in the initial scar of the index procedure was attributed to incomplete ablation during the first procedure.

Ablation procedure and endpoint

Ablation was performed with a conventional 3.5mm tip irrigated catheter at all centers. CHU Bordeaux used a LAVA-based ablation combined with non-inducibility and complete LAVA elimination. Other centers used non-inducibility as endpoint. Procedure complications were collected till 7 days after the procedure.

Follow-up

Follow-up data (in months) after both procedures were collected using device logs, hospital admissions and data from the general practitioner and cardiologist. Events as ventricular tachycardia (both sustained and non-sustained), appropriate shock and death were collected.

Statistical analysis

Continuous variables were expressed as mean ± SD for normally distributed data or median and interquartile range (IQR; 25th–75th percentile) for non-normally distributed data. Categorical data were expressed as counts and percentages. Data were tested for normality by histogram and using the Kolmogorov-Smirnov test. Continuous variables between two groups were compared using Student *t* tests. Categorical variables were compared using Fisher's exact or Pearson's chi-square tests as appropriate. All univariate predictors with P-values <0.05 were considered statistically significant. Statistical analyses were performed using PASW Statistics 18 (version 18.0.0).

Results

In total, 20 NICM patients [ARVC, n=7 (33%), myocarditis, n=1 (5%) and DCM, n=7 (33%) and other types of NICM, n=5 (25%)] were included from 9 centers (80% male 55±16yrs, LVEF 43±14%). The interval between VT ablation procedures was 28±18months. High-density maps were acquired using 226±117 endocardial and 605±711 epicardial points per procedure. Baseline patient characteristics are outlined in Table 1. The results below have been divided according to disease substrate:

Arrhythmogenic Right Ventricular Cardiomyopathy

Seven patients (patient no. 1-7; 4 male, LVEF 49±10%, age 48±16 years, Figure 1) were included with mean interval of 30±24months between procedures. An endocardial approach only was performed in 5 patients during the index procedure and patients

during the repeat procedure. A combined approach was used in 2 patients during the index procedure and in 2 patients during the repeat procedure. Endocardial ablation to eliminate epicardial LAVA was succesfully performed in both patients (patients 1 and 2).

Overall, right ventricular remodeling was observed in 6 (86%) patients (patient no. 1,2,4-7) between the two procedures with further reduction of RVEF (47±14% to 41±12%; p=0.14) and dilatation of the RV (284±147ml to 298±166ml; p=0.058). In patients with scar progression as determined by voltage mapping (n=4, 57%), RV dilatation was seen in 3 (75%) patients and decreased RVEF in 3 (75%) patients. Endocardial scar progression was seen in 4 (57%) patients (patient no. 2,4,5 and 7): bipolar progression only in 1; unipolar progression in 2 and combined progression in 1. Epicardial scar progression (epicardial maps were made during both procedures in 2 patients) was seen in one patient (patient no. 2, Figure 2): and the patient had combined progression. Data on scar evolution are given in Table 3.

In 5 patients, different VT morphologies were seen between first and second procedure. Data on VT characteristics are given in Table 2. Non-inducibility was obtained in 6 (86%) patients: 4 (57%) after first and 6 (86%) after second procedure (p=NS). At a mean follow-up of 18±11months after the last procedure, recurrence of VT was seen in one patient (14%). There were no deaths. Follow up data are given in Table 4.

Myocarditis

One patient (patient no. 8) was included with an interval of 34 months between procedures. A combined approach was performed during both procedures. LVEF (50%)

and LV volume (200ml) remained unchanged between both procedures. Endocardial or epicardial scar progression was absent. He was not inducible after the index procedure. VT morphology and VTCL were similar between both procedures. At 6-months follow-up after the second procedure, no VT recurrence or death occurred. There were no complications associated with the procedures.

Dilated and other causes of NICM

Twelve patients (patient no. 9-20; 11 male, LVEF 41±14%, age 61±14years, Figure 3) were included with mean interval of 26±14months between both procedures. An endocardial approach only was performed in 9 (75%) patients during the index procedure and 6 (50%) patients during the repeat procedure and combined approach in 3 (25%) patients during the index procedure and in 6 (50%) patients during the repeat procedure. LV remodeling was observed between the 2 procedures in 8 (67%) patients (patient no. 9-12 and 15-18), with further reduction of LVEF (41±14% to 33±16%; p=0.02) and further LV dilatation (238±121ml to 259±117ml; p=0.33).

Among the NICM patients with bipolar and/ or unipolar scar progression (n=7, 58%), LV remodeling was seen in 5 (71%). Endocardial scar progression was seen in 5 (42%) patients (patient no. 14-18): bipolar progression in 1 (8%), unipolar progression in 2 (17%) and combined progression in 2 (17%). Epicardial scar progression (epicardial mapping was performed during both procedures in 3 patients) was seen in one patient (patient no. 9). Data on scar evolution are given in Table 3.

In 8 patients, different VT morphologies were seen between first and second procedure. Data on VT characteristics are given in Table 2. Non-inducibility was achieved in 9 (75%) patients: 8 (67%) after first and 7 (58%) after second procedure (p=NS). During a follow-up period of 17±20months after the last procedure, VT recurrence was seen in 4 (33%) and death in 3 (25%) patients. VT recurrence occurred in all 3 patients who died. Follow up data are given in Table 4. Complications occurred during VT ablation in 2 (17%) patients: one dissection of the iliac artery and one pericardial effusion. A patient with combined scar progression is illustrated in Figure 4 (Supplementary online Figure).

Different causes of disease progression

The disease progressed in 15 (75%) patients with ventricular remodeling in 14 (70%) patients [ventricular dilatation in 9 (45%) patients and further decrease in EF in 9 (45%) patients], scar area progression in 10 (50%) patients [bipolar progression, n=3; unipolar progression, n=4; combined progression, n=3]. All different factors are illustrated for each patient in Table 5 to visualize their relationship.

Scar remodeling

Scar remodeling was seen in 4 (20%) of patients. We present scar remodeling separately in the Table 5, since this finding can be due to both disease progression and incomplete ablation. Ventricular remodeling was seen in 9/10 (90%) of patients with scar area progression and in all 4/4 (100%) of patients with scar remodeling.

Ablation site analysis during redo procedures

Based on the segmental division, we found that ablation sites during the redo procedure were localized in previously unablated regions of the index scar in 14 patients (70%) and in a new scar region because of scar progression, in 8 patients (40%).

During the repeat procedure, an increase in bipolar scar area in the corresponding segment -related to prior ablation- was only seen in 4 out of these 8 (50%) patients. An example of an ablation effect is shown in Figure 2 (patient no. 2).

Discussion

This is to our knowledge the first multicentric study regarding different NICM substrate entities and disease progression with consecutive epicardial maps in half of the patients. The main findings of this study are:

1. Non-ischaemic cardiomyopathy is a *progressive disease* with a highly variable individual disease course.

2. *Bipolar findings:* Endocardial bipolar scar progression is not a uniform finding and depends on the disease substrate: 29% of ARVC patients and 25% of NICM patients had scar progression. When both endocardial and epicardial substrate maps are obtained, the bipolar epicardial scar area is consistently larger.

3. *Unipolar findings:* Unipolar endocardial scar progression is seen in 29% of patients and suggests intramyocardial or epicardial disease progression. When available, we found that the unipolar endocardial surface is smaller than the epicardial surface.

4. *Factors are linked:* A strong association between ventricular remodeling and scar area progression was observed (90%).

5. *Incomplete ablation:* During the redo procedure, within new regions of the scar was necessary in the majority of patients (70%), suggesting an incomplete ablation during the index procedure.

6. *Frequent new VT:* Morphologies of recurrent VT were commonly (60%) different from those observed at the index procedure. A finding that was independent of scar progression.

NICM as a progressive disease.

This study confirms disease progression in the majority of patients (75%) in both ARVC and NICM as reported by *Riley et al* and *Liuba et al*.[4, 5]

In ARVC, they found RV dilatation and/or RV dysfunction as a uniform finding. We found RV dilatation and a decreased EF in all but one (86%). The authors furthermore found a relationship between ventricular remodeling and scar area progression since this remodeling was seen in 90% of patients with scar area progression.[4] In NICM, LVEF decreased in patients with scar area progression and remained unchanged in the patients without scar progression.[5] In this study, we found LVEF decrease was seen in 75% (6/8) of patients with scar area progression whereas only 25% of LV decrease was observed without scar area progression. We confirmed this association between scar progression and decrease in EF, present in 8/11 (73%) of patients.

Variable scar area progression.

In this present study, we confirm that scar area progression is highly variable in both ARVC (in a minority) and other NICM (in half of the patients).[4, 5]

Riley et al described a typical basal scar around the tricuspid valve in the majority of ARVC patients. Scar progression was highly variable and only found in 18% (2/11) of patients. RV dilatation and/or RV dysfunction appeared to be a uniform finding. They did however only investigate bipolar substrate maps. We investigated both bipolar and unipolar maps. In our study, scar progression was also only seen in a minority of patients: Bipolar scar progression was seen in 29% (2/7) and unipolar scar progression in 29% (2/7) patients. Interprocedural interval was longer in *Riley et al* and both studies investigated a similar small patient cohort (57±31 months vs 30±24 months and 11 vs 7 patients respectively).

Liuba et al found unipolar but not bipolar scar progression in almost half of NICM patients (46% and 8% respectively), based on endocardial substrate maps. We found both unipolar and bipolar scar progression in almost half of NICM patients (42% and 33% respectively), analyzing both endocardial and epicardial substrate maps. Our interprocedural interval and patient number was similar (32 ±20 months vs 26±14 months and 13 vs 13 patients respectively).

Difference in endocardial and epicardial unipolar scar area

In this study, we analyzed epicardial sequential scar data in 29% of patients. Low endocardial unipolar voltage predicted epicardial scar in all, but underestimated the (unipolar and bipolar) amount of scar. One would expect similar scar sizes if unipolar recording investigates the transmural voltage. We hypothesize that the larger unipolar epicardial scar size is mostly due to epicardial fat. Differences in catheter vector orientation and contact force are other plausible explanations. From the endocardium,

the epicardial fat appears at the outer side of the myocardial wall, further away from the electrode mapping range.

Frequent new VT morphologies observed during redo

In 60% of patients, we encountered at least one new VT morphology was observed during the redo procedure. We encountered new VT morphologies in ARVC and NICM patients, with or without scar progression. Potential explanations for this finding include exit site modification only during the index RF ablation, scar remodelling, or disease progression. Consistent with our findings, *Riley et al* identified new VT morphologies in 8 on 11 patients (73%) with ARVC.[5] Similar findings were reported by *Liuba et al* in NICM patients. Specifically, they found at least one new VT morphology in

7 of 8 patients (88%) and new VT morphologies in patients with or without scar progression.[4]

Ablation in previously untouched scar regions during redo

During the redo procedure, ablation is performed at new (previously untouched index scar) regions inside the scar in the majority (70%) of patients, suggesting an incomplete index ablation. More extensive index ablation could improve outcome in these patients. Interestingly, we only found evidence of an earlier RF effect in half of the patients, confirming the results of *Liuba et al* where they found 57% of RF effect during the second procedure. The authors of both manuscripts discussed above, also adjusted for

ablation lesions outside the low voltage area, but did not discuss regional ablation sites inside the scar to compare between both procedures.[4,5]

Limitations

This is a retrospective study. Follow-up time and patient population is still limited and real long-term follow-up is needed. The lack of serial epicardial maps in all patients limits the interpretation on intramyocardial and epicardial scar progression. Point-by-point mapping with the ablation catheter is limited in point density and a multipolar catheter is only rarely used. We did however exclude all maps of patients without the conventional fill threshold.

Conclusion

Disease progression is the rule in NICM with recurrent VT. It is associated to a lesser extend to an inhomogeneous increase in endocardial scar progression in <50% of patients. However, a majority of redo ablations are perfomed in previously unablated scar suggesting that a more extensive index ablation could improve the single procedure outcome.

Funding

Dr Berte B received an education EHRA (European Heart Rhythm Association) grant.

This worl was supported by by the following grant numbers: IHU LIRYC ANR-10-IAHU-04 and Equipex MUSIC ANR-11-EQPX-0030.

References

[1] Dinov B, Fiedler L, Schonbauer R, Bollmann A, Rolf S, Piorkowski C, Hindricks G, Arya A: Outcomes in catheter ablation of ventricular tachycardia in dilated nonischemic cardiomyopathy compared with ischemic cardiomyopathy: results from the Prospective Heart Centre of Leipzig VT (HELP-VT) Study. Circulation 2014; 129:728-736.

[2] Mathuria N, Tung R, Shivkumar K: Advances in ablation of ventricular tachycardia in nonischemic cardiomyopathy. Current cardiology reports 2012; 14:577-583.

[3] Tokuda M, Tedrow UB, Kojodjojo P, Inada K, Koplan BA, Michaud GF, John RM, Epstein LM, Stevenson WG: Catheter ablation of ventricular tachycardia in nonischemic heart disease. Circulation Arrhythmia and electrophysiology 2012; 5:992-1000.

[4] Liuba I, Frankel DS, Riley MP, Hutchinson MD, Lin D, Garcia FC, Callans DJ, Supple GE, Dixit S, Bala R, Squara F, Zado ES, Marchlinski FE: Scar Progression in Patients with Nonischemic Cardiomyopathy and Ventricular Arrhythmias: Scar progression in NICM. Heart rhythm : the official journal of the Heart Rhythm Society 2014; 11:755-62.

[5] Riley MP, Zado E, Bala R, Callans DJ, Cooper J, Dixit S, Garcia F, Gerstenfeld EP, Hutchinson MD, Lin D, Patel V, Verdino R, Marchlinski FE: Lack of uniform progression of endocardial scar in patients with arrhythmogenic right ventricular dysplasia/cardiomyopathy and ventricular tachycardia. Circulation Arrhythmia and electrophysiology 2010; 3:332-338.

[6] Wijnmaalen AP, van der Geest RJ, van Huls van Taxis CF, Siebelink HM, Kroft LJ, Bax JJ, Reiber JH, Schalij MJ, Zeppenfeld K: Head-to-head comparison of contrast-enhanced magnetic resonance imaging and electroanatomical voltage mapping to assess post-infarct scar characteristics in patients with ventricular tachycardias: real-time image integration and reversed registration. European heart journal 2011; 32:104-114.

[7] Cano O, Hutchinson M, Lin D, Garcia F, Zado E, Bala R, Riley M, Cooper J, Dixit S, Gerstenfeld E, Callans D, Marchlinski FE: Electroanatomic substrate and ablation outcome for suspected epicardial ventricular tachycardia in left ventricular nonischemic cardiomyopathy. Journal of the American College of Cardiology 2009; 54:799-808.

[8] Hutchinson MD, Gerstenfeld EP, Desjardins B, Bala R, Riley MP, Garcia FC, Dixit S, Lin D, Tzou WS, Cooper JM, Verdino RJ, Callans DJ, Marchlinski FE: Endocardial unipolar voltage mapping to detect epicardial ventricular tachycardia substrate in patients with nonischemic left ventricular cardiomyopathy. Circulation Arrhythmia and electrophysiology 2011; 4:49-55.

[9] Spears DA, Suszko AM, Dalvi R, Crean AM, Ivanov J, Nanthakumar K, Downar E, Chauhan VS: Relationship of bipolar and unipolar electrogram voltage to scar transmurality and composition derived by magnetic resonance imaging in patients with nonischemic cardiomyopathy undergoing VT ablation. HRTHM 2012; 9:1837-1846.

[10] Desjardins B, Yokokawa M, Good E, Crawford T, Latchamsetty R, Jongnarangsin K, Ghanbari H, Oral H, Pelosi F, Jr., Chugh A, Morady F, Bogun F: Characteristics of intramural scar in patients with nonischemic cardiomyopathy and relation to intramural ventricular arrhythmias. Circulation Arrhythmia and electrophysiology 2013; 6:891-897.

[11] d'Avila A, Houghtaling C, Gutierrez P, Vragovic O, Ruskin JN, Josephson ME, Reddy VY: Catheter ablation of ventricular epicardial tissue: a comparison of standard and cooled-tip radiofrequency energy. Circulation 2004; 109:2363-2369.

[12] van Huls van Taxis CF, Wijnmaalen AP, Piers SR, van der Geest RJ, Schalij MJ, Zeppenfeld K: Real-time integration of MDCT-derived coronary anatomy and epicardial fat: impact on epicardial electroanatomic mapping and ablation for ventricular arrhythmias. JACC Cardiovascular imaging 2013; 6:42-52.

[13] Piers SR, van Huls van Taxis CF, Tao Q, van der Geest RJ, Askar SF, Siebelink HM, Schalij MJ, Zeppenfeld K: Epicardial substrate mapping for ventricular tachycardia ablation in patients with non-ischaemic cardiomyopathy: a new algorithm to differentiate between scar and viable myocardium developed by simultaneous integration of computed tomography and contrast-enhanced magnetic resonance imaging. European heart journal 2013; 34:586-596.

Figure legends

Figure 1.

Graph illustrating all seven ARVC patients with endocardial (endo) and epicardial (epi) scar area presented as percentage of total area, during index and redo procedure. Encircling in red if endocardial progression, in blue if epicardial progression occured and in green if combined progression. Upper panel demonstrates bipolar results and lower panel the unipolar results.

Figure 2.

Voltage maps (CARTO®3, Biosense Webster) of pt 2 with ARVC. Endocardial (bipolar : <0.5mV; 0.5-,1.5mV; >1.5mV and unipolar: <0.5mV-<5.5mV) and epicardial (bipolar: <0.5mV; 0.5-1mV; >1mV and unipolar: <0.5mV-<7.95mV) voltage side-by-side. The first row represents AP view and the second row PA view. The upper panel shows the index procedure and the lower panel shows the second procedure. During the index procedure, endocardial ablation to eliminate epicardial local abnormal ventricular activity (LAVA) was performed outside the low voltage area (LVA) in segments 1 and 3. The effect is seen as an increase in bipolar LVA during the second procedure (arrows). However, an increase in bipolar LVA is also seen away from the prior ablation site, suggesting disease progression (arrow).

Figure 3.

Graph illustrating all twelve NICM patients with endocardial (endo) and epicardial (epi) scar area presented as percentage of total area, during index and redo procedure. Encircling in red if endocardial progression and in blue if epicardial progression

occurred. Upper panel demonstrates bipolar results and lower panel the unipolar results.

Figure 4 (supplementary online Figure).

Voltage maps (CARTO®3, Biosense Webster) of pt 9 with NICM. Endocardial (bipolar : <0.5mV; 0.5-1.5mV; >1.5mV and unipolar: <0.5mV-<5.5mV) and epicardial (bipolar: <0.5mV; 0.5-1mV; >1mV and unipolar: <0.5mV-<7.95mV) voltage side-by-side. The first row represents AP view and the second row PA view. The upper panel shows the index procedure and the lower panel shows the second procedure. An increase in both bipolar and unipolar voltage is appreciated in this patient.

Table 1. Baseline characteristics.

Pt	sex	age (yrs) at index procedure	time interval between procedures (mo)	type of NICM	ICD/ CRT-D	ACE=1, ALD=2, DIUR=3	BB=1, SOT=2, AMIO=3	assist device
1	M	45	17	ARVC	ICD	1,2,3	1	
2	F	49	25	ARVC	ICD	1	1,3	
3	M	70	25	ARVC	ICD	1,2,3	1	
4	F	64	34	ARVC	ICD	1,2,3	1,3	
5	F	22	82	ARVC	ICD		2	
6	M	44	14	ARVC	ICD		1,2,3	
7	M	45	12	ARVC	ICD	1,2,3	1,2,3	
8	M	35	34	MYO	ICD		1,3	
9	M	59	13	DCM	ICD	1,2,3	1,3	
10	M	63	19	DCM	ICD	1,2,3	3	LVAD
11	M	77	26	DCM	ICD	1,2,3	1,3	
12	M	74	46	DCM	ICD	1,2,3	1	
13	M	21	19	DCM	ICD	1	1	
14	M	59	59	DCM	ICD	1,2,3	1,3	
15	M	55	15	DCM	ICD	1	1,3	
16	F	60	20	NICM	ICD	1,2,3	1	
17	M	72	15	NICM	ICD		1	
18	M	70	16	NICM	ICD	1,2,3	1,3	
19	M	61	28	NICM	ICD	1,3	1,2	
20	M	55	34	NICM	ICD	1,2,3	3	

Abbreviations: Pt, patient; yrs, years; M, male; F, female; mo, months; DCM, dilated cardiomyopathy, ARVC, arrhythmogenic right ventricular cardiomyopathy; ICD, intracardiac cardioverter defibrillator, ACE, ace-inhibitor; ald, aldactone; diur, lis-diureticum; BB, beta blocker; sot, sotalol; amio, amiodarone; LVAD, left ventricular assist device.

Table 2. VT and hemodynamic characteristics.

Pt	VTCL index (ms)	VTCL second (ms)	Different VT morphology	LVEF (NICM) index second	RVEF (ARVC) index second	volume index (ml)	volume second (ml)
1	360	600	1	55% 55%	**50% 45%**	316	**385**
2	320	200		60% 60%	60% 60%	101	**156**
3			1	50% 50%	30% 30%	405	367
4	300-540	200-300		35% 30%	**25% 20%**	494	**585**
5	545	545		35% 61%	**60% 35%**	102	106
6	390	440	1	50% 50%	**50% 45%**	131	**184**
7	290	440	1	56% 55%	**55% 50%**	225	**258**
8	320	300		50% 50%		212	202
9	380	400	1	**35% 20%**		542	557
10	320	400	1	15% 15%		185	**215**
11	295	340		**40% 25%**		180	**299**
12	370	310		**35% 15%**		305	300
13	400	375		60% 60%		114	92
14	470	320	1	50% 50%		245	242
15	400	450		**55% 37%**		204	**317**
16			1	25% 25%		111	**214**
17	300	460	1	**55% 49%**		229	213
18	315-430	550	1	**25% 20%**		323	222
19	300-375	315	1	50% 50%		175	183
20	460	280-360	1	**41% 20%**			

Ventricular remodeling is highlighted in **bold.**

Abbreviations: Pt, patient; VTCL, ventricular tachycardia cycle length; ms, milliseconds; LVEF, left ventricular ejection fraction; ml, milliliters; NICM; non-ischaemic cardiomyopathy; ARVC, arrhythmogenic right ventricular cardiomyopathy; VT, ventricular tachycardia.

Table 3. Scar data.

Pt	epi acces at index	epi access at redo	scar location index	scar location second	% endo bipolar LVA index	% endo bipolar LVA second	% epi bipolar LVA index	% epi bipolar LVA second	% endo unipolar LVA index	% endo unipolar LVA second	% epi unipolar LVA index	% epi unipolar LVA second
1	1	1	TV and RVOT	TV and RVOT	29	32	57	54	57	53	74	58
2	1	1	anterior free wall	TV and RVOT and basal inferior free wall	11	28	26	34	61	58	58	54
3	0	1	TV and freewall and RVOT	TV and freewall and RVOT	56	56			73	68		
4	0	0	TV and freewall and RVOT	TV and freewall and RVOT	52	56			82	95		
5	1	1	TV and posterolateral	TV and free wall	8	17			23	27		
6	1	0	TV and inferolateral	TV and inferior	21	20			22	17		
7	0	0	TV and freewall and RVOT	TV and posterolateral and freewall and RVOT and	12	14			41	71		
8	1	0	inferolateral	inferolateral	2	1	57	54	16	13	72	67
9	1	1	lateral MV	lateral MV	14	14	27	34	57	55	69	86
10	0	0	basal septal MV	basal septal MV	19	14			66	67		
11	0	1	anterolateral	anterolateral	14	9	35	39	41	42	40	45
12	0	1	anterolateral and apical	anterolateral and apical	21	24			95	97		
13	0	1	anterolateral and apical	anterolateral and apical	10	14		55	7	9		56
14	0	0	basolateral	MV and inferolateral and apicoseptal	22	28		32	62	68		65
15	1	0	basal anterolateral	basal anterolateral	8	37			45	71		
16	0	0	basolatera	basolateral and apical	28	24			62	83		
17	0	0	MV and basal	MV and basal	20	16		30	21	31		47
18	0	1	LV: basal septal	LV: septum and apico-inferior	23	36			66	67		
19	0	0	basal posterior	inferolateral	5	4			24	25		
20	0	1	basal and inferoposterior	basal and inferoposterior	9	8	13	14	41	44	34	31

Abbreviations: Pt, patient; epi, epicardial; endo, endocardial; LVA, low voltage area; TV, tricuspid valve, MV, mitral valve; RVOT, right ventricular outflow tract.

Table 4. Procedural data and follow-up.

Pt	endo RF time (min)		epi RF time (min)		RF segments		RF outside	non-inducibility at end		recurrence of VT (mo)		death after	follow-up
	index	second	index	second	index	second	bipolar LVA	index	second	index	second	second	after second
1	14	24	5		2,9,27	1,2,9,27, 31,41	1,2	NT	0	1	no		23
2	64	80	14		1,3,30,31	1,3,9,30,31	1,3	0	1	24	no		6
3	53	44			1	1,2,3,9,10		1	1	12	no		24
4	20	30			2,3	2,3		0	1	18	no		36
5	5	6		25	2,9	2,3,9,10,26		1	1	0.5	no		17
6		17	3		27	9		1	1	13	5		5
7	31	9			7	1,2,9		1	1	6	no		14
8			21	26	29,33,37,38, 42	29,33,37, 42		0	0	32	no		6
9	40		20		20,21,32,36, 38, 42	13,20,21,32,33	32,36	NT	NT	7	1		1
10	36	ethanol injection			12,14,15	12,13,14		1	1	6		1	1
11	25	22	23	10	13,14,19,20, 21	19,20,21, 39	39	1	1	1	no		26
12	21	8			12,16	15,16,17	15,16	0	1	0.3		1	1
13	15			14	16,17	16,17		1	1		no		47
14	4	33		18	12	6,12,13,14, 20,2125,38,39,43	20,21	1	0	19		1	3
15	8			17	12,13	12,15,16		0	0	12	no		36
16	38	18			13,14,16,17, 21, 24	19,22	19,22	1	1	12	no		28
17	14			11	14,19,23	39,4	19	1	0	14	61		61
18	14	24			12,13,15,16, 18,21	6,7,12,21,24	5,13,15	1	1	15	5		5
19	13	19			13,14,19,28	1,19		0	0	1	1		1
20	33	18		24	19,20,39	19,2		0	0	32	no		6

Abbreviations: Pt, patient; epi, epicardial; endo, endocardial; RF, radiofrequency energy; mo, months; NT, not tested.

Table 5. Different factors of recurrence of VT

Pt	Disease	Decreased EF	Ventricular dilatation	New VT morphology	Bipolar scar progression	Unipolar scar progression	Ventricular remodeling	Scar progression	Disease progression	Scar remodeling * (new VT)	Incomplete ablation (same VT)	Ablation in prior untouched scar
1	ARVC	1	1	1			1		1	1		1
2	ARVC		1		1		1	1	1		1	1
3	ARVC			1						1		1
4	ARVC	1	1			1	1	1	1		1	
5	ARVC	1			1		1	1	1		1	1
6	ARVC	1	1	1			1		1	1		1
7	ARVC	1	1	1		1	1	1	1			1
8	NICM										1	
9	NICM	1		1	1	1	1	1	1			1
10	NICM		1	1			1		1	1		1
11	NICM	1	1			1	1	1	1		1	1
12	NICM	1					1		1			
13	NICM										1	
14	NICM			1	1	1		1	1			1
15	NICM	1	1		1	1	1	1	1		1	1
16	NICM		1	1			1	1	1	1		
17	NICM	1		1		1	1	1	1			1
18	NICM	1		1	1		1	1	1			1
19	NICM			1						1		1
20	NICM			1						1		
		55%	45%	60%	30%	35%	70%	50%	75%	20%	35%	70%

* Scar remodeling can be due to disease progression or incomplete ablation. 1 means the factor is present.

Abbreviations: Pt, patient; EF, ejection fraction; VT, ventricular tachycardia; ARVC, arrhythmogenic right ventricular cardiomyopathy; NICM, other non-ischaemic cardiomyopathy.

Figure 1. Scar evolution between both procedures in ARVC patients.

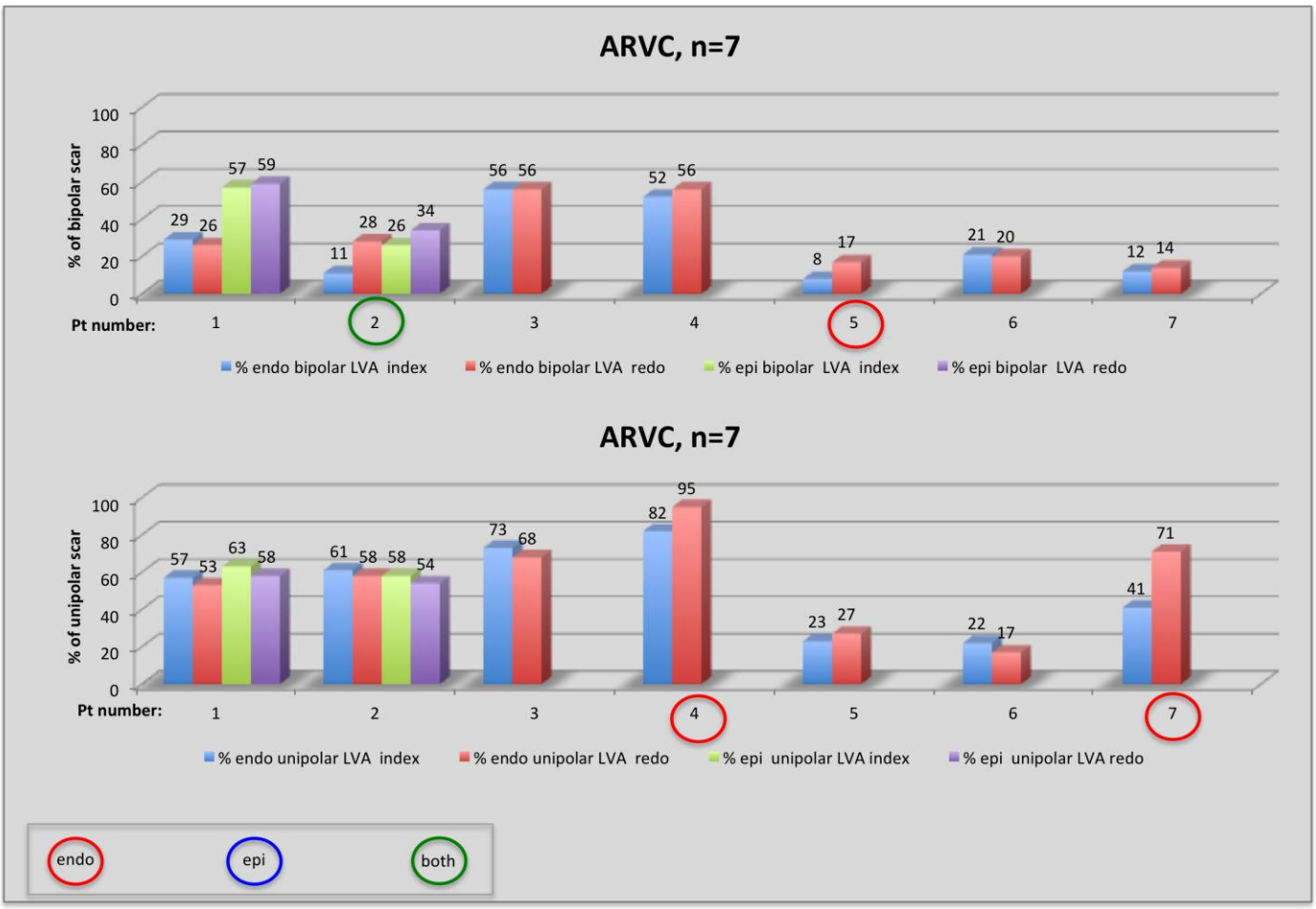

Figure 2. Example of an ARVC patient with RF effect and scar area progression.

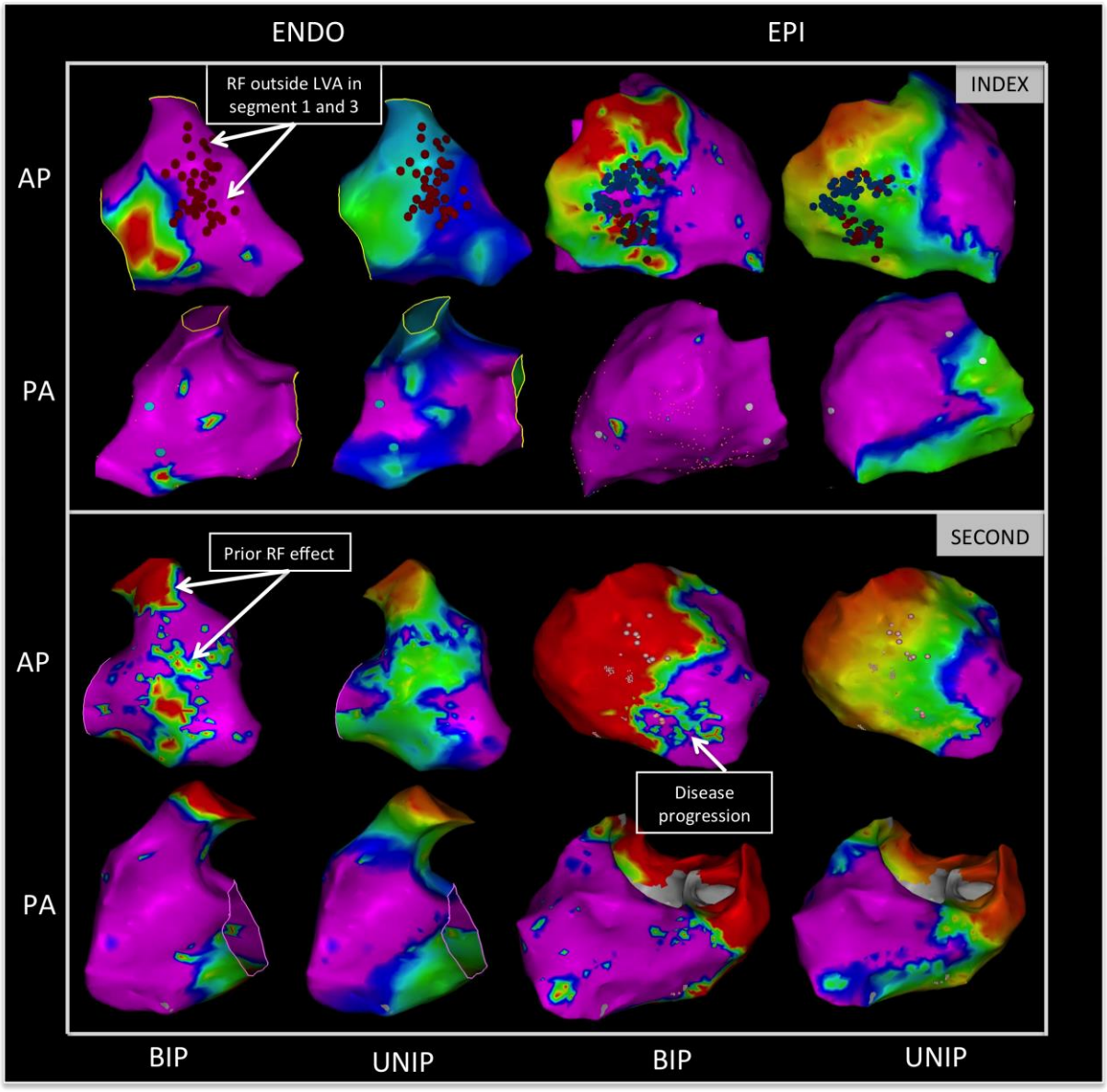

Figure 3. Scar evolution between both procedures in NICM patients. .

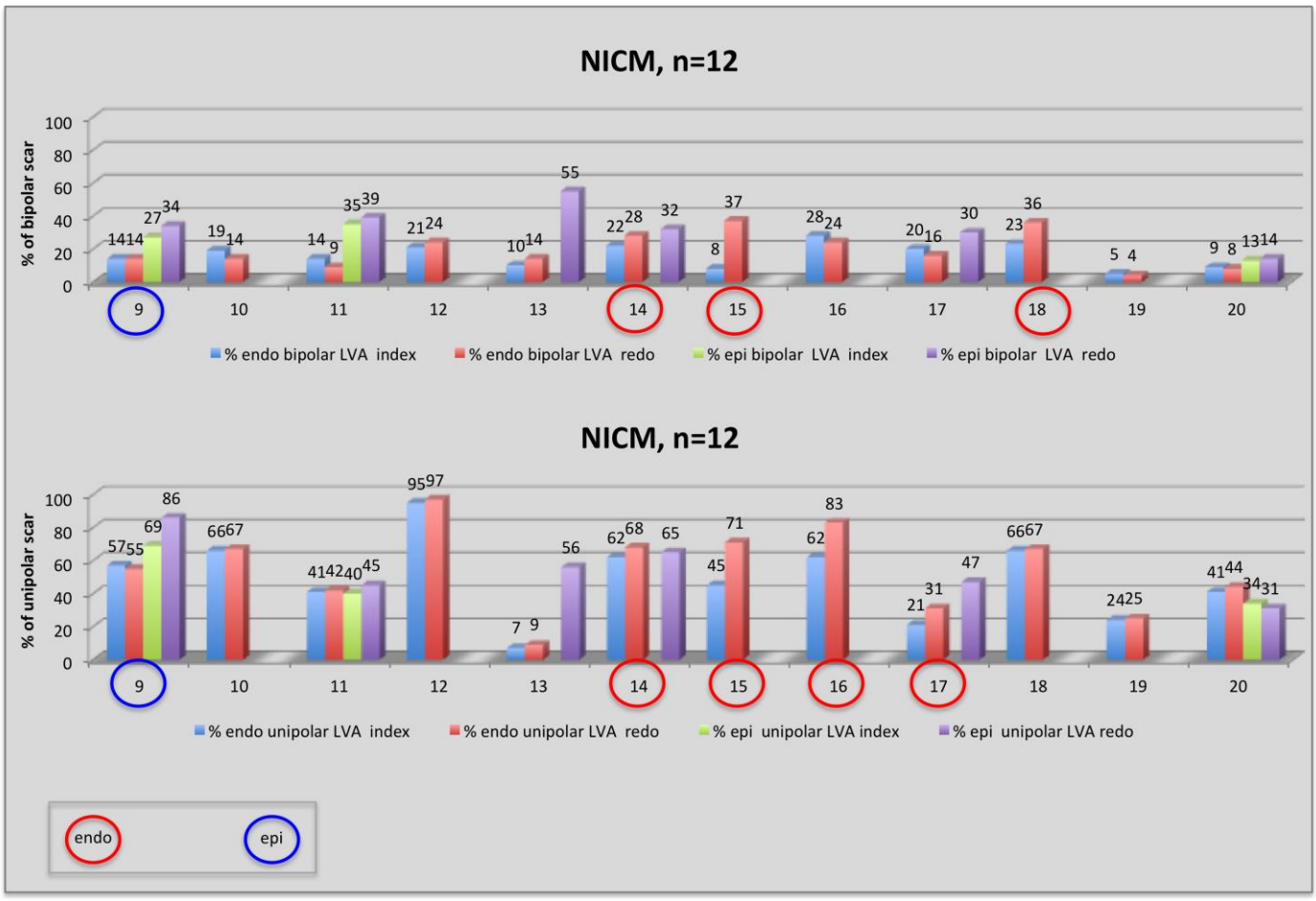

C. *In myocarditis:* Post-myocarditis ventricular tachycardia in patients with epicardial-only scar: a specific entity requiring a specific approach.

Berte B, Sacher F, Cochet H, Mahida S, Yamashita S, Lim H, Denis A, Derval N, Hocini M, Haïssaguerre M, Jaïs P. J Cardiovasc Electrophysiol. 2015 Jan;26(1):42-50.

1. Study outline

In this study, we retrospectively investigated a specific subset of NICM patients with a subepicardial only scar, defined by EAM imaging. Twelve of 189 (6.3%) NICM patients were included. An electro-anatomical mapping system was used in all to obtain automatic high-amplitude normal activity (HANA) voltage maps. Local abnormal ventricular activity (LAVA) was identified in normal voltage regions >1.5mV in 35% of cases. To better understand the scar, manually adapted LAVA voltage maps were created. This led to a better correlation between LAVA and low voltage with only 3% of LAVA in normal voltage regions and a better quantitative correlation with the scar on imaging. Attempts to eliminate epicardial LAVA using endocardial RF ablation (a strategy demonstrated as effective in ICM and ARVC) at the opposing site was unsuccessful in all because of preserved wall thickness. Therefore an epicardial approach and RF delivery was needed in all cases.[94]

2. Implications

The role of VT ablation for NICM patients is expanding. Different challenges are seen in this patient population. For instance, the scar is more often intramural and wall thinning thickness is often not present. We have identified a wall thickness threshold at 5mm, above which endocardial ablation fails to eliminate epicardial substrate. Preprocedural imaging using DE-MRI and MDCT are often the only and therefore critical tools to help to understand the disease and scar in the individual patient. Imaging can furthermore help to guide the ablation strategy and influences the decision to perform an epicardial approach from the outset. In addition, imaging is paramount to identify the course of the phrenic nerve and coronary artery system to avoid complications, especially in the subset of patients with inferolateral subepicardial scar.

Automatically created peak-to-peak substrate maps using electro-anatomical mapping systems focus on far field ventricular HANA signals, since they have the largest peak-to-peak amplitude. Near-field LAVA maps, still created manually, could be created automatically by the EAM systems to help to understand and define scar, LAVA and conduction into the scar.

3. Manuscript

Postmyocarditis Ventricular Tachycardia in Patients with Epicardial-Only Scar : A Specific Entity Requiring a Specific Approach

BENJAMIN BERTE, M.D., FREDERIC SACHER, M.D., PH.D., HUBERT COCHET, M.D., PH.D., SAAGAR MAHIDA, M.B.CH.B., PH.D., SEIGO YAMASHITA, M.D., PH.D., HAN LIM, M.B.B.S., PH.D., ARNAUD DENIS, M.D., NICOLAS DERVAL, M.D., MÉLÈZE HOCINI, M.D., MICHEL HAÏSSAGUERRE, M.D., PH.D., and PIERRE JAÏS, M.D., PH.D.

From the Hôpital Cardiologique du Haut-L'évêque, Université de Bordeaux, LIRYC Institut: IHU LIRYC ANR-10-IAHU-04 et Equipex MUSIC ANR-11-EQPX-0030, Bordeaux, France

Epicardial-Only VT Ablation. ***Background:*** **Nonischemic cardiomyopathy is a heterogeneous condition providing a favorable substrate for ventricular tachycardia (VT).**

Objective: **The purpose of this study is to further characterize the substrate in a subset of postmyocarditis patients with epicardial-only scar.**

Methods: **Twelve postmyocarditis patients (11 male, 49 ± 14 years, left ventricular ejection fraction 49 ± 12%) with VT and epicardial-only scar were included for analysis comparing automatic high-amplitude normal activity (HANA) maps to manually adjusted maps of based on local abnormal ventricular activity (LAVA) electrograms when present. A combined endocardial (endo) and epicardial (epi) approach was used in 11/12 with usual bipolar/unipolar voltage thresholds and analyzed using image integration.**

Results: **A delayed enhancement MRI scar area of 52 cm^2 (38, 59) and multidetector CT wall thinning area of 18 cm^2 (14, 35) was found. Bipolar voltage substrate mapping (160 points [101, 239] endo, 553 points [232, 713] epi and LAVA were found only epicardially [443 LAVA points] in all) illustrated a low-voltage area of HANA: 1 cm^2 (0, 10) endo, 25 cm^2 (22, 39) epi and LAVA: 1 cm^2 (0, 10) endo, 39 cm^2 (28, 51) epi. Manual maps performed better than automatic maps for delineating low-voltage area with a higher overlap with scar area on delayed enhancement magnetic resonance imaging (DE-MRI; 76% [66, 94] vs. 45% [35, 62]; P = 0.04). In addition, manual voltage maps also showed a higher overlap with location of LAVA (LAVA in normal voltage area: 3% [0, 9] vs. 35% [32, 41]; P < 0.05).**

Conclusion: **In postmyocarditis patients with epicardial-only scar, automatic voltage mapping may miss or minimize the electrical VT substrate. DE-MRI and manual LAVA-based voltage mapping are necessary to optimize scar delineation. Epicardial access is critical for mapping and ablation in this condition.**
(J Cardiovasc Electrophysiol, Vol. 26, pp. 42-50, January 2015)

cardiac DE-MRI, epicardial scar, LAVA, myocarditis, VT ablation

Background

Nonischemic cardiomyopathy (NICM) is a heterogeneous condition providing a favorable substrate for ventricular tachycardia (VT) amenable to catheter ablation.[1] Different definitions for targets and different end points for VT ablation have been used. We use the local abnormal ventricular activity (LAVA) concept as it encompasses poorly coupled surviving fibers in the scar and therefore is not limited to late potentials. The target and end point of LAVA-based VT ablation procedures are, respectively, LAVA and complete LAVA elimination, which is associated with improved outcome and mortality benefit and this irrespective of VT inducibility at the end of the procedure.[2,3] The outcome of VT ablation in NICM is worse compared to ischemic cardiomyopathy[4,5] and the arrhythmogenic substrate is less clearly defined. Patients with NICM display distinctive scar characteristics and more commonly present with patchy epicardial or intramural scar.[6] NICM patients also display distinctive electrogram (EGM) characteristics: The distribution of LAVA in NICM is typically epicardial, since almost all LAVA appear in low-voltage areas.[2,7] Correlation between low-voltage area, LAVA signals, and ischemic scar on MRI has been demonstrated.[8-11]

The purpose of this study is to better determine the specific characteristics of epicardial-only scar in postmyocarditis patients using delayed enhancement magnetic resonance imaging (DE-MRI), multidetector computed tomography (MDCT), local EGM (automatic voltage mapping and manual adjustment), and LAVA characteristics.

Dr. Berte received an educational EHRA grant.

Drs. Jaïs, Haïssaguerre, Hocini, and Sacher have received lecture fees from Biosense Webster and St. Jude Medical.

Other authors: No disclosures.

Address for correspondence: Dr. Frédéric Sacher, M.D., PH.D., Hôpital Cardiologique du Haut-Lévêque, 33604 Bordeaux-Pessac, France. Fax: 33-5-57656509; E-mail: frederic.sacher@chu-bordeaux.fr

Manuscript received 2 June 2014; Revised manuscript received 7 August 2014; Accepted for publication 19 August 2014.

doi: 10.1111/jce.12555

Methods

Patient Selection

Between 2008 and 2013, 12 postmyocarditis patients (11 male, 49 ± 14 years) with epicardial-only scar undergoing VT ablation were selected for this retrospective analysis. All patients included in this analysis had only epicardial LAVA and had recurrent episodes of drug-refractory VT. Scar location was further delineated using DE-MRI, MDCT, and electroanatomical mapping (EAM) system. All patients underwent chest X-ray, 12-lead ECG, and a pre- or periprocedural coronary angiography. The study was approved by the Institutional Review Board at Hôpital Haut-L'évêque.

MRI/MDCT Imaging

DE-MRI was performed prior to ablation using a 1.5 T MRI scanner equipped with a 32-channel cardiac coil (Avanto, Siemens Medical Solutions, Erlangen, Germany). This 3-dimensional (3-D), inversion-recovery–prepared, ECG-gated, respiration-navigated gradient-echo pulse sequence with fat saturation was initiated 15 minutes after intravenous injection of 0.2 mmol/kg gadoterate meglumine. Contrast-enhanced, ECG-gated cardiac MDCT was performed immediately following MRI study using a 64-slice CT scanner (SOMATOM Definition, Siemens Medical Solutions, Forchheim, Germany). Identical body positions were used for CT and MRI. Images were acquired during an expiratory breath hold with tube current modulation set on end diastole. CT angiographic images were acquired during the injection of a 120 mL bolus of iomeprol 400 mg I/mL (Bracco, Milan, Italy) at a rate of 4 mL/s, and reconstructed at the same phase as the one used for DE imaging. Scar on MRI was defined as delayed enhancement of gadolinium and scar on MDCT was defined as a zone of wall thinning <5 mm. All preprocedural images were incorporated using dedicated software (the MUSIC platform) in order to create a 3-D model with anatomical and scar information. This model was then integrated in the EAM system and used for fusion of scar area, wall thinning, phrenic nerve, and coronary artery visualization.[12]

Electrophysiology (EP) Study and Ablation Technique

An endocardial and epicardial substrate map was constructed in all patients. Automatic peak-to-peak voltage measurement of the electroanatomical (EAM) system was used. Electroanatomical maps (endocardial and/or epicardial) were merged with MRI/MDCT images in CARTO®3 (Biosense Webster, Diamond Bar, CA, USA) or Ensite™ Velocity (St. Jude Medical, St. Paul, MN, USA) system. A percutaneous anterior epicardial approach was gained prior to the transseptal puncture. A steerable sheath (small curve Agilis™, St. Jude Medical) was used during the procedure. Epicardial mapping was performed using a 20-electrode mapping catheter (Pentaray®NAV, Biosense Webster) and/or an ablation catheter (Navistar® Thermocool®, Biosense Webster). Endocardial mapping was performed using an ablation catheter (Navistar® Thermocool®, Biosense Webster) after obtaining retrograde or transseptal access. When transseptal access was performed, a steerable sheath (long curve Agilis™, St. Jude Medical) was used. High-density substrate mapping and pacemapping was performed in the region of interest. If VT was tolerated, activation and entrainment mapping was performed. Endocardial and/or epicardial ablation was performed with an irrigated catheter (Navistar® Thermocool®, Biosense Webster). Substrate-based LAVA ablation during sinus rhythm was performed in all patients. A combined end point of complete LAVA elimination and noninducibility of VT was used for these procedures.

Image Merging, EAM versus Scar

Anatomy, scar segmentation from DE-MRI, and wall thinning area on MDCT were used to generate 3-D meshes merged in the MUSIC platform and registered in the localization system. Quantitative correlation between scar size on DE-MRI, wall thinning area on MDCT, and low-voltage area on the substrate map was measured on the EAM system as a percentage of area overlap (after image integration and image merge) between the delayed enhancement area on DE-MRI, the wall thinning area on MDCT and the scar area on EAM, all measured with the area measurement tool (Fig. 1).

Two types of voltage maps were generated with the localization system. The first one was the standard map with automatic detection of the potentials for automatic peak-to-peak measurement of the amplitude. This type of map was therefore based on the analysis of the highest amplitude component of the EGM (high-amplitude normal activity, abbreviated HANA). On contrary, the second type of maps was manually adjusted and based on LAVA signals, usually delayed and of lower amplitude (Fig. 2). Each map was displayed using unipolar and bipolar signals. In an effort to better characterize the EP substrate, we investigated all the previously described thresholds in the literature for comparison with the scar as displayed by DE-MRI and CT scan (Fig. 3). The activation maps with LAVA signals being tagged were also used for similar analysis. Distance from LAVA to the scar border is measured on the EAM system with dedicated software.

Prevention of Complications

We used the left atrium with the pulmonary veins and the left atrial appendage as well as the coronary sinus to obtain an accurate merge of imaging segmentation on the EAM. When ablation was needed close to coronary artery—within 1 cm based on MDCT segmentation—a coronary angiography was performed to ascertain the good merge. A minimum distance of >5 mm from the coronary artery was set as a threshold for radiofrequency (RF) delivery. In addition to the phrenic nerve segmentation from MDCT (Fig. 4D), we performed a periprocedural pacemap of the phrenic nerve and tagged its course on the EAM substrate map. Before any ablation in this area, pacing at 10 mA and 2 milliseconds was performed to ensure the absence of phrenic nerve capture. If epicardial RF delivery was required close to the phrenic nerve, it was removed by previously described means.[13]

Statistical Analysis

For statistical analysis, we used SPSS 16 software. Continuous variables are summarized by mean ± standard deviation or median and first and third interquartile (IQ_1, IQ_3), depending on the normality of distribution, as assessed by normal probability and quartile plots. Categorical variables are represented by frequencies and percentages. Two group comparisons were measured with paired Student's *t* test. Because of insufficient data (small patient numbers)

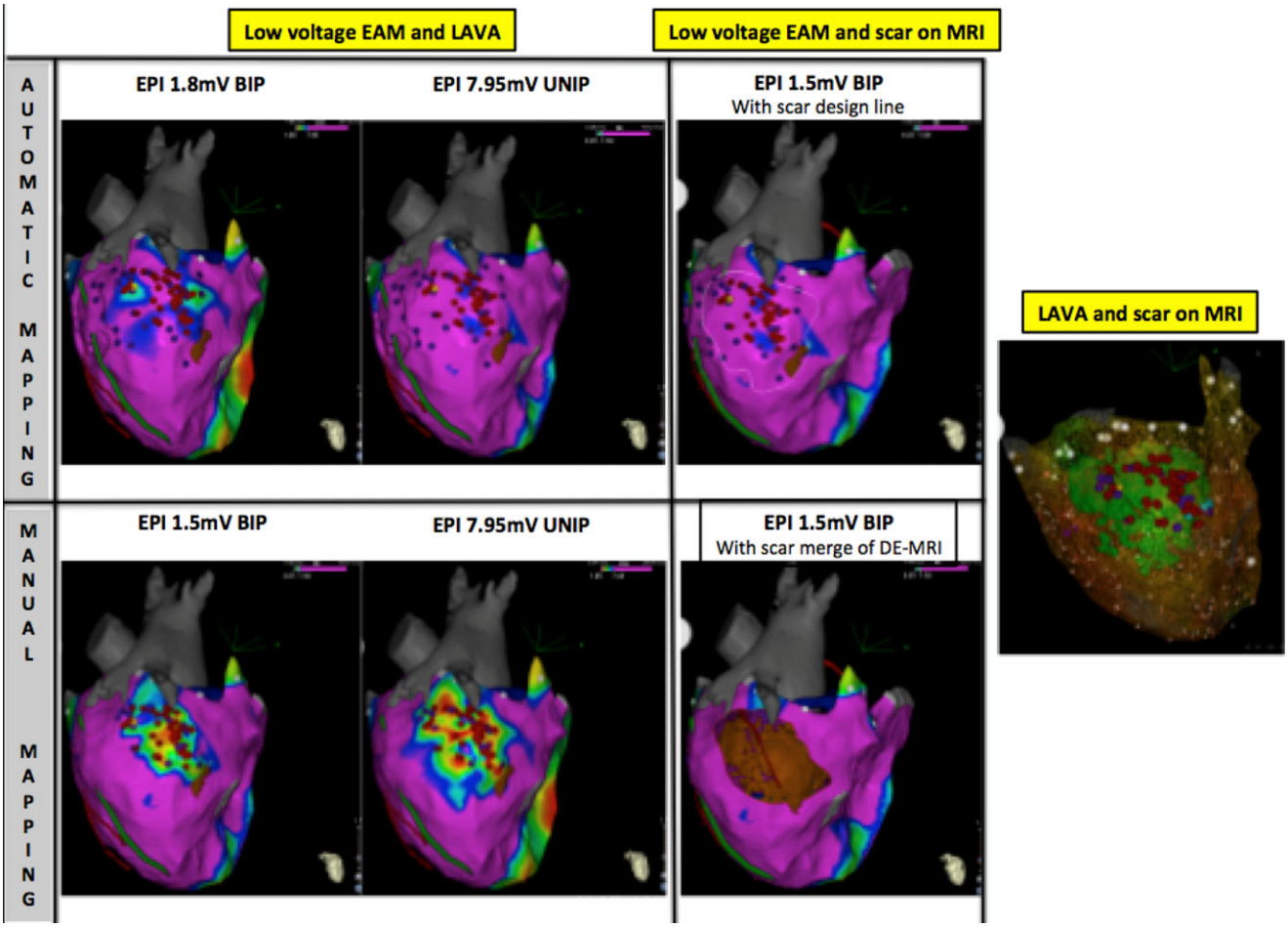

Figure 1. *Relationship between low-voltage area, LAVA, and scar on DE-MRI. Examples of epicardial substrate maps of the same patient. Upper panel: Epicardial HANA maps. Bipolar and unipolar map show both few overlap between the low-voltage area and scar on DE-MRI, presented as a white outline (third image). Lower panel: Epicardial LAVA maps. Both bipolar and unipolar map show better overlap between the low-voltage area and scar on DE-MRI. Scar is merged and substrate map is cut out in third image. Right panel: Correlation between LAVA and scar on DE-MRI.*

to make a statistical correlation coefficient, the percentage of area overlap—after image merge and image integration—between DE-MRI, MDCT, and EAM as an "*quantitative indicator of correlation*."

Results

Prevalence

Between 2008 and 2013, 189 patients with NICM underwent a VT ablation at CHU Bordeaux. Based on these findings, we found an epicardial-only scar in 6.3% of NICM patients (12/189).

Patient Characteristics

Coronary angiography in all patients demonstrated normal coronary arteries. Ten patients had an implantable cardioverter defibrillator (ICD) implanted and 8 patients had diminished (49 ± 14%) left ventricular ejection fraction. Nine patients had a clear history of myocarditis (5 ± 5 years prior to ablation) with hospitalization at the acute phase. The 3 remaining patients had a suggestive history of thoracic pain, normal coronary angiogram, and typical scar location; however, in the absence of hospitalization during the index episode. Baseline patient characteristics are summarized in Table 1.

Imaging Characteristics

Magnetic resonance imaging

DE-MRI data were obtained in 7 patients who either did not have an ICD or were awaiting ICD implantation. Scar on MRI was seen in lateral (n = 4), inferolateral (n = 2), laterobasal (n = 3), and apical (n = 3) regions of the left ventricle (multiple zones possible for 1 patient). Non-transmural epicardial-only scar was seen in all patients and surface area was 52 cm^2 (IQ_1:38, IQ_3:59). MRI characteristics are included in Table 2. Examples of epicardial-only late gadolinium enhancement are illustrated in Figure 2.

Multidetector computed tomography

MDCT data were obtained in 8 patients. Wall thinning was seen in 7 patients: lateral (n = 5) and inferolateral (n = 2). One patient did not have wall thinning on MDCT. We encountered a surface area of 18 cm^2 (IQ_1:14, IQ_3:35) using a <5 mm wall thickness cut-off. MDCT characteristics

TABLE 1

Baseline Characteristics

Patient	Age (Yrs)	M/F	LVEF (%)	ICD	AAD	Side Effects	CT Image	<5 mm Wall Thinning on MDCT	Scar Area on DE-MRI	Location of Scar on Imaging
1	57	M	40%	1	amio		NA	NA	27.3 cm^2	Inferolateral and high lateral
2	55	M	40%	1	amio	Hyperthyroid	Wall thinning lateral	50 cm^2	52 cm^2	Lateral
3	71	M	20%	CRT-D	amio	Hyperthyroid	NA	NA	NA	NA
4	55	M	60%	1	BB		NA	NA	NA	NA
5	41	F	55%	1	amio	Hyperthyroid	Wall thinning lateral	61 cm^2	79 cm^2	Lateral and apical
6	34	M	45%	1	BB		Wall thinning lateral	14 cm^2	34 cm^2	Laterobasal scar
7	33	M	55%	0	amio		Wall thinning lateral	12 cm^2	52 cm^2	Lateral and apical
8	72	M	45%	1	amio	Hyperthyroid	Wall thinning inferolateral	30 cm^2	NA	Lateral
9	31	M	67%	1	BB		Wall thinning lateral	15 cm^2	NA	Laterobasal and apical
10	42	M	45%	0	amio		No wall thinning	6 cm^2	65 cm^2	Laterobasal
11	55	M	54%	0	BB		Wall thinning inferolateral	21 cm^2	42 cm^2	Inferolateral
12	38	M	60%	1	sotalol		NA	NA	NA	NA
Mean	**49 ± 14**		**49 ± 12**							
Median								**18**	**52**	
IQR								**(IQ_1:14, IQ_3:35)**	**(IQ_1:38, IQ_3:59)**	

AAD = antiarrhythmic drugs; amio = amiodarone; BB = beta-blocker; CRT = cardiac resynchronization therapy; cm = centimeter; DE = delayed enhancement; F = female; ICD = implantable cardioverter defibrillator; IQR = interquartile range; LVEF = left ventricular ejection fraction; M = male; Yrs = years.

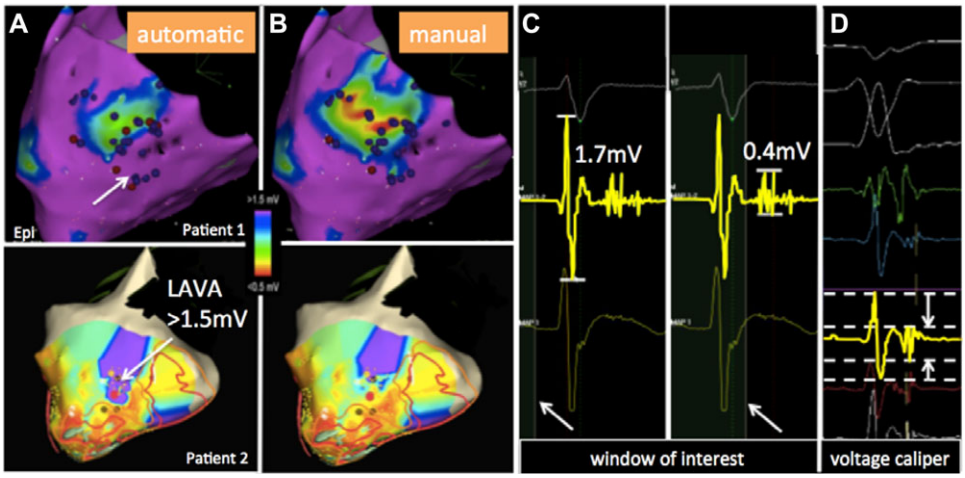

Figure 2. *Automatic EAM mapping compared to manual correction of bipolar peak-to-peak LAVA voltage. A: Automatic bipolar HANA voltage map and LAVA annotation. Few zones of low voltages and most LAVA in zones of normal bipolar voltage. Patient 1 with CARTO® 3 system (Biosense Webster) and patient 2 with EnSite™ Velocity™ system (St. Jude Medical). B: Manual bipolar LAVA voltage map shows better delineation of the low-voltage area with almost all LAVA inside this zone. Same voltage scale gives the impression of a channel inside the scar. C: CARTO® 3 system: Manual mapping by changing the window of interest to the LAVA signal (patient 1). D: EnSite™ Velocity™ system: Manual adaptation of voltage caliper to the LAVA signal (patient 2).*

TABLE 2
Mapping Characteristics

Patient	EAM System	Map Points ENDO	Map Points EPI	Low-Voltage Area, ENDO (cm^2)	HANA Low-Voltage Area, EPI (cm^2)	LAVA Low-Voltage Area, EPI (cm^2)	EPI Location of LAVA
1	CARTO 3	155	109	11	6	25	Inferolateral
2	CARTO 3	213	114	1	24	39	Lateral
3	CARTO 3	0	149	0	37	65	Inferior
4	EnSite	234	855	11,7	25	26	High lateral
5	CARTO 3	90	368	9	62	75	Inferolateral and apical
6	CARTO 3	90	259	1	11	18	Latero basal
7	EnSite	317	1,385	2,5	45	50	Inferolateral and apical
8	EnSite	253	626	12	50	53	Inferolateral basal-apical
9	CARTO 3	105	524	0	30	39	Lateral basal-apical
10	CARTO 3	165	581	0	24	41	Lateral
11	CARTO 3	446	1,334	0	19	28	Inferolateral
12	CARTO 3	140	665	0	22	30	Inferolateral
Mean		**184 ± 119**	**581 ± 435**				
Median				**1**	**25**	**39**	
IQR				**(IQ_1:0, IQ_3:10)**	**(IQ_1:22, IQ_3:39)**	**(IQ_1:38, IQ_3:51)**	

cm = centimeter; EAM = electroanatomical mapping; ENDO = endocardial; EPI = epicardial; IQR = interquartile range.

are included in Table 2. An example of wall thinning and possible (anatomical) isthmus is illustrated in Figure 4.

EGM Characteristics

In 11/12 patients, combined endocardial and epicardial EAM maps were acquired with 160 (IQ_1:101, IQ_3:139) endocardial and 553 (IQ_1:232, IQ_3:713) epicardial map points obtained per patient. A total of 443 LAVA were recorded in the entire series, but only epicardially.

Bipolar voltage automatic HANA mapping with EAM system demonstrated a median low-voltage area of 1 cm^2 (IQ_1:0, IQ_3:10) endocardial and 25 cm^2 (IQ_1:22, IQ_3:39) epicardial and 39 cm^2 (IQ_1:28, IQ_3:51) when manual editing of the epicardial map (LAVA mapping) was performed (Fig. 3).

No endocardial unipolar low-voltage area <8.3 mV was found in the 11 patients where endocardial mapping was performed. A subanalysis in the 7 patients who received a DE-MRI was performed and a mean epicardial unipolar low-voltage area <7.95 mV of 118 ± 55 cm^2 was observed.

LAVA were found epicardially in normal unipolar and bipolar voltage regions in 35% (IQ_1:32, IQ_3:41) of the recorded EGMs with automatic EAM mapping (183 of 443 LAVA in truly normal voltage area). On the contrary, manual editing of the voltage maps toward LAVA resulted in only 3% (0, 9) of LAVA in normal voltage area (26/443 of LAVA in truly normal voltage area; automatic vs. manual; $P < 0.05$; Figs. 2 and 3; Table 3). LAVA were seen in lateral (n = 5), inferolateral (n = 6), inferior (n = 1), and apical (n = 4) regions of the left ventricle (LAVA can appear in different regions in 1 patient). All LAVA were found within 20 mm of DE-MRI scar and within 5 mm of the bipolar low-voltage area on EAM. EGM characteristics are shown in Table 2.

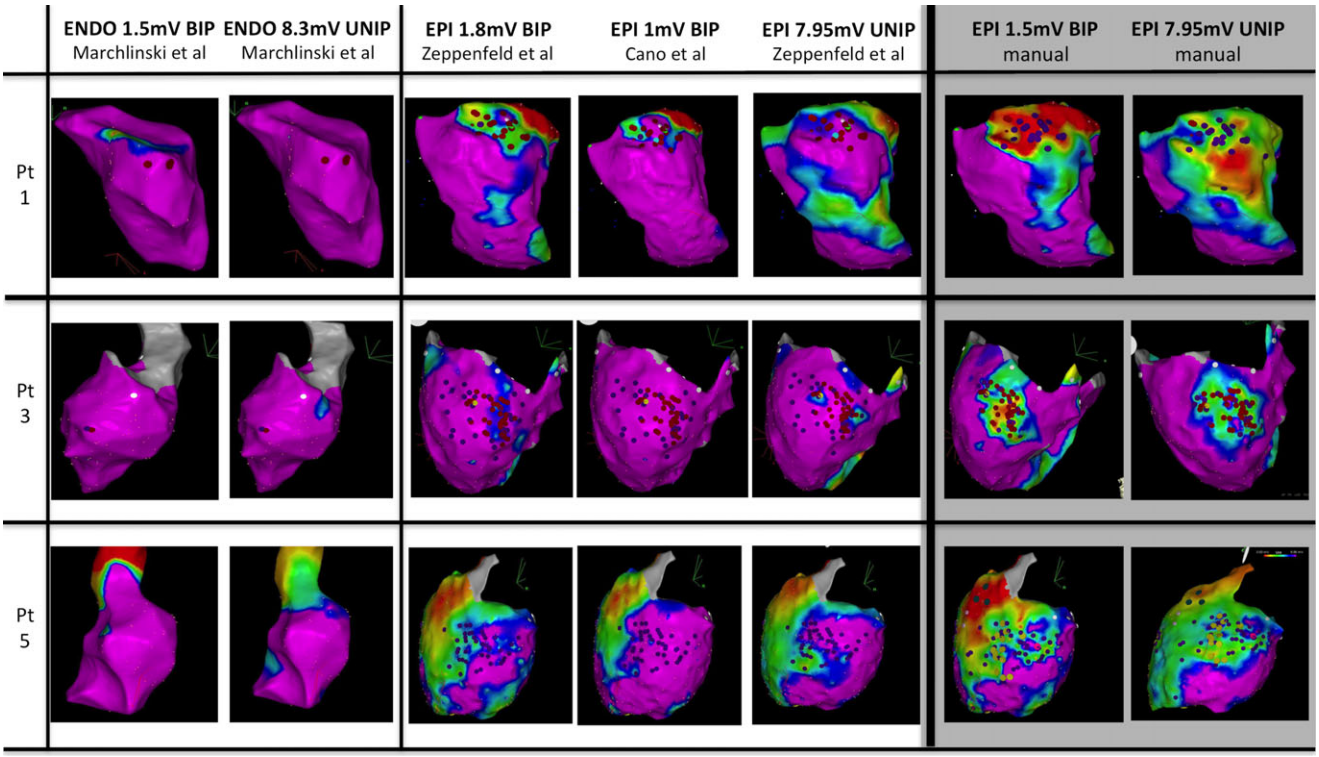

Figure 3. *Different reference values for unipolar and bipolar voltage (endocardial and epicardial) with automatic mapping versus manual adaptation. From left to right. Examples of endocardial and epicardial substrate maps of 3 patients. Left column indicates the corresponding patient, numbered as in the tables. Left section: Endocardial HANA maps. First column shows almost normal unipolar endocardial voltage in all patients. A unipolar voltage <8.3 mV suggests intramural or epicardial scar. Middle section: Epicardial HANA maps. Different bipolar and unipolar thresholds used. Thirty-five percent of LAVA in truly normal voltage regions (wide, split, and late potentials not included in this area). Right section: Manual LAVA maps. Both bipolar and unipolar maps. Only 3% of LAVA in truly normal voltage regions.*

TABLE 3
LAVA in Normal Voltage According to Automatic and Manual Mapping

Automatic versus Manual ($P < 0.05$)	LAVA in Normal Bipolar Voltage	LAVA in Low Bipolar Voltage
Automatic HANA mapping	35%	65%
Manual LAVA mapping	3%	97%

HANA = high-amplitude normal activity; LAVA = local abnormal ventricular activity.

Comparison of EAM Low-Voltage Area and Imaging

Bipolar low-voltage area versus scar on MRI

The percentage of overlap between low-voltage area and scar on DE-MRI was significantly higher with manual, as opposed to automatic measurement (76% [IQ_1:66, IQ_3:94], vs. 45% [IQ_1:35, IQ_3:62]; $P = 0.04$).

Bipolar low-voltage area versus wall thinning on MDCT

The percentage of overlap between low-voltage area and wall thinning on MDCT was similar using manual and automatic measurement (55% [IQ_1:43, IQ_3:69] vs. 64% [IQ_1:35, IQ_3:79]; $P = 0.9$).

DE-MRI and MDCT compared to manual LAVA mapping

The scar area on DE-MRI was larger than the LAVA area (52 [IQ_1:38, IQ_3:59] cm^2 vs. 39 [IQ_1:27, IQ_3:45] cm^2; $P = 0.45$) while the wall thinning area was smaller measured by MDCT (18 [IQ_1:14, 35] cm^2 vs. 39 [IQ_1:34, IQ_3:47] cm^2; $P = 0.1$).

Unipolar low-voltage area and DE-MRI

In 2 patients, 0% overlap (all low-voltage area outside the MRI scar) was found and in the remaining 5 patients a 100% area overlap was found, with an additional mean low-voltage area of 83 ± 37 cm^2 outside the MRI scar.

Combined Epicardial and Endocardial Approach

A combined epicardial and endocardial approach was used for VT ablation in 11 out of 12 patients. In the remaining patient, an epicardial approach alone was used (100% epicardial approach in all patients) because of earlier failure of endocardial ablation. In 11 patients, percutaneous epicardial access was gained. In 1 patient, surgical left lateral minithoracotomy was performed after a failed percutaneous attempt at pericardial access due to adhesions from prior cardiac surgery.

RF Ablation

In order to achieve the end point of complete LAVA elimination, an attempt to ablate epicardial LAVA recorded with a Pentaray®NAV (Biosense Webster) from inside the endocardium was performed in 7 patients and failed in all. The second end point of non-inducibility was not tested after these ablation attempts. Therefore, epicardial ablation was needed in all patients. Complete LAVA elimination was not

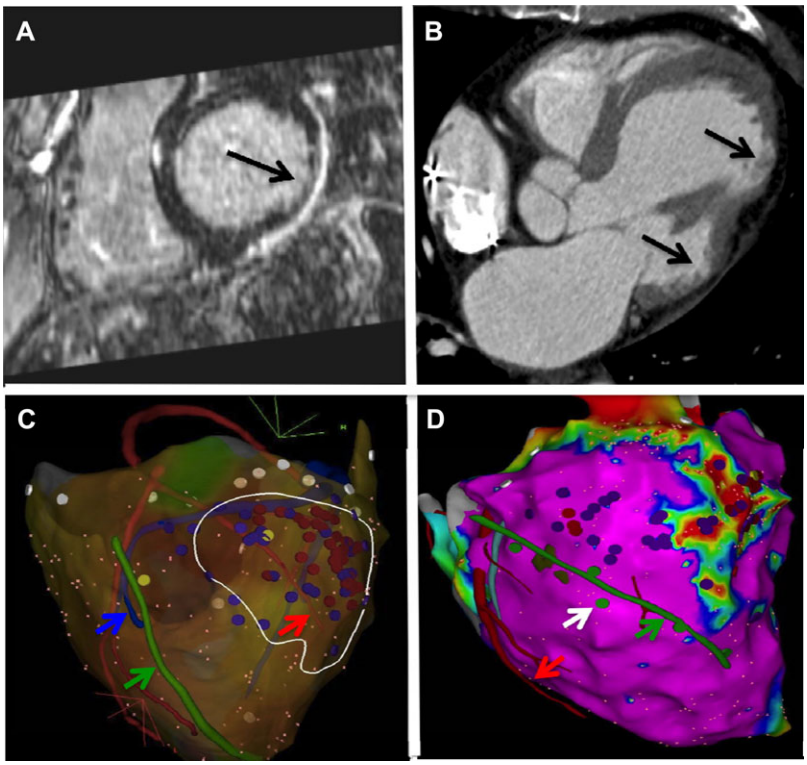

Figure 4. *Advantages of preprocedural MRI and MDCT and periprocedural phrenic imaging. A: DE-MRI image shows supepicardial scar without transmurality (black arrow). B: MDCT image shows 2 zones of focal wall thinning (black arrows) and a possible anatomical isthmus in between. C: Image merge into EAM system. MDCT segmentation of coronary arteries (red arrows), phrenic nerve (green arrow), and coronary venous system (blue arrow). Ablation is performed >5 mm away from the coronary arteries. White outline represents scar on MRI. D: Image merge into EAM system. MDCT segmentation of the phrenic nerve. Phrenic nerve capture at 20 mA, 2 milliseconds is annotated (green tags), showing good correlation with segmented phrenic nerve. No ablation was performed in areas with green tags.*

TABLE 4

Ablation Characteristics

Pt	Ablations (n)	First Ablation	Last Ablation	Total RF Time (minutes)	epi RF Time (minutes)	Procedure Time (minutes)	LAVA Elimination	Inducible at Start	Not Inducible After	FU (Months)	VT Recurrence
1	1	endo + epi		34	34	490	Complete	1	1	48	0
2	2	endo only	endo + epi	36	30	450	Complete	1	1	47	0
3	3	endo only	epi (surgical)	17	15	315	Complete	0	1	57	After 3 months
4	2	endo only	endo + epi	11	11	215	Complete	1	1	26	0
5	2	endo only	endo + epi	18	21	240	Complete	1	1	22	0
6	1	endo + epi		62	26	190	Complete	1	1	21	0
7	1	endo + epi		30	23	310	Incomplete	1	1	37	0
8	3	endo only	endo + epi	38	38	260	Complete	1	1	32	0
9	1	endo + epi		26	25	240	Complete	0	1	15	0
10	1	endo + epi		27	18	310	Complete	1	1	14	After 3 months
11	1	endo + epi		21	21	240	Incomplete	0	1	7	0
12	1	endo + epi		13	13	240	Incomplete	0	1	11	0
Mean	1.6			28 ± 14	23 ± 8	292 ± 92				28 ± 16	

endo = endocardial; epi = epicardial; FU = follow-up; min = minutes; PS = partial success; RF = radiofrequency; S = complete success; sec = second; VT = ventricular tachycardia.

achieved in 3 patients: 2 patients had LAVA with <5 mm distance from the coronary arteries and 1 patient had phrenic capture at a target ablation site. Mean total RF time was 28 ± 14 minutes with 23 ± 8 minutes of epicardial RF time and procedure time was 292 ± 92 minutes. Ablation data are included in Table 4.

Ablation End Points

The end point of complete LAVA elimination was obtained in 9 patients (75%). The end point of noninducibility was obtained in all patients at the end of the ablation procedure, but VT was only inducible in 8 patients (67%) at the start of the procedure. End point data are included in Table 4.

Complications

One complication was observed in the first patient of the series in 2008: a symptomatic left phrenic nerve paralysis, which recovered 6 months following the procedure. In 7 patients, the ablation sites were close to coronary arteries (n = 3) or to the left phrenic nerve (n = 4). Ablation was guided by merged image integration obtained from MDCT/MRI with the MUSIC platform showing phrenic nerve (Fig. 4) and coronary arteries. Three patients received saline infusion into the pericardial space in order to increase the distance to the phrenic nerve and to perform ablation safely. This strategy allowed for complete LAVA elimination.

Follow-Up

After a mean follow-up of 28 ± 16 months, recurrence of VT was seen in 2 patients (16.7%). No patients died during follow-up. Follow-up data are included in Table 4.

Discussion

The main findings of this study are the following:

(1) We demonstrate that a subgroup of postmyocarditis patients with an epicardial-only scar is found in 6.3% of NICM patients referred for VT ablation.
(2) Preprocedural imaging, particularly when using DE-MRI, can reveal this epicardial-only scar.
(3) These patients have distinct scar characteristics with no endocardial LAVA. In addition, 35% of epicardial LAVA are recorded within normal (>1.5 mV) bipolar voltage EGM demonstrating the limitations of automatic voltage map in this condition.
(4) Manual LAVA adjusted voltage mapping is feasible and superior to automatic standard voltage mapping showing better quantitative correlation with DE-MRI scar.
(5) Epicardial ablation is needed in postmyocarditis patients to achieve LAVA elimination.
(6) After a mean follow-up of >24 months, recurrence of VT occurred in 17% of patients.

The findings of the study demonstrate that automatic epicardial voltage mapping was of very little clinical value in this patient population with epicardial VT. In this subset of patients, a thin nontransmural scar is observed. Interestingly, endocardial unipolar voltage mapping was of no value in this patient population as it did not predict epicardial scar in any patient. Furthermore, epicardial unipolar voltage mapping showed no correlation with the scar in some patients and a good but not specific correlation in other patients. This is possibly due to the fact that unipolar voltage is depending on both myocardial wall thickness and scar thickness. Additional information has to be gained to treat these patients. Preprocedural MRI imaging or a careful manual annotation of epicardial abnormal potentials can help to visualize the scar.

Automatic LAVA mapping integration into an EAM system could lead to LAVA activation maps and to a better understanding of the electrical conduction inside the scar. It raises the question of spatial resolution of EGM recorded by the ablation catheter. Therefore, manual mapping is particularly useful in small scar without or with minimal wall thinning. In a recently published study, Macabelli *et al.* reported that using a bipolar epicardial voltage threshold <1 mV epicardial-only scar was only detectable in 63% of patients with postmyocarditis VT.[14] In comparison, using manual mapping with an epicardial bipolar voltage threshold of <1.5 mV, we were able to detect epicardial-only scar in 100% of patients.

Epicardial substrate mapping is more challenging due to the presence of epicardial fat. Epicardial fat can mimic low voltage but not fragmentation or prolonged duration. Manual mapping is time consuming and automatic LAVA mapping could result in better electrical scar characterization with visualization of the conduction inside the scar. An alternative to manual mapping is the annotation of abnormal potentials (split, fragmented of prolonged duration) as potential ablation targets on the substrate map.

In keeping with the findings from Cochet *et al*., we demonstrate that all LAVA appear within the scar area with a border of 20 mm.[12] Furthermore, LAVA typically were closely coupled in the border zone, of higher amplitude epicardially and appeared later after QRS onset, with low amplitude and a high degree of fragmentation deeper into the scar.

Furthermore, targeting epicardial LAVA from endocardium was ineffective at sites where neither endocardial LAVA nor wall thinning were present.[15] In these patients, an epicardial approach was required in all patients. It is our opinion that an epicardial-only ablation procedure could be considered in this subgroup of patients.

The results of this study demonstrate the importance of preablation imaging with MRI/MDCT in order to obtain a clear view of the location of the scar. MDCT does not detect areas of fibrosis directly, but rather delineates areas of wall thinning as a surrogate marker for scar. This technique is particularly useful in most types of NICM, although in myocarditis patients wall thinning is less apparent, which can explain the worse correlation compared to DE-MRI.[16] For this reason, we routinely perform a systematic MRI/MDCT acquisition before each ICD implantation.

We observed a good quantitative correlation between epicardial LAVA sites, and epicardial-only scar on DE-MRI, but smaller areas of wall thinning were observed with MDCT. These imaging findings and a normal coronary angiogram and a patient history (a clear history of acute myocarditis in 9 patients and a suggestive history in the other 3 patients) are strongly suggestive for myocarditis.

Limitations

This is only a small cohort retrospective single-center study. We further did not evaluate data in nonischemic patients with transmural scar. Further analysis is needed to evaluate epicardial bipolar peak-to-peak LAVA voltage in those patients.

Conclusion

In postmyocarditis patients with epicardial-only scar, automatic voltage mapping may miss or underestimate the electrical VT substrate. Epicardial LAVA are found in apparent normal bipolar voltage regions. DE-MRI and manual LAVA voltage mapping are necessary to visualize the entire scar.

References

1. Aliot EM, Stevenson WG, Almendral-Garrote JM, Bogun F, Calkins CH, Delacretaz E, Della Bella P, Hindricks G, Jais P, Josephson ME, Kautzner J, Kay GN, Kuck KH, Lerman BB, Marchlinski F, Reddy V, Schalij MJ, Schilling R, Soejima K, Wilber D, European Heart Rhythm Association, Registered Branch of the European Society of Cardiology, Heart Rhythm Society, American College of Cardiology, American Heart Association: EHRA/HRS Expert consensus on catheter ablation of ventricular arrhythmias: Developed in a partnership with the European Heart Rhythm Association (EHRA), a registered branch of the European Society of Cardiology (ESC), and the Heart Rhythm Society (HRS); in collaboration with the American College of Cardiology (ACC) and the American Heart Association (AHA). Heart Rhythm 2009;6:886-933.
2. Jais P, Maury P, Khairy P, Sacher F, Nault I, Komatsu Y, Hocini M, Forclaz A, Jadidi AS, Weerasooryia R, Shah A, Derval N, Cochet H, Knecht S, Miyazaki S, Linton N, Rivard L, Wright M, Wilton SB,

Scherr D, Pascale P, Roten L, Pederson M, Bordachar P, Laurent F, Kim SJ, Ritter P, Clementy J, Haissaguerre M: Elimination of local abnormal ventricular activities: A new end point for substrate modification in patients with scar-related ventricular tachycardia. Circulation 2012;125:2184-2196.

3. Vergara P, Trevisi N, Ricco A, Petracca F, Baratto F, Cireddu M, Bisceglia C, Maccabelli G, Della Bella P: Late potentials abolition as an additional technique for reduction of arrhythmia recurrence in scar related ventricular tachycardia ablation. J Cardiovasc Electrophysiol 2012;23:621-627.
4. Tokuda M, Tedrow UB, Kojodjojo P, Inada K, Koplan BA, Michaud GF, John RM, Epstein LM, Stevenson WG: Catheter ablation of ventricular tachycardia in nonischemic heart disease. Circ Arrhythm Electrophysiol 2012;5:992-1000.
5. Dinov B, Fiedler L, Schonbauer R, Bollmann A, Rolf S, Piorkowski C, Hindricks G, Arya A: Outcomes in catheter ablation of ventricular tachycardia in dilated non-ischemic cardiomyopathy in comparison to ischemic cardiomyopathy: Results from the prospective HEart centre of LeiPzig VT (HELP–VT) study. Circulation 2014;129: 728-736.
6. Liuba I, Marchlinski FE: The substrate and ablation of ventricular tachycardia in patients with nonischemic cardiomyopathy. Circ J 2013;77:1957-1966.
7. Garcia FC, Bazan V, Zado ES, Ren JF, Marchlinski FE: Epicardial substrate and outcome with epicardial ablation of ventricular tachycardia in arrhythmogenic right ventricular cardiomyopathy/dysplasia. Circulation 2009;120:366-375.
8. Oduneye SO, Pop M, Biswas L, Ghate S, Flor R, Ramanan V, Barry J, Celik H, Crystal E, Wright GA: Postinfarction ventricular tachycardia substrate characterization: A comparison between late enhancement magnetic resonance imaging and voltage mapping using an MR-guided electrophysiology system. IEEE Trans Biomed Eng 2013;60:2442-2449.
9. Wijnmaalen AP, van der Geest RJ, van Huls van Taxis CF, Siebelink HM, Kroft LJ, Bax JJ, Reiber JH, Schalij MJ, Zeppenfeld K: Head-to-head comparison of contrast-enhanced magnetic resonance imaging and electroanatomical voltage mapping to assess post-infarct scar characteristics in patients with ventricular tachycardias: Real-time image integration and reversed registration. Eur Heart J 2011;32:104-114.
10. Desjardins B, Crawford T, Good E, Oral H, Chugh A, Pelosi F, Morady F, Bogun F: Infarct architecture and characteristics on delayed enhanced magnetic resonance imaging and electroanatomic mapping in patients with postinfarction ventricular arrhythmia. Heart Rhythm 2009;6:644-651.
11. Codreanu A, Odille F, Aliot E, Marie PY, Magnin-Poull I, Andronache M, Mandry D, Djaballah W, Regent D, Felblinger J, de Chillou C: Electroanatomic characterization of post-infarct scars comparison with 3-dimensional myocardial scar reconstruction based on magnetic resonance imaging. J Am Coll Cardiol 2008;52:839-842.
12. Cochet H, Komatsu Y, Sacher F, Jadidi AS, Scherr D, Riffaud M, Derval N, Shah A, Roten L, Pascale P, Relan J, Sermesant M, Ayache N, Montaudon M, Laurent F, Hocini M, Haïssaguerre M, Jaïs P: Integration of merged delayed-enhanced magnetic resonance imaging and multidetector computed tomography for the guidance of ventricular tachycardia ablation: A pilot study. J Cardiovasc Electrophysiol 2013;24:419-426.
13. Matsuo S, Jais P, Knecht S, Lim KT, Hocini M, Derval N, Wright M, Sacher F, Haissaguerre M: Images in cardiovascular medicine. Novel technique to prevent left phrenic nerve injury during epicardial catheter ablation. Circulation 2008;117:e471.
14. Maccabelli G, Tsiachris D, Silberbauer J, Esposito A, Bisceglia C, Baratto F, Colantoni C, Trevisi N, Palmisano A, Vergara P, De Cobelli F, Del Maschio A, Della Bella P: Imaging and epicardial substrate ablation of ventricular tachycardia in patients late after myocarditis. Europace 2014;16:1363-1372.
15. Komatsu Y, Daly M, Sacher F, Cochet H, Denis A, Derval N, Jesel L, Zellerhoff S, Lim HS, Jadidi A, Nault I, Shah A, Roten L, Pascale P, Scherr D, Aurillac-Lavignolle V, Hocini M, Haissaguerre M, Jais P: Endocardial ablation to eliminate epicardial arrhythmia substrate in scar-related ventricular tachycardia. J Am Coll Cardiol 2014;63:1416-1426.
16. Komatsu Y, Cochet H, Jadidi A, Sacher F, Shah A, Derval N, Scherr D, Pascale P, Roten L, Denis A, Ramoul K, Miyazaki S, Daly M, Riffaud M, Sermesant M, Relan J, Ayache N, Kim S, Montaudon M, Laurent F, Hocini M, Haïssaguerre M, Jaïs P: Regional myocardial wall thinning at multidetector computed tomography correlates to arrhythmogenic substrate in postinfarction ventricular tachycardia: Assessment of structural and electrical substrate. Circ Arrhythm Electrophysiol 2013;6:342-350.

D. *In ARVC:* Characterization of the Left-sided Substrate in Arrhythmogenic Right Ventricular Cardiomyopathy.

Submitted as First Review to Circulation Arrhythmia and Electrophysiology.

1. Study outline

In this work we prospectively included 32 ARVC patients who underwent VT ablation at our institution between 2009 and 2014. All received MDCT imaging and RV and LV fat was defined as < -10 Hounsfield Units. A subset of 14 of the patients underwent multipolar epicardial mapping and VT ablation because of sustained VT: 9 with biventricular involvement (BIV) and 4 with RV only involvement. The aim of this study was to compare both groups for clinical characteristics, scar size and amount and density of LAVA and finally arrhythmogenicity.

The agreement between low voltage and fat on MDCT was high on the RV when using either endocardial unipolar or epicardial bipolar data, but lower on the LV. LV LAVA was found in all patients with LV involvement, and none of the others. The density of LAVA within fat areas was similar between the RV and LV.

LV intra-myocardial fat is present on imaging in the majority of patients with ARVC fulfilling the modified Task Force criteria, mostly on lateral, inferior, and apical LV segments, and with a lower burden as compared to the RV.

The number of right-sided PVCs was not different between patients with vs without LV involvement but patients with LV involvement showed a higher number of left-sided PVCs (P=0.02). In the whole population, a total of 39 VTs were observed, either spontaneously or during isoproterenol testing. Two left-sided VTs were observed in patients with LV involvement on imaging, but the association between LV involvement and left-sided VT was not significant.

2. Implications

Our data confirm the results of other radiological and histological studies regarding the high prevalence of biventricular involvement (70-80%) in ARVC. [95, 96,97] To conclude, ARVC is typically regarded as a predominantly right-sided disease with a spectrum of left-sided involvement: RV only ARVC, limited LV involvement or left-dominant involvement.[97] This spectrum translates into different LV arrhythmogenicity from no left-sided VT or PVC, to non-clinical left-sided VT but left-sided PVC in the majority and finally both clinical and non-clinical left-sided VT and PVC respectively.

This study may suggest the need to include LV involvement in the Task Force criteria, which at the present time only focus on right-disease. This is important, since the electrophysiologist needs to analyze this spectrum for the individual patient in order to decide if ablation on the left-sided scar is needed or not. Imaging can help to make this decision.

3. Manuscript

Title: Characterization of the Left-sided Substrate in Arrhythmogenic Right Ventricular Cardiomyopathy.

Manuscript number: CIRCAE/2015/003213

Author(s): Benjamin Berte, CHU Bordeaux Haut L'évêque
Arnaud Denis, Hôpital Cardiologique du Haut-Lévêque & Université Victor Segalen Bordeaux II, LIRYC Institute
Sana Amraoui, University Hospital of Bordeaux
Seigo Yamashita, Hôpital Cardiologique du Haut-Lévêque, CHU de Bordeaux
Yuki Komatsu, Hôpital Cardiologique du Haut-Lévêque, the Université Victor Segalen Bordeaux II, Institut LYRIC, Bordeaux, France
Xavier Pillois, Hôpital cardiologique du Haut Lévèque
Frédéric Sacher, Hôpital Cardiologique du Haut-Lévêque & Université Bordeaux, LIRYC Institute

Saagar Mahida, Hôpital Haut-Lévêque

Jean-Yves Wielandts, CHU Bordeaux

Jean-Marc Sellal, CHU de Nancy & University Hospital Nancy

Antonio Frontera, Bristol Heart Institute

Nora Al Jefairi, CHU Bordeaux

Nicolas Derval, Hôpital Cardiologique du Haut-Lévêque & Université

Victor Segalen Bordeaux II, LIRYC Institute

Michel Montaudon, Centre Hospitalier Universitaire de Bordeaux

François Laurent, Hôpital Cardiologique du Haut-Lévêque & Université

Victor Segalen Bordeaux II, Bordeaux, France

Mélèze Hocini, Hôpital Cardiologique du Haut-Lévêque & Université

Victor Segalen Bordeaux II, LIRYC Institute

Michel Haïssaguerre, Hôpital cardiologique du Haut-Lévêque

Pierre Jaïs, Hôpital Cardiologique Haut Lévêque

Hubert Cochet, CHU / Université de Bordeaux - IHU Liryc / INSERM U1045

Characterization of the Left-sided Substrate in Arrhythmogenic Right Ventricular Cardiomyopathy

Authors list: Benjamin Berte, MD[1,2]; Arnaud Denis, MD[1,2]; Sana Amraoui, MD[1,2]; Seigo Yamashita, MD, PhD[1,2]; Yuki Komatsu, MD[1,2]; Xavier Pillois, MD, PhD[1,2]; Frédéric Sacher, MD, PhD[1,2]; Saagar Mahida, MD[1], PhD; Jean-Yves Wielandts, MD, MSc[1,2]; Jean-Marc Sellal, MD[1,2]; Antonio Frontera, MD[1,2]; Nora Al Jefairi, MD[1]; Nicolas Derval, MD[1,2]; Michel Montaudon, MD, PhD[1,2]; François Laurent, MD[1]; Mélèze Hocini, MD[1,2]; Michel Haïssaguerre, MD[1,2]; Pierre Jaïs, MD, PhD[1,2]; Hubert Cochet, MD, PhD[1,2].

Affiliations:
[1]CHU Bordeaux, France.
[2]LIRYC Institute, IHU Bordeaux, France.

Running title: *Berte et al.* Left-sided substrate in ARVC.

Manuscript word count: 6850 words.

Corresponding author:
Hubert Cochet, MD, PhD
Hôpital Cardiologique du Haut-Lévêque, 33604 Bordeaux-Pessac, France.
Tel: +33 557656542
Fax: +33 557656880
E-mail: hcochet@wanadoo.fr

ABSTRACT

Background: The clinical and electrophysiological correlates of left ventricular (LV) substrate in arrhythmogenic right ventricular cardiomyopathy (ARVC) are largely unknown.

Methods and results: Thirty-two ARVC patients (47±14years, 6 women) were included. RV and LV dysplasia were defined from MDCT and CMR imaging. Arrhythmias were characterized as right-sided or left-sided on 12-lead ECG recordings at baseline and during isoproterenol testing. In 14 patients, the imaging substrate was compared to voltage mapping and local abnormal ventricular activity (LAVA). Imaging abnormalities were found in 32(100%) and 21(66%) patients on the RV and LV, respectively, intra-myocardial fat on MDCT being the most sensitive feature. LV involvement related to none of the Task Force criteria. Right-sided arrhythmias were more frequent than left-sided arrhythmias (P=0.003), although the latter were more frequent in case of LV involvement (P=0.02). The agreement between low voltage and fat on MDCT was high on the RV when using either endocardial unipolar or epicardial bipolar data (k=0.82 and k=0.78, respectively), but lower on the LV (k=0.54 for epicardial bipolar). LV LAVA was found in all patients with LV involvement, and none of the others. The density of LAVA within fat areas was similar between the RV and LV (P=0.57).

Conclusions: LV substrate is frequent in ARVC, but poorly identified by current diagnostic strategies. Left-sided arrhythmias are more frequent in case of LV involvement. LV fat hosts the same density of LAVA as RV fat, but is less efficiently detected by voltage mapping. These results support the need for alternative diagnostic strategies to identify LV dysplasia.

Keywords: Arrhythmogenic right ventricular dysplasia/cardiomyopathy; Left ventricle; Multi-detector computed tomography; Cardiac Magnetic Resonance

INTRODUCTION

Arrhythmogenic right ventricular cardiomyopathy (ARVC) is a condition characterized by progressive fibro-fatty replacement of the subepicardial layers of the ventricular myocardium.[1] This substrate results in the development of a complex heterogeneous scar, which increases susceptibility to ventricular arrhythmia and sudden cardiac death.[2] Although the dysplastic tissue predominantly involves the right ventricle (RV), left ventricular (LV) involvement is not uncommon. Its prevalence in ARVC patients was reported as high as 75% in imaging studies, and up to 88% in histological studies.[3-5] As a majority of studies investigating the arrhythmogenic substrate in ARVC have focused on the right ventricle, there is a relative paucity of data regarding the left-sided substrate.[2,6,7] The aim of the present study was to define the imaging and electrophysiological characteristics of the left-sided ARVC substrate.

METHODS

Population

From January 2009 to November 2014, consecutive patients referred for the diagnosis or the therapeutical management of ARVC were prospectively enrolled. The inclusion criterion was a definite ARVC diagnosis according to the modified 2010 Task Force recommendations.[8] Exclusion criteria were contra-indications to contrast-enhanced multidetector computed tomography (MDCT). All patients underwent a comprehensive diagnostic evaluation comprising clinical evaluation, ECG, signal-averaged ECG, 24-hour Holter, trans-thoracic echocardiography (TTE), and CMR unless contraindicated. These studies were analyzed according to Task Force recommendations. Implantable cardioverter defibrillators (ICDs) were considered as a contra-indication to CMR. Myocardial biopsy was not routinely performed. Genetic testing was not part of the study protocol but available results from

potential prior testing were considered for analysis. In addition, all patients underwent laboratory assessment of renal function, isoproterenol testing, as well as MDCT in order to assess intramyocardial fat. In a sub-population referred for catheter ablation, electro-anatomical maps were acquired and registered to imaging data. The study was approved by the Institutional Ethics Committee, and all patients provided informed consent.

Imaging

Contrast-enhanced ECG-gated cardiac MDCT was performed on a 64-slice CT scanner (SOMATOM Definition, Siemens Medical Solutions, Forchheim, Germany). CT angiographic images were acquired during the injection of 120mL iomeprol 400 mg I/mL (Bracco, Milan, Italy) using a biphasic injection protocol, i.e. 60mL contrast followed by 120mL of a 50:50 mixture of saline and contrast at the rate of 5ml/s. Images were reconstructed in a stack of 1mm-thick slices encompassing the whole heart in short axis orientation. Image processing was performed using dedicated software (MUSIC software, LIRYC institute - Bordeaux university / Inria - Sophia Antipolis, France). Intra-myocardial fat was defined as any myocardial voxel with attenuation less than -10HU, based on prior validation versus contact mapping.[9] This substrate was segmented using an automated image processing method, as described previously,[9-10] and distributed over a biventricular 16-segment model: the RV and LV free walls comprised 7 segments each (3 segments at basal and midventricular levels, i.e. anterior, lateral and inferior, and 1 segment at the apex), and the septum comprised 2 segments (basal and midventricular). CMR imaging was performed on a 1.5T system (Avanto, Siemens Medical Solutions, Erlangen, Germany). Cine imaging was performed using a steady state free precession sequence in 2 stacks of contiguous 6mm-thick slices encompassing the whole ventricles in short axis and 4-chamber orientations. RV and LV volumes and ejection fraction were quantified from cine images using Argus software (Siemens medical systems, Erlangen, Germany). Ventricular dilatation and systolic

dysfunction were defined based on pirorly reported normal values in males and females on the LV[11] and RV.[12] Late gadolinium enhanced imaging was performed 10 min after the injection of 0.2mmol/Kg gadoterate meglumine (Guerbet, Aulnay-sous-bois, France) using a 3D turbo Fast Low Angle Shot sequence in 3 stacks of contiguous 6mm-thick slices encompassing the whole ventricles in short axis, 2-chamber and 4-chamber orientations. Cine and late enhancement images were reviewed by 2 observers analyzing the images in consensus. On each RV and LV segment, regional wall motion was described as either normal or abnormal and regional fibrosis was described as either present or absent. After image analysis, LV involvement was considered present if one or more LV segments (excluding the 2 septal segments) exhibited either fat on MDCT, fibrosis on CMR, or wall motion abnormalities on CMR.

Arrhythmia characterization

In all patients, ventricular arrhythmias were characterized from 12-lead ECG recordings at baseline and during isoproterenol testing. Isoproterenol testing was performed after withdrawal of β-blockers, calcium channel blockers, and other antiarrhythmic agents for ≥5 half-lives. Equipment for cardiopulmonary resuscitation was readily accessible in the room during the test. A continuous infusion of isoproterenol at the rate of 45 micrograms/min was administered for 3 minutes, regardless of heart rate. The 12-lead ECG (recorded at 25 mm/s and 10 mm/mV) was continuously recorded from the beginning of infusion and until 10 minutes after the cessation of infusion. In case of VT, the infusion was immediately stopped and a β-blocker (atenolol 5 mg for 1 minute) was injected intravenously. Each episode of single premature ventricular complex (PVC), run of non-sustained VT or sustained VT was analyzed to define the VT exit site. A V1-positive morphology was always defined as a left-sided exit.[13,14] In addition, an R/S amplitude of ≥ 30% in V1 or V2 combined with a R-wave

duration ≥50% of the total QRS duration in V1 was also considered as a left-sided exit.[15] A V1-negative morphology was defined as a right-sided exit.[13,14]

Contact mapping

Contact mapping was performed using a 3D mapping system (CARTO3, Biosense Webster, Diamond Bar, CA). Endocardial mapping was performed via a femoral venous approach, and all patients also underwent epicardial mapping via a sub-xyphoid approach. High-density substrate mapping was performed on complete epicardial (a fill threshold <15 for the entire epicardium was used) and RV endocardial surfaces with a multipolar catheter (PentaRay®NAV, Biosense Webster, Diamond Bar, CA). Endocardial and epicardial bipolar voltage maps were created using peak-to-peak amplitudes of <0.5mV to indicate dense scar, from 0.5 to 1.5mV to indicate borderzone on the endocardium, and from 0.5 to 1mV to indicate borderzone on the epicardium.[16-18] In addition, endocardial and epicardial unipolar voltage maps were created using thresholds of <5.5mV and <7.95mV to define low voltage, respectively.[19-21] Besides voltage, all sites exhibiting local abnormal ventricular activity (LAVA), as defined previously,[22] were tagged on the substrate map. VT inducibility was tested at the beginning and at the end of the procedure from 2 pacing sites on RV apex and RVOT, using a decreasing pacing train (600ms-500ms-400ms) and up to 3 extrastimuli. If hemodynamically tolerated, activation mapping and ablation were performed during VT. Differentiation between right-sided and left-sided VT exits was annotated. In case of unstable or poorly tolerated VT, the 12-lead ECG alone was used to define the exit site. Ablation was conducted using complete right-sided LAVA elimination and non-inducibility of any VT as procedural endpoints. Left-sided LAVA ablation was only conducted in case a left-sided VT was observed either at baseline, during isoproterenol testing or during the stimulation protocol.

Post-hoc Analysis

Intramyocardial fat areas were mapped onto endocardial and epicardial geometries as segmented from MDCT images. The resulting patient specific 3D meshes were loaded in 3D mapping systems. The following anatomical landmarks were used to initiate point-based registration between the imaging and mapping geometries: coronary sinus, RV apex, and tricuspid annulus (3, 6, 9, and 12 o'clock). Registration was then refined using automatic surface registration. Once registration was achieved, myocardial fat and low voltage were distributed over 3 separate segmentations: RV endocardium (9 segments including the septum), RV epicardium (7 segments), and LV epicardium (7 segments). In addition, areas of fat and low voltage were manually contoured, their extent being expressed in cm^2. In order to minimize the effect of epicardial fat on low voltage area measurements, the anterior interventricular sulcus and the atrioventricular grove (defined as the first centimeter from mitral and tricuspid annuli) were not considered for segmentation when contouring epicardial low voltage areas.[23] The distribution of LAVA sites with respect to this substrate was analyzed, and the density of LAVA sites per cm^2 of substrate was assessed and compared between the RV and the LV.

Statistical analysis

Continuous variables were expressed as mean ± standard deviation for normally distributed data or median [interquartile range: 25^{th}-75^{th} percentile] for non-normally distributed data. Categorical data were expressed as counts and percentages. Data were tested for normality by using the Kolmogorov-Smirnov test. Continuous variables were compared using independent-sample parametric (unpaired Student's t-test) or non-parametric tests (Mann-Whitney) depending on data normality. Categorical variables were compared using Fisher's exact or $\chi 2$ tests, as appropriate. The agreement between fat on MDCT and low voltage was assessed using Cohen's kappa coefficients, calculated sequentially for RV endocardium, RV

epicardium and LV epicardium, and for bipolar and unipolar voltage measurements. Statistical analyses were performed using PASW Statistics 18 (version 18.0.0).

RESULTS

Population characteristics

Thirty-two patients (47±14 years, 6 women) were included. The characteristics of the studied population are shown in Table 1. All patients had a definite ARVC diagnosis, with mean numbers of minor and major Task Force Criteria of 2.1±1.2 and 1.9±1.2, respectively. The time since initial ARVC diagnosis was 36 [0-96] months. In addition to the complete ARVC diagnostic workup recommended by the Task Force, isoproterenol testing and MDCT were performed in all patients. CMR was performed in 22(69%) of the patients (including 4 patients with ICD but with available MRI preformed less than 6 months before inclusion). Genetic testing was available in 20(63%) patients, and was found to be positive for PKP2 mutation in 9(45%) of these patients. Other gene mutations were identified in 5 patients, including DSG2 (N=1), ACTN2 (N=1), TNNC1 (N=1), DSC2 (N=1) and TNEM43 (N=1). Fourteen (44%) patients were referred for VT ablation, and therefore included in the mapping sub-study.

Imaging findings

Imaging was positive for a major Task Force criterion in 18(56%) patients, for a minor Task Force criterion in 6(19%), and it was negative in 8(25%). The characteristics of ARVC substrate on imaging are summarized in Table 2. The distribution of fat on MDCT over the LV and RV walls is illustrated in Figure 1. On the RV, fibrosis and wall motion abnormalities were found on CMR in 20(91%) and 21(95%) patients, respectively, while fat was found on MDCT in 32(100%) patients. The extents of RV fat on MDCT and RV wall motion abnormalities on CMR were higher than the extent of RV fibrosis on CMR (P<0.0001 and

P<0.0001, respectively). The extent of RV fat on MDCT was higher than the extent of RV wall motion abnormalities (P=0.001). On the LV, fibrosis and wall motion abnormalities were found on CMR in 14(64%) and 2(9%) patients, respectively, while fat was found on MDCT in 21(66%) patients. The extent of LV fat on MDCT and LV fibrosis on CMR were higher than the extent of LV wall motion abnormalities (P<0.0001 and P<0.0001, respectively). No difference was found between the extent of LV fat on MDCT and LV fibrosis on CMR (P=0.33). LV involvement was present in 21(66%) of the studied population. Examples of LV involvement on imaging are shown in Figure 2.

Clinical correlates of LV involvement

Baseline clinical characteristics in patients with and without LV involvement are compared in Table 1. LV involvement related to none of the Task Force Criteria. We found no association between the presence of PKP2 gene mutation and the presence of LV substrate. The only characteristic that differed between patients with vs without LV involvement was LVEF (56±8 vs 63±8%, respectively, P=0.02), and a fair correlation was found between LVEF and the extent of LV substrate on imaging (R=-0.52, P=0.002). However, LVEF was significantly altered (i.e. <56%) in only 8(38%) of the patients with LV substrate. The analysis of spontaneous and isoproterenol-induced arrhythmias is shown in Table 3. In the whole population, right-sided PVCs were more frequent than left-sided PVCs (P=0.003). The number of right-sided PVCs was not different between patients with vs without LV involvement (P=0.25). Patients with LV involvement showed a higher number of left-sided PVCs (P=0.02). In the whole population, a total of 39 VTs were observed, either spontaneously or during isoproterenol testing. Three (8%) of these VTs were polymorphic, and therefore could not be characterized. Among the 36 monomorphic VTs, right-sided VTs were more frequent than left-sided VTs (34 right-sided VTs in 24[75%] patients vs 2 left-sided VTs in 2[6%] patients, P<0.0001). These 2 left-sided VTs were observed in patients

with LV involvement on imaging, but the association between LV involvement and left-sided VT was not significant (P=0.33).

Electrophysiological characteristics of the LV substrate

The population undergoing electrophysiological study was composed of 14 patients (43±16 years, 1 woman). LV involvement was present on imaging in 9(64%) patients. All patients underwent high density mapping of the RV endocardium (mapping density 497±264 points/map) and biventricular epicardium (mapping density 567±261 points/map). The agreement between low voltage and intra-myocardial fat on imaging is shown in Table 4. The higher agreement was found when using RV endocardial unipolar and RV epicardial bipolar data. Lower agreements were found on the LV. Contact mapping characteristics of LV and RV fat, as defined by MDCT, are compared in Table 5. As compared to RV fat, LV fat was found to be smaller (P<0.0001), and less efficiently detected on voltage mapping (P=0.02 on both bipolar and unipolar voltage data). Although the number of LAVAs was higher on the RV than on the LV (P<0.0001), LAVAs were found within LV fat areas in all patients with LV involvement, and the density of LAVA within the fatty substrate defined on MDCT was similar between the RV and LV (P=0.57). An example of LV substrate on contact mapping and imaging is shown in Figure 3.

Procedural results

A mean of 2.0±0.8 VTs were induced, all of which with RV morphology except for one non-clinical left-sided VT in one patient. A mean of 107±49 LAVAs were identified during sinus rhythm, including LV LAVAs in all 9 patients with LV substrate on imaging, and in none of the 5 patients with no LV substrate on imaging. After a mean of 29±9min of RF ablation (endocardial ablation: 20±6min and epicardial ablation: 9±7min), complete RV LAVA elimination could be achieved in 8/14(57%) patients, and non-inducibility of VT in 13/14(93%) patients, the remaining patient being not tested because the VT induced at

baseline was poorly tolerated. In the patient with inducible left-sided VT, LV LAVA could be successfully eliminated by epicardial ablation, resulting in the loss of VT inducibility. After a median follow-up of 19 months, VT recurrence was observed in 5/14(36%) patients, with no difference between patients with vs without LV involvement (respectively 33% vs 40%, P=NS).

DISCUSSION

The main findings of this study are that (i) LV intra-myocardial fat is present on imaging in the majority of patients with ARVC fulfilling the modified Task Force criteria, mostly on lateral, inferior, and apical LV segments, and with a lower burden as compared to the RV (ii) LV involvement relates to none of the Task Force criteria, although mild LV systolic dysfunction and left-sided arrhythmias are more frequent, (iii) LV fat hosts the same density of LAVA as RV fat, but is less efficiently detected by voltage mapping.

Distribution of structural substrate in ARVC

This study shows that RV fat in ARVC patients predominates in basal lateral, basal inferior, and mid lateral segments, and is rarely found in the septum. The method used to segment intra-myocardial fat from MDCT is based on prior validation studies demonstrating good correlation with contact mapping data[9] and Task Force criteria.[10] The distribution of RV fat is consistent with prior histological[3,24] and contact mapping studies.[18,25] In the current study, RV substrate was also assessed with the use of MRI. Results indicate that wall motion abnormalities on cine images are more efficient in describing the extent of RV dyplasia than fibrosis on late gadolinium enhancement, which is likely to be due to spatial resolution issues when studying fibrosis on the thin RV wall.[5,26,27] In the present study, RV wall motion abnormalities were found in 95% of the patients, but imaging was positive for a major or minor Task Force criterion in only 75% of the patients. This indicates that RV volume and

ejection fraction cut-off values recommended by the Task Force are the factors limiting imaging sensitivity.[8] In the present study, LV fat was found on MDCT in 66% of ARVC patients, mostly in inferior, lateral, and apical segments, and with a lower burden as compared to the RV. The prevalence of LV substrate is consistent with prior imaging reports,[4,5,28,29] and superior to the one usually reported in mapping studies.[5,30] The regional distribution of the LV substrate is also consistent with prior studies.[31-33] The lower burden of LV substrate as compared to the RV might be explained by a selection bias, patients being included in the present study based on Task Force criteria, which are designed to identify RV dysplasia. This outlines the limitations of the current diagnostic strategy in detecting LV variants of arrhythmogenic dysplasia/cardiomyopathy.[7] MRI results indicate that as opposed to the RV substrate, fibrosis on late gadolinium enhancement is more efficient in detecting LV dysplasia than wall motion abnormalities, which are usually absent. This result suggests that although the use of tissue characterization methods is not recommended by the Task Force, these are of great value to detect LV involvement in ARVC.[31]

Clinical correlates of LV involvement in ARVC

Our results show that LV involvement in ARVC relates to none of the Task Force criteria. This can be explained by the fact that Task Force criteria are essentially dependent on the burden of RV substrate. Indeed, diffuse RV dysplasia can be seen in the absence of LV involvement, and conversely LV variants of arrhythmogenic cardiomyopathy with minimal RV involvement have been reported.[31] In the present study we found a fair inverse correlation between the presence of LV fat and LVEF. However, significant LV systolic dysfunction was only present in 38% of the patients with LV involvement. This further outlines the need for tissue characterization methods to identify LV dysplasia, which is often non-transmural and therefore has limited impact on global and regional systolic function. Genetic testing was available in 20 patients, and no relationship was found between PKP2 gene mutation and the

presence of LV dysplasia. Other less prevalent gene mutations could not be analyzed because of sample size limitations. In the present study, arrhythmogenicity was assessed from 12-lead ECG recordings at baseline and during isoproterenol testing. The rationale to use isoproterenol testing was that the ARVC substrate is known to show explosive response to isoproterenol,[34] and we hypothesized that an increased sensitivity would be of value to detect left-sided arrhythmias, which were expected to be less frequent than right-sided arrhythmias. As expected, our results show that right-sided PVCs are more frequent than left-sided PVCs in ARVC, although left-sided PVCs are more frequent in patients with LV involvement on imaging than in those without. This demonstrates that LV involvement is associated with a certain degree of arrhythmogenicity. However, we found no significant difference in the prevalence of left-sided VTs, which is likely due to the limited sample size (only 2 left-sided VTs were observed, both in patients with LV involvement).

Electrophysiological characteristics of the LV substrate in ARVC

This study shows that RV endocardial voltage mapping is more accurate in detecting RV dysplasic substrate when using unipolar than bipolar data. This is consistent with a prior study, and has been explained by the limitation of endocardial bipolar voltage in detecting subepicardial scar, whereas unipolar is more sensitive to distant substrate.[17,21] Conversely, RV epicardial voltage mapping shows a higher agreement with MDCT-derived fat when using bipolar than unipolar data. This is also consistent with prior reports and can be explained by an overestimation of the substrate on unipolar voltage data, due to epicardial fat interposition.[9,35] This study is to our knowledge the first to report on the accuracy of voltage mapping to detect LV dysplasia. Our results show that voltage mapping is less efficient on the LV than on the RV. This can be explained by the fact that fat is usually non-transmural on the LV, resulting in false negative voltage measurements due to far field signal from the adjacent healthy myocardium. The poor sensitivity of voltage mapping in detecting subepicardial scar

on the LV is likely responsible for the underestimation of left-sided ARVC involvement in contact mapping studies. However, an accurate delineation of the diseased LV myocardium would be of value as our results show that the prevalence and density of LAVA within LV fat areas are similar to those observed on the RV. Therefore, there seems to be no difference between RV and LV fat in terms of arrhythmogenicity, and the higher prevalence of right-sided arrhythmias in ARVC patients appears to be merely the consequence of a selection based on Task Force criteria, in which the RV substrate only is targeted.

Study limitations

The first limitation of this study is the absence of predominantly LV forms of arrhythmogenic dysplasia. This is the consequence of a selection based on Task Force criteria, which was mandatory in the absence of alternate diagnostic strategy focusing on LV dysplasia. We acknowledge that the absence of endomyocardial biopsy is a limit to this study. Indeed, evidence of LV fibro-fatty replacement on histology might have been used to identify LV variants. However, our results show that LV dysplasia rarely involves the septum but rather predominates in the subepicardial layers of the LV free wall, and performing biopsies on such locations would be extremely challenging. This outlines the diagnostic dilemma in identifying LV variants of arrhythmogenic cardiomyopathy, which are likely to be largely underestimated by current diagnostic approaches, and easily mistaken on imaging for other types of cardiac diseases characterized by subepicardial scar, such as post-myocarditis, sarcoidosis, dilated cardiomyopathy or idiopathic myocardial fibrosis.[36,37] Because imaging, clinical and electrophysiological characteristics show substantial limitations, this differential diagnosis might be assisted by genetic testing in the near future. Unfortunately in the present study genotyping was only available in 20 patients, and PKP2 was the only gene mutation sufficiently prevalent to be analyzed.[38] Therefore, additional research is desirable to look for a potential specific genetic substrate associated with LV dysplasia. Another limitation is that

the characterization of the RV substrate was based on combined endocardial and epicardial mapping data, whereas we only mapped the LV substrate epicardially. However, the LV substrate being usually non-transmural on imaging, we hypothesized that few electrophysiological substrate would be present on LV endocardium.

CONCLUSION

LV intra-myocardial fat is present on imaging in the majority of patients fulfilling the modified Task Force criteria for ARVC, mostly on lateral, inferior, and apical LV segments, and with a lower burden as compared to the RV. This substrate is poorly identified by imaging methods performed within the frame of Task Force recommendations. LV involvement relates to none of the Task Force criteria, although mild LV systolic dysfunction and left-sided arrhythmias are more frequent. LV fat hosts the same density of LAVA as RV fat, but is less efficiently detected by voltage mapping. These results support the need for alternate diagnostic strategies to identify LV dysplasia.

FUNDING SOURCES

Dr Berte received an educational EHRA Grant. This manuscript was made possible by the following grants: Equipex MUSIC ANR-11-EQPX-0030 and IHU LIRYC ANR-10-IAHU-04.

DISCLOSURES

Drs Jaïs, Haïssaguerre, Hocini, and Sacher have received lecture fees from Biosense Webster and St. Jude Medical. The other authors report no conflicts.

REFERENCES

1. Marcus FI, Fontaine GH, Guiraudon G, Guiraudon G, Frank R, Laurenceau JL, Malergue C, Grosgogeat Y. Right ventricular dysplasia: a report of 24 adult cases. Circulation. 1982;65:384-98.
2. Sen-Chowdhry S, Syrris P, Ward D, Asimaki A, Sevdalis E, McKenna WJ. Clinical and genetic characterization of families with arrhythmogenic right ventricular dysplasia/cardiomyopathy provides novel insights into patterns of disease expression. Circulation. 2007;115:1710 –1720.
3. El Demellawy D, Nasr A, Alowami S. An updated review on the clinicopathologic aspects of arrhythmogenic right ventricular cardiomyopathy. The American journal of forensic medicine and pathology. 2009;30:78-83.
4. Nakajima T, Kimura F, Kajimoto K, Kasanuki H, Hagiwara N. Utility of ECG-gated MDCT to differentiate patients with ARVC/D from patients with ventricular tachyarrhythmias. Journal of cardiovascular computed tomography. 2013;7:223-33.
5. Marra MP, Leoni L, Bauce B, Corbetti F, Zorzi A, Migliore F, Silvano M, Rigato I, Tona F, Tarantini G, Cacciavillani L, Basso C, Buja G, Thiene G, Iliceto S, Corrado D. Imaging study of ventricular scar in arrhythmogenic right ventricular cardiomyopathy: comparison of 3D standard electroanatomical voltage mapping and contrast-enhanced cardiac magnetic resonance. Circulation Arrhythmia and Electrophysiology. 2012;5:91-100.
6. Horimoto M, Funayama N, Satoh M, Igarashi T, Sekiguchi M. Histological evidence of left ventricular involvement in arrhythmogenic right ventricular dysplasia. Japanese circulation journal. 1989;53:1530-4.
7. Mackey-Bojack SM, Roe SJ, Titus JL. Sudden death with circumferential subepicardial fibrofatty replacement: left-sided arrhythmogenic ventricular cardiomyopathy. The American journal of forensic medicine and pathology. 2009;30:209-14.
8. Marcus FI, McKenna WJ, Sherrill D, Basso C, Bauce B, Bluemke DA, Calkins H, Corrado D, Cox MG, Daubert JP, Fontaine G, Gear K, Hauer R, Nava A, Picard MH, Protonotarios N, Saffitz JE, Sanborn DM, Steinberg JS, Tandri H, Thiene G, Towbin JA, Tsatsopoulou A,

Wichter T, Zareba W. Diagnosis of arrhythmogenic right ventricular cardiomyopathy/dysplasia: proposed modification of the Task Force Criteria. Circulation 2010;121:1533-41.

9. Komatsu Y, Jadidi A, Sacher F, Denis A, Daly M, Derval N, Shah A, Lehrmann H, Park CI, Weber R, Arentz T, Pache G, Sermesant M, Ayache N, Relan J, Montaudon M, Laurent F, Hocini M, Haïssaguerre M, Jaïs P, Cochet H. Relationship between MDCT-imaged myocardial fat and ventricular tachycardia substrate in arrhythmogenic right ventricular cardiomyopathy. Journal of the American Heart Association. 2014;3(4). [Epub ahead of print]
10. Cochet H, Denis A, Komatsu Y, Jadidi AS, Aït Ali T, Sacher F, Derval N, Relan J, Sermesant M, Corneloup O, Hocini M, Haïssaguerre M, Laurent F, Montaudon M, Jaïs P. Automated quantification of right ventricular fat at contrast-enhanced cardiac multidetector CT in arrhythmogenic right ventricular cardiomyopathy. Radiology. 2015 Jan 5:141140. [Epub ahead of print]
11. Maceira AM, Prasad SK, Khan M, Pennell DJ. Normalized left ventricular systolic and diastolic function by steady state free precession cardiovascular magnetic resonance. Journal of Cardiovascular Magnetic Resonance. 2006;8:417-26.
12. Maceira AM, Prasad SK, Khan M, Pennell DJ. Reference right ventricular systolic and diastolic function normalized to age, gender and body surface area from steady-state free precession cardiovascular magnetic resonance. European Heart Journal. 2006;27:2879-88.
13. Asirvatham SJ. Correlative anatomy for the invasive electrophysiologist: outflow tract and supravalvar arrhythmia. Journal of cardiovascular electrophysiology. 2009;20:955-68.
14. Bala R, Marchlinski FE. Electrocardiographic recognition and ablation of outflow tract ventricular tachycardia. Heart rhythm : the official journal of the Heart Rhythm Society. 2007;4:366-70.
15. Ouyang F, Fotuhi P, Ho SY, Hebe J, Volkmer M, Goya M, Burns M, Antz M, Ernst S, Cappato R, Kuck KH. Repetitive monomorphic ventricular tachycardia originating from the aortic sinus cusp: electrocardiographic characterization for guiding catheter ablation. Journal of the American College of Cardiology. 2002;39:500-8.

16. Cano O, Hutchinson M, Lin D, Garcia F, Zado E, Bala R, Riley M, Cooper J, Dixit S, Gerstenfeld E, Callans D, Marchlinski FE. Electroanatomic substrate and ablation outcome for suspected epicardial ventricular tachycardia in left ventricular nonischemic cardiomyopathy. Journal of the American College of Cardiology. 2009;54:799-808.
17. Dinov B, Schratter A, Schirripa V, Fiedler L, Bollmann A, Rolf S, Sommer P, Hindricks G, Arya A. Procedural Outcomes and Survival after Catheter Ablation of Ventricular Tachycardia in Relation to Electroanatomical Substrate in Patients with Nonischemic Dilated Cardiomyopathy: The Role of Unipolar Voltage Mapping. Circulation Arrhythmia and electrophysiology. 2011;4:49-55.
18. Corrado D, Basso C, Leoni L, Tokajuk B, Bauce B, Frigo G, Tarantini G, Napodano M, Turrini P, Ramondo A, Daliento L, Nava A, Buja G, Iliceto S, Thiene G. Three-dimensional electroanatomic voltage mapping increases accuracy of diagnosing arrhythmogenic right ventricular cardiomyopathy/dysplasia. Circulation 2005;111:3042-50.
19. Hutchinson MD, Gerstenfeld EP, Desjardins B, et al. Endocardial unipolar voltage mapping to detect epicardial ventricular tachycardia substrate in patients with nonischemic left ventricular cardiomyopathy. Circulation Arrhythmia and electrophysiology 2011;4:49-55.
20. Piers SR, van Huls van Taxis CF, Tao Q, van der Geest RJ, Askar SF, Siebelink HM, Schalij MJ, Zeppenfeld K. Epicardial substrate mapping for ventricular tachycardia ablation in patients with non-ischaemic cardiomyopathy: a new algorithm to differentiate between scar and viable myocardium developed by simultaneous integration of computed tomography and contrast-enhanced magnetic resonance imaging. European Heart Journal 2013;34:586-96.
21. Polin GM, Haqqani H, Tzou W, Hutchinson MD, Garcia FC, Callans DJ, Zado ES, Marchlinski FE. Endocardial unipolar voltage mapping to identify epicardial substrate in arrhythmogenic right ventricular cardiomyopathy/dysplasia. Heart rhythm : the official journal of the Heart Rhythm Society 2011;8:76-83.
22. Jais P, Maury P, Khairy P, Sacher F, Nault I, Komatsu Y, Hocini M, Forclaz A, Jadidi AS, Weerasooryia R, Shah A, Derval N, Cochet H, Knecht S, Miyazaki S, Linton N, Rivard L, Wright M, Wilton SB, Scherr D, Pascale P, Roten L, Pederson M, Bordachar P, Laurent F,

Kim SJ, Ritter P, Clementy J, Haïssaguerre M. Elimination of local abnormal ventricular activities: a new end point for substrate modification in patients with scar-related ventricular tachycardia. Circulation 2012;125:2184-96.

23. Desjardins B, Morady F, Bogun F. Effect of epicardial fat on electroanatomical mapping and epicardial catheter ablation. Journal of the American College of Cardiology. 2010;56:1320-7.
24. Fontaliran F, Fontaine G, Fillette F, Aouate P, Chomette G, Grosgogeat Y. Nosologic frontiers of arrhythmogenic dysplasia Quantitative variations of normal adipose tissue of the right heart ventricle. Archives des Maladies de Coeur et Vaisseaux 1991;84:33–8.
25. Marchlinski FE, Zado E, Dixit S, Gerstenfeld E, Callans DJ, Hsia H, Lin D, Nayak H, Russo A, Pulliam W. Electroanatomic substrate and outcome of catheter ablative therapy for ventricular tachycardia in setting of right ventricular cardiomyopathy. Circulation 2004;110:2293-8.
26. Tandri H, Saranathan M, Rodriguez ER, Martinez C, Bomma C, Nasir K, Rosen B, Lima JA, Calkins H, Bluemke DA. Noninvasive detection of myocardial fibrosis in arrhythmogenic right ventricular cardiomyopathy using delayed-enhancement magnetic resonance imaging. Journal of the American College of Cardiology 2005;45:98-103.
27. Bomma C, Rutberg J, Tandri H, Nasir K, Roguin A, Tichnell C, Rodriguez R, James C, Kasper E, Spevak P, Bluemke DA, Calkins H. Misdiagnosis of arrhythmogenic right ventricular dysplasia/cardiomyopathy. Journal of cardiovascular electrophysiology 2004;15:300-6.
28. Lindstrom L, Nylander E, Larsson H, Wranne B. Left ventricular involvement in arrhythmogenic right ventricular cardiomyopathy - a scintigraphic and echocardiographic study. Clinical physiology and functional imaging 2005;25:171-7.
29. El Ghannudi S, Nghiem A, Germain P, Jeung MY, Gangi A, Roy C. Left ventricular involvement in arrhythmogenic right ventricular cardiomyopathy - a cardiac magnetic resonance imaging study. Clinical Medicine Insights Cardiology 2014;8:27-36.
30. Berruezo A, Fernández-Armenta J, Mont L, Zeljko H, Andreu D, Herczku C, Boussy T, Tolosana JM, Arbelo E, Brugada J. Combined endocardial and epicardial catheter ablation in

arrhythmogenic right ventricular dysplasia incorporating scar dechanneling technique. Circulation Arrhythmia and electrophysiology 2012;5:111-21.

31. Sen-Chowdhry S, Syrris P, Prasad SK, Hughes SE, Merrifield R, Ward D, Pennell DJ, McKenna WJ. Left-dominant arrhythmogenic cardiomyopathy: an under-recognized clinical entity. Journal of the American College of Cardiology 2008;52:2175–2187.
32. De Pasquale CG, Heddle WF. Left sided arrhythmogenic ventricular dysplasia in siblings. Heart 2001;86:128–130.
33. Michalodimitrakis M, Papadomanolakis A, Stiakakis J, Kanaki K. Left side right ventricular cardiomyopathy. Medicine Science and Law. 2002;42:313–317.
34. Denis A, Sacher F, Derval N, Lim HS, Cochet H, Shah AJ, Daly M, Pillois X, Ramoul K, Komatsu Y, Zemmoura A, Amraoui S, Ritter P, Ploux S, Bordachar P, Hocini M, Jaïs P, Haïssaguerre M. Diagnostic value of isoproterenol testing in arrhythmogenic right ventricular cardiomyopathy. Circulation Arrhythmia and electrophysiology 2014;7:590-7.
35. van Huls van Taxis CF, Wijnmaalen AP, Piers SR, van der Geest RJ, Schalij MJ, Zeppenfeld K. Real-time integration of MDCT-derived coronary anatomy and epicardial fat: impact on epicardial electroanatomic mapping and ablation for ventricular arrhythmias. JACC Cardiovascular imaging 2013;6:42-52.
36. Vasaiwala SC, Finn C, Delpriore J, Leya F, Gagermeier J, Akar JG, Santucci P, Dajani K, Bova D, Picken MM, Basso C, Marcus F, Wilber DJ. Prospective study of cardiac sarcoid mimicking arrhythmogenic right ventricular dysplasia. Journal of Cardiovascular Electrophysiology. 2009;20:473–476.
37. Pieroni M, Dello Russo A, Marzo F, Pelargonio G, Casella M, Bellocci F, Crea F. High prevalence of myocarditis mimicking arrhythmogenic right ventricular cardiomyopathy differential diagnosis by electroanatomic mapping-guided endomyocardial biopsy. Journal of the American College of Cardiology. 2009;53:681–689.
38. Gerull B, Heuser A, Wichter T, Paul M, Basson CT, McDermott DA, Lerman BB, Markowitz SM, Ellinor PT, MacRae CA, Peters S, Grossmann KS, Drenckhahn J, Michely B, Sasse-

Klaassen S, Birchmeier W, Dietz R, Breithardt G, Schulze-Bahr E, Thierfelder L. Mutations in the desmosomal protein plakophilin-2 are common in arrhythmogenic right ventricular cardiomyopathy. Nature Genetics. 2004;36:1162–1164.

TABLES

Table 1. Patient characteristics

	Total population (N=32)	no LV involvement (N=11)	LV involvement (N=21)	P value
age (years)	47±14	48±14	47±14	0.85
male gender	26 (81)	8 (73)	18 (86)	0.39
time since initial ARVC diagnosis (months)	36 [IQR 0-96]	24 [IQR 0-72]	36 [IQR 12-106]	0.23
ICD	14 (44)	7 (64)	7 (33)	0.11
Imaging CMR/TTE				
CMR performed	22 (69)	8 (73)	14 (67)	0.74
LVEDV (mL/m2)	79±9	77±7	80±10	0.56
LVEF (%)	59±8	63±8	56±8	0.02
RVEDV (mL/m2)	114±25	107±22	118±26	0.33
RVEF (%)	38±10	42±11	37±9	0.19
CMR/TTE positive for major criterion	18 (56)	4 (36)	14 (67)	0.11
CMR/TTE positive for minor criterion	6 (19)	1 (9)	5 (24)	0.33
ECG				
TWI V1, V2, V3	20 (63)	9 (82)	11 (53)	0.11
TWI V1, V2	2 (6)	0 (0)	2 (10)	0.31
TWI extending beyong V3 and RBBB	2 (6)	0 (0)	2 (10)	0.31
Epsilon wave	8 (25)	1 (10)	7 (33)	0.14
Late potentials on SAECG	23 (72)	7 (64)	16 (76)	0.47
TAD≥55ms	9 (28)	4 (36)	5 (24)	0.47
Arrhythmias				
VT of LBBB morphology and sup. axis	12 (38)	6 (55)	6 (29)	0.16
VT of RV outflow morphology	7 (22)	2 (18)	5 (24)	0.73
VT of unknown morphology	5 (16)	2 (18)	3 (14)	0.78
>500 PVCs / 24h	15 (47)	4 (36)	11 (52)	0.40
Family History				
ARVC in 1st degree relative	2 (6)	2 (18)	0 (0)	0.09
Premature SD in 1st degree relative	2 (6)	1 (9)	1 (5)	0.64
Genetic testing performed for PKP2 mutation	20 (63)	8 (73)	12 (57)	0.40
PKP2 mutation present	9 (45)	3 (38)	6 (50)	0.61
Endomyocardial biopsy performed	0 (0)	0 (0)	0 (0)	NA
ARVC diagnosis				
number of major criteria	1.9±1.2	2.3±1.3	1.8±1.2	0.28
number of minor criteria	2.1±1.2	1.7±1.1	2.3±1.2	0.17

ARVC : arrhythmogenic right ventricular cardiomyopathy ; ICD : implantable cardioverter defibrillator ; CMR : cardiac magnetic resonance ; TTE : trans-thoracic echocardiography ; LV : left ventricle ; RV : right ventricle ; EDV : end-diastolic volume ; EF : ejection fraction; TWI: T wave inversion; RBBB: right bundle branch block; SAECG: signal averaged electrocardiogram; TAD: terminal activation duration; VT: ventricular tachycardia; LBBB: left bundle branch block; SD: sudden death; PVC: premature ventricular contraction.

Table 2. Characteristics of ARVC substrate on imaging

	RV	LV	P value
CMR (N=22)			
end-diastolic volume (mL/m2)	114±25	79±9	-
dilatation present	13 (59%)	0 (0%)	<0.0001
ejection fraction (%)	38±10	59±8	-
systolic dysfunction present †	17 (77%)	6 (27%)	0.0005
fibrosis present	20 (91%)	14 (64%)	0.03
extent of fibrosis (nb segts) †	2.9±1.8	1.7±1.7	0.03
wall motion abnormality present	21 (95%)	2 (9%)	<0.0001
extent of wall motion abnormality (nb segts) †	4.1±2.0	0.1±0.47	<0.0001
MDCT (N=32)			
fat present	32 (100%)	21 (66%)	0.0002
extent of fat (nb segts) †	5.1±2.1	1.8±1.7	<0.0001

† the extent of fibrosis, wall motion abnormalities and fat are based on 9 segments on the RV (including septal segments), and 7 segments on the LV (excluding septal segments). ARVC: arrhythmogenic right ventricular cardiomyopathy; CMR: cardiac magnetic resonance; MDCT: multi-detector computed tomography; LV: left ventricle; RV: right ventricle.

Table 3. Arrhythmogenicity in patients with vs without left-sided substrate

	no LV involvement (N=11)	LV involvement (N=21)	P value
Right-sided arrhythmias			
spontaneous PVC morphologies	1.6±0.7	1.5±0.8	0.68
isoproterenol-induced PVC morphologies	1.1±0.9	1.4±1.3	0.48
total PVC morphologies	1.8±0.8	2.3±1.2	0.25
spontaneous VT morphologies	1.0±0.7	1.0±0.9	0.88
isoproterenol-induced VT morphologies	0.4±0.5	0.2±0.4	0.23
total VT morphologies	1.3±0.8	1.0±0.8	0.36
Left-sided arrhythmias			
spontaneous PVC morphologies	0.4±0.5	0.8±0.7	0.10
isoproterenol-induced PVC morphologies	0.3±0.5	1.0±0.9	0.03
total PVC morphologies	0.7±0.8	1.4±0.7	0.02
spontaneous VT morphologies	0.0±0.0	0.1±0.4	0.22
isoproterenol-induced VT morphologies	0.0±0.0	0.1±0.2	0.50
total VT morphologies	0.0±0.0	0.1±0.3	0.33

LV: left ventricle; PVC: premature ventricular complex; VT: ventricular tachycardia

Table 4. Agreement between MDCT-fat and low voltage

	k coefficient	P value
Right ventricle		
endocardial bipolar low voltage	0.612	<0.001
endocardial unipolar low voltage	0.821	<0.001
epicardial bipolar low voltage	0.777	<0.001
epicardial unipolar low voltage	0.504	<0.001
Left ventricle		
epicardial bipolar low voltage	0.544	<0.001
epicardial unipolar low voltage	0.263	<0.001

MDCT: multi-detector computed tomography

Table 5. Left and right-sided substrate characteristics on contact mapping

	RV substrate (N=14)	LV substrate (N=9)	P value
MDCT fat			
fat present	14 (100)	9 (100)	-
fat area (cm^2)	103±45	16±13	<0.0001
Low voltage			
bipolar low voltage present on endocardium	14 (100)	NA	-
bipolar low voltage area on endocardium (cm^2)	71±28	NA	-
bipolar low voltage present on epicardium	14 (100)	6 (67)	0.02
bipolar low voltage area on epicardium (cm^2)	142±69	8±10	<0.0001
unipolar low voltage present on endocardium	14 (100)	NA	-
unipolar low voltage area on endocardium (cm^2)	128±34	NA	-
unipolar low voltage present on epicardium	14 (100)	6 (67)	0.02
unipolar low voltage area on epicardium (cm^2)	199±70	15±13	<0.0001
LAVA			
presence of LAVA on endocardium	13 (93)	NA	-
nb of LAVA on endocardium	51±29	NA	-
presence of LAVA on epicardium	14 (100)	9 (100)	NS
nb of LAVA on epicardium	72±26	12±10	<0.0001
LAVA density within fat on epicardium (/cm^2)	0.6±0.3	0.9±0.6	0.57

LAVA: local abnormal ventricular activity; MDCT: multi-detector computed tomography; LV: left ventricle; RV: right ventricle

FIGURES

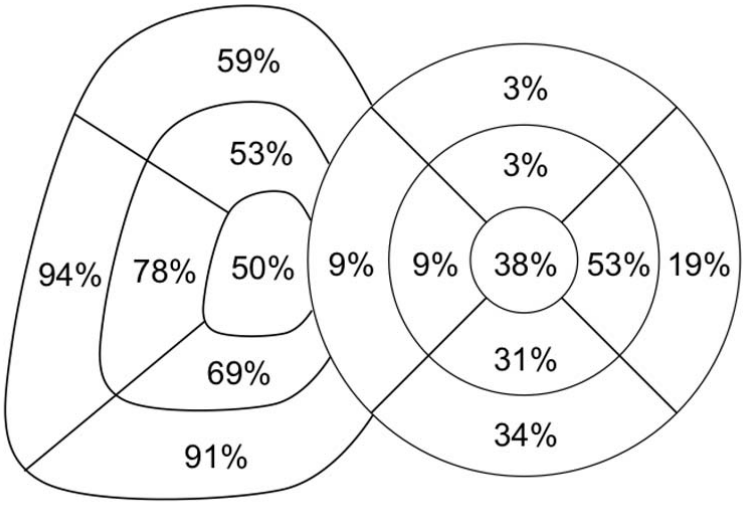

Figure 1: distribution of MDCT-derived intra-myocardial fat. The prevalence of fat is indicated for each of the RV and LV segments. MDCT: multi-detector computed tomography; LV: left ventricle; RV: right ventricle.

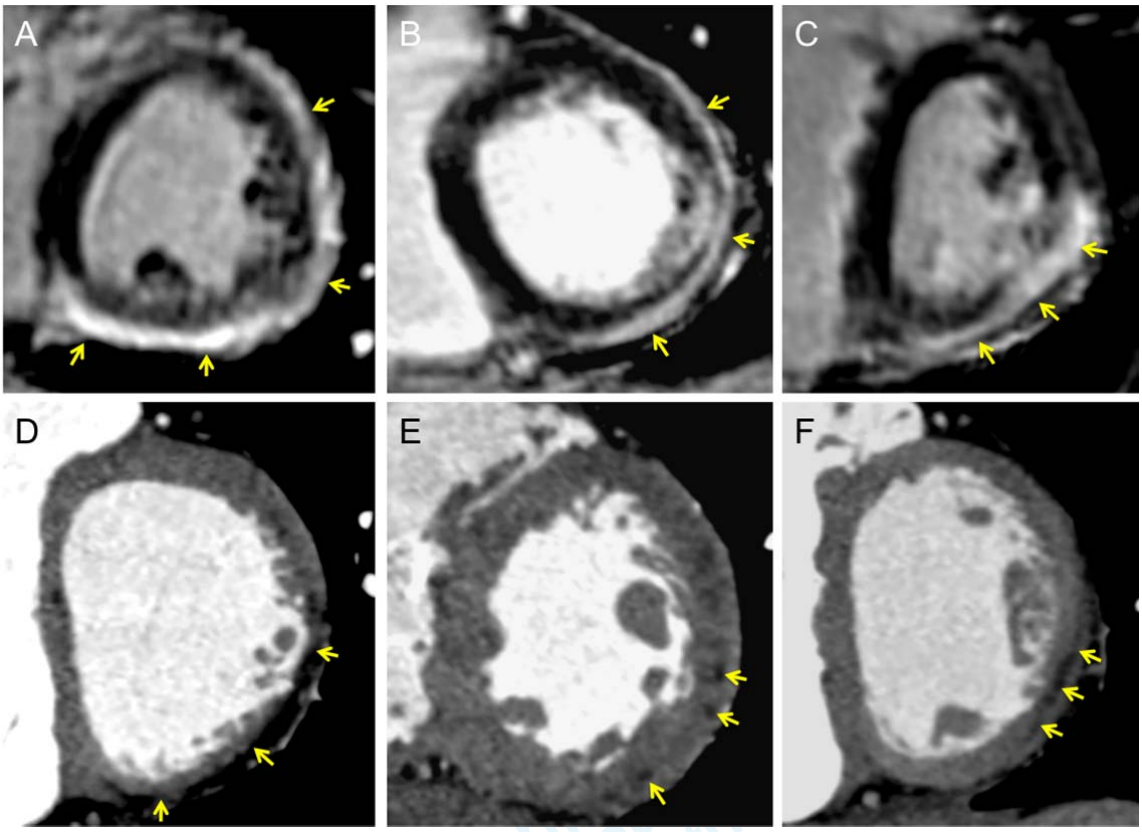

Figure 2: examples of left-sided ARVC substrate on imaging. Top row: late gadolinium-enhanced CMR shows sub-epicardial enhancement consistent with fibrosis on inferior and lateral LV wall in 3 patients (yellow arrows in A, B, and C). Bottom row: iodine-enhanced cardiac-gated MDCT shows intra-myocardial hypo-attenuation consistent with fatty replacement in 3 patients. All patients had a definite ARVC diagnosis based on Task Force criteria. ARVC: arrhythmogenic right ventricular cardiomyopathy; CMR: cardiac magnetic resonance; LV: left ventricle; MDCT: multi-detector computed tomography.

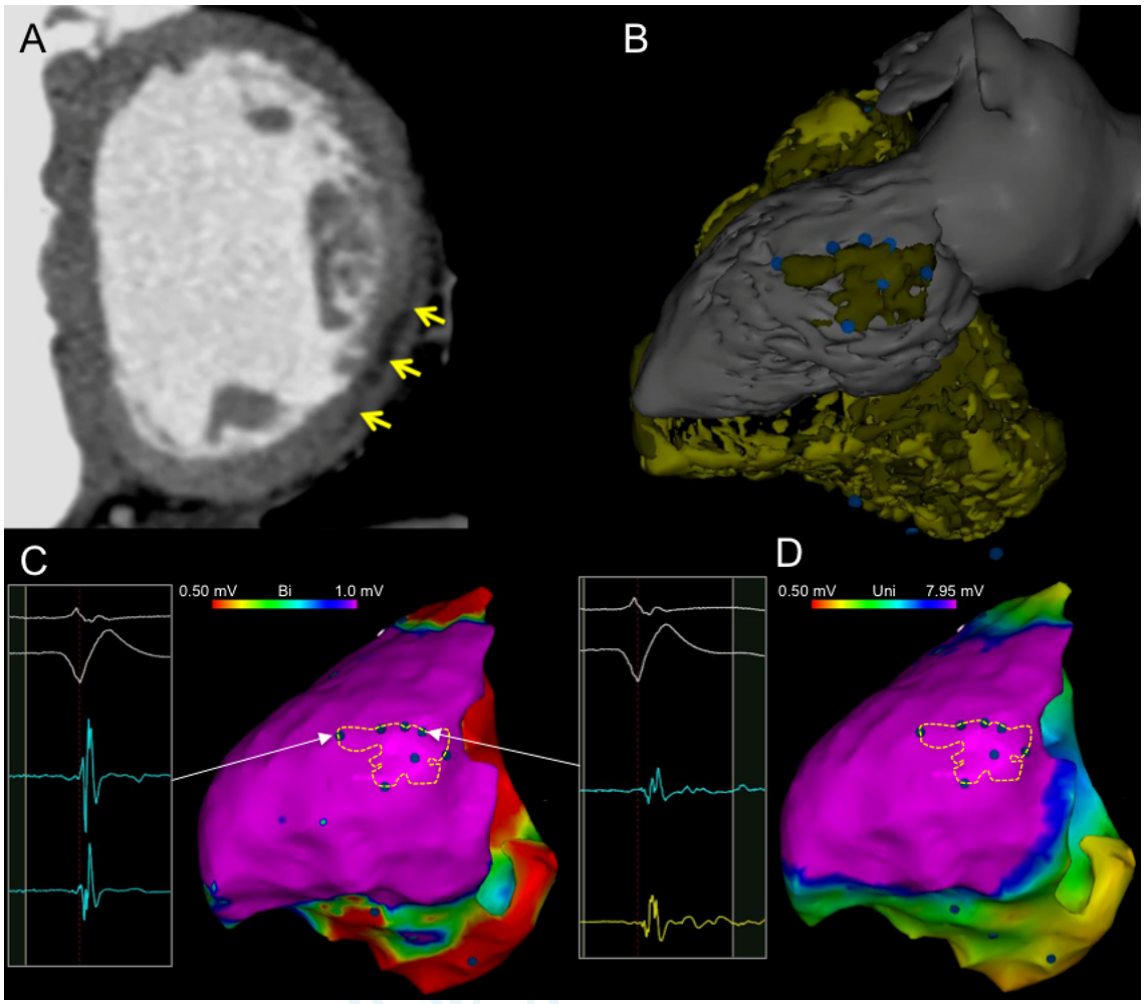

Figure 3: example of left-sided ARVC substrate on imaging and contact mapping. Contrast enhanced cardiac gated MDCT shows hypo-attenuation consistent with intra-myocardial fat on posterolateral LV wall (arrows in A). The 3D model derived from MDCT segmentation shows diffuse RV fat, and focal postero-lateral LV fat (yellow surface in B indicates fat). Bipolar and unipolar voltage mapping (C and D, respectively) shows diffuse low voltage on the RV, but no low voltage on the LV, including at the site of intra-myocardial fat (yellow dashed contour in C and D). Local abnormal ventricular activity is found within LV fat area (blue dots, arrows and signals in C). ARVC: arrhythmogenic right ventricular cardiomyopathy; LV: left ventricle; MDCT: multi-detector computed tomography; RV: right ventricle.

References

1. Sacher F, Tedrow UB, Field ME, et al. Ventricular tachycardia ablation: evolution of patients and procedures over 8 years. Circulation Arrhythmia and electrophysiology 2008;1:153-61.
2. Liuba I, Frankel DS, Riley MP, et al. Scar Progression in Patients with Nonischemic Cardiomyopathy and Ventricular Arrhythmias: Scar progression in NICM. Heart rhythm : the official journal of the Heart Rhythm Society 2014.
3. Riley MP, Zado E, Bala R, et al. Lack of uniform progression of endocardial scar in patients with arrhythmogenic right ventricular dysplasia/cardiomyopathy and ventricular tachycardia. Circulation Arrhythmia and electrophysiology 2010;3:332-8.
4. Komatsu Y, Daly M, Sacher F, et al. Endocardial ablation to eliminate epicardial arrhythmia substrate in scar-related ventricular tachycardia. Journal of the American College of Cardiology 2014;63:1416-26.
5. Miani D, Pinamonti B, Bussani R, Silvestri F, Sinagra G, Camerini F. Right ventricular dysplasia: a clinical and pathological study of two families with left ventricular involvement. British heart journal 1993;69:151-7.
6. Horimoto M, Funayama N, Satoh M, Igarashi T, Sekiguchi M. Histological evidence of left ventricular involvement in arrhythmogenic right ventricular dysplasia. Japanese circulation journal 1989;53:1530-4.
7. Sen-Chowdhry S, Syrris P, Ward D, Asimaki A, Sevdalis E, McKenna WJ. Clinical and genetic characterization of families with arrhythmogenic right ventricular dysplasia/cardiomyopathy provides novel insights into patterns of disease expression. Circulation 2007;115:1710-20.

IV. Epicardial mapping of scar

In part IV, the epicardial scar is discussed in more detail. An epicardial approach for mapping and ablation is associated with different technical issues, considerations and potential complications. Preprocedural imaging with MDCT and DE-MRI are useful and important to identify possible difficulties that can be expected, such as a endocardial thrombus, a phrenic nerve in the vicinity of the scar region, significant wall thinning with the risk of perforation, anatomical isthmuses to predict possible LAVA locations and epicardial adhesions.

In this chapter, the epicardial access technique is explained, followed by a feasibility analysis of an epicardial only mapping and ablation procedure. Finally the usefulness of imaging in guiding the epicardial ablation is analyzed.

Figure 1. Anterior percutaneous subxyphoidal epicardial puncture technique.[22]

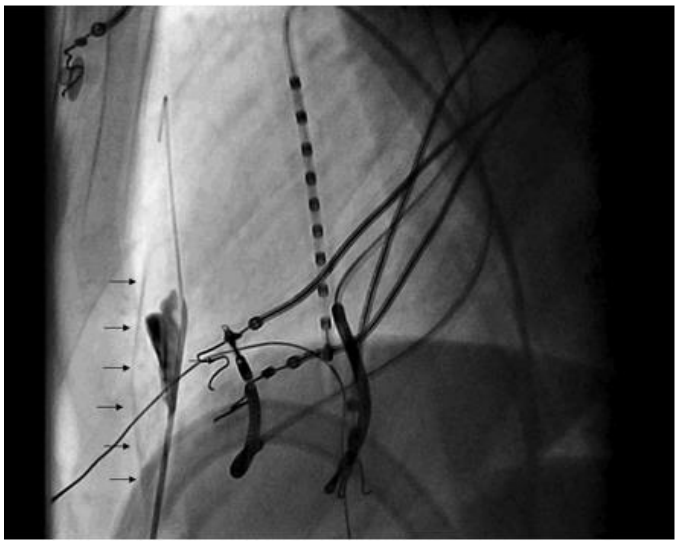

Left lateral fluoroscopic view. Tuohy needle into the pericardial space with tip away from the pericardium. Guidewire within the perciardial space. Contrast (arrows) within the pericardial space and staining in the mediastinum.

A. Safety and prevention of complications during percutaneous epicardial access for the ablation of cardiac arrhythmias.

Lim HS, Sacher F, Cochet H, Berte B, Yamashita S, Mahida S, Zellerhoff S, Komatsu Y, Denis A, Derval N, Hocini M, Haïssaguerre M, Jaïs P. Heart Rhythm. 2014 Sep; 11(9):1658-65.

1. Study outline

In this hands-on section, we explained the anterior epicardial puncture technique using the Tuohy needle from a subxyphoidal access using a conscious sedation with midazolam and sufentamil.[5, 22] We believe that this approach helps to avoid potential organ damages, particularly by not penetrating into the peritoneal space. A detailed knowledge of the anatomical structures in the vicinity, medical history of the patient, the absolute and relative contra-indications, possible complications and preventive measures are needed. Furthermore, a practical work-flow in case of emergencies agreed with the cardiac surgeons needs to be created as urgent cardiac surgery can be necessary.

2. Implications

The number of patients referred for VT ablation in NICM is increasing.[9] Because of a more intramural or epicardial scar predominance in this subset of patients (e.g. in ARVC, myocarditis and DCM) more epicardial access and ablation is needed.[9] In-depth knowledge of this technique is paramount. In the future, better image integration and 3D rotational angiography of the coronary artery system could help to further reduce the complication rate.

3. Manuscript

HANDS ON

Safety and prevention of complications during percutaneous epicardial access for the ablation of cardiac arrhythmias

Han S. Lim, MBBS, PhD, Frédéric Sacher, MD, Hubert Cochet, MD, Benjamin Berte, MD, Seigo Yamashita, MD, Saagar Mahida, MBChB, Stephan Zellerhoff, MD, Yuki Komatsu, MD, Arnaud Denis, MD, Nicolas Derval, MD, Mélèze Hocini, MD, Michel Haïssaguerre, MD, Pierre Jaïs, MD

From the Hôpital Cardiologique du Haut-Lévêque, CHU Bordeaux, Université Victor Segalen Bordeaux II, France; and INSERM U1045 - L'Institut de Rythmologie et Modeling Cardiaque, Bordeaux, France.

Introduction

Since its introduction, percutaneous epicardial access is increasingly being performed to facilitate catheter ablation of ventricular tachycardias (VTs) with epicardial circuits, difficult cases of idiopathic VTs, focal atrial tachycardia, and accessory pathways that cannot be successfully targeted endocardially.[1] A thorough understanding of the clinical anatomy and potential complications is vital in order to perform a safe procedure.[2] In this article, we present the clinical anatomy related to epicardial access, the technique of performing a subxiphoid epicardial puncture, and various measures to prevent complications.

Anatomy

Epicardial access

Needle entry in the subxiphoid approach is typically 2–3 cm below the xiphoid process (Figure 1). Accurate palpation of the xiphoid process is paramount, as this determines the subsequent needle angle and point of entry into the pericardial space. The xiphisternum may be difficult to palpate in certain patients because it articulates with the posterior aspect of the sternum.[3] In these cases, the location can be identified and predicted by palpation of the adjacent costal margin.

The layers traversed by the needle include the skin, superficial fascia, anterior rectus sheath/linea alba, rectus abdominis muscle, and posterior rectus sheath. The needle then travels over the dome of the diaphragm (avoiding the subdiaphragmatic vessels) before reaching the fibrous and parietal serous layers of the pericardium (Figure 2).[3]

The internal mammary arteries lie at the margins of the sternum, typically 1 cm from the sternal edge. It bifurcates into the superior epigastric and musculophrenic arteries at about the sixth intercostal space. The risk of damaging the artery is increased if the needle entry or direction is too lateral (Figure 1).

The left lobe of the liver is near the xiphisternum and may be particularly at risk in patients with congestive heart failure and hepatomegaly.

The right ventricular (RV) marginal artery is situated at the acute margin of the RV, where the pericardium reflects to become the diaphragmatic pericardium, and may rarely continue along the diaphragmatic wall of the RV to become a short posterior descending artery. In cases of abnormally dilated RVs, the marginal artery may be at risk during epicardial access or ablation (Figure 1A).[2]

Pericardial space

The pericardial sac is situated posterior to the sternum and at the level of the second to sixth costal cartilages (Figure 1 and Online Supplemental Teaching Slides). To help maintain its position, the fibrous pericardium, the outermost layer of the sac, has attachments to the sternum anteriorly and the central tendon of the diaphragm inferiorly and it fuses with the adventitia of the great vessels superiorly.[3] The inner fibrous pericardium is lined by the parietal serous pericardium. The parietal serous pericardium reflects on itself to form the visceral serous pericardium, which is adherent to the epicardium. The pericardial cavity is the potential space between the outer parietal layer and the inner visceral layer of the serous pericardium. In about 1 in 10,000 patients, the pericardium is congenitally absent.[4] Features suggestive of this rare disorder include electrocardiographic changes,

KEYWORDS Percutaneous epicardial access; Safety; Complications; Technique

ABBREVIATIONS **LA** = left atrium/atrial; **LAO** = left anterior oblique; **LV** = left ventricle/ventricular; **RV** = right ventricle/ventricular; **VT** = ventricular tachycardia (Heart Rhythm 2014;11:1658–1665)

Dr Lim was supported by the Neil Hamilton Fairley Early Career Fellowship from the National Health and Medical Research Council of Australia. **Address reprint requests and correspondence:** Dr Frédéric Sacher, Hôpital Cardiologique du Haut-Lévêque, 33604 Bordeaux-Pessac, France. E-mail address: frederic.sacher@chu-bordeaux.fr.

1547-5271/$-see front matter http://dx.doi.org/10.1016/j.hrthm.2014.05.041

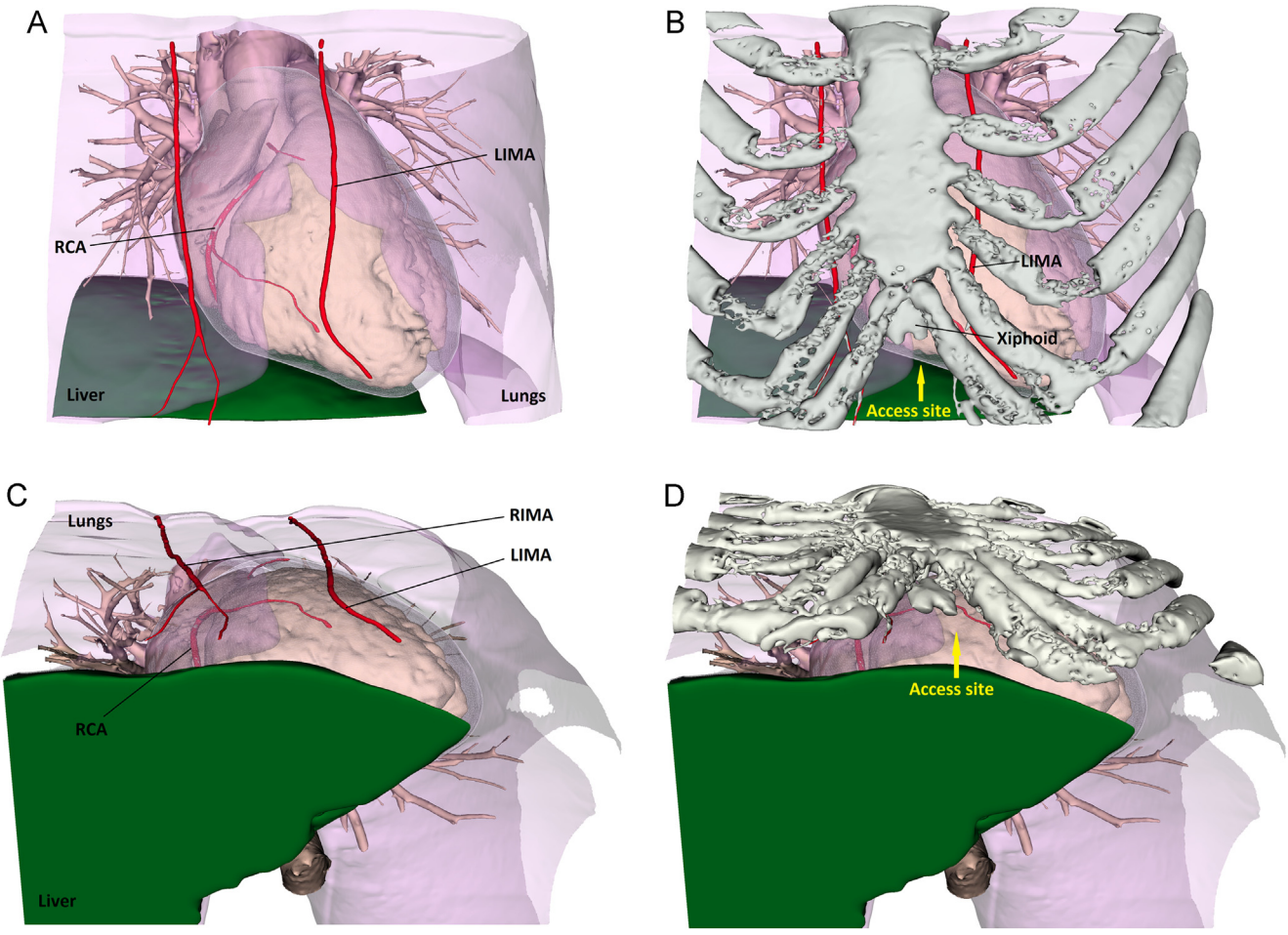

Figure 1 Anatomy of subxiphoid pericardial access. Anteroposterior and transverse views are shown. Needle entry should be 2–3 cm below the xiphoid and directed superiorly at a shallow angle to avoid diaphragmatic puncture. The internal mammary arteries course about 1 cm from the sternal edge. The RV marginal artery lies at the acute margin of the RV. Note that the left lobe of the liver crosses the midline. See text for further details. LIMA = left internal mammary artery; RCA = right coronary artery (with acute marginal branch); RIMA = right internal mammary artery; RV = right ventricle/ventricular.

cardiac displacement, and a sharp aortopulmonary window on the chest radiograph, which can be confirmed by computed tomography or magnetic resonance imaging.

Within the pericardial sac, the catheter moves freely over most of the epicardial surface, apart from specific regions bound by the pericardial reflections, such as the oblique and transverse sinuses, and the pulmonary vein recesses (Online Supplemental Figure 1).[5] The oblique sinus is a cul-de-sac along the posterior left atrial (LA) wall and is bound in between the pericardial reflections of the left and right pulmonary veins and superiorly by the transverse sinus/LA roof. Its inferior opening is bound by the 2 inferior pulmonary veins.[5] The ligament of Marshall is situated at the posterolateral aspect of the LA, and the fold of Marshall may be seen to the left of the oblique sinus. The transverse sinus is a tunnel-shaped anatomical space between the great vessels (which are enclosed in a common pericardial sleeve) and the roof of the LA, connecting the left and right sides of the pericardial cavity. The right pulmonary artery lies superior to the transverse sinus, and the roof of the LA forms its floor.

The phrenic nerves lie near the pericardium. The left phrenic nerve passes behind the left brachiocephalic vein, over the aortic arch and pulmonary trunk, over the LA appendage, and in the majority of patients laterally over the obtuse margin of the left ventricle (LV) and in a minority anteriorly close to the left anterior descending artery.[6,7] The right phrenic nerve descends along the brachiocephalic vein, the right anterolateral border of the superior vena cava, passes close to the anterior wall of the right superior pulmonary vein, and then along the lateral aspect of the right atrial wall.

Technique of epicardial access

Patient preparation

In our institution, patients are under conscious sedation (with the administration of midazolam and sufentanil or remifentanil) and a generous amount of local anesthetic is given along the course of the needle under sterile conditions to ensure adequate anesthesia. Anticoagulation is ceased and baseline coagulation profile, hemoglobin level, platelet

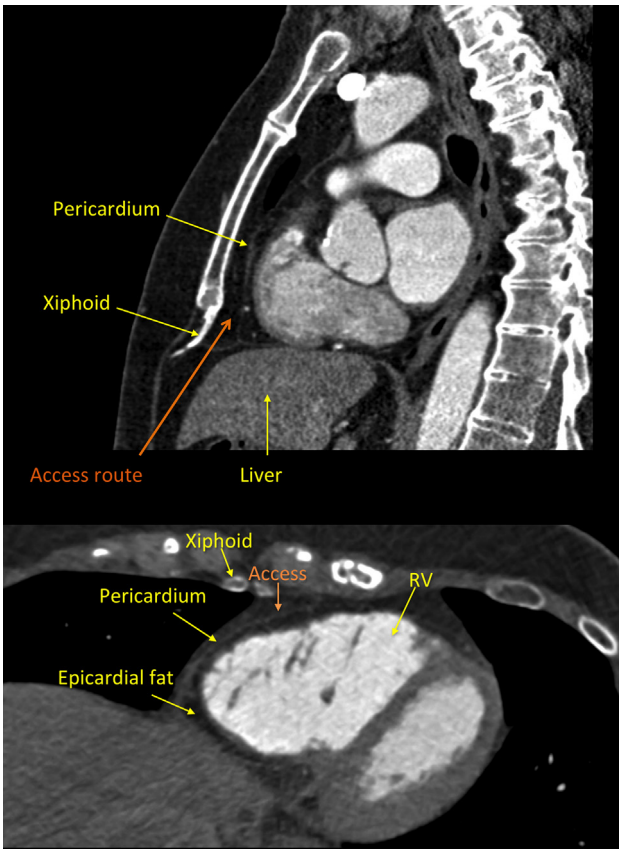

Figure 2 Magnetic resonance imaging views for pericardial access. Top panel: Sagittal view; bottom panel: transverse view). The needle traverses the superficial fascia, anterior rectus sheath, rectus abdominis muscle, and posterior rectus sheath and then over the dome of the diaphragm before reaching the fibrous and parietal serous layers of the pericardium. RV = right ventricle.

count, and biochemistry are checked. Cardiac surgeons are notified of an epicardial procedure and are on standby. A quadripolar catheter is positioned via femoral venous access at the RV apex to provide a fluoroscopic landmark. Pacing threshold is determined should the patient enter VT, and pace termination is required. Further anatomical landmarks such as the lateral LV wall and coronary sinus are also gleaned from patients with existing defibrillators and biventricular pacemakers. The patient is positioned supine with arms beside the body and the fluoroscopic C-arm is positioned at the left lateral position (90°).[8] Fluoroscopic settings for this stage of the procedure are adjusted to obtain maximum definition (eg, 15 frames/s).

Epicardial access

We use a blunt-tipped Tuohy needle (Tuohy bevel, 18 gauge, 1.3 × 80 or 150 mm; Braun, Kronberg, Germany) designed to enter virtual spaces (Online Supplemental Figure 2). Other needles that are used include the Pajunk needle (Pajunk Medical Systems, Norcross, GA). The bevel of the needle should point upward away from the cardiac border in an anterior approach as the needle is advanced and enters the pericardial space to decrease the risk of RV perforation. There are 2 possible approaches to access the pericardial space: the anterior approach (our usual approach) and the posterior approach (see below and Table 2 for further discussion). Needle entry is typically 2–3 cm below the xiphoid process, at the midline (Figure 1). The needle is angled superficially at about 20° to the horizontal plane and superiorly along the midline. In cases of severe scoliosis, fine adjustments need to be made and preprocedural imaging is of pronounced value (Online Supplemental Figure 3). Hereon, the needle is advanced slowly under fluoroscopic guidance as it passes through the subcutaneous tissue and over the dome of the diaphragm (Figure 3A). The most superficial route is taken with the needle underneath the sternum to avoid penetrating the abdominal cavity and damaging a subdiaphragmatic vessel. Gentle downward pressure at the epigastrium helps to steer the left lobe of the liver away from the path of the needle.

Once over the dome of the diaphragm, the needle can be angled slightly further (at about 30°), depending on the anterior or posterior approach (Figure 3B). The left lateral projection offers the advantage of assessing the depth of the needle angle, preventing an overly shallow angle that may not get beneath the sternum, resulting in intense pain from the periosteum, and avoiding the diaphragm at its initial course due to an overly deep angle.[8] Not only does this decrease the risk of injury to the subdiaphragmatic vessels, but in the setting where the diaphragm is punctured, the increased resistance of the diaphragm may suddenly give way to the much softer pericardial layers beneath, obscuring any tactile sensation and increasing the risk of inadvertent RV puncture.

With optimum fluoroscopic settings (and if required a cine image for increased clarity), the motion of the heart border can be imaged (Online Supplemental Movie 1 and Online Supplemental Figure 4). The needle is advanced carefully with gentle suction and should approach the heart border at an oblique angle on the left lateral projection. As the needle approaches the heart border, the needle stylet is removed and a luer lock tip syringe with undiluted contrast is connected to the needle and small amounts of contrast (<1 mL) are injected to assess the location of the needle tip. Care must be taken not to inject too much contrast at each point, as this will obscure the fluoroscopic image, rendering further assessment exceedingly difficult. If too much contrast is injected, the operator may consider waiting to allow the contrast to dissipate before attempting a second puncture. Before reaching the pericardial space, contrast injection usually results in pooled contrast in the mediastinal space (Figure 3C and Online Supplemental Movie 3), an outline of the dome of the diaphragm if the needle is subdiaphragmatic, or patchy contrast in the pleural space if the needle is too laterally directed. Contrast pooling along the inferior wall may indicate the presence of pericardial adhesions.

As the needle traverses the pericardial layers, occasionally tenting of the parietal layer is observed (Figure 3D and Online Supplemental Movie 4). Often gentle pressure coupled with the respiratory movement of the heart is sufficient to cross this parietal layer. Otherwise fine rotating movements (without changing the angle or direction of the

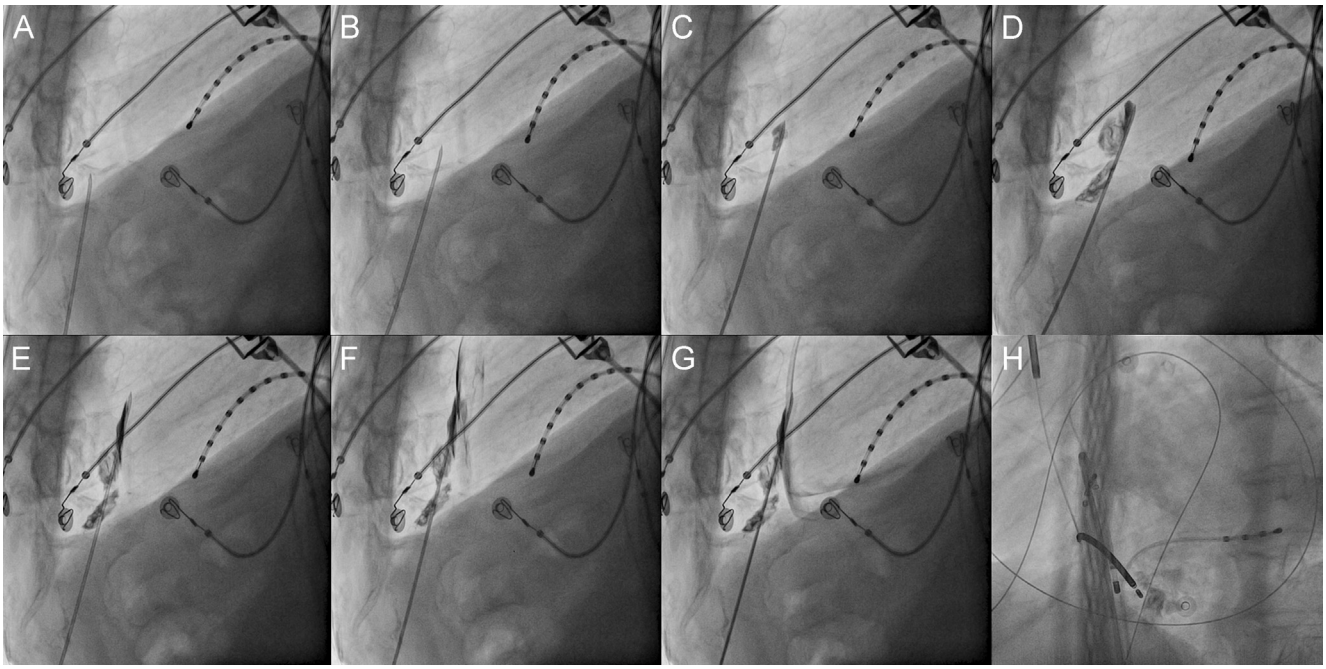

Figure 3 Technique for pericardial access. Initial needle angle is superficial to avoid the diaphragm. The heart border can be seen on the cine image (Online Supplemental Movie). **A:** Once over the dome of the diaphragm, the needle depth can be adjusted under the lateral projection, depending on an anterior or posterior approach. **B:** As the needle approaches the cardiac border, a luer lock needle with contrast is connected and gentle aspiration is applied as the needle is advanced. The cardiac silhouette can be appreciated under optimized fluoroscopic settings or during cine imaging. Contrast injection should be minimal as this may obscure the view. Contrast injection stains the mediastinum. **C:** A small degree of resistance can be felt against the fibrous pericardium. Contrast injection reveals tenting of the pericardium. **D:** A sensation of "give" may be felt as the needle enters the pericardial space. The needle bevel is pointed away from the myocardium to decrease the risk of perforation. **E:** Contrast injection into the pericardial space produces a thin lining that outlines the pericardium around the cardiac silhouette. **F:** Wire insertion into the pericardial space should be free and unrestricted. **G:** Confirmation of wire placement in the pericardial space is obtained in the left anterior oblique projection, demonstrating the guidewire wrapping around the left and right heart borders and crossing multiple cardiac chambers. Movies of each step of the procedure are available in the Online Supplement.

needle) may be needed to create a cut through the membrane. With experience, a sensation of "give" is palpable as the needle enters into the pericardial space (Figure 3E) and a small volume of pericardial fluid can sometimes be aspirated.

Within the pericardial space, 4 conditions should be met: (1) no blood is continually aspirated; (2) contrast injection results in a thin outline of the pericardium around the cardiac silhouette (Figure 3F and Online Supplemental Movie 5);

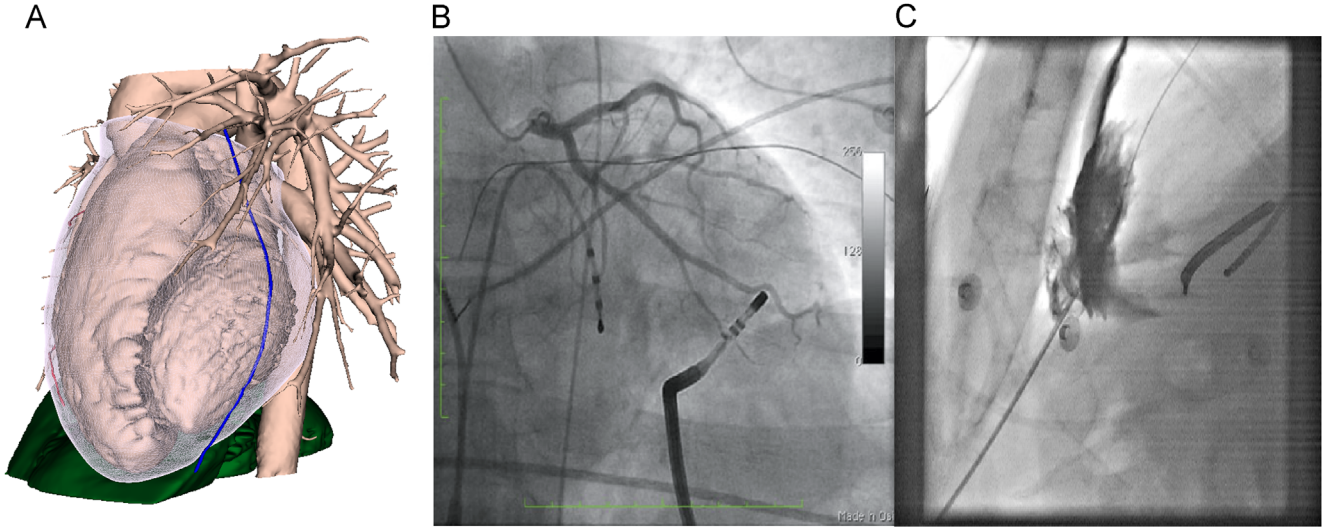

Figure 4 Potential complications. **A:** Phrenic nerve injury. The left phrenic nerve has a variable course over the left ventricular free wall. **B:** Coronary vessel injury. Coronary angiography should always be performed before epicardial ablation. In this case during epicardial mapping of ventricular tachycardia, coronary angiography revealed the ablation catheter displacing a marginal branch of the left circumflex artery at the site of interest (see the Online Supplemental Movie). Adapted from Komatsu et al[15] with permission. **C:** Inadvertent RV puncture. The wire is inadvertently inserted into the RV, which is invariably accompanied by premature ventricular complexes. Note that excessive contrast in difficult cases obscures the operator's view (see the Online Supplemental Movie). RV = right ventricle/ventricular.

(3) the guidewire that is passed through is unrestricted (Figure 3G and Online Supplemental Movie 6), wraps around the left and the right cardiac silhouette, and crosses multiple heart chambers in the left anterior oblique (LAO) projection; and (4) no premature ventricular complexes are observed. The guidewire should be advanced generously and observed to hug both the left and right heart borders and to cross multiple chambers of the heart in the LAO projection (Figure 3H and Online Supplemental Movie 7). The anteroposterior projection alone is inadequate, as a guidewire entering the RV outflow tract and pulmonary artery may give a false impression of being in the pericardial space.

Once the guidewire is confirmed to be in the pericardial space, the needle is removed and an adequate incision is made in the skin, as restrictions in the skin and subcutaneous tissue can be uncomfortable to the patient and can reduce tactile feedback to the operator during catheter manipulation. In our center, a 10-F short sheath with the dilator is then used to dilate the tract. This allows smooth passage of the epicardial sheath (Agilis EPI Steerable Introducer, small curve, St Jude Medical, Inc, St Paul, MN). The sheath can be advanced a few centimeters beyond the epicardial access site to prevent loss of access.

Exchange of catheters and sheath management

The side port of the epicardial sheath is connected to a suction tube with a 3-way tap, which allows continued suction even when a catheter is in place. The aspirated fluid should be examined for any blood stains and the amount of pericardial bleeding assessed.

During exchange and insertion of catheters, suction may be turned off just before catheter insertion to allow some fluid and less friction in the pericardial space, which may be more comfortable for the patient. The epicardial sheath should never be left alone without a catheter or guidewire and dilator in place, as under tension the tip of the sheath may potentially lacerate an epicardial structure. Irrigation of the ablation catheter is maintained at 2 mL/min during mapping and at usual settings during ablation. Pericardial fluid should be drained periodically (or the sheath maintained in constant suction), particularly during ablation, to avoid fluid accumulation in the pericardial space.

Avoiding complications

Knowledge of the potential complications related to epicardial access is crucial in order to perform a safe puncture. Table 1 summarizes the potential complications and relevant preventive measures discussed below.

Inadvertent RV puncture

Inadvertent RV puncture may occur in 4.5%–17% of the cases with attempted epicardial access[2,9]; however, the majority were not associated with serious consequences (<80 mL of pericardial bleeding).[2] Continual aspiration of blood, runs of premature ventricular complexes, lack of thin-walled contrast lining the pericardium, and inappropriate positioning of the guidewire in the LAO projection indicate inadvertent RV puncture (Figure 4C and Online Supplemental Movie 9). It is important to recognize that this has happened so as not to proceed with sheath insertion. In such cases, rather than starting anew, the needle should be withdrawn slightly and the guidewire readvanced into the pericardial space, and the position of the needle tip reconfirmed with the above criteria.

Various further techniques can be employed to minimize trauma to the RV. One method involves the telescoping technique. In this technique, a stiff needle (eg, Pajunk needle) is first used to navigate the subcutaneous tissue. Once the needle enters near the heart, the stylet from the stiff needle is replaced by a long micropuncture needle and small amounts of contrast (1 mL) are injected as the needle approaches the pericardium. Since the micropuncture needle does not offer the tactile feel of a larger needle, contrast injection is mandatory to confirm pericardial access, with this needle-in-needle approach. Once access has been obtained through the micropuncture needle, a micropuncture wire is inserted through the needle into the pericardium and the rest of the steps are analogous to gaining pericardial access with traditional needles.

Pericardial bleeding

Pericardial bleeding may be noted even in uncomplicated procedures, and it is not uncommon to observe 10–30 mL of aspirated blood-stained fluid after the puncture that usually settles in 5–10 minutes.[10,11] However, any continual bleeding should alert the operator of a possible complication. If hemostasis is not achieved, surgical repair should be considered urgently. To minimize bleeding, no anticoagulation should be given before epicardial access.

Injury to the subdiaphragmatic vessels and liver/abdominal viscera

Infrequently, injury to the subdiaphragmatic vessels or abdominal viscera may occur if the angle of the needle is too deep or the skin entry is too low (Online Supplemental Figure 5). Care must be taken in patients with known heart failure and hepatomegaly. Adequate palpation of the level of the xiphoid process, gentle downward pressure in the epigastrium to steer the liver away from the course of the needle, assessing the depth of the needle in the left lateral projection to avoid the diaphragm, and maintenance of the needle trajectory with no sideways movements help prevent this complication. Abdominal pain, rebound tenderness, and progressive hypotension are warning signs of an intra-abdominal bleed and hemoperitoneum. Hence, conscious sedation may promote periprocedural and early postoperative detection in this setting. Blood transfusions and surgical repair may be indicated.[9]

Coronary vessel damage

The acute marginal branch of the RV courses along the margin of the RV. In cases of arrhythmogenic RV dysplasia or where the RV is abnormally dilated, this artery may be at

Table 1 Potential complications with epicardial access and preventive measures

Potential complication	Incidence	Preventive measure
Inadvertent RV puncture	4.5%–17% (without significant bleeding)[2,9]	1. Ensure no continual aspiration of blood 2. Ensure contrast injection results in a thin outline of the pericardium around the cardiac silhouette 3. Ensure guidewire that is passed through is unrestricted, wraps around the left and the right cardiac silhouette and crosses multiple heart chambers in the LAO projection 4. Ensure no premature ventricular complexes are observed 5. Do not insert sheath until confirmed in the pericardial space
Pericardial bleed	10%–30% (mild, self-limiting)[11] 4.5% (intrapericardial bleeding >80 mL)[2] 0.6% (delayed tamponade)[2]	1. Avoid anticoagulation before epicardial access 2. Examine aspirated pericardial fluid 3. Consider surgical repair if hemostasis not achieved
Injury to subdiaphragmatic vessels and abdominal viscera	0.5%[9]	1. Beware in cases of congestive heart failure and hepatomegaly 2. Ensure adequate palpation of the level of the xiphoid process 3. Apply gentle downward and leftward pressure in the epigastrium to steer the liver away from the course of the needle 4. Adjust needle angle from the left lateral projection to avoid the diaphragm 5. Maintain trajectory of the needle with no sideways movements
Coronary vessel damage	0.6% (coronary artery stenosis)[2] 0.6% (myocardial infarction)[2]	1. Beware in cases of abnormally dilated RV (acute marginal artery) 2. Monitor pericardial aspirate 3. Perform coronary angiography before ablation and if suspected vessel damage
Phrenic nerve injury	0% (during epicardial puncture)[2] Maneuvers to avoid injury during ablation[6]	1. Perform high-output pacing for phrenic nerve capture 2. Consider methods to interpose the ablation site and the phrenic nerve
Pneumopericardium	Uncommon	1. Results in decreased defibrillator threshold 2. Minimize introduction of air during sheath insertion and catheter exchange 3. Evacuate any air in the pericardium 4. Ensure adequate placement of defibrillator patches, electrocardiographic patches, and electroanatomic mapping patches
Pericarditis (postprocedural)	Mild symptomatic pericarditis in almost all patients[2] 0.6% (severe pericardial reaction)[2]	1. Remove the catheter and sheath at the end of the procedure when no further bleeding is observed 2. Administer anti-inflammatory agents 3. Consider steroid injection into the pericardial space
Pleuritis (postprocedural)	Not uncommon	1. Administer anti-inflammatory agents

LAO = left anterior oblique; RV = right ventricular.

risk during epicardial access or ablation.[2] During mapping and ablation, particular care should be taken in the septal and basal areas, where coronary arteries are known to traverse. The susceptibility to coronary artery damage is inversely proportional to the proximity of the ablation catheter and the size of the vessel.[12] A minimal distance of 5 mm should be maintained between the ablation catheter and the coronary vessel.[13] Acute coronary arterial vasospasm during epicardial mapping has also been reported, requiring intracoronary nitrates and intra-aortic balloon counterpulsation in some cases.[14] Coronary angiography should always be performed before ablation (Figure 4B and Online Supplemental Movie 8). Multimodality imaging such as multidetector computed tomography and magnetic resonance imaging of the course of the coronary arteries and phrenic nerves (Figure 4A) integrated with the 3-dimensional electroanatomic map provides further information on these important epicardial structures.[15]

Phrenic nerve injury

Before ablation, over the lateral LV and at areas near the course of the phrenic nerve, pacing maneuvers should always be performed at high output (20 mA, pulse width of 2 ms) to exclude phrenic nerve capture (Figure 4A).[6] It is important to note that a response will not be elicited in patients who are paralyzed under general anesthesia. Several methods exist to avoid injury to the phrenic nerve, including interposing a sheath, balloon, saline, or air in the pericardium between the ablation catheter and the nerve.[16]

Pneumopericardium

During the exchange of catheters, care must be taken to minimize the introduction of air into the pericardial space. Air in the pericardium may result in an increase in the transthoracic defibrillator threshold, which can be highly detrimental during a VT procedure.[17] Pericardial air is easily

imaged by fluoroscopy around the apex and should be evacuated when detected.

Injury to the esophagus

The esophagus lies behind the posterior wall of the LA. Although rarely encountered, damage to this structure may result in severe complications such as atrio-esophageal fistulas.

Pericarditis

Mild pericarditis with chest pain after an epicardial procedure is experienced in almost every patient.[2] They are often self-limiting and respond well to anti-inflammatory agents. To prevent excessive pericardial irritation, the catheter and sheath are removed at the end of the procedure, except in cases of continued bleeding. Data from animal studies favor the injection of steroids into the pericardial space to minimize postprocedure pericarditis and adhesion formation.[18] Although we do not routinely administer steroids, some centers administer 0.5–1 mg/kg of methylprednisolone into the pericardial space at the end of the procedure in the hope of reducing pericardial inflammatory reaction.[10] In limited cases, severe inflammatory pericarditis may impede epicardial access during repeat procedures.

Injury to the lung/pleuritis

In one series, inadvertent entry of the guidewire into the pleural space occurred in 1.5% of the patients during attempted epicardial access, without pneumothorax or complications.[2] Pulmonary lesions may occur as a result of epicardial ablation, although the clinical significance is unknown. Patients may also experience symptomatic pleuritis postprocedure, which usually responds well to anti-inflammatory agents.

Anterior vs posterior approach for epicardial access

The anterior or posterior approach to the pericardium may be chosen chiefly based on the target site of ablation. The anterior approach allows easier access to the anterior surface of the heart and ventricles, while the posterior approach allows easier access to the inferior ventricular walls and posterior LA walls. If repeat percutaneous access is attempted in a patient, a posterior approach may be preferred because of higher preponderance of adhesions situated anteriorly.[19] However, our strategy is to always start with the anterior approach as we consider this the safest approach. With the anterior approach, the inferior/posterior regions of the heart remain accessible either indirectly by looping the catheter around the heart or in cases of pericardial puncture within 2–3 cm from the apex, directly by bending the steerable sheath downward. A shallow angle is used in the anterior approach and needle entry may be slightly lower than usual to facilitate the shallow angle, while a deeper angle is used in the posterior approach and needle entry may be relatively closer to the xiphoid than in the anterior approach. The needle angles for each approach can be further adjusted in the left lateral projection. The needle bevel is pointed upward in an anterior approach and downward generally in a posterior approach, away from the myocardium to minimize the risk of cardiac perforation. The needle is pointed superiorly along the midline in an anterior approach, which allows entry into the pericardial space anterior to the RV, while in a posterior approach the needle is pointed slightly leftward toward the left midclavicle. These factors are summarized in Table 2.

Patients with prior epicardial access or prior cardiac surgery

The pericardial space can be reaccessed in the majority of patients with prior epicardial procedures (95% in one series), whereas previous cardiac surgery and the presence of pericardial adhesions is a frequent cause of failure to achieve percutaneous epicardial access (73% in the same series) (Online Supplemental Figure 6).[2] In patients with previous cardiac surgery, a limited surgical approach with the creation of a subxiphoid pericardial window is an alternative and safe option.[20]

Table 2 Anterior vs posterior approach for epicardial access

Factor/technique	Anterior approach	Posterior approach
Factors		
Target region	• Anterior wall of ventricles • Left atrial and right atrial appendage	• Inferior wall of ventricles • Posterior left atrial wall • Epicardial left ventricular lead placement
Prior cardiac surgery (if the percutaneous approach is attempted)		• Preferable as adhesions predominantly situated anteriorly from surgical opening of the pericardial sac
Technique		
Needle trajectory	• Superiorly along the midline	• Slightly leftward, aiming toward the left midclavicle
Needle angle	• Shallow angle (~20°) • Needle entry may be slightly lower than usual owing to the shallow needle angle • Gentle downward pressure to steer the left lobe of the liver away from the needle path	• Slightly deeper angle (20°–30°) • Needle angle can be adjusted once the needle tip passes over the dome of the diaphragm in the left lateral projection
Needle bevel	• Bevel is pointed upward, away from the myocardium	• Bevel pointed downward generally, away from the myocardium

Introducing a second pericardial catheter

A second pericardial catheter may be introduced in certain cases when additional epicardial mapping is required during ablation. The second pericardial puncture is facilitated significantly by the injection of air (50–100 mL) into the pericardial space via the first sheath. Air collects superiorly and creates a space between the pericardial layers, enabling a second puncture with minimal risk of RV perforation. The injected air is then removed to permit effective defibrillation during the rest of the procedure.

Conclusion

Percutaneous epicardial access is a valuable adjunct for catheter ablation of complex arrhythmias. However, knowledge of potential complications and pertinent preventive measures is vital to ensure safe implementation of the procedure.

Appendix

Supplemenety data

Supplementary data associated with this article can be found in the online version at http://dx.doi.org/10.1016/j.hrthm.2014.05.041.

References

1. Sosa E, Scanavacca M, d'Avila A, Pilleggi F. A new technique to perform epicardial mapping in the electrophysiology laboratory. J Cardiovasc Electrophysiol 1996;7:531–536.
2. Sacher F, Roberts-Thomson K, Maury P, et al. Epicardial ventricular tachycardia ablation a multicenter safety study. J Am Coll Cardiol 2010;55:2366–2372.
3. Loukas M, Walters A, Boon JM, Welch TP, Meiring JH, Abrahams PH. Pericardiocentesis: a clinical anatomy review. Clin Anat 2012;25:872–881.
4. Van Son JA, Danielson GK, Schaff HV, Mullany CJ, Julsrud PR, Breen JF. Congenital partial and complete absence of the pericardium. Mayo Clin Proc 1993;68:743–747.
5. Lachman N, Syed FF, Habib A, Kapa S, Bisco SE, Venkatachalam KL, Asirvatham SJ. Correlative anatomy for the electrophysiologist, Part I: The pericardial space, oblique sinus, transverse sinus. J Cardiovasc Electrophysiol 2010;21:1421–1426.
6. Fan R, Cano O, Ho SY, Bala R, Callans DJ, Dixit S, Garcia F, Gerstenfeld EP, Hutchinson M, Lin D, Riley M, Marchlinski FE. Characterization of the phrenic nerve course within the epicardial substrate of patients with non-ischemic cardiomyopathy and ventricular tachycardia. Heart Rhythm 2009;6:59–64.
7. Sanchez-Quintana D, Cabrera JA, Climent V, Farre J, Weiglein A, Ho SY. How close are the phrenic nerves to cardiac structures? Implications for cardiac interventionalists. J Cardiovasc Electrophysiol 2005;16:309–313.
8. Weerasooriya R, Jais P, Sacher F, Knecht S, Wright M, Lellouch N, Nault I, Matsuo S, Hocini M, Clementy J, Haissaguerre M. Utility of the lateral fluoroscopic view for subxiphoid pericardial access. Circ Arrhythm Electrophysiol 2009;2:e15–e17.
9. Sosa E, Scanavacca M. Epicardial mapping and ablation techniques to control ventricular tachycardia. J Cardiovasc Electrophysiol 2005;16:449–452.
10. Tedrow U, Stevenson WG. Strategies for epicardial mapping and ablation of ventricular tachycardia. J Cardiovasc Electrophysiol 2009;20:710–713.
11. Yamada T. Transthoracic epicardial catheter ablation. Circ J 2013;77:1672–1680.
12. Sosa E, Scanavacca M, d'Avila A. Transthoracic epicardial catheter ablation to treat recurrent ventricular tachycardia. Curr Cardiol Rep 2001;3:451–458.
13. Viles-Gonzalez JF, de Castro Miranda R, Scanavacca M, Sosa E, d'Avila A. Acute and chronic effects of epicardial radiofrequency applications delivered on epicardial coronary arteries. Circ Arrhythm Electrophysiol 2011;4:526–531.
14. Koruth JS, Aryana A, Dukkipati SR, Pak HN, Kim YH, Sosa EA, Scanavacca M, Mahapatra S, Ailawadi G, Reddy VY, d'Avila A. Unusual complications of percutaneous epicardial access and epicardial mapping and ablation of cardiac arrhythmias. Circ Arrhythm Electrophysiol 2011;4:882–888.
15. Komatsu Y, Sacher F, Cochet H, Jais P. Multimodality imaging to improve the safety and efficacy of epicardial ablation of scar-related ventricular tachycardia. J Cardiovasc Electrophysiol 2013;24:1426–1427.
16. Matsuo S, Jais P, Knecht S, Lim KT, Hocini M, Derval N, Wright M, Sacher F, Haissaguerre M. Images in cardiovascular medicine: novel technique to prevent left phrenic nerve injury during epicardial catheter ablation. Circulation 2008;117:e471.
17. Yamada T, McElderry HT, Platonov M, Doppalapudi H, Kay GN. Aspirated air in the pericardial space during epicardial catheterization may elevate the defibrillation threshold. Int J Cardiol 2009;135:e34–e35.
18. d'Avila A, Neuzil P, Thiagalingam A, Gutierrez P, Aleong R, Ruskin JN, Reddy VY. Experimental efficacy of pericardial instillation of anti-inflammatory agents during percutaneous epicardial catheter ablation to prevent postprocedure pericarditis. J Cardiovasc Electrophysiol 2007;18:1178–1183.
19. d'Avila A, Koruth JS, Dukkipati S, Reddy VY. Epicardial access for the treatment of cardiac arrhythmias. Europace 2012;14:ii13–ii18.
20. Soejima K, Couper G, Cooper JM, Sapp JL, Epstein LM, Stevenson WG. Subxiphoid surgical approach for epicardial catheter-based mapping and ablation in patients with prior cardiac surgery or difficult pericardial access. Circulation 2004;110:1197–1201.

B. Epicardial only mapping and ablation of VT: a case series.

Berte B, Yamashita S, Sacher F, Cochet H, Hooks D, Aljefairi N, Amraoui S, Denis A, Derval N, Hocini M, Haïssaguerre M, Jaïs P. Europace. 2015 Apr 2. pii: euv072. [Epub ahead of print]

1. Study outline

In this work, we retrospectively analyzed all 296 patients who underwent a VT ablation at our center between 2011 and 2014. Four patients underwent an epicardial only procedure. Two ICM patients had a proven endocardial LV thrombus (by imaging). One myocarditis patient had a prior endocardial only procedure at another center. The fourth patient had a complicated epicardial puncture with mild bleeding. Complete epicardial LAVA elimination was obtained in 2 patients. Non-inducibility was obtained in 2 patients. After a follow-up of 21±12 months, 1patient had recurrence of VT.

2. Implications

Epicardial only ablation seems feasible and effective and useful in a limited subset of patients with incessant VT. However, endpoints are more difficult to evaluate and long-term follow-up is needed. In myocarditis patients with subepicardial only scar (III.C) we hypothesize that an epicardial only approach could be effective since no endocardial LAVA is found.[98] In ICM with an endocardial thrombus, this approach could be used as an epicardial ablation to eliminate endocardial LAVA, the opposite of earlier published work, if wall thinning <5mm is present.[67]

3. Manuscript

Europace Advance Access published April 2, 2015

Europace
doi:10.1093/europace/euv072

CLINICAL RESEARCH

Epicardial only mapping and ablation of ventricular tachycardia: a case series

Benjamin Berte, Seigo Yamashita, Frederic Sacher, Hubert Cochet, Darren Hooks, Nora Aljefairi, Sana Amraoui, Arnaud Denis, Nicolas Derval, Meleze Hocini, Michel Haïssaguerre, and Pierre Jaïs*

Hôpital Cardiologique du Haut-L'évêque, CHU Bordeaux, and LIRYC Institute, IHU Bordeaux, Bordeaux-Pessac 33604, France

Received 13 December 2014; accepted after revision 3 March 2015

Aims Ventricular tachycardia (VT) ablation for ventricular arrhythmias is a validated approach, typically performed endocardially, or combined with an epicardial approach if endocardial ablation failed or in case of non-ischaemic cardiomyopathy. We report our experience with epicardial only procedure in a subset of patients with incessant VT or VT storm.

Methods and results This was a single centre retrospective study. Between 2011 and 2014, all patients referred for VT ablation were reviewed at CHU Bordeaux. All patients with an epicardial only (anterior percutaneous approach) mapping and ablation procedure were included. In total, 296 patients underwent a VT ablation and 4 (all male, 70 ± 7 years, 27 ± 11% left ventricular ejection fraction) of them underwent an epicardial only procedure: two ischaemic patients had an endocardial left ventricular thrombus and incessant VT. One patient post-myocarditis had a failed a previous endocardial procedure without local abnormal ventricular activity (LAVA). The fourth patient had a dilated cardiomyopathy and a complicated epicardial puncture followed by mild continuous bleeding (200 mL) precluding anticoagulation associated with left ventricular endocardial access. Local abnormal ventricular activity elimination was verified only epicardially in all and obtained in two patients and non-inducibility was tested and achieved in the two patients without thrombus. No further complications occurred. After a mean follow-up of 21 ± 12 months, one patient (25%) had recurrence of VT and no patient death was observed.

Conclusion Epicardial only ablation seems feasible and effective and useful in a limited subset of patients with incessant VT. However, endpoints are more difficult to evaluate and long-term follow-up is needed.

Keywords Ablation • Endocardial thrombus • Epicardial • Imaging • LAVA • Ventricular tachycardia

Introduction

Ablation of scar-related ventricular tachycardia (VT) is a validated technique, often in conjunction with implantable cardioverter-defibrillator (ICD) therapy.[1,2] Substrate-based ablation widened the use of VT ablation for both ischaemic ischaemic cardiomyopathy (ICM) and non-ischaemic cardiomyopathy (NICM).

An endocardial only ablation approach is the most used technique.[1,3] The epicardial access is usually used after a failed endocardial approach and rarely as a combined approach during the index procedure.[4,5] Epicardial ablation is a relatively safe approach with a major complication rate around 8% in tertiary centres.[6] Moreover, an epicardial only ablation has been reported to be safe and effective after a failed endocardial approach.[7]

In ICM—with subendocardial or transmural scar and because of wall thinning—an endocardial only approach is effective in the vast majority of patients.[8] However, more than two-thirds of patients selected for an epicardial approach after a failed endocardial procedure showed an epicardial ablation target.[9]

In NICM—with subepicardial or intramural scar—an epicardial access can be of added value.[8] In arrhythmogenic right ventricular cardiomyopathy, epicardial scar is larger than endocardial scar and epicardial access can be used to map epicardial scar and local abnormal ventricular activity (LAVA) from the epicardium, while ablating from the endocardium, due to wall thinning.[10] In patients post-myocarditis with subepicardial scar only, endocardial LAVA is usually absent and epicardial only ablation is needed in most if not all.[11,12]

* Corresponding author. Tel: +33 5 57 65 64 71; fax: +33 5 57 65 65 09. *E-mail address*: pierre.jais@chu-bordeaux.fr

What's new?

- This is to our experience the first case series of epicardial only mapping and ablation of VT feasible in a very limited subset of patients.
- Specific problems to evaluate endpoints are encountered.

Pre-procedural imaging with multidetector computed tomography (MDCT) and delayed enhancement magnetic resonance imaging (DE-MRI) can help to visualize scar, important anatomical structures (such as the phrenic nerve and the coronary artery system), wall thinning, ventricular aneurysm, ventricular (and atrial) thrombus, and calcification MRI.[13–16] The knowledge of the presence of a subepicardial scar can help the operator to use an epicardial approach.[17] A left ventricular endocardial thrombus is a contra-indication for endocardial mapping and ablation, due to the risk for stroke.

In this study, we report our experience of an epicardial only approach for mapping and ablation in a very limited subset of patients.

Methods

All VT ablations between 2011 and 2014 were reviewed at CHU Bordeaux. All epicardial only (both mapping and ablation) procedures were included irrespective of an earlier endocardial mapping. Procedure time, radiofrequency time, electroanatomical substrate and activation maps, endpoints (LAVA elimination and inducibility), complications, and follow-up were analysed.

A pre-procedural mesh with scar and anatomical information was integrated in the mapping system and ICD therapy was disabled before the procedure. After obtaining groin access, a RV apex catheter was positioned as anatomical landmark and for pacing. An anterior percutaneous subxyphoidal puncture approach was used to obtain access to the pericardial space.[18,19] A steerable short curve—regular size or epicardial sheath (Agilis, St Jude Medical)—was used to access the pericardial space. Suction was applied on the sheath when needed to increase catheter stability, contact, and electrogram quality. An irrigated multipolar mapping catheter (PentaRay, Biosense Webster) was used for high-density mapping.

Local abnormal ventricular activity was manually tagged on the substrate maps. Local abnormal ventricular activities are surviving fibres inside the scar tissue and often have a lower bipolar voltage and sharp appearance.[6] They can be fractionated and late but can in fact appear everywhere during the QRS complex, depending on their anatomy and position inside the scar, as previously demonstrated.[7] Their main characteristic is poor electrical coupling to the surrounding tissue, which manifests as local delay or Wenkebach behaviour during pacing at faster rates. This is the reason why we prefer to use the term LAVA and not late potentials, since this implies performance of active pacing manoeuvres to unmask/identify LAVA in doubt. All late potentials are LAVA, but not all LAVAs are late potentials.

Although different epicardial voltage cut-offs are suggested (<1.81 and <1 mV), we used the usual epicardial bipolar low-voltage threshold of <1 mV and unipolar low-voltage thresholds of <7.95 mV.[1,4] We used unipolar voltage in this subset to have a better understanding of the endocardial and/or transmural scar extent and to improve our image merge.

After completion of the substrate map in sinus rhythm, the electroanatomical mapping (EAM) map was merged with the three-dimensional image model and the mapping catheter was exchanged for an irrigated ablation catheter (Thermocool SF, Biosense Webster or Coolpath Duo, St Jude Medical).

When the merged image demonstrated a phrenic nerve within 5 mm, we performed detailed high output (10 mA, 2 ms) pacing to tag the phrenic nerve on the EAM map. In case we expect a close distance (<5 mm) from a coronary artery on the merged image, a coronary angiogram was performed in different views by an experienced invasive cardiologist. If LAVAs were found >5 mm away from the major coronary arteries or no phrenic nerve capture was confirmed, LAVA-based ablation was performed in that region. If LAVAs were found <5 mm from the phrenic nerve, an injection of saline (with close monitoring of signs of tamponade) was performed to displace the phrenic nerve from the potential ablation site.

In the absence of an endocardial thrombus, a VT induction protocol was performed from the RV apex (600–500–400 ms drive train with up to three extrastimuli) and an activation map was made when tolerated. Furthermore, entrainment mapping was performed to identify the critical isthmus, based on a short post-pacing interval <30 ms, a stimulus-to-QRS duration of 40–70 ms and concealed entrainment. Ablation was started with the aim to terminate VT during ablation. When an induction protocol was contra-indicated, the critical isthmus was detected based on substrate mapping, manual LAVA tagging, pacemapping, and prolonged stimulation-to-QRS duration.

Ablation was performed using a conventional ablation catheter without contact force, using a power-controlled mode is used with mean power delivery of 25 W with an irrigation at 8 mL/min during 60–90 s. We did not titrate to achieve certain impedance changes.

After LAVA-based ablation, a re-map was made, using the multipolar PentaRay mapping catheter to confirm the endpoint of complete LAVA elimination and an additional ablation was performed when needed.

At the end of the procedure, the epicardial Agilis sheath was replaced by a pigtail catheter and an active suction was performed to evacuate all intrapericardial liquid. A routine transthoracic ultrasound evaluation of the pericardial space was then performed and if re-assuring, the pigtail catheter was removed without application of intrapericardial corticoids. All patients routinely received a therapeutic dose of non-steroidal anti-inflammatory drugs (NSAIDs) during 5 days.

Follow-up data (in months) after procedures were collected using device logs, hospital admissions, and data from the general practitioner and cardiologist. All patients were routinely seen in clinic at 1, 3, 6, 12, and 24 months. Records were kept of all instances of VT (sustained and non-sustained), with or without the need of therapy [anti-tachycardia pacing (ATP) or shock], as well as any deaths.

Results

A total of 296 patients underwent a VT ablation procedure at CHU Bordeaux. A subset of four patients (all male, 70 ± 7 years old) underwent an epicardial only procedure for mapping and ablation. A three-dimensional mapping system was used in all patients (Ensite™: $n = 3$, St Jude Medical and CARTO® 3: $n = 1$, Biosense Webster) to create a high-density map (mean 696 ± 414 map points epicardial/map), using a multipolar mapping catheter (PentaRay, Biosense Webster). All patients had a diminished left ventricular ejection fraction (mean LVEF 27 ± 11%) and were on amiodarone and beta-blockers. Three patients had incessant VT and one had a ventricular storm. All patients carried an ICD and had multiple ICD shocks

Table 1 Baseline characteristics

Patient	Sex	Age (years)	Disease	Procedure number	Amiodarone	BB-ACE-statin	VTCL (ms)	Axis	ICD	ICD shocks	GFR (mL/min)	NYHA	LVEF	Reason for procedure	Reason for epi only procedure
1	M	70	MYO	2	1	1	490	RBBB	1	1	75	II	41%	Incessant VT	endo LAVA absent surgical epi access
2	M	73	ICM	1	1	1	300	RBBB	1	1	70	II	20%	Incessant VT	LV endocardial thrombus
3	M	60	ICM	1	1	1	350	RBBB	1	1	53	II	30%	VT storm	LV endocardial thrombus
4	M	77	DCM	1	1	1	350	RBBB	1	1	39	III	16%	Incessant VT	Bleeding after epi puncture

BB, beta-blockers; ACE, ace-inhibitors; VTCL, ventricular tachycardia cycle length; GFR, glomerulary filtration rate; NYHA, New York Heart Association Class; epi, epicardial; MYO, post-myocarditis; DCM, dilated cardiomyopathy; RBBB, right bundle branch block; endo, endocardial.

Table 2 Procedural data

Patient	EAM system	epi map points	epi bipolar LVA (cm^2)	epi LAVA	Imaging	Scar location	Ablation during VT	epi mapping	epi adhesions	Procedure time (min)	epi RF time (min)	Non-inducibility	LAVA elimination
1	Ensite	626	53	1	MDCT + DE-MRI	Apico-inferoseptal and lateral	1	PentaRay	1	175	38	1	Complete
2	CARTO 3	322	166	1	DE-MRI	Anterior	0	PentaRay	1	190	10	Not tested	Complete
3	Ensite + Mediguide	1140	121	1	MDCT	Anterior	0	PentaRay	1	240	21	Not tested	Incomplete
4	Ensite	NA	NA	1	MDCT	Basal-mid inferoseptal	1	PentaRay	0	120	9	1	Incomplete

epi, epicardial; LVA, low-voltage area.

before admission. Pre-procedural imaging was used in all (MDCT: $n = 3$ and DE-MRI: $n = 2$) and demonstrated a subepicardial scar in one patient, a transmural scar in one patient, and an endocardial left ventricular thrombus in two patients.

Baseline characteristics and procedural data are illustrated in *Tables 1* and *2*. All patients are discussed in detail as follows.

Myocarditis patient with recurrence of ventricular tachycardia after endocardial only procedure ($n = 1$)

Patient 1 (represented in *Figure 1*) presented with subepicardial only inferolateral scar. Multidetector computed tomography and DE-MRI imaging showed an anatomical isthmus between two regions of focal wall thinning. An earlier endocardial approach demonstrated the absence of endocardial LAVA. Because of incessant VT, a repeat procedure was proposed but without any endocardial access. An epicardial only procedure was conducted. After the completion of the substrate map and image integration, only the stable clinical VT was induced and the isthmus was confirmed using entrainment mapping, at the site of the anatomical isthmus, found on imaging. A coronary angiogram was made and confirmed a safe potential ablation site. Ablation was performed during VT and the clinical VT was stopped during the first RF application and was not inducible afterwards. Further LAVA elimination was performed until complete LAVA elimination was obtained. Only beta-blocker therapy was continued afterwards (*Table 3*).

Ischaemic patients with a left ventricular thrombus on multidetector computed tomography ($n = 2$)

Patients 2 and 3 (represented in *Figures 2* and *3*) were referred for VT ablation and had an endocardial left ventricular (LV) thrombus on MDCT imaging. None of them had undergone CABG.

Patient 2 presented with a persistent thrombus despite of anticoagulant therapy (warfarin) initiated 3 months ago. The thrombus was not visible on routine echocardiography. This patient was taken to the laboratory because of prior incessant VT episodes. He was therefore intubated and ventilated and received amiodarone intravenously. After extubation—1 week before the procedure—he did not show spontaneous VT episodes anymore.

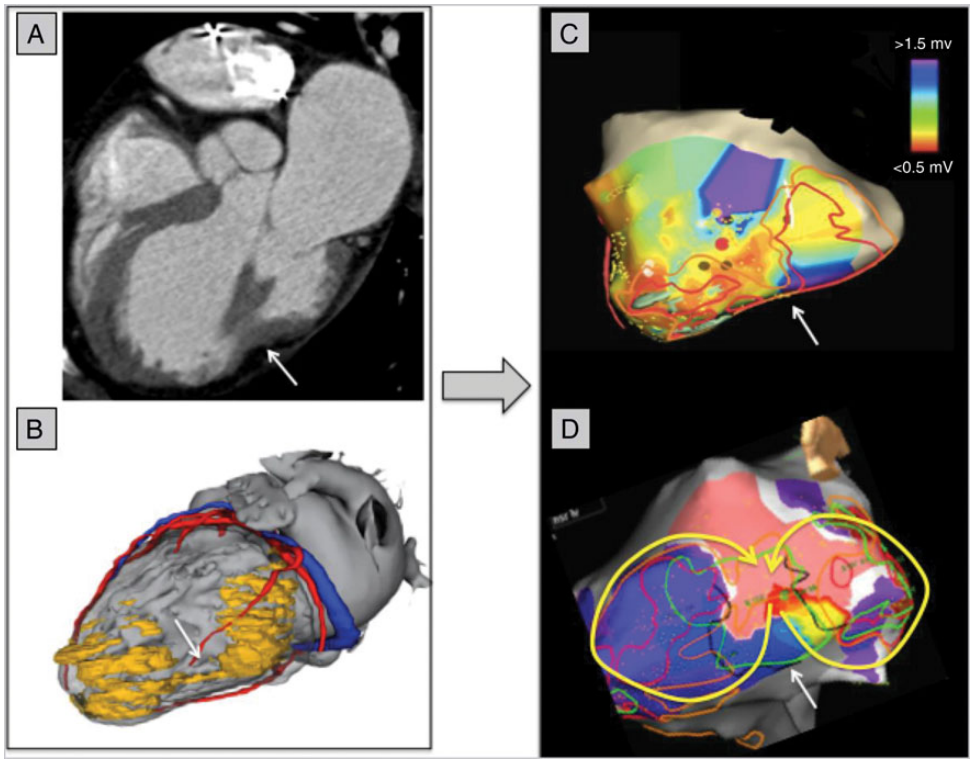

Figure 1 Patient 1 with post-myocarditis subepicardial only scar (lateral view). (*A*) Multidetector computed tomography image of the left ventricle, showing two lateral zones of focal wall thinning with an anatomical epicardial isthmus in between (white arrow). (*B*) Three-dimensional mesh (derived from merged information of MDCT and MRI) made using Music software (INRIA, Nice and CHU Bordeaux, France) with coronary artery system in red, coronary venous system in blue, and two zones of scar (wall thinning) in yellow with an isthmus in between (white arrow). (*C*) Epicardial bipolar voltage map, using the EnSite™ Velocity™ system (St Jude Medical). Purple is normal voltage >1.5 mV, green is borderzone >0.5 to <1.5 mV, and grey is dense scar <0.5 mV. Brown LAVA dots are manually tagged and seen inside the anatomical isthmus (white arrow). Successful ablation site is tagged in red. (*D*) Activation map of the clinical incessant VT, showing a figure-of-eight circuit trough the isthmus. Ablation is performed during VT and the first application at the narrow VT exit site stopped the VT.

Table 3 Complications and follow-up

Patient	Complications	VT recurrences	ATP	ICD shocks	LVEF 6 months later (%)	Follow-up (months)
1	0	0	0	0	50	30
2	0	0	0	0	36	32
3	0	0	0	0	33	6
4	200 mL epicardial bleeding	1	0	1	20	15

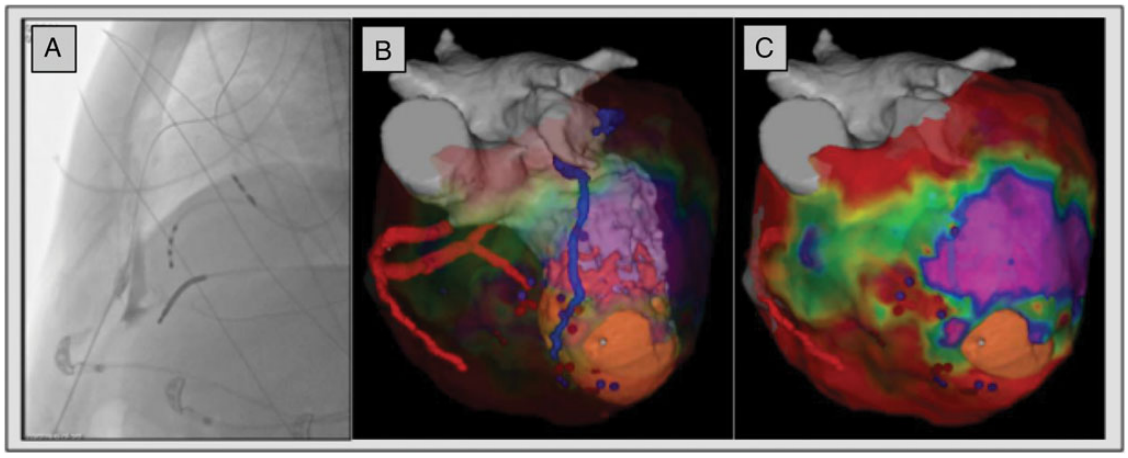

Figure 2 Patient 2 with ischaemic cardiomyopathy and an endocardial thrombus [anteroposterior (AP) view]. (*A*) Percutaneous anterior subxyphoidal epicardial puncture with Tuhoy needle using the left lateral fluoroscopic view. Contrast inside the pericardial space is seen and a guidewire freely moves within the pericardial space. A quadripolar catheter (Bard) inside the RV apex is used as anatomical landmark. Atrial and ventricular leads of intracardiac defibrillator are visible. (*B*) Merged image of transparant epicardial voltage map and three-dimensional mesh (derived from DE-MRI) made using Music® software with coronary artery system in red, coronary venous system in blue, and scar in orange. Local abnormal ventricular activity tagged in purple and ablation points are tagged in red. (*C*) Epicardial bipolar voltage map with merged image and EAM image, using the CARTO®3 system (Biosense Webster). Purple is normal voltage >1.5 mV, green is borderzone >0.5 to <1.5 mV, and red is dense scar or epicardial fat <0.5 mV. A hole is visible at the pericardial adhesions above the apical scar.

Epicardial access was obtained and the voltage map created showed an anterior scar. A coronary angiogram was performed and demonstrated no main coronary artery in the vicinity of the ablation site. A LAVA-based ablation was performed in sinus rhythm, based on substrate mapping, prolonged stimulus to QRS duration and pacemapping, and complete epicardial LAVA elimination was achieved. Therefore, it was decided to end amiodarone therapy after the procedure.

In patient 3, there was a large endocardial thrombus, with calcifications and severe wall thinning predominating at the basal and apical aspects of the myocardial infarction scar. In between these two areas, a relatively preserved wall thickness region suggested the possibility of an epicardial isthmus on the MDCT imaging. After obtaining epicardial access, difficulties were encountered to map in the direct surroundings of basal anterior aneurysm, because of pericardial adhesions. However, LAVAs were recorded in the borderzone of the low-voltage area and clustered in the pre-procedural identified isthmus. An induction protocol was not performed to avoid the risk for thrombus migration during a DC shock and pacemapping with long stimulation-to-QRS time was used to identify interesting sites. No coronary angiogram was performed since the image merge only revealed a small branch in the surroundings of the ablation site. Ablation was performed in sinus rhythm using substrate mapping, pacemapping, and prolonged stimulus to QRS duration. Endpoint reached was incomplete epicardial LAVA elimination but inducibility was not tested, because of the thrombus. Amiodarone and beta-blocker therapy were continued after the procedure.

Patient with dilated cardiomyopathy with complicated epicardial puncture ($n = 1$)

Patient 4 received resynchronization therapy and prior His ablation because of persistent atrial fibrillation in a referral centre. Because of the disease substrate and surface ECG morphology of the VT, an epicardial approach was used from onset. The epicardial puncture was followed by a continuous bleeding finally limited to a total of 200 ml. After completion of the epicardial substrate map, it was decided not to obtain endocardial access, because of the disease substrate on imaging and mapping and to avoid further bleeding possibly associated with the heparin infusion needed for an endocardial

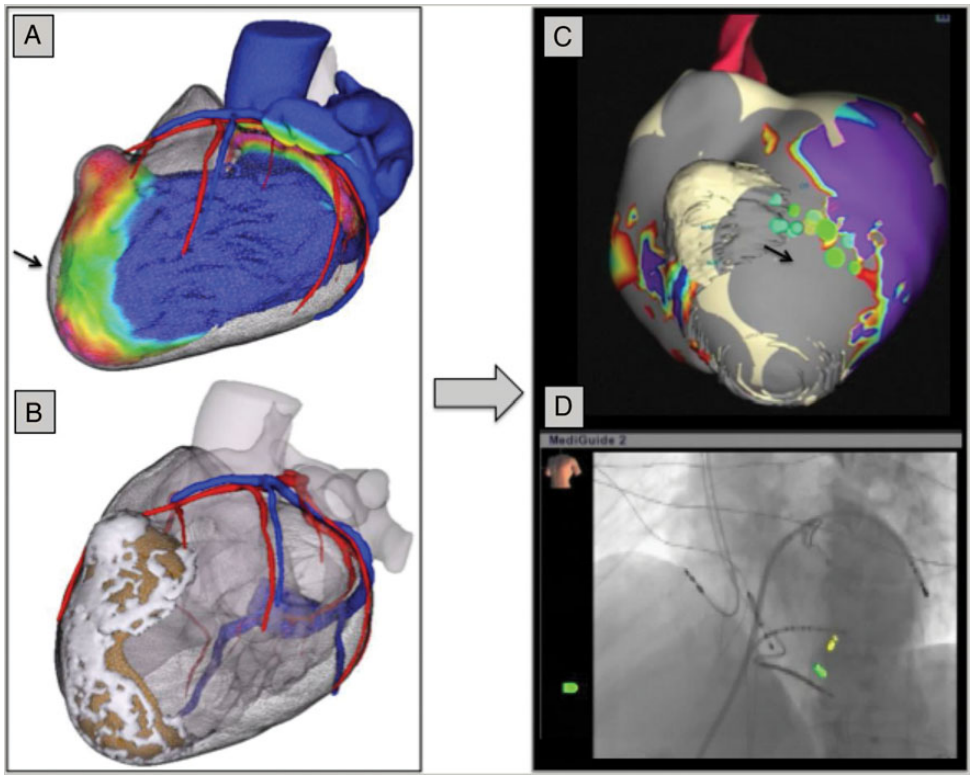

Figure 3 Patient 3 with ischaemic cardiomyopathy and an endocardial thrombus (lateral view). (*A*) Multidetector computed tomography colour-coded wall thickness map showing an anterior left ventricular aneurysm with wall thinning (blue is normal thickness and red is <3 mm with intermediate thickness in green). An epicardial isthmus can be seen (black arrow). (*B*) Three-dimensional mesh (derived from MDCT) made using Music® software with coronary artery system in red, coronary venous system in blue, scar with calcification in white, and large mural thrombus in brown. (*C*) Epicardial bipolar voltage map with merged image and EAM image, using the EnSite™ Velocity™ system (St Jude Medical). Purple is normal voltage >1.5 mV, green is borderzone >0.5 to <1.5 mV, and grey is dense scar <0.5 mV. Green LAVA dots are manually tagged and seen besides the aneurysm inside the anatomical isthmus (black arrow). (*D*) Fluoroscopic anteroposterior (AP) image using the MediGuide™ system. Anterior epicardial access, using a steerable sheath (Agilis™, St Jude Medical). Magnetic sensors of MediGuide-compatible catheters (both St Jude Medical) show the tip of the ablation catheter (Saphire™ BLU™) in yellow and a decapolar catheter (LiveWire™) in green. Atrial and ventricular leads of intracardiac defibrillator are visible.

procedure. Epicardial LAVAs were found as well as sites of perfect pacemap matching the clinical VT. The area of interest was not in direct vicinity to a coronary artery or to the left phrenic nerve. The clinical VT was induced and entrainment manoeuvres confirmed the isthmus site. Ablation at that site was performed during VT and stopped the clinical VT. Complete epicardial LAVA elimination was not obtained due to a more intramural LAVA location, but VT was no longer inducible in the end. The pericardial bleeding stopped spontaneously 30 min after the procedure. It was then decided to extract the pigtail catheter after 3 h of monitoring using ultrasound monitoring. The patient did receive standard NSAID therapy during 5 days and did not present any clinical or electrocardiographic signs of pericarditis. No prolongation of his hospital stay was required. Prior anti-arrhythmic treatment (amiodarone and beta-blocker therapy) was continued.

Follow-up

After a mean follow-up of 21 $\pm$ 12 months, recurrence of the clinical VT was seen in one patient (25%) and no mortality was observed.

Discussion

This is the first case series reporting on epicardial only mapping and ablation in a limited subset of patients. The main findings of this study were:

(1) An epicardial only VT ablation procedure is feasible.
(2) This purely epicardial approach seems to be associated with acceptable short-term success.
(3) Endpoints are more difficult to verify since LAVA elimination is only evaluated epicardially, and VT inducibility was not performed in the presence of endocardial thrombus.

This approach seems especially useful for the patients referred for VT ablations with an endocardial thrombus, a clear contra-indication for an endocardial approach. We do believe that in this context, this approach compares favourably with surgery which would be associated with a significantly higher risk in these fragile patients. We further presume that this approach can potentially shorten procedure time (compared with a combined procedure) in unstable selected patients

since no endocardial access is obtained and no endocardial mapping is used. The complication that occurred is related to the epicardial access and not to the strategy in itself. We expect a similar complication rate of any epicardial procedure but these case series are too small to draw any conclusions about safety.

In patients with secondary wall thinning (ICM and arrhythmogenic right ventricular cardiomyopathy), there is a reasonable chance that epicardial ablation can eliminate endocardial LAVA. We have previously demonstrated that the opposite approach, eliminating epicardial LAVA using endocardial ablation, works if the wall thickness does not exceed 5 mm.[20]

The first patient did undergo prior endocardial mapping. We did not exclude this patient, since myocarditis patients with subepicardial only scar on imaging could in fact benefit from purely epicardial mapping and ablation procedures. We have observed in a previous series that in these patients with preserved LV wall thickness and using the current ablation tools, the likelihood for eliminating epicardial LAVA using endocardial RF delivery was null.[10] This case series illustrates the feasibility. In this subset, an epicardial only approach could be effective, since no LAVAs were found endocardially in all patients.[11]

Limitations

This is a single centre heterogeneous and small cohort retrospective study. The follow-up period is relatively short. A larger population and longer follow-up is needed prospectively to validate this approach.

Conclusion

An epicardial only VT ablation procedure is feasible and demonstrates good outcome at short-term follow-up. This approach should however only be used in experienced centres in a very selective patient population.

Funding

B.B. received an EHRA grant. This manuscript is made possible by IHU LIRYC ANR-10-IAHU-04 and Equipex MUSIC ANR-11-EQPX-0030 Bordeaux, France.

Conflict of interest: B.B. received an educational EHRA Grant. P.J., M.H., M.H., and F.S. have received lecture fees from Biosense Webster and St Jude Medical.

References

1. Aliot EM, Stevenson WG, Almendral-Garrote JM, Bogun F, Calkins CH, Delacretaz E *et al.* EHRA/HRS Expert Consensus on Catheter Ablation of Ventricular Arrhythmias: developed in a partnership with the European Heart Rhythm Association (EHRA), a Registered Branch of the European Society of Cardiology (ESC), and the Heart Rhythm Society (HRS); in collaboration with the American College of Cardiology (ACC) and the American Heart Association (AHA). *Europace* 2009; **11**:771–817.
2. Pedersen CT, Kay GN, Kalman J, Borggrefe M, Della-Bella P, Dickfeld T *et al.* EHRA/HRS/APHRS expert consensus on ventricular arrhythmias. *Europace* 2014;**16**:1257–83.
3. Wissner E, Stevenson WG, Kuck K-H. Catheter ablation of ventricular tachycardia in ischaemic and non-ischaemic cardiomyopathy: where are we today? A clinical review. *Eur Heart J* 2012;**33**:1440–50.
4. Schmidt B, Chun KR, Baensch D, Antz M, Koektuerk B, Tilz RR *et al.* Catheter ablation for ventricular tachycardia after failed endocardial ablation: epicardial substrate or inappropriate endocardial ablation? *Heart Rhythm* 2010;**7**:1746–52.
5. Proclemer A, Dagres N, Marinskis G, Pison L, Lip GY. Blomstrom-Lundqvist C *et al.* Current practice in Europe: how do we manage patients with ventricular tachycardia? European Heart Rhythm Association survey. *Europace* 2013;**15**:167–9.
6. Della Bella P, Brugada J, Zeppenfeld K, Merino J, Neuzil P, Maury P *et al.* Epicardial ablation for ventricular tachycardia: a European multicenter study. *Circ Arrhythm Electrophysiol* 2011;**4**:653–9.
7. Brugada J, Berruezo A, Cuesta A, Osca J, Chueca E, Fosch X *et al.* Nonsurgical transthoracic epicardial radiofrequency ablation: an alternative in incessant ventricular tachycardia. *J Am Coll Cardiol* 2003;**41**:2036–43.
8. Dinov B, Fiedler L, Schonbauer R, Bollmann A, Rolf S, Piorkowski C *et al.* Outcomes in catheter ablation of ventricular tachycardia in dilated nonischemic cardiomyopathy compared with ischemic cardiomyopathy: results from the prospective Heart Centre of Leipzig VT (HELP-VT) study. *Circulation* 2014;**129**:728–36.
9. Sarkozy A, Tokuda M, Tedrow UB, Sieria J, Michaud GF, Couper GS *et al.* Epicardial ablation of ventricular tachycardia in ischemic heart disease. *Circ Arrhythm Electrophysiol* 2013;**6**:1115–22.
10. Komatsu Y, Daly M, Sacher F, Cochet H, Denis A, Derval N *et al.* Endocardial ablation to eliminate epicardial arrhythmia substrate in scar-related ventricular tachycardia. *J Am Coll Cardiol* 2014;**63**:1416–26.
11. Berte B, Sacher F, Cochet H, Mahida S, Yamashita S, Lim HS *et al.* Post-myocarditis ventricular tachycardia in patients with epicardial-only scar: a specific entity requiring a specific approach. *J Cardiovasc Electrophysiol* 2015;**26**:42–50.
12. Maccabelli G, Tsiachris D, Silberbauer J, Esposito A, Bisceglia C, Baratto F *et al.* Imaging and epicardial substrate ablation of ventricular tachycardia in patients late after myocarditis. *Europace* 2014;**16**:1363–72.
13. Cochet H, Komatsu Y, Sacher F, Jadidi AS, Scherr D, Riffaud M *et al.* Integration of merged delayed-enhanced magnetic resonance imaging and multidetector computed tomography for the guidance of ventricular tachycardia ablation: a pilot study. *J Cardiovasc Electrophysiol* 2013;**24**:419–26.
14. Komatsu Y, Sacher F, Cochet H, Jais P. Multimodality imaging to improve the safety and efficacy of epicardial ablation of scar-related ventricular tachycardia. *J Cardiovasc Electrophysiol* 2013;**24**:1426–7.
15. Wijnmaalen AP, van der Geest RJ, van Huls van Taxis CF, Siebelink HM, Kroft LJ, Bax JJ *et al.* Head-to-head comparison of contrast-enhanced magnetic resonance imaging and electroanatomical voltage mapping to assess post-infarct scar characteristics in patients with ventricular tachycardias: real-time image integration and reversed registration. *Eur Heart J* 2011;**32**:104–14.
16. Blomström Lundqvist C, Auricchio A, Brugada J, Boriani G, Bremerich J, Cabrera JA *et al.* The use of imaging for electrophysiological and devices procedures: a report from the first European Heart Rhythm Association Policy Conference, jointly organized with the European Association of Cardiovascular Imaging (EACVI), the Council of Cardiovascular Imaging and the European Society of Cardiac Radiology. *Europace* 2013;**15**:927–36.
17. Andreu D, Ortiz-Perez JT, Boussy T, Fernandez-Armenta J, de Caralt TM, Perea RJ *et al.* Usefulness of contrast-enhanced cardiac magnetic resonance in identifying the ventricular arrhythmia substrate and the approach needed for ablation. *Eur Heart J* 2014;**35**:1316–26.
18. Jais P, Maury P, Khairy P, Sacher F, Nault I, Komatsu Y *et al.* Elimination of local abnormal ventricular activities: a new end point for substrate modification in patients with scar-related ventricular tachycardia. *Circulation* 2012;**125**:2184–96.
19. Komatsu Y, Daly M, Sacher F, Derval N, Pascale P, Roten L *et al.* Electrophysiologic characterization of local abnormal ventricular activities in postinfarction ventricular tachycardia with respect to their anatomic location. *Heart Rhythm* 2013;**10**:1630–7.
20. Komatsu Y, Daly M, Sacher F, Cochet H, Denis A, Derval N *et al.* Endocardial ablation to eliminate epicardial arrhythmia substrate in scar-related ventricular tachycardia. *J Am Coll Cardiol* 2014;**63**:1416–26.

C. The role of high-resolution image integration to visualize left phrenic nerve and coronary arteries during epicardial ventricular tachycardia ablation.

Yamashita S, Sacher F, Mahida S, Berte B, Lim HS, Komatsu Y, Amraoui S, Denis A, Derval N, Laurent F, Montaudon M, Hocini M, Haïssaguerre M, Jaïs P, Cochet H. Circ Arrhythm Electrophysiol. 2015 Apr;8(2):371-80.

1. Study outline

Although epicardial VT ablation has been proven to be effective, particularly in non-ischemic cardiomyopathy (NICM), its effectiveness is limited by the risk for damaging vulnerable structures such as coronary arteries (CAs) and phrenic nerve (PN). This study analyzed the feasibility of MDCT to detect and segment the left phrenic nerve and coronary arteries in 95 patients (ICM: 54 patients, NICM: 23 patients and ARVC: 18 patients), referred for VT ablation. In addition, anatomical distribution was analyzed according to scar and LAVA. MDCT detected the phrenic nerve in 81 patients (85%). All detected PNs were located close to the tip of the left atrial appendage (9±6mm, rage: 1-29mm). In contrast, the course of the PN along the left ventricular free wall was highly variable (65±15% of base to apex distance, range: 20-88%). Epicardial LAVAs were observed within 1 cm from CAs in 35/44 (80%) patients. Epicardial LAVAs were observed within 1 cm from PN in 18/44 (37%) patients.

The prevalence of LAVA adjacent to CAs was higher in NICM and ARVC than in ICM (100% vs. 86% vs. 53%). The prevalence of LAVAs adjacent to PN was higher

in NICM than in ICM (93% vs. 27%). Epicardial LAVAs could not be eliminated due to the proximity to CAs or PN in 8 patients (18%).

2. Implications

This imaging study highlights several advantages of preprocedural MDCT for epicardial mapping and ablation. MDCT has a higher spatial resolution then DE-MRI. MDCT accurately delineates the PN in a high proportion of patients and high resolution integrated imaging is valuable in minimizing risk of PN and CA damage during epicardial VT ablation, regardless of the underlying etiology of VT. Knowledge of the individual course of the phrenic nerve and coronary arteries can help to use preventive measures as endocardial ablation for epicardial LAVA, pericardial saline or air injection to displace the phrenic nerve, intracoronary temperature control and safety perimeter of >5mm etc. A limitation is still the lack of perfect image integration into the EAM systems, which should be improved.

3. Manuscript

Title: The role of high-resolution image integration to visualize left phrenic nerve and coronary arteries during epicardal ventricular tachycardia ablation

Manuscript number: CIRCAE/2014/002420R2

Author(s): Seigo Yamashita, Hôpital Cardiologique du Haut-Lévêque, CHU de Bordeaux
Frédéric Sacher, Hôpital Cardiologique du Haut-Lévêque & Université Bordeaux, LIRYC Institute
Saagar Mahida, Hôpital Haut-Lévêque
Benjamin Berte, CHU Bordeaux Haut L'évêque
Han Lim, Hôpital Cardiologique du Haut-Lévêque, CHU Bordeaux, Université Victor Segalen Bordeaux II; INSERM U1045 - L'Institut de Rythmologie et Modeling Cardiaque

Yuki Komatsu, Hôpital Cardiologique du Haut-Lévêque, the Université Victor Segalen Bordeaux II, Institut LYRIC, Bordeaux, France

Sana Amraoui, University Hospital of Bordeaux

Arnaud Denis, Hôpital Cardiologique du Haut-Lévêque & Université Victor Segalen Bordeaux II, LIRYC Institute

Nicolas Derval, Hôpital Cardiologique du Haut-Lévêque

François Laurent, Hôpital Cardiologique du Haut-Lévêque & Université Victor Segalen Bordeaux II, Bordeaux, France

Michel Montaudon, Centre Hospitalier Universitaire de Bordeaux

Mélèze Hocini, Hôpital Cardiologique du Haut-Lévêque & Université Victor Segalen Bordeaux II, LIRYC Institute

Michel Haïssaguerre, Hôpital cardiologique du Haut-Lévêque

Pierre Jaïs, Hôpital Cardiologique Haut Lévêque

Hubert Cochet, CHU / Université de Bordeaux - IHU Liryc / INSERM U1045

The role of high-resolution image integration to visualize left phrenic nerve and coronary arteries during epicardal ventricular tachycardia ablation

Seigo Yamashita, M.D., Ph.D.[1], Frédéric Sacher, M.D., Ph.D.[1,3], Saagar Mahida, M.B.Ch.B., Ph.D.[1], Benjamin Berte, M.D.[1], Han Lim, M.B.B.S., Ph.D.[1], Yuki Komatsu, M.D.[1], Sana Amraoui, M.D.[1], Arnaud Denis, M.D.[1,3], Nicolas Derval, M.D.[1,3], François Laurent, M.D.[2,3], Michel Montaudon, M.D., Ph.D.[2,3], Mélèze Hocini, M.D.[1,3], Michel Haïssaguerre, M.D., Ph.D.[1,3], Pierre Jaïs, M.D., Ph.D.[1,3], and Hubert Cochet, M.D., Ph.D.[2,3]

1. Department of Cardiac Electrophysiology, Hôpital Cardiologique du Haut-Lévêque, CHU de Bordeaux, Pessac, France

2. Department of Cardiovascular Imaging, Hôpital Cardiologique du Haut-Lévêque, CHU de Bordeaux, Pessac, France

3. Institut Liryc / Equipex Music, Université de Bordeaux-Inserm U1045, Pessac, France

Funding sources: LIRYC ANR-10-IAHU-04, Equipex MUSIC ANR-11-EQPX-0030IHU

Conflicts of interest: None declared

Word count: 6996

Running title: Role of MDCT for epicardial VT ablation

Subject code: 22, Ablation/ICD/surgery

Address for correspondence:

Seigo Yamashita, M.D.

Department of Cardiac Electrophysiology, Hôpital Cardiologique du Haut-Lévêque

Avenue de Magellan, Bordeaux-Pessac, 33604, France

Fax: +33 5 57 65 64 19

Tel: +33 5 56 79 56 79

E-mail: seigoy722@yahoo.co.jp

Abstract

Background: Epicardial ventricular tachycardia (VT) ablation is associated with risks of coronary artery (CA) and phrenic nerve (PN) injury. We investigated the role of multidetector CT (MDCT) in visualizing CA and PN during VT ablation.

Methods and results: Ninety-five consecutive patients (86 males, age 57±15) with VT underwent cardiac MDCT. The PN detection rate and anatomical variability were analyzed. In 49 patients undergoing epicardial mapping, real-time MDCT integration was used to display CAs/PN locations in 3D mapping systems. Elimination of local abnormal ventricular activities (LAVA) was used as ablation endpoint. The distribution of CAs/PN with respect to LAVA was analyzed and compared between VT etiologies. MDCT detected PN in 81 patients (85%). Epicardial LAVAs were observed in 44/49 patients (15 ICM, 15 NICM, 14 ARVC) with a mean of 35±37 LAVA points/patient. LAVAs were located within 1cm from CAs and PN in 35(80%) and 18(37%) patients, respectively. The prevalence of LAVA adjacent to CAs was higher in NICM and ARVC than in ICM (100% vs. 86% vs. 53%, P<0.01). The prevalence of LAVAs adjacent to PN was higher in NICM than in ICM (93% vs. 27%, P<0.001). Epicardial ablation was performed in 37 patients (76%). Epicardial LAVAs could not be eliminated due to the proximity to CAs or PN in 8 patients (18%).

Conclusions: The epicardial electrophysiological VT substrate is often close to CAs and PN in patients with NICM. High-resolution image integration is useful to minimize risks of PN

and CA injury during epicardial VT ablation.

Abstract: 247 words

Key words: Ventricular tachycardia, Epicardial ablation, Imaging, Coronary artery, Phrenic nerve

Introduction

Catheter ablation is an effective treatment strategy for recurrent and drug-refractory scar-related ventricular tachycardia (VT). Potential strategies for VT ablation include targeting of the critical isthmus of the VT circuit during sustained VT[1-3] and/or substrate-based ablation during sinus rhythm (SR), particularly in patients with poorly tolerated or non-inducible VT.[4-6] Targeting local abnormal ventricular activities (LAVAs) has recently been proposed as an effective approach for scar-related VT ablation.[7]

In a proportion of VT patients, an epicardial approach is required to fully eliminate the arrhythmogenic substrate. Although epicardial VT ablation has been proven helpful particularly in non-ischemic cardiomyopathy (NICM) which is typically associated with epicardial scar,[8] its effectiveness is limited by the risk for damaging vulnerable structures such as coronary arteries (CAs) and phrenic nerve (PN).[9-11] According to current guidelines, coronary angiography is recommended prior and after epicardial radiofrequency (RF) deliveries[12]. However, it cannot be repeated before every RF application.

Real-time high-resolution image integration of multidetector computed tomography (MDCT) is emerging as an important adjunctive imaging technique for characterization of the arrhythmogenic substrate in patients with scar-related VT.[13,14] MDCT has also the advantage of allowing sub millimetric reconstruction of CAs and PN. In the present study, we assessed the ability of MDCT to allow safe ablation procedures by displaying high resolution

reconstruction of CAs and PN, and sought to define the anatomical relationship of CAs and PN locations with the electrophysiological substrates (LAVAs) according to the VT etiology in patients undergoing epicardial VT ablation for scar-related VT.

Methods

Study population

Ninety-five consecutive patients with drug-refractory and scar-related VT were enrolled in this study. VT etiology was categorized as ICM, NICM or arrhythmogenic right ventricular cardiomyopathy (ARVC). All patients underwent pre-procedural MDCT. The PN detection rate and anatomical variability was analyzed. In patients undergoing epicardial mapping, real-time MDCT integration was used to display CAs and PN in 3D mapping systems. In this sub population, we analyzed the distribution of CAs/PN with respect to epicardial LAVAs and the impact of visualizing PN/CAs on VT ablation. The study was approved by the Institutional Review Board, and all patients provided informed consent.

Image acquisition

High-resolution CT imaging was performed 2-3 days prior to the ablation procedure. Contrast-enhanced ECG-gated cardiac MDCT was performed on a 64-slice CT scanner (SOMATOM Definition, Siemens Medical Solutions, Forchheim, Germany). Images were acquired during an expiratory breath hold with tube current modulation set on end-diastole.

CT angiographic images were acquired during the injection of a 120 mL bolus of iomeprol 400 mg I/mL (Bracco, Milan, Italy) at a rate of 5 mL/s.

Image processing

Image processing was performed by using a dedicated in-house software solution (MUSIC software, Liryc - Université de Bordeaux / Inria - Sophia Antipolis, France). Myocardial and vascular structures were segmented on the MDCT series. Segmented images were used to generate 3D surface meshes of the endocardium, epicardium, CAs, coronary sinus (CS) and PN. Myocardial structural substrate was also segmented, defined as areas of wall thinning <5mm in ICM and NICM, or myocardial hypodensity in ARVC.[14,15] The resulting 3D objects were imported into 3D-mapping systems (EnSite NavX, St. Jude Medical, St. Paul, MN, USA; or CARTO3, Biosense Webster, Diamond Bar, CA, USA). All imaging models were available for real-time integration during the subsequent electrophysiological procedures.

Trans-axial images were reviewed by 2 observers in consensus in order to evaluate the detection rate of PN on MDCT data. When detected, the course of the left PN in the mediastinum and along the LV free wall was analyzed as follows: the minimum distance to the left atrial appendage tip was measured and the location of the PN along the LV free wall was expressed in % of base to apex distance, as measured on a 4-chamber reconstruction. The detection and anatomical variability of left PN on MDCT are illustrated in **Figure 1**.

Electrophysiological Study

The electrophysiological study and ablation were conducted with conscious sedation. Vascular sheaths were inserted via the right femoral vein, right femoral artery and subxiphoid area under local anesthesia as needed. A steerable quadripolar or decapolar catheter (2–5–2 mm, Xtrem, Sorin, France; or Dynamic, BARD Electrophysiology, Lowell, Massachusetts) was positioned in the right ventricular apex or coronary sinus, respectively. The left ventricle (LV) was accessed by transseptal (BRK Needle, Agilis sheath, St. Jude Medical) and/or retrograde approach with or without pericardial access for additional epicardial mapping (Tuohy needle, Agilis sheath, St. Jude Medical).

Indications for epicardial access included; 1) suspicion of an epicardial origin of VT based on imaging, 2) absence of LAVAs on endocardium, 3) persistence of clinical VT after ablation from the endocardial aspect, 4) absence of contraindications to epicardial access such as prior cardiac surgery. After LV access was attained, a 50U/kg heparin bolus was administered intravenously, aiming for an activated clotting time >250 seconds during procedure. Endocardial and epicardial electroanatomical mapping (EAM) was performed during SR using CARTO3 or NavX systems. An irrigated catheter with a 3.5mm-tip (NaviStar Thermocool, Biosense Webster) and/or a multipolar high-density mapping catheter (PentaRay, Biosense Webster) was used for mapping, and peak to peak amplitudes of 0.5 to 1.5mV and <0.5mV were used to define the low voltage and the dense scar zone, respectively. After creating the voltage map during SR, inducibility was assessed by extra

stimulation with 2 drive trains (600ms and 400ms) with up to 3 extrastimuli decremented to 200ms from the right ventricular apex.

Image integration

After creating a complete endocardial mapping geometry including the CS, left atrium (with 4 pulmonary veins and left atrial appendage), mitral annulus, left ventricular endocardium, and aortic root, point-based registration with the imaging model was initiated using a first set of coupled points on the aforementioned landmarks. Of note, the rhythm during the acquisition of the 3D geometry was the same as the one during pre-procedure MDCT acquisition in all patients (1 AF, 11 pacing, 37 SR). The patient with AF was adequately rate controlled during both procedures. There was no significant difference in heart rate between the two procedures (MDCT vs. 3D mapping; 65±15 bpm vs. 64±14 bpm, p=0.89). In case the Navx system was used, field scaling was first applied to the geometry (to compensate for variations in impedance between the heart chambers and venous structures), then the acquired geometry was fused to the MDCT model with 4-8 landmarks (left ventricular apex, aortic root, mitral valve, CS and pulmonary veins). Secondary, fusion points were applied additionally at sites of local mismatch between the 2 superimposed geometries (**Figure 2**). This process molded the created geometry surface onto the MDCT surface and bended the 3D navigation space within the geometry, thereby improving the accuracy of image registration.[16] When using CARTO platform, registration was refined using automatic

surface registration. In addition, a 6F-decapolar catheter (Xtrem, Sorin, France; or Dynamic, BARD Electrophysiology, Lowell, Massachusetts) was placed into the CS as distally as possible to partly enter an anterior or lateral vein. This catheter was used as a spatial reference to detect a potential shift of the map, thereby monitoring the accuracy of MDCT registration throughout the procedure (**Figure 2**).

Ablation

In patients with inducible and hemodynamically tolerated VT, ablation was performed using conventional activation and entrainment mapping techniques. After restoration of SR, substrate-based ablation targeting LAVA was performed. In case of non-inducible or poorly tolerated VT, only LAVA-based ablation was performed. LAVAs include all identified poorly coupled signals, and are defined as (1) sharp, high-frequency ventricular potentials distinct from the far-field ventricular electrogram, (2) potentials occurring after the far-field ventricular electrogram in SR, and (3) potentials that may display double or multiple components separated by very low-amplitude signals or an isoelectric interval. When LAVAs were buried in the QRS complex and fused with the far-field ventricular electrogram, pacing maneuvers were performed to distinguish LAVA from far-field ventricular electrogram.[7]

RF power was applied at a maximum of 50W endocardially and 35W epicardially with a temperature limit of 42 degrees for 60 seconds. Low RF power (25W) was restricted to sites close to the conduction system or CAs. Based on previous reports from Sacher F. et al.

demonstrating larger lesions due to catheter parallel orientation during epicardial ablation,[17] power delivery during epicardial ablation was limited to 35 watts. The endpoint of the procedure was the elimination of LAVA and non-inducibility of clinical VT by extra stimuli with the same protocol as before ablation.

The management of epicardial LAVAs was performed as follows: as a rule, RF energy was always delivered first endocardially, while monitoring LAVAs from the epicardium with a multipolar high-density mapping catheter, in order to minimize the risk of extracardiac damage. When epicardial LAVAs were within 1cm from PN on MDCT segmentation, PN capture was confirmed by pacing with 25mA/2ms. In case endocardial ablation failed to eliminate epicardial LAVAs, 100-300 ml of saline were infused in the pericardium prior to epicardial ablation and radiofrequency was delivered after confirming the loss of phrenic capture during pacing. When LAVAs were within 5mm from the CAs on the integrated image, a coronary angiography was performed, and a decision was made whether or not to deliver RF energy epicardially. The presence or absence of CA and PN injury were assessed by monitoring 12 lead-ECG (ST-T change) and diaphragmatic movement.

Statistical Analysis

Quantitative data were expressed as the mean ± SD when normally distributed, and median [interquartile range] otherwise. Comparison between groups was analyzed by using unpaired Student's t-test or Wilcoxon rank-sum test based on the distribution of the values.

The chi-square test was used to analyze categorical variables, unless the expected values in any cells were <5, in which case Fisher exact test was used. Comparisons of continuous variables regarding etiologies were made using one-way ANOVA or Kruskal-Wallis test based on the distribution of the values. Logistic regression analysis was used to identify significant predictors of PN detection on MDCT. All tests were 2-tailed, and P<0.05 was considered significant. Statistical analyses were performed using the MedCalc software package, version 11.2 (MedCalc Software, Mariakerke, Belgium).

Results

Patient Characteristics

The clinical characteristics of the patient cohort are summarized in **Table 1**. The mean age of total population was 57±15 years. The VT etiology was ICM in 54/95(57%), NICM in 23/95(24%), and ARVC in 18/95(19%). Forty-nine patients had an epicardial approach and a PN visible on MDCT (18 ICM, 17 NICM and 14 ARVC). Image integration was successfully performed in all patients and the mean surface registration error in the CARTO system was 3.9±1.1 mm. In cases in which the NavX system was used 36±19 points were used for image integration.

Phrenic nerve (PN) detection and anatomical variability on MDCT

The left PN was detected in 81/95(85%) patients on MDCT (**Figure 3**). The clinical

characteristics associated with PN detection are shown in **Table 2**. Univariable analysis showed that PN was more likely to be detected when patients were older and when epicardial fat was present over the left ventricular free wall. At multivariable analysis, the presence of epicardial fat was an independent predictor for detecting PN (OR: 10.9, 95% CI: 2.39-50.03, P=0.003). All detected PNs were located close to the tip of the left atrial appendage (9±6mm, rage: 1-29mm). In contrast, the course of the PN along the left ventricular free wall was highly variable (65±15% of base to apex distance, range: 20-88%).

Mapping results in patients with both endocardial and epicardial approach

In the 49 patients with both endocardial and epicardial mapping, the mean number of mapping points during endocardial and epicardial EAM were 424±267 and 706±557, respectively. Endocardial and epicardial LAVAs were observed in 30(61%) and 44(90%) patients (endo/epi: 16(89%)/15(83%) in ICM, 5(29%)/15(88%) in NICM and 9(64%)/14(100%) in ARVC). The mean number of LAVA points/patient was 22±24 on the endocardium, and 35±37 on the epicardium. Two patients (4%) demonstrated no LAVA in both endocardium and epicardium (1 NICM, 1 ICM). On the endocardium, the low-voltage area and the prevalence of LAVA was higher in patients with ICM as compared with NICM and ARVC (71 [50-110] vs. 20 [2-36] vs. 36 [21-62] cm^2; P<0.001, 89% vs. 29% vs. 64%; P=0.001). On the epicardium, the low voltage area and the prevalence of LAVA were similar between VT etiologies (**Table 3, Figure 3, 4**).

Distribution of LAVA with respect to coronary arteries (CAs) and phrenic nerve (PN)

Epicardial LAVAs were observed within 1cm from CAs in 35/44(80%) patients. The prevalence of LAVA adjacent to CAs was higher in patients with NICM and ARVC than in those with ICM (NICM vs. ARVC vs. ICM: 100% vs. 86% vs. 53%, P=0.005). The coronary artery involved was predominantly the right coronary artery in ARVC patients, and the left circumflex artery in NICM patients. Epicardial LAVAs were observed within 1cm from PN in 18/44(37%) patients. The prevalence of LAVAs adjacent to PN was higher in NICM than in ICM and ARVC (NICM 93% vs. ICM 27% vs. ARVC 0%, P<0.001) (**Table 3, Figure 3, 4**).

Ablation

Out of the 49 patients with endocardial and epicardial mapping, 47 exhibited LAVAs, which were located on the epicardium in 44 patients. Epicardial ablation was performed in 37/49(76%) patients. Prior to epicardial ablation, coronary angiography was performed in 11/37(30%) patients due to the proximity of CAs. In these patients, the distance between coronary and catheter tip was not found to be different on the 3D registered image versus on coronary angiography (3.7±1.9 vs. 5.1±3.4mm, respectively, P=0.36). Saline infusion was performed in 6/37(16%) patients due to the proximity of PN. In all 6 patients, phrenic pacing confirmed the PN location as displayed from MDCT segmentation. Out of the 47 patients with LAVA, complete LAVA elimination in both the endocardium and epicardium was achieved in 31 patients (66%). Of note, complete LAVA elimination was only achievable in

44%(7/16) of NICM patients (**Table 3**). Out of the 16 patients with incomplete LAVA elimination, the proximity of CAs and PN was involved in 12(75%). Out of the 44 patients with epicardial LAVAs, incomplete elimination due to the proximity to CAs was observed in 8 patients (18%) (7 NICM, 1 ARVC) (**Table 4**, **Figure 5**). This proximity (<5mm) was confirmed by coronary angiography in all 8 patients. In 3 patients, a proximity between a LAVA site and a CA was found on the registered 3D image, but coronary angiography demonstrated that the catheter tip was >5mm away from CA, resulting in possible LAVA elimination from the epicardium. Furthermore in 4 patients (9%, all NICM), LAVAs close to PN could not be eliminated despite saline or air insufflation of the pericardium (due to persisting phrenic capture). On the other hand, out of the 35 patients with epicardial LAVA close to CAs, LAVAs could be eliminated by endocardial ablation in 15 (43%, 6 ICM, 9 ARVC). Out of the 18 patients with epicardial LAVA close to PN, LAVAs could be eliminated by endocardial ablation in 3/18 patients (17%, 3 ICM) (**Table 4, Figure 5**). Moreover, LAVA close to CAs in ICM and ARVC could be eliminated from endocardial aspect more frequently than that in NICM (**Table 4**). Minor complications (200-300ml of pericardial blood) related to epicardial access were observed in 2 procedures. No major complications related to PN or CAs injury occurred, either during mapping or ablation.

Discussion

Main findings

The present study demonstrates the feasibility of using MDCT to detect CAs/PN and reports on the distribution of PN/CAs with respect to the electrophysiological VT substrate (LAVA) in the most common VT etiologies. Specifically, we demonstrate that: (1) MDCT accurately delineates the PN in a high proportion of patients, (2) the prevalence of epicardial LAVA sites close to PN and CAs is higher in patients with NICM as compared to those with ICM, (3) high resolution integrated imaging is valuable in minimizing risk of PN and CA damage during epicardial VT ablation, regardless of the underlying etiology of VT.

Visualization of the left phrenic nerve (PN) on MDCT

In this study, MDCT could detect the PN and describe its course in 85% patients. The patients in whom the PN could be detected were likely to be older and to exhibit epicardial fat over the left ventricular free wall. A prior study had reported that the PN could be identified in 74% patients, and that the patients in whom PN was not detected were older and more commonly women.[18] The discrepancy between our results and those from this prior study may be explained by the differences between the studied populations, and particularly by the limited number of females included in the present study (9/74). The relationship with epicardial fat has not been previously studied, and could be explained by the increased contrast between PN and surrounding tissues in the presence of fat. Indeed, the visualization of the PN is easier when low fat densities surround it as opposed to when

no fat is present over the left ventricular wall, because in the latter the PN can be confounded with the adjacent myocardium. The present study is to our knowledge the first report on the anatomical variability of left PN course along the left ventricle. Our results shows that the PN is consistently close to the tip of the left atrial appendage, and therefore this location is of value to detect the proximal part of its course along the heart. In contrast, the course of the PN along the left ventricular free wall was found to be highly variable, with some patients exhibiting a basal course, and others exhibiting an apical course. This inter-patient variability substantiate the use of non-invasive imaging to characterize the course of the left PN and its relationship with the structural substrate of VT prior to epicardial ablation.

Relationship between LAVA and coronary arteries (CAs) / phrenic nerve (PN)

This study demonstrates a clustering of epicardial LAVAs in the vicinity of CAs in NICM and ARVC, and in the vicinity of the PN in NICM, which is consistent with several prior reports. Garcia et al. reported that the critical isthmuses of VT circuits in ARVC are more commonly found in a triangle at the basal lateral aspect of the right ventricle, adjacent to the right CA.[8] In non-ischemic DCM, abnormal electrograms are known to be more frequent on the basal lateral aspect of the left ventricle, and therefore often close to the left circumflex artery.[19-21] As for PN location, Roger et al. reported that 7/10 (70%) patients with NICM exhibited phrenic capture within the low-voltage area, and stressed out the importance PN

identification and protection before epicardial ablation.[9] These results indicate that epicardial ablation in patients with NICM and ARVC is at higher risk of CAs and PN injury.

In ICM, the lower prevalence of LAVA adjacent to PN and CAs can be explained by the lower number of epicardial LAVA in this condition as compared to NICM and ARVC. Indeed, the wavefront of necrosis during ischemia spreads from the endocardium to the epicardium,[22] which results in more scar border zones and VT electrophysiological substrate on the endocardium.[23] In addition, a relationship between LAVA location and PN is obviously mostly encountered when myocardial infarction is in the circumflex territory. Moreover, from a pathophysiological point of view, the coronary damage caused in the substrate vicinity should have less impact on cardiac function in ICM patients, as the territory is often already nonviable. For these reasons the issue of CAs and PN damage during epicardial VT ablation may be less critical in ICM than in ARVC and NICM.

Role of real-time CAs and PN integration during epicardial ablation

The role of epicardial ablation for VT is expanding. Prior studies have reported acute CA injury, CA spasms and CA occlusions during epicardial procedures.[24,25] The use of coronary angiography and a safety distance of more than 5mm between the CA and the ablation catheter tip are recommended.[12,26] However, the introduction of substrate-based strategies has increased the amount of ablation during VT procedures, and it is simply not possible to perform coronary angiography prior to each epicardial RF delivery. Moreover coronary

angiography is associated with additional procedural risk and exposure to iodinated contrast. In the current study coronary angiography was performed before RF application only in case of a close proximity (<5mm) with CAs as displayed by MDCT. Amongst patients who underwent angiography, we demonstrated a good correlation between coronary anatomy on angiography and on registered imaging. However it is important to note that in 27% of cases that underwent angiography, integrated imaging underestimated the distance between the ablation site and CAs. Furthermore, image integration is associated with substantial registration errors (3.9±1.1mm in the CARTO system). Therefore, in patients with a proximity (<5mm) to CAs on registered imaging, angiography remains desirable. Overall, MDCT imaging limited the use of coronary angiography to only 22% (11/49) of epicardial procedures without complications related to CAs injury in the present study. It is also important to note that in the present study, 80% of patients had putative epicardial targets within 1cm of CAs. This observation further highlights the importance of accurate delineation of coronary anatomy in patients undergoing epicardial ablation.

PN injury and subsequent diaphragmatic palsy is also a well-recognized complication during epicardial ablation. While pre-procedure MDCT is associated with additional radiation exposure, it is associated with a number of advantages compared to conventional techniques for delineating PN and CA and alternative imaging techniques such as magnetic resonance imaging (MRI). High output pacing was shown to accurately detect the left PN.[9]

However, epicardial pacing prior to each ablation is time-consuming, and the registration of PN course as identified on MDCT could help reducing the need for pacing in areas sufficiently far from MDCT-derived PN segmentation. In the current study, the use of MDCT resulted in a limited number of pacing maneuvers (only performed in 24% of epicardial procedures). When proximity to PN is identified, the use of saline[27] or air[28] injection within the pericardium has been proposed to prevent PN damage. In the present study, this strategy was not always successful and LAVAs close to PN could not be eliminated in 4 patients (8%, all NICM).

Finally, while MRI is an effective imaging technique, MDCT provides images with higher spatial resolution (<0.5mm) than MRI, and is more suitable for detecting coronary arteries and phrenic nerve.

Strategy to eliminate epicardial LAVAs

In the present study, the first strategy applied for the elimination of epicardial LAVAs was to attempt endocardial ablation while monitoring LAVA elimination from the epicardium. This strategy proved successful in most patients with ICM and ARVC, whereas it failed in all patients with NICM. This can be explained by the lower wall thickness encountered in ischemic scars and dysplasic RV walls, as compared to the relatively preserved wall thickness in NICM.[29,30] These findings support the use of endocardial ablation as a first line strategy in ICM and ARVC, epicardial ablation being required for resistant sites only, with the

use of image integration to minimize the risk of CAs and PN injury. In patients with NICM, our results suggest that a combined endocardial and epicardial ablation approach may be required in most cases.

Study limitations

The main limitation of this study is related to its observational design. The impact of CAs/PN integration on patient outcome should be evaluated in a prospective and randomized fashion. Another potential limitation is the heterogeneity of VT etiologies in the group with NICM, which can include primitive and secondary dilated cardiomyopathies, granulomatosis, myocarditis. However, we used NICM as a category because each of these etiologies would have been too rare to produce substantial results. Secondary, the 3-dimensional reconstruction of CAs from coronary angiography was not obtained in this study, thus the accuracy of CA localization on integrated imaging could not be accurately assessed. We used the longest distance on 2-dimensional view among several views (left and right anterior oblique, cranial and caudal view) between the catheter tip and CA. To clarify this accuracy animal studies should be conducted to analyze the localization of ablation lesions close to CA versus histology.

Conclusion

Real-time integration of PN and CAs during VT ablation is feasible with the use of MDCT. The epicardial substrate of VT is frequently adjacent to CAs and PN, particularly in patients with NICM. MDCT registration is useful to select the optimal strategy for VT ablation, minimizing the risk of CAs and PN injury.

Funding Sources

None.

Conflict of Interest Disclosures

None.

References

1. Stevenson WG, Wilber DJ, Natale A, Jackman WM, Marchlinski FE, Talbert T, Gonzalez MD, Worley SJ, Daoud EG, Hwang C, Schuger C, Bump TE, Jazayeri M, Tomassoni GF, Kopelman HA, Soejima K, Nakagawa H; Multicenter Thermocool VT Ablation Trial Investigators. Irrigated radiofrequency catheter ablation guided by electroanatomic mapping for recurrent ventricular tachycardia after myocardial infarction: the multicenter thermocool ventricular tachycardia ablation trial. *Circulation.* 2008;118:2773-2782.
2. Morady F, Frank R, Kou WH, Tonet JL, Nelson SD, Kounde S, De Buitleir M, Fontaine G.

Identification and catheter ablation of a zone of slow conduction in the reentrant circuit of ventricular tachycardia in humans. *J Am Coll Cardiol.* 1988;11:775-782.

3. Verma A, Marrouche NF, Schweikert RA, Saliba W, Wazni O, Cummings J, Abdul-Karim A, Bhargava M, Burkhardt JD, Kilicaslan F, Martin DO, Natale A. Relationship between successful ablation sites and the scar border zone defined by substrate mapping for ventricular tachycardia post-myocardial infarction. *J Cardiovasc Electrophysiol.* 2005;16:465-471.
4. Marchlinski FE, Callans DJ, Gottlieb CD, Zado E. Linear ablation lesions for control of unmappable ventricular tachycardia in patients with ischemic and nonischemic cardiomyopathy. *Circulation.* 2000;101:1288-1296.
5. Cesario DA, Vaseghi M, Boyle NG, Fishbein MC, Valderrábano M, Narasimhan C, Wiener I, Shivkumar K. Value of high-density endocardial and epicardial mapping for catheter ablation of hemodynamically unstable ventricular tachycardia. *Heart Rhythm.* 2006;3:1-10.
6. Bogun F, Good E, Reich S, Elmouchi D, Igic P, Lemola K, Tschopp D, Jongnarangsin K, Oral H, Chugh A, Pelosi F, Morady F. Isolated potentials during sinus rhythm and pace-mapping within scars as guides for ablation of post-infarction ventricular tachycardia. *J Am Coll Cardiol.* 2006;47:2013-2019.
7. Jaïs P, Maury P, Khairy P, Sacher F, Nault I, Komatsu Y, Hocini M, Forclaz A, Jadidi AS,

Weerasooryia R, Shah A, Derval N, Cochet H, Knecht S, Miyazaki S, Linton N, Rivard L, Wright M, Wilton SB, Scherr D, Pascale P, Roten L, Pederson M, Bordachar P, Laurent F, Kim SJ, Ritter P, Clementy J, Haïssaguerre M. Elimination of local abnormal ventricular activities: a new end point for substrate modification in patients with scar-related ventricular tachycardia. *Circulation.* 2012;125:2184-2196.

8. Garcia FC, Bazan V, Zado ES, Ren JF, Marchlinski FE. Epicardial substrate and outcome with epicardial ablation of ventricular tachycardia in arrhythmogenic right ventricular cardiomyopathy/dysplasia. *Circulation.* 2009;120:366-375.
9. Fan R, Cano O, Ho SY, Bala R, Callans DJ, Dixit S, Garcia F, Gerstenfeld EP, Hutchinson M, Lin D, Riley M, Marchlinski FE. Characterization of the phrenic nerve course within the epicardial substrate of patients with nonischemic cardiomyopathy and ventricular tachycardia. *Heart Rhythm.* 2009;6:59-64.
10. Killu AM, Friedman PA, Mulpuru SK, Munger TM, Packer DL, Asirvatham SJ. Atypical complications encountered with epicardial electrophysiological procedures. *Heart Rhythm.* 2013;10:1613-1621.
11. Sacher F, Roberts-Thomson K, Maury P, Tedrow U, Nault I, Steven D, Hocini M, Koplan B, Leroux L, Derval N, Seiler J, Wright MJ, Epstein L, Haissaguerre M, Jais P, Stevenson WG. Epicardial ventricular tachycardia ablation a multicenter safety study. *J Am Coll Cardiol.* 2010;55:2366-2372.

12. Aliot EM, Stevenson WG, Almendral-Garrote JM, Bogun F, Calkins CH, Delacretaz E, Della Bella P, Hindricks G, Jaïs P, Josephson ME, Kautzner J, Kay GN, Kuck KH, Lerman BB, Marchlinski F, Reddy V, Schalij MJ, Schilling R, Soejima K, Wilber D; European Heart Rhythm Association (EHRA); Registered Branch of the European Society of Cardiology (ESC); Heart Rhythm Society (HRS); American College of Cardiology (ACC); American Heart Association (AHA). EHRA/HRS Expert Consensus on Catheter Ablation of Ventricular Arrhythmias: developed in a partnership with the European Heart Rhythm Association (EHRA), a Registered Branch of the European Society of Cardiology (ESC), and the Heart Rhythm Society (HRS); in collaboration with the American College of Cardiology (ACC) and the American Heart Association (AHA). *Heart Rhythm.* 2009;6:886-933.

13. Cochet H, Komatsu Y, Sacher F, Jadidi AS, Scherr D, Riffaud M, Derval N, Shah A, Roten L, Pascale P, Relan J, Sermesant M, Ayache N, Montaudon M, Laurent F, Hocini M, Haïssaguerre M, Jaïs P. Integration of merged delayed-enhanced magnetic resonance imaging and multidetector computed tomography for the guidance of ventricular tachycardia ablation: a pilot study. *J Cardiovasc Electrophysiol.* 2013;24:419-426.

14. Komatsu Y, Cochet H, Jadidi A, Sacher F, Shah A, Derval N, Scherr D, Pascale P, Roten L, Denis A, Ramoul K, Miyazaki S, Daly M, Riffaud M, Sermesant M, Relan J, Ayache N,

Kim S, Montaudon M, Laurent F, Hocini M, Haïssaguerre M, Jaïs P. Regional myocardial wall thinning at multidetector computed tomography correlates to arrhythmogenic substrate in postinfarction ventricular tachycardia: assessment of structural and electrical substrate. *Circ Arrhythm Electrophysiol.* 2013;6:342-350.

15. Komatsu Y, Jadidi A, Sacher F, Denis A, Daly M, Derval N, Shah A, Lehrmann H, Park CI, Weber R, Arentz T, Pache G, Sermesant M, Ayache N, Relan J, Montaudon M, Laurent F, Hocini M, Haïssaguerre M, Jaïs P, Cochet H. Relationship between MDCT-imaged myocardial fat and ventricular tachycardia substrate in arrhythmogenic right ventricular cardiomyopathy. *J Am Heart Assoc.* 2014;3. pii: e000935. doi: 10.1161/JAHA.114.000935.
16. Brooks AG, Wilson L, Kuklik P, Stiles MK, John B, Shashidhar, Dimitri H, Lau DH, Roberts-Thomson RL, Wong CX, Young GD, Sanders P. Image integration using NavX Fusion: initial experience and validation. *Heart Rhythm.* 2008;5:526-535.
17. Sacher F, Wright M, Derval N, Denis A, Ramoul K, Roten L, Pascale P, Bordachar P, Ritter P, Hocini M, Dos Santos P, Haissaguerre M, Jais P. Endocardial versus epicardial ventricular radiofrequency ablation: utility of in vivo contact force assessment. *Circ Arrhythm Electrophysiol.* 2013;6:144-150.
18. Matsumoto Y, Krishnan S, Fowler SJ, Saremi F, Kondo T, Ahsan C, Narula J, Gurudevan S. Detection of phrenic nerves and their relation to cardiac anatomy using

64-slice multidetector computed tomography. *Am J Cardiol.* 2007;100:133-137.

19. Soejima K, Stevenson WG, Sapp JL, Selwyn AP, Couper G, Epstein LM. Endocardial and epicardial radiofrequency ablation of ventricular tachycardia associated with dilated cardiomyopathy: the importance of low-voltage scars. *J Am Coll Cardiol.* 2004;43:1834-1842.
20. d'Avila A, Splinter R, Svenson RH, Scanavacca M, Pruitt E, Kasell J, Sosa E. New perspectives on catheter-based ablation of ventricular tachycardia complicating Chagas' disease: experimental evidence of the efficacy of near infrared lasers for catheter ablation of Chagas' VT. *J Interv Card Electrophysiol.* 2002;7:23-38.
21. Sarabanda AV, Sosa E, Simões MV, Figueiredo GL, Pintya AO, Marin-Neto JA. Ventricular tachycardia in Chagas' disease: a comparison of clinical, angiographic, electrophysiologic and myocardial perfusion disturbances between patients presenting with either sustained or nonsustained forms. *Int J Cardiol.* 2005;102:9-19.
22. Reimer KA, Lowe JE, Rasmussen MM, Jennings RB. The wavefront phenomenon of ischemic cell death. 1. Myocardial infarct size vs duration of coronary occlusion in dogs. *Circulation.* 1977;56:786-794.
23. Ciaccio EJ, Ashikaga H, Kaba RA, Cervantes D, Hopenfeld B, Wit AL, Peters NS, McVeigh ER, Garan H, Coromilas J. Model of reentrant ventricular tachycardia based on infarct border zone geometry predicts reentrant circuit features as determined by

activation mapping. *Heart Rhythm.* 2007;4:1034-1045.

24. Koruth JS, Aryana A, Dukkipati SR, Pak HN, Kim YH, Sosa EA, Scanavacca M, Mahapatra S, Ailawadi G, Reddy VY, d'Avila A. Unusual complications of percutaneous epicardial access and epicardial mapping and ablation of cardiac arrhythmias. *Circ Arrhythm Electrophysiol.* 2011;4:882-888.
25. Bossert T, Bittner HB, Gummert JF, Mohr FW. Coronary artery spasm of the native right coronary artery during off-pump coronary surgery of the left coronary artery system. *Clin Res Cardiol.* 2006;95:115-118.
26. D'Avila A, Gutierrez P, Scanavacca M, Reddy V, Lustgarten DL, Sosa E, Ramires JA. Effects of radiofrequency pulses delivered in the vicinity of the coronary arteries: implications for nonsurgical transthoracic epicardial catheter ablation to treat ventricular tachycardia. *Pacing Clin Electrophysiol.* 2002;25:1488-1495.
27. Di Biase L, Burkhardt JD, Pelargonio G, Dello Russo A, Casella M, Santarelli P, Horton R, Sanchez J, Gallinghouse JG, Al-Ahmad A, Wang P, Cummings JE, Schweikert RA, Natale A. Prevention of phrenic nerve injury during epicardial ablation: comparison of methods for separating the phrenic nerve from the epicardial surface. *Heart Rhythm.* 2009;6:957-961.
28. Matsuo S, Jaïs P, Knecht S, Lim KT, Hocini M, Derval N, Wright M, Sacher F, Haïssaguerre M. Images in cardiovascular medicine. Novel technique to prevent left

phrenic nerve injury during epicardial catheter ablation. *Circulation.* 2008;117:e471.

29. Sacher F, Roberts-Thomson K, Maury P, Tedrow U, Nault I, Steven D, Hocini M, Koplan B, Leroux L, Derval N, Seiler J, Wright MJ, Epstein L, Haissaguerre M, Jais P, Stevenson WG. Epicardial ventricular tachycardia ablation a multicenter safety study. *J Am Coll Cardiol.* 2010 May 25;55:2366-2372.

30. Komatsu Y, Daly M2, Sacher F, Cochet H, Denis A, Derval N, Jesel L, Zellerhoff S, Lim HS, Jadidi A, Nault I, Shah A, Roten L, Pascale P, Scherr D, Aurillac-Lavignolle V, Hocini M, Haïssaguerre M, Jaïs P. Endocardial Ablation to Eliminate Epicardial Arrhythmia Substrate in Scar-Related Ventricular Tachycardia. *J Am Coll Cardiol.* 2014;63:1416-1426.

Table 1. Patients' characteristics

	Total population (n = 95)	Endo/Epi population (n = 49)
Patient age, years	57 ± 15	53 ± 15
Male	86 (91%)	45 (92%)
Body mass index, kg/m^2	27 ± 4.3	27 ± 4.4
ICM	54 (57%)	18 (40%)
NICM	23 (24%)	17 (34%)
ARVC	18 (19%)	14 (28%)
LVEF, %	37 ± 15	41 ± 15
Prior VT ablation	15 (16%)	11 (22%)
ICD/CRTD	76 (80%)	41 (84%)

ARVC indicates arrhythmogenic right ventricular cardiomyopathy; CRTD, cardiac resynchronization therapy defibrillator; ICD, implanted cardioveter defibrillator; ICM, ischemic cardiomyopathy; LVEF, left ventricular ejection fraction; NICM, non-ischemic cardiomyopathy; VT, ventricular tachycardia.

Table 2. Patients' characteristics in patients with and without PN detection and predictors for detecting PN by MDCT

	PN detection	No PN detection	Univariable-analysis		Multivariable-analysis	
	(N=81)	(N=14)	OR (95% CI)	P-value	OR (95% CI)	P-value
Patient age, years	58 ± 14	49 ± 18	**1.04 (1.00-1.08)**	**0.037**	1.01 (0.96-1.05)	0.82
Male gender	74 (91%)	12 (86%)	1.76 (0.33-9.51)	0.53		
Body mass index, kg/m^2	26 ± 5.8	27 ± 4.0	1.05 (0.90-1.22)	0.54		
ICM	32 (51%)	7 (64%)				
NICM	15 (24%)	2 (18%)	1.64 (0.30-8.86)	0.57		
ARVC	16 (25%)	2 (18%)	1.75 (0.33-9.41)	0.51		
Epicardial fat over LV wall	62 (77%)	3 (21%)	**12.0 (3.02-47.39)**	**0.001**	**10.9 (2.39-50.03)**	**0.003**
Pericardial effusion	4 (4.9%)	2 (14%)	0.31 (0.05-1.89)	0.24		
ICD/CRTD	67 (83%)	9 (64%)	2.66 (0.77-9.15)	0.13		

ARVC indicates arrhythmogenic right ventricular cardiomyopathy; CRTD, cardiac resynchronization therapy defibrillator; ICD, implanted cardioveter defibrillator; ICM, ischemic cardiomyopathy; MDCT, multi-detected computed tomography; NICM, non-ischemic cardiomyopathy; OR, odds ratio; PN, phrenic nerve.

Table 3. Clinical variables according to VT etiology

	ICM (N=18)	NICM (N=17)	ARVC (N=14)	P-value
Patient age, years	66 ± 9	48 ± 10	42 ± 15	**<0.001**
Male	17 (94%)	15 (88%)	13 (93%)	0.79
LVEF, %	30 [23-37]	40 [25-45]	60 [59-65]	**<0.001**
Prior Aablation	1.2 ± 0.5	1.1 ± 0.3	1.8 ± 1.1	0.06
Endocardium				
Mapping points ,n/pt	392 [247-523]	230 [187-449]	486 [301-845]	**0.01**
Low voltage area, cm^2	71 [50-110]	20 [2-36]	36 [21-62]	**<0.001**
Presence of LAVA	16 (89%)	5 (29%)	9 (64%)	**0.001**
LAVA points, n/pt	21 [15-34]	13 [7-19]	12 [10-15]	0.11
Epicardium				
Mapping points, n/pt	431 [322-744]	768 [341-1034]	541 [414-821]	0.48
Low voltage area, cm^2	55 [45-105]	49 [39-85]	114 [88-131]	**0.004**
Presence of LAVA	15 (83%)	15 (88%)	14 (100%)	0.42
LAVA points, n/pt	14 [9-21]	35 [21-48]	42 [28-46]	**0.003**
LAVA <1cm from CAs	8/15 (53%)	15/15(100%)	12/14 (86%)	**0.005**
LAVA <1cm from PN	4/15 (27%)	14/15 (93%)	0/14 (0%)	**<0.001**

Epicardial ablation	12 (67%)	15 (88%)	10 (71%)	0.30
Coronary angiography	0 (0%)	9 (53%)	2 (14%)	**<0.001**
RF time (endocardium), min	23 [17-32]	9 [5-24]	29 [14-42]	0.06
RF time (epicardium), min	5 [2-12]	22 [13-29]	13 [8-15]	**0.006**
Total procedure time, min	295 [240-320]	310 [250-375]	300 [280-300]	0.51
Complete LAVA elimination	12/17 (71%)	7/16 (44%)	12/14 (86%)	**0.04**

CA indicates coronary artery; EAM, endoanatomical mapping; ICM, ischemic cardiomyopathy; LAVA, local abnormal ventricular activity; LVEF, left ventricular ejection fraction; NICM, non-ischemic cardiomyopathy; PN, phrenic nerve; RF, radiofrequency.

Table 4. Results of ablation for LAVAs close to CAs and PN

	ICM		NICM		ARVC	
	<1cm from CAs	<1cm from PN	<1cm from CAs	<1cm from PN	<1cm from CAs	<1cm from PN
Elimination from endo	6/8 (75%)*	3/4 (75%)†	0/15 (0%)*‡	0/14 (0%)†	9/12 (75%)‡	-
Elimination from epi	2/8 (25%)	1/4 (25%)	8/15 (53%)	10/14 (71%)	4/12 (33%)	-
Incomplete elimination	0/8 (0%)	0/4 (0%)	7/15 (47%)§	4/14 (29%)	1/12 (8%)§	-
Minor/major complication	2/0		0/0		0/0	

In this table, the rate of elimination from endo/epi and incomplete elimination was compared between each etiology.

ARVC indicates arrhythmogenic right ventricular cardiomyopathy; CAs, coronary arteries; ICM, ischemic cardiomyopathy; LAVA, local abnormal ventricular activity; NICM, non-ischemic cardiomyopathy; PN, phrenic nerve; *‡, P<0.001;†, P=0.005; §, P=0.04.

Figure legends

Figure 1. Phrenic nerve course identified by MDCT. (A) Trans-axial MDCT images in a 57 year-old man showing PN location over the pericardium (arrow). (B) Illustration of the high variability of PN course over the left ventricular free wall (left panel: apical course in a 47 year-old man; right panel: basal course in a 66 year-old man). PN: phrenic nerve.

Figure 2. Imaging integration on Navx system and monitoring the registration with a coronary sinus catheter. (A) After field scaling and registration with 4 points (left ventricular apex, mitral annulus, aortic root and coronary sinus), additional fusion points on the local mismatch sites (yellow points) were applied. (B) Real-time integrated image can be monitored with a 6F decapolar catheter during procedure (white arrow). MDCT: multidetector computed tomography.

Figure 3. Relationship between LAVAs, low-voltage, coronary arteries, phrenic nerve, and structural substrate in a 58 year-old man with post-myocarditis VT. (A) LAVAs and epicardial voltage map registered to MDCT geometry: some LAVAs were located outside the epicardial low-voltage (<1.5mV). (B) LAVAs registered to MDCT-defined CAs/PN and CT-defined substrate: most LAVAs located inside the CT-defined structural substrate (wall thinning

<5mm); some LAVAs located close to LCx artery (pink arrows) and PN (yellow arrows). Phrenic capture sites (yellow dots) on CARTO corresponded to the PN location of integrated image. LAVA: local abnormal ventricular activity; CAs: coronary arteries; PN: phrenic nerve; LCx: left circumflex artery.

Figure 4. Relationship between LAVAs, coronary arteries, phrenic nerve, and structural substrate in patients with ischemic cardiomyopathy (A) and arrhythmogenic right ventricular cardiomyopathy (B). (A) Epicardial voltage map registered to MDCT data in a 57 year-old man with ICM. MDCT image demonstrated a wall thinning area (<5mm) around left ventricular apex, and LAVAs (white dots) were located on its border zone. One LAVA was close to PN (white arrow). (B) Epicardial voltage map registered to MDCT data in a 60 year-old man with ARVC. LAVAs (purple dots) were located close to the MDCT-defined structural substrate (myocardial fat densities), some LAVAs being located close to the RCA (white arrow). ICM: ischemic cardiomyopathy; ARVC: arrhythmogenic right ventricular cardiomyopathy; LAVA: local abnormal ventricular activity; PN: phrenic nerve; RCA: right coronary artery.

Figure 5. Epicardial LAVA close to a coronary artery in a 41 year-old man with post-myocarditis VT (A)-(C) and epicardial LAVA elimination from endocardial ablation in

ARVC patient (same patient as in Figure 4B) (D)(E). Fluoroscopic image (A) and image integration in 3D mapping system (B) both show a close contact (red arrow) between the catheter tip demonstrating LAVA (C) and the left circumflex artery, preventing epicardial ablation in patient with post-myocarditis. (D) Endocardial ablation is performed while monitoring LAVA elimination from the epicardium (red arrows in E) in patient with ARVC. RV: right ventricle; RAO: right anterior oblique; LAVA: local abnormal ventricular activity; HDM: high-density mapping catheter; RF: radiofrequency catheter; CS: coronary sinus.

Figure 1.

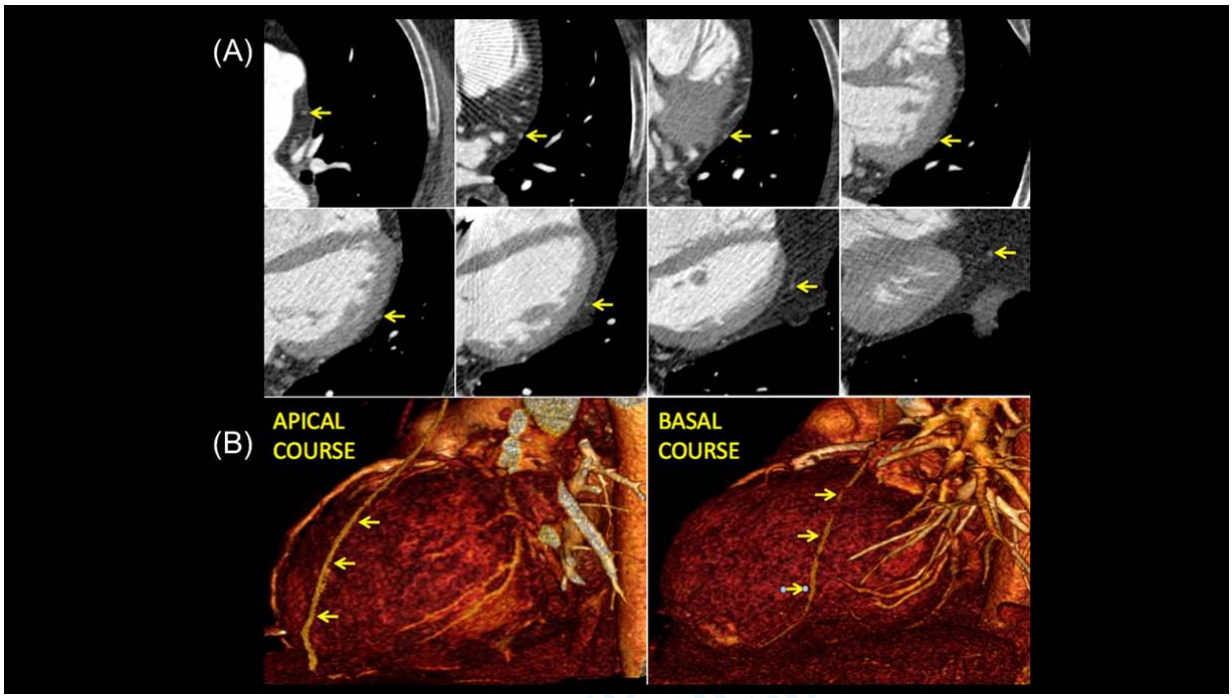

Figure 2.

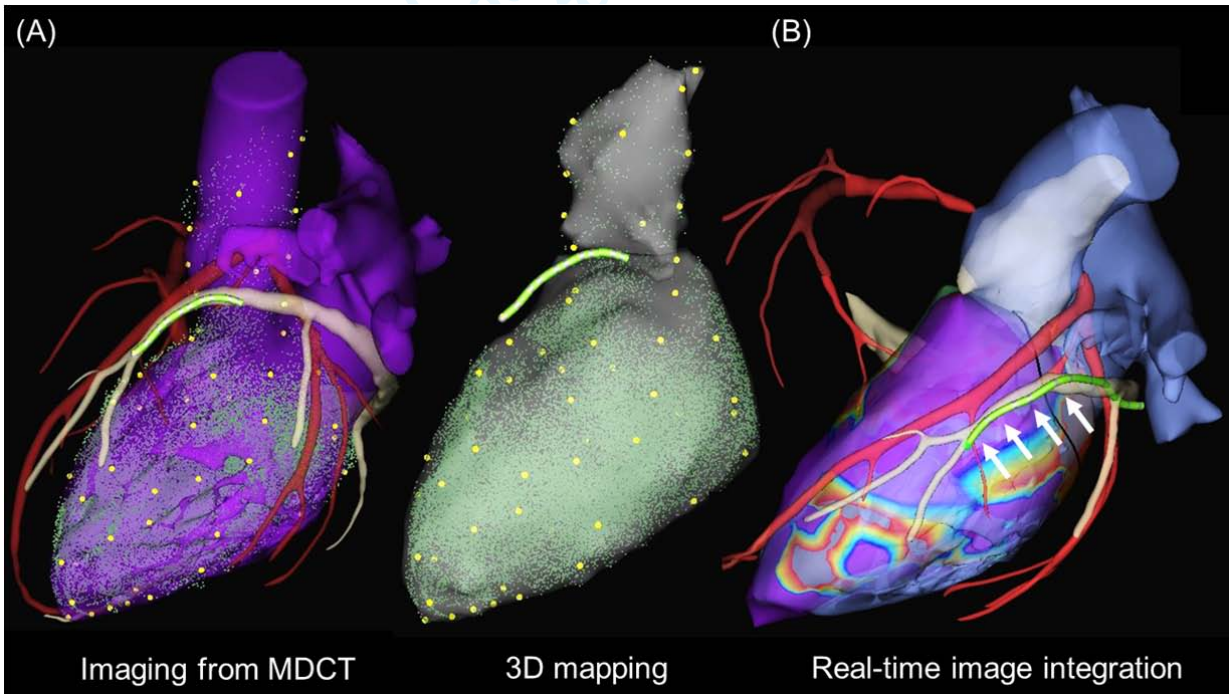

Figure 3.

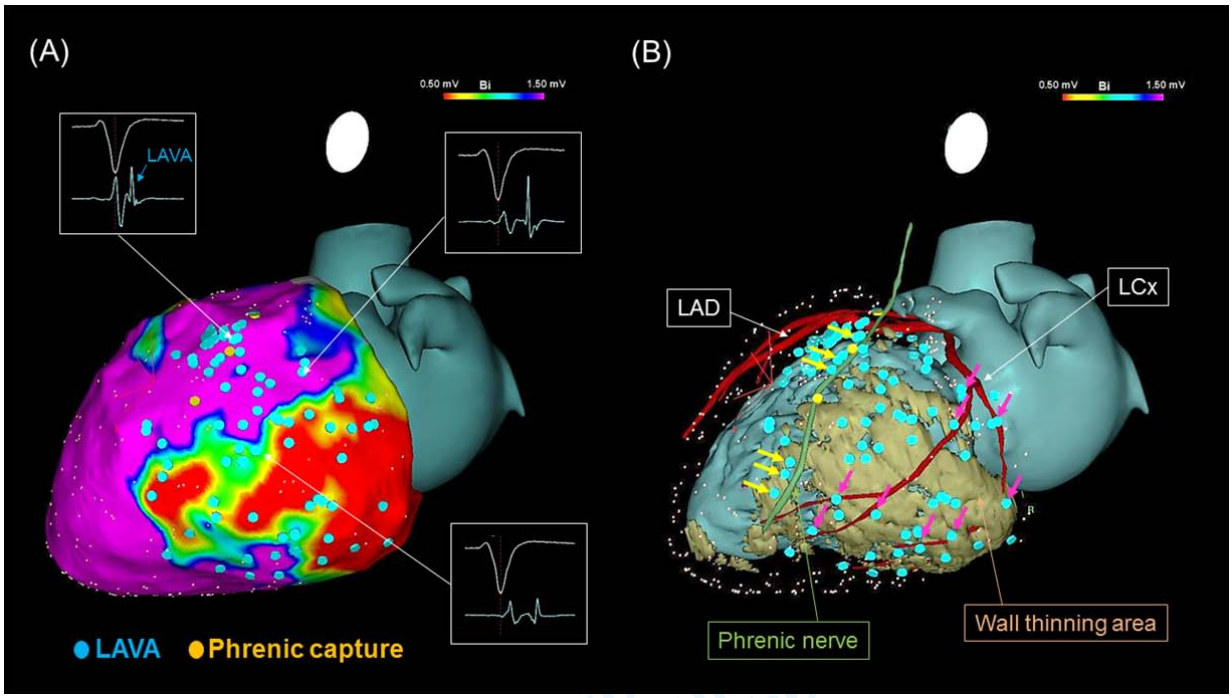

Figure 4.

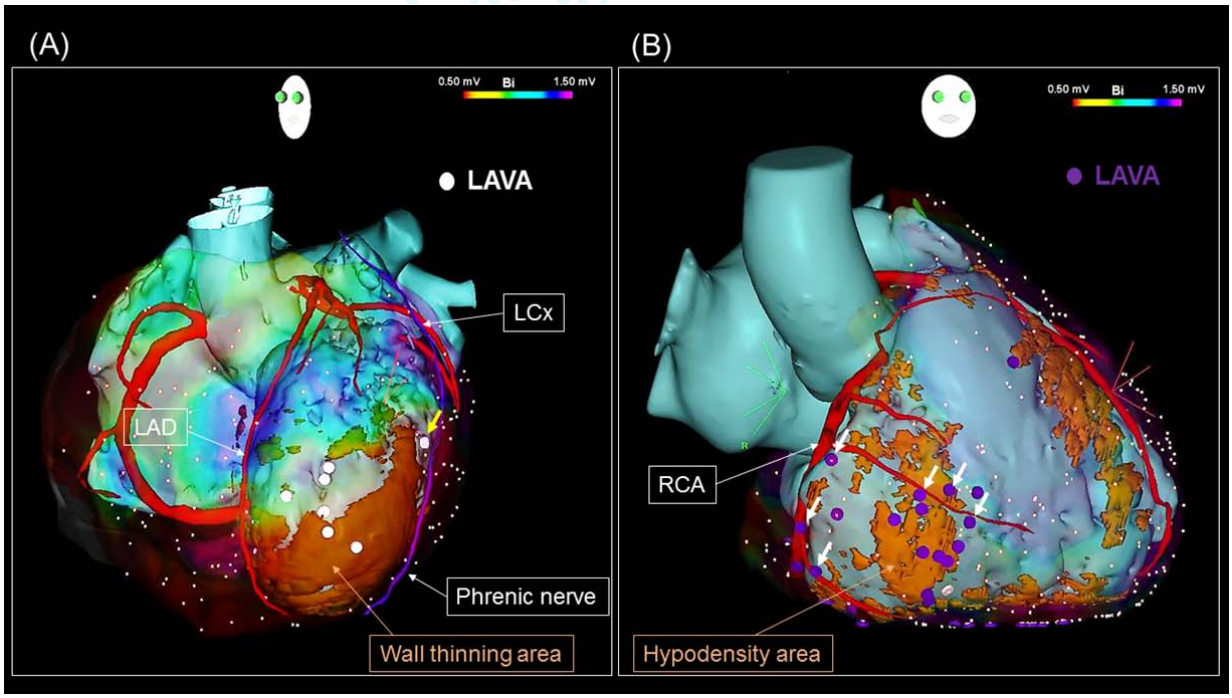

Figure 5.

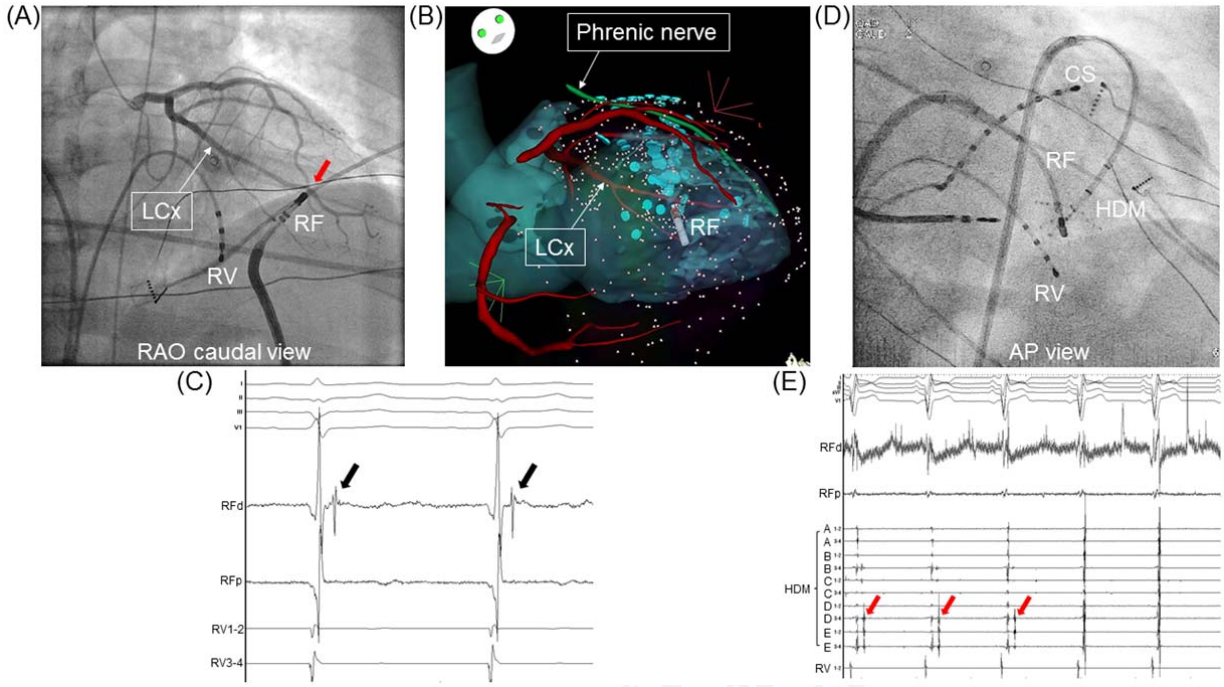

References

1. Jais P, Maury P, Khairy P, et al. Elimination of local abnormal ventricular activities: a new end point for substrate modification in patients with scar-related ventricular tachycardia. Circulation 2012;125:2184-96.
2. Sosa E, Scanavacca M, d'Avila A, Pilleggi F. A new technique to perform epicardial mapping in the electrophysiology laboratory. Journal of cardiovascular electrophysiology 1996;7:531-6.
3. Sacher F, Tedrow UB, Field ME, et al. Ventricular tachycardia ablation: evolution of patients and procedures over 8 years. Circulation Arrhythmia and electrophysiology 2008;1:153-61.
4. Berte B, Sacher F, Cochet H, et al. Postmyocarditis ventricular tachycardia in patients with epicardial-only scar: a specific entity requiring a specific approach. Journal of cardiovascular electrophysiology 2015;26:42-50.
5. Komatsu Y, Daly M, Sacher F, et al. Endocardial Ablation to Eliminate Epicardial Arrhythmia Substrate in Scar-Related Ventricular Tachycardia. Journal of the American College of Cardiology 2014.

V. Mapping and ablation of scar-related VT: LAVA and intramural scar

Different techniques to perform substrate mapping and ablation are available (please refer to Introduction). In part V, we first describe our specific mapping and LAVA tagging technique, using the LAVA approach. In collaboration with the INRIA institute (Institut National de Recherche en Informatique et en Automatique, Sofia Antipolis, Nice) we attempted to predict LAVA locations with imaging data.

The last three sections (C.D. and E.) highlight the difficulties of intramural or septal scar mapping and ablation, particulary difficult to map and to treat, especially in the absence of wall thinning. Preprocedural imaging can help to detect intramural scar. Different ablation techniques are discussed as irrigated needle ablation, bipolar ablation and ethanol ablation.

Figure 1. Example of an intraseptal focus and iatrogenic scar.

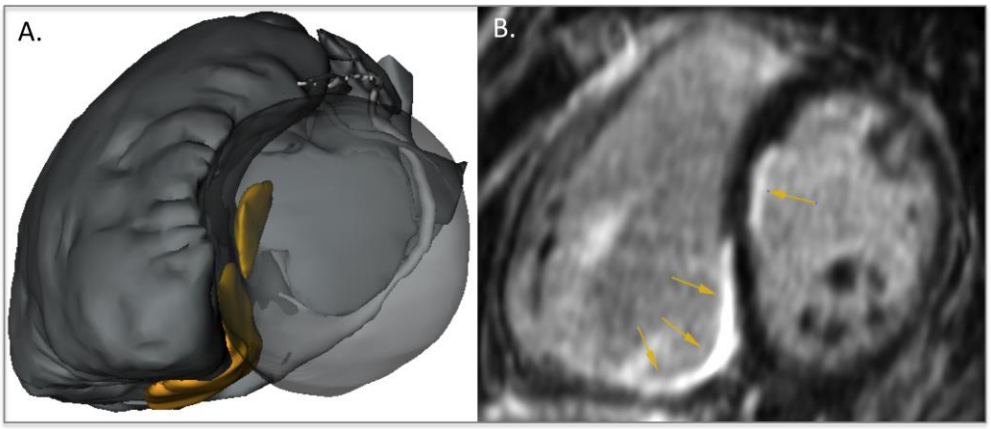

A. Merged MDCT and DE-MRI model (MUSIC) with effects of conventional RF ablation as iatrogenic scar in yellow. No transmural lesion can be made with conventional RF. **B.** DE-MRI with iatrogenic scar in white (arrows). No transmurality obtained after multiple ablation attempts.

A. Substrate Mapping and Ablation for VT: The LAVA Approach.

Sacher F, Lim HS, Derval N, Denis A, Berte B, Yamashita S, Hocini M, Haissaguerre M, Jaïs P.
J Cardiovasc Electrophysiol. 2015 Apr;26(4):464-71.

1. Study outline

In this manuscript, we describe the method used at our institution. Late potential ablation was described by different authors as Arenal, Bogun and Nogami.[15, 24, 99] Our center published the results of the LAVA approach with, for the first time, the end point of elimination of abnormal potentials, in 2012.[22] Local abnormal ventricular activity (LAVA) is a global term that incorporates all abnormal ventricular signals (late and double potentials, fragmented signals) that represent surviving near-field electrical activity. They can occur anywere during the QRS complex and can be identified by pacing maneuvers. Their main charachteristic is their poor coupling to the surrounding tissue. Manual tagging of these LAVA signals on the substrate map can help to identify potential ablation sites and can be used as an additional endpoint, combined with non-inducibility.

2. Implications

VT non-inducibility and/or inducibility of unstable VT are limitations of ablation techniques who cannot be performed in sinus rhythm. The LAVA approach is an effective mapping and ablation technique that can be used to treat patients referred

for VT ablation (both ICM and NICM) in SR and during VT with an objective endpoint.

3. Manuscript

TECHNIQUES, TECHNOLOGY, AND INNOVATIONS
Section Editor: Samuel J. Asirvatham, M.D.

Substrate Mapping and Ablation for Ventricular Tachycardia: The LAVA Approach

FREDERIC SACHER, M.D., PH.D., HAN S. LIM, M.B.B.S., NICOLAS DERVAL, M.D., ARNAUD DENIS, M.D., BENJAMIN BERTE, M.D., SEIGO YAMASHITA, M.D., MELEZE HOCINI, M.D., MICHEL HAISSAGUERRE, M.D., and PIERRE JAÏS, M.D.

From the Hôpital Cardiologique du Haut-Lévêque, LIRYC Institute, Bordeaux University, INSERM 1045, Bordeaux-Pessac France

Substrate Mapping and Ablation. ***Introduction:*** **Catheter ablation of ventricular tachycardia (VT) is proven effective therapy particularly in patients with frequent defibrillator shocks. However, the optimal endpoint for VT ablation has been debated and additional endpoints have been proposed. At the same time, ablation strategies aiming at homogenizing the substrate of scar-related VT have been reported.**

Methods and Results: **Our method to homogenize the substrate consists of local abnormal ventricular activity (LAVA) elimination. LAVA are high-frequency sharp signals that represent near-field signals of slowly conducting tissue and hence potential VT isthmuses. Pacing maneuvers are sometimes required to differentiate them from far-field signals. Delayed enhancement on cardiac MRI and/or wall thinning on multidetector computed tomography are also extremely helpful to identify the areas of interest during ablation. A strategy aiming at careful LAVA mapping, ablation, and elimination is feasible and can be achieved in about 70% of patients with scar-related VT. Complete LAVA elimination is associated with a better outcome when compared to LAVA persistence even when VT is rendered noninducible.**

Conclusion: **This is a simple approach, with a clear endpoint and the ability to ablate in sinus rhythm. This strategy significantly benefits from high-definition imaging, mapping, and epicardial access.** *(J Cardiovasc Electrophysiol, Vol. pp. 1-8)*

catheter ablation, imaging, ventricular tachycardia

Introduction

Catheter ablation of ventricular tachycardia (VT) is proven effective therapy particularly in patients with frequent defibrillator shocks.[1] Various substrate modification techniques have been described for unmappable or hemodynamically intolerable VT.[2-13] Late potential (LP) ablation has been described as a target for VT ablation.[8,11] Noninducibility, despite significant limitations, remained the endpoint in most of these studies. However, recently the optimal endpoint for VT ablation has been debated.[1]

Interestingly, Nogami *et al*.[14] targeted LPs in patients with arrhythmogenic right ventricular dysplasia. They proposed change in LP as an endpoint for ablation and postulated that qualitative analyses of serial signal-averaged ECGs could be useful during long-term follow-up.

We recently showed that elimination of local abnormal ventricular activities (LAVA) during sinus rhythm or ventricular pacing was an effective endpoint for substrate-based VT ablation.[1,15] This review will describe the identification of LAVA, their relation to the scar based on imaging studies and how to use them as an endpoint for VT ablation.

How to Identify LAVA

Definition of LAVA

Local abnormal ventricular activity (LAVA) is a global term that incorporates all abnormal ventricular signals that represent near-field signals of slowly conducting tissue and hence potential VT isthmuses. Most LAVA reside in scar or border-zone tissue and will appear as LPs. However, this is not always the case depending on its location, such as septal versus lateral and endocardial versus epicardial.[16]

The electrophysiological definition and properties of LAVA include the following:

The work described in this review was supported by a Fondation Leducq Grant (Grant number: 09 CVD 03) and grants from the Agence Nationale de la Recherche (IHU LIRYC ANR-10-IAHU-04 and Equipex MUSIC ANR-11-EQPX-0030).

F. Sacher reports honoraria relevant to this topic from Biosense Webster and St. Jude Medical. M. Hocini and M. Haissaguerre report research support from Biosense Webster, St. Jude Medical, and CardoInsight; they are stakeholders in CardioInsight. P. Jais reports travel and lecture fees from Biosense Webster and St. Jude Medical. Other authors: No disclosures.

Address for correspondence: Frederic Sacher, M.D., Ph.D., Hôpital Cardiologique du Haut-Lévêque, LIRYC Institute, Bordeaux University, INSERM 1045, Bordeaux-Pessac 33604, France. Fax: +33 55 765 6509; E-mail: frederic.sacher@chu-bordeaux.fr

Manuscript received 3 September 2014; Revised manuscript received 28 September 2014; Accepted for publication 8 October 2014.

doi: 10.1111/jce.12565

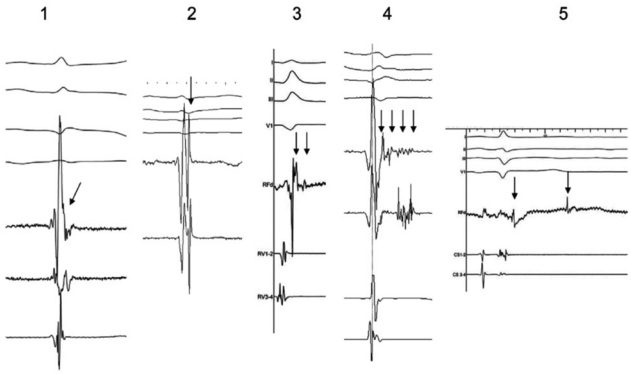

Figure 1. *Electrogram recordings from different patients showing various characteristics of local abnormal ventricular activities (LAVAs; arrows). (A) The potential representing LAVA is fused with the terminal portion of the far-field ventricular signal, making it difficult to identify the LAVA as a separate signal. (B) LAVA potential occurs just after and with a slightly higher frequency than the far-field ventricular potential. LAVAs in 1 and 2 occur within the QRS complex. (C) LAVA is a double-component potential that closely follows the far-field ventricular signal. The early component is a high-frequency potential that is almost fused with the preceding far-field ventricular potential. It occurs within the terminal portion of the QRS complex. Another low-amplitude signal follows an isoelectric interval and represents the late component of LAVA, which occurs after the QRS complex. (D) LAVAs are represented by pluricomponent signals without isoelectric intervals. These signals can be visualized distinctly from the preceding far-field ventricular signal. (E) Double-component LAVA signal. Although the early component is recorded just after the QRS complex, the late component is recorded after the inscription of the T wave on the surface ECG. Reproduced from Ref. (15).*

(1) sharp ventricular potential of high-frequency (high dV/dP) ± low-amplitude signal, but this is not always the case (Fig. 1);
(2) distinct from the far-field ventricular electrogram (sinus rhythm or pacing);
(3) occurring anytime during (rarely) or after the V EGM in sinus rhythm or before the V EGM during VT (Fig. 2);
(4) sometimes displaying fractionation (Fig. 1), double or multiple components separated by very low-amplitude signals, or an isoelectric interval;
(5) poorly coupled to the rest of the myocardium as demonstrated by the maneuvers detailed below.

Settings

To be able to identify these signals it is important to use high amplification with a low level of noise (Fig. 3). LAVA voltage may be extremely different from almost 1.5 mV in the border zone and in the absence of transmural scar to less than 0.05 mV in dense scar. In the absence of clear LAVA in area of dense scar (<0.5 mV), we use pacing to identify slow conduction area (long S-QRS) versus electrically unexcitable scar as described by Soejima *et al*.[6]

In terms of filters, we typically use 30–250 Hz as high- and low-pass filters.

In our experience, the pattern of the LAVA signal may be different depending on the catheter used and in particular the size of the electrode and the spacing between electrodes. The smaller the size of the electrode and the interelectrode space, the sharper is the signal (Fig. 4). Hence, LAVA will be easier to identify using catheters with small and shortly interspaced electrodes.

Techniques to Identify LAVA

During mapping, the signal recorded by the catheter is always a combination of far-field and near-field potentials. When multiple components are observed in the ventricular electrogram, the LAVA signals are typically made of high-frequency sharp potentials, while far-field signals have a lower dV/dT. In order to unmask LAVA, we suggest several different pacing techniques:

(1) Pacing from the right ventricle, particularly with a shortly coupled S2, may create some delay between the far-field and the poorly coupled near-field potential.
(2) Pacing from the catheter recording the potential of interest may be performed. The stimulus to QRS (S-QRS) delay will be prolonged when pacing a poorly coupled fiber especially when the pacing strength is reduced to threshold. As a consequence, the QRS morphology may also change, as the exit from the fibrotic region may be different.
(3) LAVA may be identified during local ectopics by the observation of sequential ventricular electrograms (Fig. 3). In case of local ectopy, the near-field activity (first potential) and the delay to the far-field one (second potential) provides insight to the time needed for the activation front to conduct from the surviving bundle to the surrounding ventricular tissue.
(4) An abnormally long intramyocardial conduction time may be identified by pacing endocardially while recording epicardially.

Relationship Between Imaging and LAVA

Preprocedural imaging is extremely useful to guide ablation and to prevent complications (coronary artery anatomy, phrenic nerve)[17] (Fig. 5). In our center, cardiac magnetic resonance imaging (MRI) with high-resolution sequences (voxel size: 1.25 × 1.25 × 2.5 mm^3) and/or multidetector computed tomography scan (MDCT) are routinely performed before VT ablation in the absence of contraindication.

Delayed enhancement (DE) on MRI as well as wall thinning (WT) on MDCT are well correlated with low voltage area <1.5 mV on electroanatomic mapping (EAM)[18] and the presence of LAVA.[19,20] Previous studies demonstrate that EAM voltage maps consistently underestimate scar when compared to DE-MRI.[19,21] With regard to LAVA, >90% are found in DE-MRI areas (Fig. 6). Wall thinning <5 mm on MDCT to identify scar areas is particularly relevant in patients with ischemic cardiomyopathy but less accurate in nonischemic cardiomyopathy. In ischemic cardiomyopathy, there is a 99% overlap between DE areas on MRI and WT on MDCT. With this extremely high percentage of overlap, cardiac MDCT may be reliably performed to estimate scar size in patients with ischemic cardiomyopathy and ICD. Ninety percent of LAVA are seen in areas with wall thinning <5 mm. Not surprisingly, very late LAVA occur almost exclusively in WT area <3 mm.[20]

There is also potential utility for imaging post-VT ablation. DE-MRI allows the quantification of the extend of ablation, specifically the level of transmurality[22,23] and the delineation of nonablated areas.

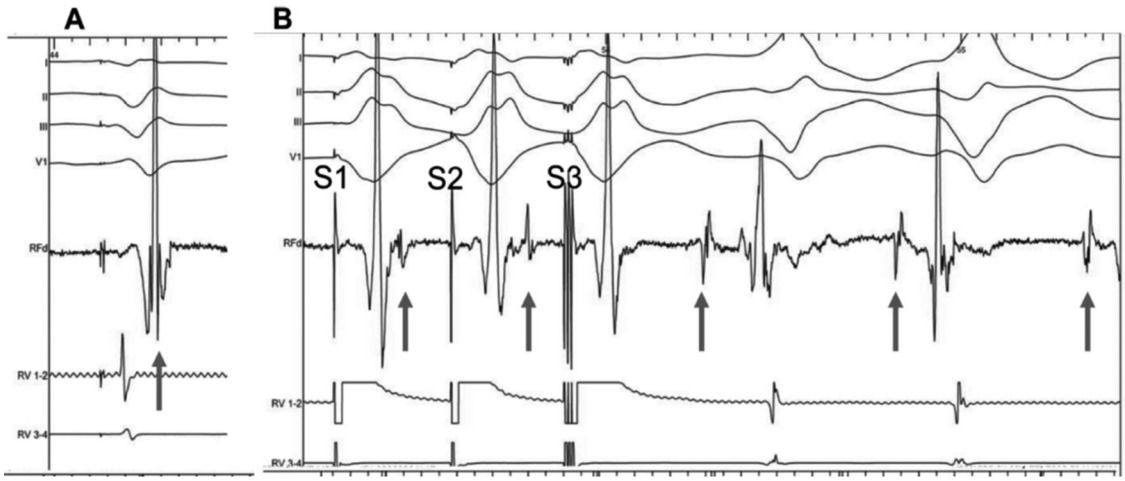

Figure 2. *Role of local abnormal ventricular activities (LAVAs) in the induction of ventricular tachycardia (VT) and the influence of radiofrequency energy on LAVAs. Before radiofrequency energy delivery (RF): (A) At first sight, the local ventricular electrogram during baseline paced rhythm looks simple. However, in the terminal portion of this simple-looking signal, a very high-frequency component (LAVA) can be identified. (B) Programmed electric stimulation from the right ventricle (RV) unmasks the LAVA potential by increasing the delay from the far-field signal. The delay observed during RV pacing suggests poor coupling of the muscle bundle generating the LAVA signal. The delay is maximal with S3, which is associated not only with a change in the polarity of LAVA but also with the induction of VT. Reproduced from Ref. (15).*

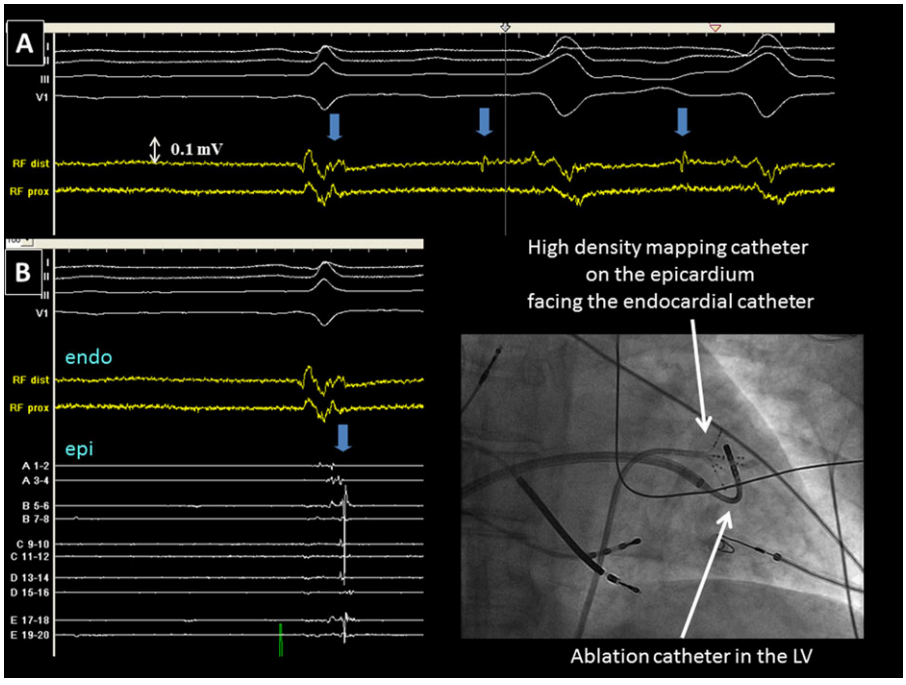

Figure 3. *Panel A displays a low-voltage electrogram (0.1 mV) recorded with a thermocool catheter (Biosense Webster, Diamond Bar, CA, USA) positioned in the left ventricle via transeptal access through an Agilis sheath (large curve, St. Jude Medical, St. Paul, MN, USA). Due to the very low voltage and absence of late component, it is difficult to determine whether there is a LAVA component or not. During spontaneous PVCs, a LAVA (blue arrow) becomes apparent ahead of the QRS proving its presence in the previous sinus beat. Panel B represents the same electrogram with additional electrograms (A1–2 to E19–20) recorded with a high-density mapping catheter (Pentaray, Biosense Webster) on the epicardium facing the ablation catheter. On these electrograms, the presence of LAVA (blue arrow) becomes obvious. When an epicadial access is obtained, we monitor epicardial electrograms while delivering RF endocardially at the facing site to ensure transmural LAVA elimination. For a high quality, full color version of this figure, please see Journal of Cardiovascular Electrophysiology's website: www.wileyonlinelibrary.com/journal/jce*

LAVA Ablation

Mapping

Epicardial access and mapping are routinely performed in patients with nonischemic cardiomyopathy or arrhythmogenic right ventricular dysplasia in the absence of contraindication.[24] In patients with ischemic cardiomyopathy, we would obtain epicardial access in case of previous failed procedure in the absence of a history of cardiac surgery. When epicardial access is obtained, we typically start with the epicardial voltage map before accessing the left endocardium.

Bipolar cut-off of <0.5 mV (scar), 0.5–1.5 mV (border zone) and >1.5 mV (normal)[4,25] is used to create a voltage map in sinus rhythm with a high-density mapping catheter (typically Pentaray® catheter, Biosense Webster, Diamond Bar, CA, USA). During point acquisition, all LAVA points recorded either spontaneously or during pacing maneuvers are annotated on the map. Pacing maneuvers are typically performed at the border zone of the scar where LAVA are more often found hidden within the far-field ventricular electrogram (Fig. 6). Areas with S-QRS >50 milliseconds during pacing are also annotated. Multipolar mapping catheter allows quick and high-density mapping of LAVA with a good

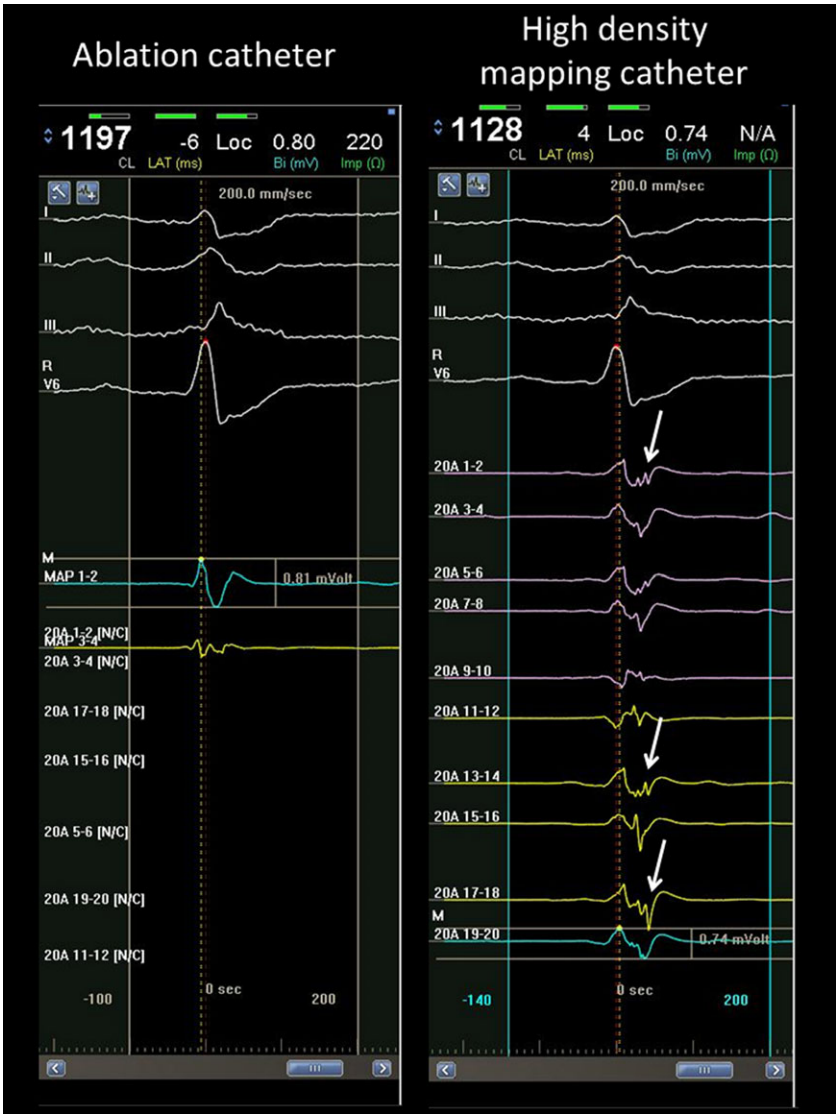

Figure 4. *Comparison of signals recorded at the same spot with an ablation catheter (Thermocool SF, electrode size: 3.5-mm tip, Biosense Webster, Diamond Bar, CA, USA) and a high-density mapping catheter (Pentaray, Biosense Webster) with small and short interspace electrodes. (electrode size: 1 mm; space between electrodes: 2–6–2 mm). While LAVA can be identified with the Pentaray (arrow), no LAVA potential can be seen with the ablation catheter. For a high quality, full color version of this figure, please see Journal of Cardiovascular Electrophysiology's website: www.wileyonlinelibrary.com/journal/jce*

spatial resolution owing to small and closely interspaced electrodes.

Ablation

Prior to ablation, an attempt to induce VT is made in every patient in our laboratory. If VT is inducible and well tolerated, conventional approach (activation and entrainment mapping) is used and ablation is performed at sites of critical isthmuses displaying mid-diastolic potentials. However, even in these favorable situations, we would aim for LAVA elimination as other VTs may still occur. An irrigated tip catheter is always used for ablation. The power varies from 30 to 50 Watts endocardially. In arrhythmogenic right ventricular dysplasia or when ablating epicardially, the power is usually limited to 30–35 Watts. For most of our patients, ablation is conducted in sinus rhythm once information on VT inducibility has been obtained. Usually, noninducibility is observed before complete LAVA elimination. However, radiofrequency (RF) delivery is continued until complete elimination is achieved to prevent other VTs from potentially occurring.

Ablation is preferentially started on LAVA situated within the QRS or slightly after the ventricular electrogram (Fig. 6) in an attempt to interrupt the potential channels that conduct to other areas displaying later LAVA signals. In essence, the early LAVAs are targeted first. Of note, ablation is also performed in scar areas, where no apparent signal is seen on the ablation catheter but capture is achieved with a long S-QRS interval. The lack of a visible signal may mean that either the signal amplification is not gained enough to detect the local abnormal EGM or the noise level is too high.

Even with epicardial mapping, ablation is generally started endocardially to prevent from collateral damages that are more likely to occur with epicardial ablation. This holds true even if more LAVA are recorded epicardially. In such situations, we monitor the transmural effect of endocardial RF applications by recording the disappearance of epicardial LAVA during endocardial ablation. This is performed by placing high-density mapping catheter epicardially juxtapositioned to the endocardial site during ablation.[26]

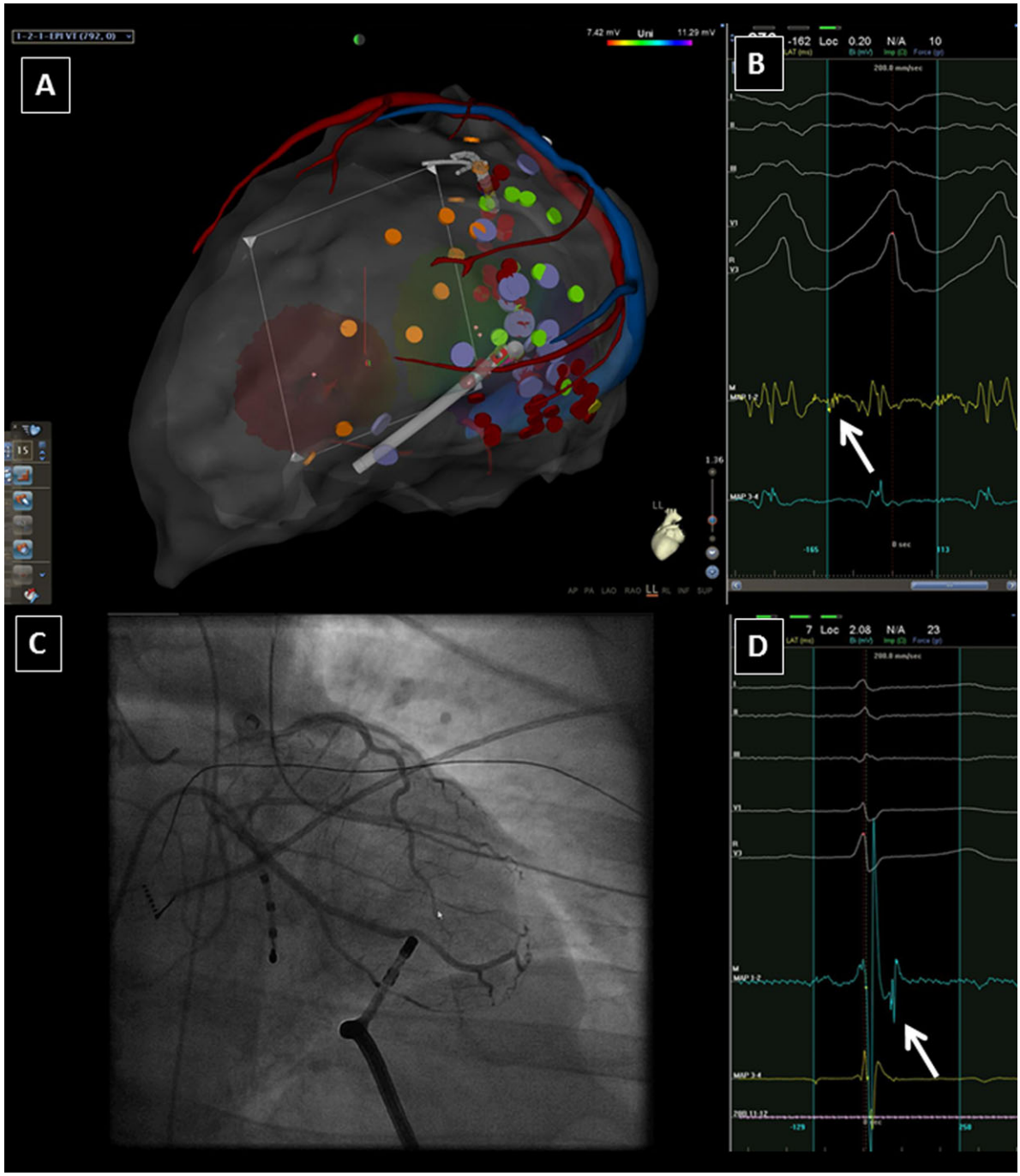

Figure 5. *Patient with myocarditis sequellae that underwent epicardial VT ablation. A cardiac MDCT was performed prior ablation and anatomical structures (coronary arteries, venous system, phrenic nerve [not displayed here], epicardium, endocardium [not displayed here], and wall thinning [not displayed here]) were segmented and imported into the CARTO 3 (Biosense Webster) system. VT was induced and well tolerated. Based on the merge of the MDCT, the site where mid-diastolic potentials (panel B, arrow) were recorded with the ablation catheter was situated on a coronary artery. After pace-terminating the VT, LAVA was observed in sinus rhythm (panel D, arrow). A coronary angiography was performed and confirmed the presence of a coronary artery (panel C) at that site and therefore the accuracy of the merge.*

LAVA as an Endpoint

Our procedural endpoint is LAVA elimination. Hence, we encourage remapping with a small pole, tightly spaced catheter once identified areas of LAVA have been targeted. If there are remaining LAVA, consolidative ablation is applied. Complete LAVA elimination can be achieved in 67% of patients with structural heart disease. VT inducibility is retested again when no LAVA remain on remapping or certain LAVA cannot be eliminated, for example, due to a deep scar or the presence of an adjacent coronary artery. In such cases, we find that most of the time monomorphic VT is no longer inducible. However, should monomorphic VT be induced, the VT would be targeted.

While inducibility of any VT is a poor prognostic sign, the lack of inducibility does not mean VT will not recur. In

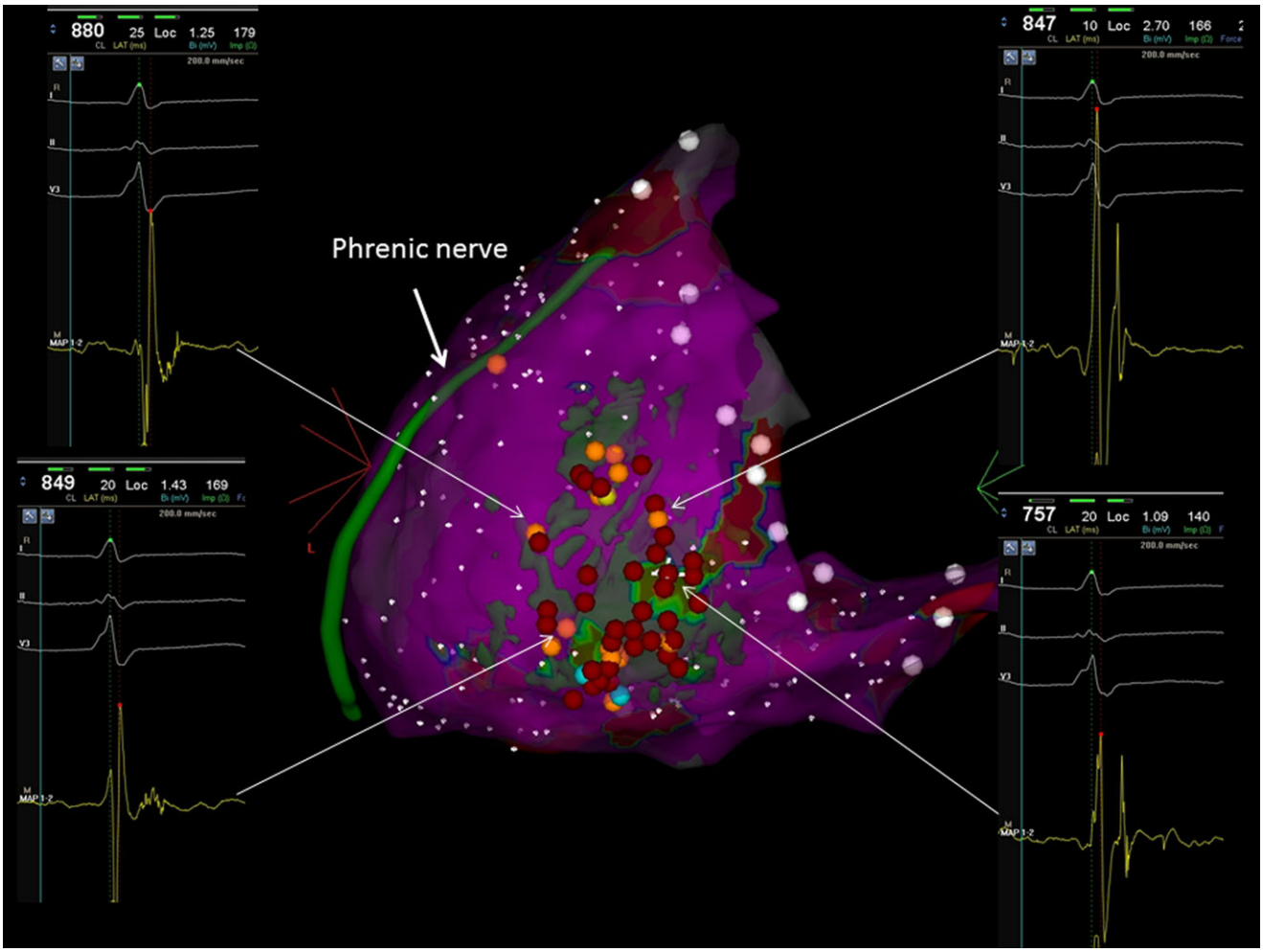

Figure 6. *Epicardial voltage map with merged delayed enhancement area in semitransparent green. Early LAVA are typically found in border-zone area. Merged DE-MRI is extremely helpful to focus on area of interest and not forget any area of scar. In this patient, ablation of early LAVA in border zone area allowed us to eliminate LAVA within the center of the scar.*

this respect, we have shown that LAVA elimination is a better predictor of success.[15] Thus, we feel the procedural endpoint of ablation should be the lack of VT inducibility (even in cases of multiple VTs) and the elimination of LAVA after remapping. Of note, this cannot always be achieved. Our data suggest that incomplete LAVA elimination is associated with a significantly higher risk of recurrent VT (hazard ratio [HR] 3.031, 95% confidence interval (CI; 1.915–4.798), $P < 0.001$) and mortality (HR 2.779, 95% CI (1.562–4.947), $P = 0.001$). In contrast, failure to achieve noninducibility postablation is independently associated with recurrent VT (HR 1.937, 95% CI (1.229–3.055), $P = 0.004$) but not mortality.

Are There Any Differences from Other Scar Homogenization Strategies?

Other groups also have described scar homogenization in VT ablation.[27,28] LAVA-based ablation leads to similar ablation maps. However, there are differences and LAVA-guided ablation may allow for less extensive ablation, especially if early-coupled LAVAs are targeted first, compared to complete scar homogenization as described by Di Biase *et al.*[27] In the latter approach, the entire low voltage area on EAM is targeted, focusing on delayed fragmented signals within the scar tissue. In that approach, any epicardial signal that lasts longer than 70 milliseconds, has 4 or more deflections, or is less than 1.5 mV and is not felt to be within dense scar is targeted. Such an approach may result in the most extensive ablation and indeed was reported to have 74 ± 21 minutes of ablation time versus 23 ± 11 minutes with our LAVA experience. However, this scar homogenization technique was associated with a very good VT outcome without an increase in complication rate.

On the other hand, we feel that limiting ablation to LPs may miss some potential VT isthmuses. LP as described by Vergara *et al.*[28] are defined as any low voltage EGM (<1.5 mV) with a single component or multiple continuous delayed electrical components, separated from the higher amplitude component of the local ventricular EGM by at least 20 milliseconds and recorded after the surface QRS end. In contrast, LAVA signals do not necessarily need to be after the QRS. In fact, in our experience roughly 20% of LAVA occur prior to the end of the QRS. Early-coupled LAVA may be more important for targeting the entrance to channels. Interestingly, if these early coupled LAVA signals are targeted, other LPs may disappear. However, this strategy is similar to LAVA elimination. A success rate of 90% at 13 months in cases of complete LP elimination versus 25% in cases of incomplete abolition is reported.

Conclusion

LAVA is present in about 90% of patients with ICM, NICM, and ARVC. A strategy aiming at careful LAVA mapping, ablation, and elimination is feasible and can be achieved in about 70% of patients. Complete LAVA elimination is associated with a better outcome when compared to LAVA persistence even when VT is rendered noninducible.

This is a simple approach, with a clear endpoint and the ability to ablate in sinus rhythm. This strategy significantly benefits from high-definition imaging, mapping, and epicardial access.

References

1. Aliot EM, Stevenson WG, Almendral-Garrote JM, Bogun F, Calkins CH, Delacretaz E, Bella PD, Hindricks G, Jais P, Josephson ME, Kautzner J, Kay GN, Kuck KH, Lerman BB, Marchlinski F, Reddy V, Schalij MJ, Schilling R, Soejima K, Wilber D; European Heart Rhythm Association, European Society of Cardiology, Heart Rhythm Society: EHRA/HRS Expert Consensus on Catheter Ablation of Ventricular Arrhythmias: Developed in a partnership with the European Heart Rhythm Association (EHRA), a Registered Branch of the European Society of Cardiology (ESC), and the Heart Rhythm Society (HRS); in collaboration with the American College of Cardiology (ACC) and the American Heart Association (AHA). Europace 2009;11:771-817.
2. Cassidy DM, Vassallo JA, Buxton AE, Doherty JU, Marchlinski FE, Josephson ME: The value of catheter mapping during sinus rhythm to localize site of origin of ventricular tachycardia. Circulation 1984;69:1103-1110.
3. Miller JM, Kienzle MG, Harken AH, Josephson ME: Subendocardial resection for ventricular tachycardia: Predictors of surgical success. Circulation 1984;70:624-631.
4. Marchlinski FE, Callans DJ, Gottlieb CD, Zado E: Linear ablation lesions for control of unmappable ventricular tachycardia in patients with ischemic and nonischemic cardiomyopathy. Circulation 2000;101:1288-1296.
5. Soejima K, Suzuki M, Maisel WH, Brunckhorst CB, Delacretaz E, Blier L, Tung S, Khan H, Stevenson WG: Catheter ablation in patients with multiple and unstable ventricular tachycardias after myocardial infarction: Short ablation lines guided by reentry circuit isthmuses and sinus rhythm mapping. Circulation 2001;104:664-669.
6. Soejima K, Stevenson WG, Maisel WH, Sapp JL, Epstein LM: Electrically unexcitable scar mapping based on pacing threshold for identification of the reentry circuit isthmus: Feasibility for guiding ventricular tachycardia ablation. Circulation 2002;106:1678-1683.
7. Kottkamp H, Wetzel U, Schirdewahn P, Dorszewski A, Gerds-Li JH, Carbucicchio C, Kobza R, Hindricks G: Catheter ablation of ventricular tachycardia in remote myocardial infarction: Substrate description guiding placement of individual linear lesions targeting noninducibility. J Cardiovasc Electrophysiol 2003;14:675-681.
8. Arenal A, Glez-Torrecilla E, Ortiz M, Villacastin J, Fdez-Portales J, Sousa E, del Castillo S, Perez de Isla L, Jimenez J, Almendral J: Ablation of electrograms with an isolated, delayed component as treatment of unmappable monomorphic ventricular tachycardias in patients with structural heart disease. J Am Coll Cardiol 2003;41:81-92.
9. Arenal A, del Castillo S, Gonzalez-Torrecilla E, Atienza F, Ortiz M, Jimenez J, Puchol A, Garcia J, Almendral J: Tachycardia-related channel in the scar tissue in patients with sustained monomorphic ventricular tachycardias: Influence of the voltage scar definition. Circulation 2004;110:2568-2574.
10. Hsia HH, Lin D, Sauer WH, Callans DJ, Marchlinski FE: Anatomic characterization of endocardial substrate for hemodynamically stable reentrant ventricular tachycardia: Identification of endocardial conducting channels. Heart Rhythm 2006;3:503-512.
11. Bogun F, Good E, Reich S, Elmouchi D, Igic P, Lemola K, Tschopp D, Jongnarangsin K, Oral H, Chugh A, Pelosi F, Morady F: Isolated potentials during sinus rhythm and pace-mapping within scars as guides for ablation of post-infarction ventricular tachycardia. J Am Coll Cardiol 2006;47:2013-2019.
12. Oza S, Wilber DJ: Substrate-based endocardial ablation of postinfarction ventricular tachycardia. Heart Rhythm 2006;3:607-609.
13. de Chillou C, Groben L, Magnin-Poull I, Andronache M, Magdi Abbas M, Zhang N, Abdelaal A, Ammar S, Sellal JM, Schwartz J, Brembilla-Perrot B, Aliot E, Marchlinski FE: Localizing the critical isthmus of post-infarct ventricular tachycardia: The value of pace mapping during sinus rhythm. Heart Rhythm 2014;11:175-181.
14. Nogami A, Sugiyasu A, Tada H, Kurosaki K, Sakamaki M, Kowase S, Oginosawa Y, Kubota S, Usui T, Naito S: Changes in the isolated delayed component as an endpoint of catheter ablation in arrhythmogenic right ventricular cardiomyopathy: Predictor for long-term success. J Cardiovasc Electrophysiol 2008;19:681-688.
15. Jais P, Maury P, Khairy P, Sacher F, Nault I, Komatsu Y, Hocini M, Forclaz A, Jadidi AS, Weerasooryia R, Shah A, Derval N, Cochet H, Knecht S, Miyazaki S, Linton N, Rivard L, Wright M, Wilton SB, Scherr D, Pascale P, Roten L, Pederson M, Bordachar P, Laurent F, Kim SJ, Ritter P, Clementy J, Haissaguerre M: Elimination of local abnormal ventricular activities: A new end point for substrate modification in patients with scar-related ventricular tachycardia. Circulation 2012;125:2184-2196.
16. Komatsu Y, Daly M, Sacher F, Derval N, Pascale P, Roten L, Scherr D, Jadidi A, Ramoul K, Denis A, Jesel L, Zellerhoff S, Lim HS, Shah A, Cochet H, Hocini M, Haissaguerre M, Jais P: Electrophysiologic characterization of local abnormal ventricular activities in postinfarction ventricular tachycardia with respect to their anatomic location. Heart Rhythm 2013;10:1630-1637.
17. Komatsu Y, Sacher F, Cochet H, Jais P: Multimodality imaging to improve the safety and efficacy of epicardial ablation of scar-related ventricular tachycardia. J Cardiovasc Electrophysiol 2013;24:1426-1427.
18. Tian J, Jeudy J, Smith MF, Jimenez A, Yin X, Bruce PA, Lei P, Turgeman A, Abbo A, Shekhar R, Saba M, Shorofsky S, Dickfeld T: Three-dimensional contrast-enhanced multidetector CT for anatomic, dynamic, and perfusion characterization of abnormal myocardium to guide ventricular tachycardia ablations. Circ Arrhythm Electrophysiol 2010;3:496-504.
19. Cochet H, Komatsu Y, Sacher F, Jadidi AS, Scherr D, Riffaud M, Derval N, Shah A, Roten L, Pascale P, Relan J, Sermesant M, Ayache N, Montaudon M, Laurent F, Hocini M, Haissaguerre M, Jais P: Integration of merged delayed-enhanced magnetic resonance imaging and multidetector computed tomography for the guidance of ventricular tachycardia ablation: A pilot study. J Cardiovasc Electrophysiol 2013;24:419-426.
20. Komatsu Y, Cochet H, Jadidi A, Sacher F, Shah A, Derval N, Scherr D, Pascale P, Roten L, Denis A, Ramoul K, Miyazaki S, Daly M, Riffaud M, Sermesant M, Relan J, Ayache N, Kim S, Montaudon M, Laurent F, Hocini M, Haissaguerre M, Jais P: Regional myocardial wall thinning at multidetector computed tomography correlates to arrhythmogenic substrate in postinfarction ventricular tachycardia: Assessment of structural and electrical substrate. Circ Arrhythm Electrophysiol 2013;6:342-350.
21. Wijnmaalen AP, van der Geest RJ, van Huls van Taxis CF, Siebelink HM, Kroft LJ, Bax JJ, Reiber JH, Schalij MJ, Zeppenfeld K: Head-to-head comparison of contrast-enhanced magnetic resonance imaging and electroanatomical voltage mapping to assess post-infarct scar characteristics in patients with ventricular tachycardias: Real-time image integration and reversed registration. Eur Heart J 2011;32:104-114.
22. Cochet H, Sacher F, Chaumeil A, Jais P: Steam pop during radiofrequency ablation: Imaging features on magnetic resonance imaging and multidetector computed tomography. Circ Arrhythm Electrophysiol 2014;7:559-560.
23. Berte B, Sacher F, Mahida S, Yamashita S, Lim HS, Denis A, Derval N, Hocini M, Haissaguerre M, Cochet H, Jais P: Impact of septal radiofrequency ventricular tachycardia ablation: Insights from magnetic resonance imaging. Circulation 2014;130:716-718.
24. Lim HS, Sacher F, Cochet H, Berte B, Yamashita S, Mahida S, Zellerhoff S, Komatsu Y, Denis A, Derval N, Hocini M, Haissaguerre M, Jais P: Safety and prevention of complications during percutaneous epicardial access for the ablation of cardiac arrhythmias. Heart Rhythm 2014;11:1658-1665.
25. Callans DJ, Ren JF, Michele J, Marchlinski FE, Dillon SM: Electroanatomic left ventricular mapping in the porcine model of healed anterior myocardial infarction. Correlation with intracardiac echocardiography and pathological analysis. Circulation 1999;100:1744-1750.
26. Komatsu Y, Daly M, Sacher F, Cochet H, Denis A, Derval N, Jesel L, Zellerhoff S, Lim HS, Jadidi A, Nault I, Shah A, Roten L, Pascale P, Scherr D, Aurillac-Lavignolle V, Hocini M, Haissaguerre M, Jais P: Endocardial ablation to eliminate epicardial arrhythmia substrate in

scar-related ventricular tachycardia. J Am Coll Cardiol 2014;63:1416-1426.

27. Di Biase L, Santangeli P, Burkhardt DJ, Bai R, Mohanty P, Carbucicchio C, Dello Russo A, Casella M, Mohanty S, Pump A, Hongo R, Beheiry S, Pelargonio G, Santarelli P, Zucchetti M, Horton R, Sanchez JE, Elayi CS, Lakkireddy D, Tondo C, Natale A: Endo-epicardial homogenization of the scar versus limited substrate ablation for the treatment of electrical storms in patients with ischemic cardiomyopathy. J Am Coll Cardiol 2012;60:132-141.
28. Vergara P, Trevisi N, Ricco A, Petracca F, Baratto F, Cireddu M, Bisceglia C, Maccabelli G, Della Bella P: Late potentials abolition as an additional technique for reduction of arrhythmia recurrence in scar related ventricular tachycardia ablation. J Cardiovasc Electrophysiol 2012;23:621-627.

B. *Needle ablation:* Irrigated needle ablation creates larger and more transmural ventricular lesions compared to standard unipolar ablation in an ovine model.

Submitted as First Review to Circulation Arrhythmia and Electrophysiology.

1. Study outline

In this animal study, we compared the lesions made by a new irrigated needle catheter to conventional radiofrequency (RF) lesions. VT recurrence can occur after VT ablation due to incomplete and/or non-transmural ventricular lesion formation, especially in NICM patients with no or limited wall thinning or in the presence of intramural scar. Thirteen sheep were included and 120 left ventricular endocardial RF ablation lesions were created in healthy tissue: 60 lesions with a conventional irrigated ablation catheter (Thermocool, Biosense Webster) and 60 lesions with an irrigated needle catheter (Biosense Webster). In the animals where needle RF was performed, DE-MRI was performed both in-vivo (1.5T) and ex-vivo (9.3T). Finally, histological analysis was performed.

The needle lesions were twice as large and twice as deep as conventional lesions (1030±362mm^3 vs. 488±384mm^3 and 9.9±2.7mm vs. 5±2.4mm) and more transmural lesions were created with needle RF vs conventional RF (62.5% vs. 17%). No complications occured using both strategies. All needle lesions were seen on DE-MRI, both directly post-procedural on conventional MRI as on ex-vivo high density MRI.

2. Implications

Patients with an intramural or septal scar are particularly challenging to treat and frequently experience recurrences following VT ablation. This is mainly due to the lack of efficacy to create deep and transmural lesions using conventional RF energy. Irrigated needle ablation is a promising, novel technique which appears to be safe and effective in the treatment of scar-related VT arising from deep intramural circuits. Since needle RF lesions can be visualized on conventional MRI, this can help to evaluate efficacy and transmurality of lesion formation directly after the VT ablation procedure. Ex-vivo high-density MRI is a very effective tool to analyze the lesion volume and transmurality with almost histological accuracy.

3. Manuscript

Irrigated needle ablation creates larger and more transmural ventricular lesions compared to standard unipolar ablation in an ovine model.

Authors list: Benjamin Berte MD[1,2]; Hubert Cochet MD, PhD[1,2]; Julie Magat MD, PhD[2]; Jérôme Naulin[2]; Frédéric Sacher MD, PhD[1,2]; Daniele Ghidoli[3]; Xavier Pillois PhD[1]; Frédéric Casassus MD[1]; Seigo Yamashita MD, PhD[1]; Saagar Mahida MD, PhD[1]; Nicolas Derval MD[1]; Mélèze Hocini MD[1,2]; Bruno Quesson PhD[2]; Olivier Bernus PhD[2]; Rukshen Weerasooriya MD, PhD[4]; Michel Haïssaguerre MD[1,2]; Pierre Jaïs MD, PhD[1,2].

Affiliations:

[1] Hôpital Haut-l'évêque, departments of Cardiology and Radiology, CHU Bordeaux, FR

[2] LIRYC institute, IHU Bordeaux, FR

[3] Biosense Webster, research and development department, Ann Arbor, Los Angeles, USA

[4] Department of Cardiology, Royal Perth Hospital, AU

Running title: Berte *et al.* Needle ablation for scar related VT.

Conflicts of interest: Dr Berte received an educational EHRA grant.

Dr Jaïs receives consulting fees from Biosense Webster. Mr Ghidoli is an employee of Biosense Webster.

Word count: 6199 words.

Corresponding author:

Pierre Jaïs, MD

Hôpital Cardiologique du Haut-Lévêque, 33604 Bordeaux-Pessac, France.

Tel: +33 5 57 65 64 71; Fax: +33 5 57 65 65 09

E-mail: pierre.jais@chu-bordeaux.fr

Irrigated needle ablation creates larger and more transmural ventricular lesions compared to standard unipolar ablation in an ovine model.

ABSTRACT

Introduction: VT recurrence can occur after VT ablation due to incomplete and/or non-transmural ventricular lesion formation. We sought to compare the lesions made by a novel irrigated needle catheter to conventional radiofrequency (RF) lesions.

Methods: Thirteen female sheep (4.6±0.7yrs, 54±8kg) were studied. In 7 sheep, 60s RF applications were performed using an irrigated needle catheter. In 6 sheep, conventional lesions were made using a 4mm-irrigated catheter. 1.5 T in vivo and high-density MRI (9.4Tesla) were performed on explanted hearts from animals receiving needle RF. Conventional lesion volume was calculated as $(1/6)*\pi*(A*B^2+C*D^2/2)$. Needle lesion volume was measured as $\Sigma(\pi*r^2)/2$ with a slice thickness of 1mm. The dimensions of all lesions were also measured on gross pathology. Additional histological analysis of the needle lesions was performed.

Results: 120 endocardial left ventricular ablation lesions (conventional, n=60; needle, n=60) were created. At necropsy, more lesions were found using needle vs. conventional RF (90% vs. 75%, $p<0.05$). Comparing needle vs. conventional RF: Lesion volume was larger (1030±362mm3 vs. 488±384mm3, $p<0.001$), lesion depth was increased (9.9±2.7mm vs. 5±2.4mm, $p<0.001$) and more transmural lesions were created (62.5% vs. 17%, $p<0.01$). Pericardial contrast injection was observed in 4 apical attempts using needle RF, however with no adverse effects. Steam pops occurred in 3 attempts using conventional RF.

Conclusions: Irrigated needle ablation is associated with more frequent, larger, deeper, and more often transmural lesions compared to conventional irrigated ablation. This technology might be of value to treat intramural or epicardial VT substrates resistant to conventional ablation.

ABSTRACT WORD COUNT: 247

INTRODUCTION

Ventricular tachycardia (VT) ablation is associated with a relatively high recurrence rate. Outcomes of VT ablation are worse in non-ischaemic cardiomyopathy (NICM) as compared to ischaemic cardiomyopathy (ICM).[1, 2] One of the factors contributing to high recurrence rates may be the inability to perform transmural lesions. Formation of transmural lesions is particularly important in patients with intramural arrhythmogenic substrates and preserved wall thickness. In this context, techniques such as selective intracoronary ethanol injection or bipolar ablation have demonstrated promise however have not been widely adopted.[3-6]

A promising novel technology for ablation of intramural VT circuits of foci is the retractable needle catheter technique. A number of recent studies have demonstrated that the technique may be useful in patients with VT resistant to conventional ablation.[7-10] However, characteristics of lesions following needle ablation, both in healthy and scarred tissue, have not been fully defined. Further, optimal ablation settings are not yet established (saline infusion rate through the needle and the catheter, power titration, and ablation time). The aim of this study was 1) to evaluate lesion formation using a retractable needle catheter versus conventional ablation and 2) to evaluate the safety of VT ablation using the needle catheter.

METHODS

Animal Preparation

The experimental protocol was compliant with the Guiding Principles for the Use and Care of Animals published by the National institutes of Health (NIH Publication No. 85-23, Revised 1996). Animals were sedated with an intramuscular injection of 20mg/kg

ketamine hydrochloride and anaesthetized with sodium pentobarbital (10mg/kg). Slow intravenous infusion of saline maintained hydration throughout surgery, and anesthesia was maintained using continuous intravenous infusion of ketamine (500mg/hour) and pentobarbital (150mg/hour). The trachea was intubated through a midline cervical incision for connection to a respirator (Siemens Servo B, Berlin, Germany). Sheep were then ventilated using room air supplemented with oxygen. An intravenous catheter was placed in the internal jugular vein for infusion of drugs and fluids. Arterial blood gases were monitored at 30minute intervals (Radiometer, Copenhagen, Denmark), and ventilation parameters were adjusted to maintain blood gases within physiological ranges.

Substrate mapping

The left ventricle (LV) was accessed via a retrograde aortic approach, and a short 7 or 8Fr sheath was placed in the right femoral artery. In both groups, bipolar voltage map of left ventricular endocardium was acquired by using ablation catheters (Thermocool or needle catheter, Biosense Webster, Diamond Bar, CA) and a CARTO® system. Conventional voltage thresholds were applied (<0.5mV as dense scar, 0.5-1.5mV as border zone, >1.5mV as normal tissue). All ablation lesions were created in healthy tissue (normal voltage) and were manually annotated as three-dimensional tags on the map in order to compare the lesions with the magnetic resonance imaging (MRI) data after postprocedural image integration.

Catheter Ablation

The deflectable needle catheter has a distal bipole with an extendable/retractable 27gauge nitinol needle. The needle has an embedded thermocouple and has a central lumen through

which saline can be infused and the lumen of the catheter is flushed separately. A position sensor within the catheter tip is compatible with the CARTO® system (Biosense Webster). The needle can be retracted completely within the catheter tip and completely expanded has a needle length of 12mm (common used lengths vary between 4-8mm). At the distal handle, a manual adjustable system can adjust the wanted needle length in mm and enables retraction and expansion of the needle. The bipolar recordings Abl1-2 were made between the needle and the distal electrode. Abl3-4 was made between the ring electrode and the distal electrode. Abl1-2 was very noisy and not interpretable with the needle retracted, but became visible following needle deployment. Impedance is only recorded with the needle extracted. Pacing in both unipolar (0.5-500Hz, between needle tip and catheter electrode in the inferior caval vein) and bipolar (30-500Hz, between needle tip and distal electrode) mode and electrogram (EGM) recordings are possible from the catheter electrodes and the needle tip.

Needle ablation group

The needle was fully retracted during manipulation within the left ventricle. Ablation sites were tagged on the substrate map. In an attempt to comprehensively analyse the effect of needle ablation, lesions were delivered in multiple different areas of the left ventricle.

When good contact and perpendicular tip position were expected by tactile feedback and fluoroscopy, the needle was expanded during fluoroscopy to evaluate needle deployment. ST elevation on the unipolar tip electrode and ectopic beats were frequently observed during this maneuver. Contrast injection of 1-2ml of Omnipaque 300mg/ml) was performed under fluoroscopic view to evaluate contrast staining and to rule out

perforation. After contrast injection, the needle was flushed during 60-90seconds (defined as waiting time). Ablation was then performed, using a power controlled mode (25-35Watts) with an ablation duration of 60s at an infusion rate of 2ml/min flow trough the needle lumen and 1-2ml/min flow rate trough the catheter lumen. Ablation was started at 25Watts and up titrated to 35Watts if a stable decline in impedance was observed. An application was considered if RF was delivered for ≥10seconds (s). The choice of flow settings was based on the available data from animal and clinical studies and from our own experimental data demonstrating larger needle lesions using 2ml/min vs. 1ml/min flow (unpublished data).[9,10] From a theoretical perspective, the saline infusion acts as a virtual electrode and potentially cools the needle tip.[9,10]

Needle perforations with contrast injection into the pericardial space were not considered as RF applications, since RF was not delivered in this situation.

In case of stable sinus rhythm, bipolar EGM voltage was measured before and after ablation, with the needle deployed in the myocardium, using an EP Recording System (LabSystem™ PRO, Bard EP, Lowell, MA). Pacing thresholds were also analyzed before and after ablation using a stimulator (UHS 3000, Biotronik, Berlin, Germany). Because this device has a maximal limit on pacing thresholds of 10mA, we considered any threshold >10mA as 11mA.

Conventional ablation group

Endocardial ablation sites were selected on the substrate map in healthy left ventricular areas. Each ablation site was tagged on the substrate map. When good contact was expected by tactile feedback and fluoroscopy, a conventional ablation (Thermocool,

Biosense Webster, Diamond Bar, CA) was performed for a duration of 60s using a power-controlled mode (30-35Watts) and 30ml/min irrigation rate. An application was considered if RF was delivered for ≥10s.

Magnetic resonance imaging

MRI was performed in 5/7 animals from the needle ablation group. In vivo late-gadolinium enhanced MRI was performed immediately after the ablation procedure to assess whether acute lesions could be assessed non-invasively. Imaging was performed using a 1.5T device (Avanto, Siemens Medical Systems, Erlangen, Germany) equipped with a 32-channel cardiac coil. Late gadolinium enhanced imaging was initiated 15 min after the injection of 0.2mmol.kg^{-1} gadoterate meglumine (Dotarem, Laboratoires Guerbet, Aulnay-sous-bois, France). Images were acquired using a three-dimensional, ECG-gated, respiratory-navigated and inversion recovery-prepared Turbo Fast Low Angle Shot sequence with fat saturation. Sequence parameters were: voxel size 1.25x1.25x2.5mm, TR/TE 6.1/2.2ms, flip angle 22°, inversion time 260 to 320ms depending on the results of a TI scout scan performed immediately before acquisition, parallel imaging with GRAPPA technique with R=2, 42 reference lines, acquisition time 5 to 10 min depending on the animal's heart and breath rate.

Ex vivo high-resolution MRI (9.4T) was performed on explanted hearts from the same animals. The aim was to assess tissue characteristics at lesion site (needle trajectory, necrotic core and haemorrhagic halo), and to enable accurate three-dimensional lesion measurement (volume, transmurality). Animals were sacrificed after in vivo MRI acquisitions, and the hearts were rapidly removed and flushed with cold cardioplegic

solution, followed by a fixed perfusion during 1.5 hours with a 1L solution of 4% formalin in phospate buffered saline (PBS) containing 2ml gadoterate meglumine (Dotarem, Guerbet). Imaging was carried out with the heart removed from formalin and placed in a plastic container immersed with fomblin (Aldrich), a perfluoropolyether for susceptibility matching. Imaging was performed on a 9.4T system (Bruker BioSpin MRI, Ettlingen, Germany) with an open bore access of 30cm, using a 7-element transmit/receive array coil. The whole heart was imaged in short axis orientation using a three-dimensional Turbo Fast Low Angle Shot sequence with the following parameters: voxel size 80x80x235µm, TR/TE 25/9ms, flip angle 30°, acquisition time of about 110h per animal.

On these high-resolution images, lesions were identified and labeled by reviewing the lesion tags on the three-dimensional electro-anatomic map. MRI signal characteristics were assessed at each lesion site. Lesions were described as present or absent, transmural or non-transmural. Lesions were considered as transmural when extending from the endocardium to less than 2mm from the epicardium. Additionally, lesion volume was measured by three-dimensional manual segmentation using the software OsiriX 3.9.4 (Osirix Foundation, Geneva, Switzerland).

Gross Pathology and Histology

Gross anatomic examination was performed immediately after animal sacrifice in all animals from the conventional ablation group (N=6), and in 2 animals from the needle ablation group. In the 5 animals from the needle group who underwent MRI, gross pathology examination was performed after fixation. Lesions were identified and labeled by reviewing the lesion tags on the three-dimensional electro-anatomic map. Lesions were described as present or absent, transmural or non-transmural. Lesions were considered as

transmural when extending from the endocardium to less than 2mm from the epicardium. The 3 dimensions were measured on each lesion using a micrometer (±0.1mm), with surrounding inflammation being excluded from lesion sizing.

The volume of conventional RF lesions was considered as half a prolate ellipsoid (missing cap) and computed as follows: lesion volume = $(1/6)*\pi*(A*B^2 + C*D^2/2)$ as described by Wittkampf *et al.*[11] The volume of needle RF lesions was calculated as the sum of all slice surfaces (π x width^2 /2 for each slide) of 1mm section thickness on ex vivo high resolution 3D MRI data (surrogate for histological slices), as described by Sapp *et al.*[8] Hence, high field MR lesion volume measurements were only available in 5/7 animals from the needle ablation group.

Histological assessment was performed in 5 animals from the needle ablation group (the same that underwent MRI). After fixation in formaldehyde, explants were processed using an automatic tissue treatment (LEICA TP1020) for embedding in paraffin (LEICA EG1150H). Serial 6µm-thick sections were cut using a Microtome (LEICA RM2255) and stained with Trichrome Masson, following standard procedures. Paraffin sections were deparaffinized with toluene and rehydrated in graded series of ethanol and distilled water before staining (Tissue colouring using HMS70 from MicroMicrom). After staining, the sections were analyzed by a certified anatomical pathologist using a dedicated Microscope (NIKON Eclipse) and imaging software (NIS Elements D version 4.12).

Statistical analysis

Continuous variables were expressed as mean ± SD for normally distributed data or median and interquartile range (IQR; 25th–75th percentile) for non-normally distributed

data. Categorical data were expressed as counts and percentages. Data were tested for normality using the Kolmogorov-Smirnov test. Continuous variables were compared between groups using parametric (Student *t*) or non-parametric (Mann-Whitney) tests, depending on data normality. Categorical variables were compared using Fisher's exact or Pearson's chi-square tests as appropriate. A P-value <0.05 was considered to indicate statistical significance. Statistical analyses were performed using PASW Statistics 18 (version 18.0.0).

RESULTS

Population characteristics

Thirteen female sheep (4.6±0.7years, 54±8kg) were included, and divided into 2 groups, one undergoing ablation with the conventional irrigated catheter (n=6), and the other undergoing ablation with the needle irrigated ablation catheter (n=7). A total of 120 ablation lesions (conventional RF, n=60; needle RF, n=60) were created in the 13 sheep. A mean waiting time between contrast staining and RF application in the needle RF group was 79±23 s. The needle was deployed from 3 to 8 mm in all animals with a mean length of 6±1 mm. Apical lesions were performed with 3 mm deployment length in all cases. Baseline characteristics are presented in Table 1. Macroscopic lesion assessment was feasible in all 13 animals. It was performed on wet tissue in 8 animals, and after fixation in the 5 animals that underwent MRI. *In vivo* and *ex vivo* MRI studies were feasible in all 5 animals in which they were attempted. Histological analysis was feasible in all of these 5 animals.

Procedural data

Among the 120 RF applications, there were no differences in RF duration between groups (58±10 s in needle group vs. 55±13 s in conventional group, p= 0.33), and effective mean

power delivered between both groups (29±5.8Watts in needle group vs. 30±1.8Watts in conventional group, p=0.39). Using the needle catheter, contrast injection into the pericardial space occurred in four attempts at the apex, while the needle was deployed at 3 mm. Following the identification of pericardial injection, the needle was retracted and the animal was observed during ten minutes. There was no evidence of tamponade in any of the four cases. Short runs of ventricular tachycardia were frequently observed during RF application. Sustained ventricular arrhythmias were observed in 4 cases (3 monomorphic VT, 1 VF) In these 3cases of sustained ventricular tachycardia, the needle was retracted and no further measurements were performed (sinus rhythm was necessary for bipolar voltage measurement). In the case of ventricular fibrillation, the needle was retracted, the animal received one DC chock and returned into sinus rhythm.

Pacing thresholds and voltage measurements are shown in Table 2 and an example is given in Figure 1. Pacing threshold measurement was feasible both before and after ablation on 53 needle RF applications sites. Thresholds increased from 6.2±2.9mA before ablation to 9.8±2.5mA after ablation ($p<0.001$). A threshold above >10mA was observed on 2/53 sites before ablation and 19/53 sites after ablation ($p<0.001$). Bipolar voltage could be reliably measured before and after RF on 28 needle RF applications sites. A decrease in bipolar voltage was consistently observed after ablation (2.7±2.7mV before RF vs. 0.7±0.4mV after RF, $p<0.001$). In the conventional RF group, 3 steam pops occurred during ablation, however no tamponade was observed. One episode of ventricular fibrillation was observed during ablation, requiring multiple shocks. All 13 animals survived the complete ablation procedure.

Lesion characteristics on gross pathology and MRI

After the ablation procedure, more lesions were found on necropsy in the needle RF group as compared to the conventional ablation group (needle vs. conventional; 54/60 [90%] vs. 45/60 [75%], $p<0.05$). Lesion volume was more than twice as large in the needle RF group (needle vs. conventional; 1030±362mm^3 vs. 488±384mm^3, $p<0.001$). Needle RF lesions were also deeper (needle vs. conventional; 9.9±2.7mm vs. 5.2±2.4mm, $p<0.001$) and more likely to be transmural (needle vs. conventional; 62.5% vs. 17%, $p<0.01$). All transmural lesions using conventional RF were found near the LV apex where a wall thickness of ≤3mm was measured. Ablation and lesion characteristics are outlined in Table 3. A comparison between conventional and needle RF lesions is given in Figure 2.

In vivo and ex vivo imaging features

In vivo MRI studies were feasible using a clinical 1.5T scanner in all 5 animals from the needle ablation group. In these animals, RF applications had been performed on 50 sites. Late gadolinium enhanced imaging was performed within 60 min of the ablation procedure in all animals, and allowed for the visualization of lesions at all sites of RF application (50/50). All lesions demonstrated characteristics consistent with coagulative necrosis, i.e. a halo of intense enhancement surrounding a dark core. Lesions were of ellipsoid shape, with a center located within midwall layers.

Ex vivo MRI studies with a 9.4T scanner were feasible in all 5 animals. Of note however, the size of the hearts did not enable a complete left ventricular coverage. Therefore, the apex was not included in the field of view, and apical RF application sites could not be analyzed. Nonetheless, lesions were identified at all RF application sites present in the imaging field of view (41/41). All lesions showed similar features, i.e. a halo of hypointense signal compatible with hemorrhagic tissue, surrounding a highly heterogeneous necrotic core.

Lesions appeared to be of ellipsoid or teardrop shape, with a center located within midwall layers. The needle trajectory was clearly visible in all cases. Comparative examples of *in vivo* and *ex vivo* MRI are illustrated in Figure 3 and additional examples of 9.4T *ex vivo* MRI are shown in Figure 4.

Histological features

Histological abnormalities were observed in all 54 lesions identified on gross pathology. At the core of the ablation lesions hyper contracted muscle fibers (monophasic muscular degeneration) were observed. In some cases, fragmented sarcoplasm with an intact nucleus was observed. In addition, discrete micro-haemorrhage and vascular congestion was seen. When present, Purkinje fibres were vacuolated and fragmented.

At the lesion border zone, muscle fibres appeared less contracted and were characterized with a brilliant red appearance of the sarcoplasm with Masson's trichrome staining. The needle trajectory after RF delivery, when visible, was characterized by torn and hyper contracted fibres (boiled appearance of the fibers). The needle trajectory of a puncture attempt without RF delivery was characterized by small amount of mechanical tearing of myofibers, but not the brilliant red appearance of the sarcoplasm and the disarray of the Purkinje fibers. These findings suggest that the latter changes are due to tissue heating of RF delivery on top of the mechanical disruption of myofibers. Necrosis but no fibrosis was seen within the lesions, as the specimens were fixated at the acute phase.

Finally, a degenerated musculature was seen from the center towards the borderzone. Macroscopic, histological and MRI appearance of the same RF lesion are illustrated in Figure 5. Additional histological examples are demonstrated in Figure 6.

Discussion

The main findings of the present study are: (i) RF deliveries by an irrigated needle ablation catheter results in more frequent lesions. The lesions are larger, deeper, and more often transmural than those induced by conventional irrigated catheters, (ii) needle RF ablation appears to be feasible and safe in the left ventricle, and (iii) these lesions can be qualitatively and quantitatively assessed with the use of *in vivo* and *ex vivo* MRI.

Lesion size in needle vs. conventional RF catheters

Multiple previous studies have reported that conventional ablation catheters fail to create deep or transmural lesions.[8, 12] The present study demonstrates that lesions created by the irrigated needle catheter are significantly larger and deeper than those created by a conventional irrigated catheter. This finding may be of interest for ablation of VT circuits refractory to conventional ablation due to deep intramural locations. It also offers the possible treatment of epicardial targets from the endocardium, sparing the need for epicardial access. This could be of major interest particularly when epicardial targets are covered by coronary artery braches.

In addition to needle catheters, a number of techniques have attempted to overcome the challenges of ablating intramural VT circuits. Sacher *et al* reported that the use of contact force sensing catheters is associated with a higher prevalence of lesions at necropsy in animal models.[13] However, the size and depth of the lesions was not significantly improved (<5 mm). Transcoronary ethanol ablation has been reported to be effective for the management of intramural VT resistant to conventional RF ablation.[3, 5] However, ethanol ablation is limited by the anatomy of the coronary artery system and the challenge of controlling lesion size.[5]

Bipolar ablation is another technique that has been demonstrated to increase lesion size. The ability of the method to induce transmural lesions has been demonstrated in animal and computer modeling studies.[14] However to this day, the use of bipolar ablation in humans has only been evaluated in small case series with heterogeneous clinical results.[4, 6, 15]

Preliminary results of epicardial ablation using an open-chest approach are included as supplementary material (Additional online Figure 1). The needle catheter was held manually with moderate pressure, approximately 3cm from the needle tip. This technique could be used during a hybrid surgical approach using a mini-thoracotomy. We have however not investigated the possibility of needle ablation using a subxyphoid approach, since we hypothesized we could not have a favourable angulation towards the epicardium and the potential harm of direct puncture of coronary arteries with the needle tip. With direct optical visualization, it could be investigated, however once again, we believe correct angulation maybe a challenge.

Because our results indicate that irrigated needle ablation catheters are able to create intramural lesions of consistent size, this technique can be viewed as a promising alternative in patients refractory to conventional ablation, as recently suggested by the results of a first clinical study.[10]

In vivo lesion efficacy evaluation of needle ablation

Sacher *et al* previously demonstrated an EGM reduction >50% in approximately half of applications using conventional ablation. EGM reduction was more frequent when a lesion was found at necropsy compared to the absence of lesion.[16] Our findings relating to needle RF application compare favorably to this report. We demonstrated an EGM reduction of

>50% during all RF applications. Potential explanations for these findings include the fact that we used contrast staining and we evaluated ventricular premature beats with needle extraction and ST elevation before RF delivery. We believe these measures help to select for potential effective RF applications. Consistent with the findings relating to EGM reduction, 100% of needle RF lesions were identified using MRI. Intramural bipolar pacing did increase after ablation when feasible. All these measurements can potentially help to evaluate efficacy of lesion formation, but this has to be further investigated.

Safety of needle ablation

This animal study did not demonstrate major complications associated with needle ablation. To avoid perforation, the needle deployment did not exceed 8 mm. At apical sites, needle length was limited to 3mm. However, 4 perforations were observed, as identified by iodine contrast injection. The very small size of the needle probably explains the absence of tamponade in such situation. All pericardial contrast blushes occurred at apical needle positions. These findings suggest that RF application with the needle should be avoided or limited to less than 3 mm needle length in structurally remodeled areas with severe wall thinning. Further, in area with thinner myocardial tissue such as the left ventricular apex and right ventricular free wall, needle RF should be delivered with caution.

Two VF episodes were observed in this series, one due to needle deployment and one to RF delivery with conventional catheter. Sheep are prone to develop VF when the ventricles are targeted and this risk should probably not be extrapolated to humans.

Interestingly, in a recent feasibility study in humans, Sapp *et al* reported complications in 3/8 patients (1 tamponade and 2 heart block).[10] These findings highlight the point that the

safety of needle ablation should be further studied in larger cohorts of patients undergoing VT ablation. In this context, the integration of wall thickness maps derived from pre-procedural imaging into 3D mapping systems might be helpful to define the needle deployment length that is most appropriate for a given site.[17]

The appearance of the needle trajectory on high-density MRI and histology, could potentially raise concerns regarding fistula creation following needle ablation. Of note however in their limited clinical series Sapp *et al* did not report any clinical fistulae after a mean follow-up of 12 months. Further studies in larger cohorts of patients are necessary to fully address this question.[10]

Finally, coronary injury may remain a concern, as the lesions are often transmural. Needle ablation may not obviate the need for performing a coronary angiogram before and after ablation, Even if preliminary clinical data from Sapp *et al* did not show acute coronary syndromes more data are needed.[10]

Use of MRI to characterize ablation lesions

Our results demonstrate that both *in vivo* and *ex vivo* MRI can be used to identify RF lesions and quantify lesion size. In the current study, *in vivo* MRI was performed on a clinical scanner using a clinically available imaging protocol. This free-breathing method, initially developed to image atrial fibrosis, was chosen because of its higher spatial resolution as compared to conventional late gadolinium enhancement methods acquired during one breath-hold.[18] Using this method, lesions were depicted on all sites of needle RF application. This finding suggests both that myocardial damage is consistently observed after needle RF ablation, and that in *vivo MRI* can identify these lesions with high

sensitivity. The ability of MRI to assess acute ablation lesions is consistent with prior reports using conventional ablation in humans as well as to a recent animal study.[19, 20,21]

In the current study, we also performed ex vivo MRI on explanted hearts using a high field strength MRI system (9.4 Tesla). The rationale to add *ex vivo* MRI data was to provide structural information on ablation lesions with high spatial resolution and with minimal organ deformation. Indeed, accurate sizing of needle ablation lesions could not be directly derived from the lesion dimensions measured on gross pathology, because the shape of the lesions was highly variable, as opposed to conventional ablation lesions that can be considered as half a prolate ellipsoid. Therefore, three-dimensional segmentation was considered more robust. In addition, *ex vivo* MRI facilitated the comparison to electroanatomical map and the labeling of ablation sites because the global shape of the organ was preserved.

We believe that our MRI results illustrate the use of MRI in the post-ablation setting, either *in vivo* to document lesion formation and transmurality at the acute stage, or *ex vivo* as a surrogate for histology to overcome the issue of spatial registration with procedural data.

Limitations

The first limitation of this study is that ablation was performed in healthy tissue only. Therefore, the reported lesion size might apply to patients with non-scar related VT, but lesion formation in patients with scar-related VT should be addressed in future studies. However, scar related VT is usually associated with thinner myocardium and conventional RF is more likely to create transmural lesions. Furthermore, lesions were characterized at the acute stage, and further research is therefore required to describe the definite result of

needle RF ablation at the chronic stage. Another potential limitation is the absence of contact force in the group with conventional ablation catheters. However, although this contact force was shown to be associated with a higher rate of lesions on pathology, the size of the lesions do not seem to be improved.[13] Finally, MRI characterization was only used in the needle ablation group, given the limited availability of MRI, prolonged scanning times (>120 hours) and the fact that previous studies have reported on MRI imaging following conventional ablation, we focussed our imaging on the needle group.[19,20,21] The description of conventional ablation lesions on MRI has already been reported, and the sizing of these lesions from gross pathology measurements was shown to be similar and feasible.[21]

Conclusion

Needle RF ablation appears to be feasible and safe in the left ventricle. Lesions induced by an irrigated needle ablation catheter are more frequent, larger, deeper, and more often transmural than those induced by conventional irrigated catheters. These lesions can be qualitatively and quantitatively assessed at the acute stage with the use of *in vivo* and *ex vivo* MRI.

Acknowledgements

We would like to thank Marlène Dumond and Samantha Delmond from CIC-IT BioDiMI, Bordeaux and Lionel Couraud for the histological analysis of our specimen.

This manuscript was made possible with the following grants: ANR-10-IAHU-04 and Equipex MUSIC ANR-11-EQPX-0030.

References

1. Wissner E, Stevenson WG, Kuck KH. Catheter ablation of ventricular tachycardia in ischaemic and non-ischaemic cardiomyopathy: Where are we today? A clinical review. *European heart journal*. 2012;33:1440-1450
2. Dinov B, Fiedler L, Schonbauer R, Bollmann A, Rolf S, Piorkowski C, Hindricks G, Arya A. Outcomes in catheter ablation of ventricular tachycardia in dilated nonischemic cardiomyopathy compared with ischemic cardiomyopathy: Results from the prospective heart centre of leipzig vt (help-vt) study. *Circulation*. 2014;129:728-736
3. Tokuda M, Sobieszczyk P, Eisenhauer AC, Kojodjojo P, Inada K, Koplan BA, Michaud GF, John RM, Epstein LM, Sacher F, Stevenson WG, Tedrow UB. Transcoronary ethanol ablation for recurrent ventricular tachycardia after failed catheter ablation: An update. *Circulation. Arrhythmia and electrophysiology*. 2011;4:889-896
4. Koruth JS, Dukkipati S, Miller MA, Neuzil P, d'Avila A, Reddy VY. Bipolar irrigated radiofrequency ablation: A therapeutic option for refractory intramural atrial and ventricular tachycardia circuits. *Heart rhythm : the official journal of the Heart Rhythm Society*. 2012;9:1932-1941
5. Sacher F, Sobieszczyk P, Tedrow U, Eisenhauer AC, Field ME, Selwyn A, Raymond JM, Koplan B, Epstein LM, Stevenson WG. Transcoronary ethanol ventricular tachycardia ablation in the modern electrophysiology era. *Heart rhythm : the official journal of the Heart Rhythm Society*. 2008;5:62-68
6. Berte B, Sacher F, Mahida S, Yamashita S, Lim HS, Denis A, Derval N, Hocini M, Haissaguerre M, Cochet H, Jais P. Impact of septal radiofrequency ventricular tachycardia ablation: Insights from magnetic resonance imaging. *Circulation*. 2014;130:716-718
7. Reddy VY, Neuzil P, Taborsky M, Ruskin JN. Short-term results of substrate mapping and radiofrequency ablation of ischemic ventricular tachycardia using a saline-irrigated catheter. *Journal of the American College of Cardiology*. 2003;41:2228-2236
8. Sapp JL, Cooper JM, Soejima K, Sorrell T, Lopera G, Satti SD, Koplan BA, Epstein LM, Edelman E, Rogers C, Stevenson WG. Deep myocardial ablation lesions can be created with a retractable needle-tipped catheter. *Pacing and clinical electrophysiology : PACE*. 2004;27:594-599
9. Sapp JL, Cooper JM, Zei P, Stevenson WG. Large radiofrequency ablation lesions can be created with a retractable infusion-needle catheter. *Journal of cardiovascular electrophysiology*. 2006;17:657-661
10. Sapp JL, Beeckler C, Pike R, Parkash R, Gray CJ, Zeppenfeld K, Kuriachan V, Stevenson WG. Initial human feasibility of infusion needle catheter ablation for refractory ventricular tachycardia. *Circulation*. 2013;128:2289-2295
11. Wittkampf FH, Nakagawa H, Foresti S, Aoyama H, Jackman WM. Saline-irrigated radiofrequency ablation electrode with external cooling. *Journal of cardiovascular electrophysiology*. 2005;16:323-328
12. Sacher F, Tedrow UB, Field ME, Raymond JM, Koplan BA, Epstein LM, Stevenson WG. Ventricular tachycardia ablation: Evolution of patients and procedures over 8 years. *Circulation. Arrhythmia and electrophysiology*. 2008;1:153-161
13. Sacher F, Wright M, Derval N, Denis A, Ramoul K, Roten L, Pascale P, Bordachar P, Ritter P, Hocini M, Dos Santos P, Haissaguerre M, Jais P. Endocardial versus epicardial ventricular radiofrequency ablation: Utility of in vivo contact force assessment. *Circulation. Arrhythmia and electrophysiology*. 2013;6:144-150

14. Gonzalez-Suarez A, Trujillo M, Koruth J, d'Avila A, Berjano E. Radiofrequency cardiac ablation with catheters placed on opposing sides of the ventricular wall: Computer modelling comparing bipolar and unipolar modes. *International journal of hyperthermia : the official journal of European Society for Hyperthermic Oncology, North American Hyperthermia Group*. 2014;30:372-384
15. Teh AW, Reddy VY, Koruth JS, Miller MA, Choudry S, D'Avila A, Dukkipati SR. Bipolar radiofrequency catheter ablation for refractory ventricular outflow tract arrhythmias. *Journal of cardiovascular electrophysiology*. 2014;25:1093-1099
16. Sacher F, Derval N, Jadidi A, Scherr D, Hocini M, Haissaguerre M, Dos Santos P, Jais P. Comparison of ventricular radiofrequency lesions in sheep using standard irrigated tip catheter versus catheter ablation enabling direct visualization. *Journal of cardiovascular electrophysiology*. 2012;23:869-873
17. Komatsu Y, Cochet H, Jadidi A, Sacher F, Shah A, Derval N, Scherr D, Pascale P, Roten L, Denis A, Ramoul K, Miyazaki S, Daly M, Riffaud M, Sermesant M, Relan J, Ayache N, Kim S, Montaudon M, Laurent F, Hocini M, Haïssaguerre M, Jaïs P. Regional myocardial wall thinning at multidetector computed tomography correlates to arrhythmogenic substrate in postinfarction ventricular tachycardia: Assessment of structural and electrical substrate. *Circulation. Arrhythmia and electrophysiology*. 2013;6:342-350
18. Oakes RS, Badger TJ, Kholmovski EG, Akoum N, Burgon NS, Fish EN, Blauer JJ, Rao SN, DiBella EV, Segerson NM, Daccarett M, Windfelder J, McGann CJ, Parker D, MacLeod RS, Marrouche NF. Detection and quantification of left atrial structural remodeling with delayed-enhancement magnetic resonance imaging in patients with atrial fibrillation. *Circulation*. 2009;119:1758-1767
19. Lardo AC, McVeigh ER, Jumrussirikul P, Berger RD, Calkins H, Lima J, Halperin HR. Visualization and temporal/spatial characterization of cardiac radiofrequency ablation lesions using magnetic resonance imaging. *Circulation*. 2000;102:698-705
20. Dickfeld T, Kato R, Zviman M, Nazarian S, Dong J, Ashikaga H, Lardo AC, Berger RD, Calkins H, Halperin H. Characterization of acute and subacute radiofrequency ablation lesions with nonenhanced magnetic resonance imaging. *Heart rhythm : the official journal of the Heart Rhythm Society*. 2007;4:208-214
21. Celik H, Ramanan V, Barry J, Ghate S, Leber V, Oduneye S, Gu Y, Jamali M, Ghugre N, Stainsby JA, Shurrab M, Crystal E, Wright GA. Intrinsic contrast for characterization of acute radiofrequency ablation lesions. *Circulation. Arrhythmia and electrophysiology*. 2014;7:718-727

Table 1. Baseline characteristics

	Conventional RF	Needle RF
No of sheep	6	7
Weigth (kg)	59±9	50±5
Age (yrs)	5±1	4
Macroscopy after euthanazia	Direct: n=6	Direct: n=2, After fixation: n=5
Waiting time (s)	NA	79±23s after contrast injection
Irrigation (ml/min)	Pump flow: 24±9	Needle flow: 2 Gap flow: 1.6±0.5
Needle length (mm)	NA	6±1

Table 2. EGM and threshold measurements

	Needle RF	
No of RF applications	60	
No of threshold measurements	53	
Unipolar threshold before RF	6.2±2.9mA	
Unipolar threshold after RF	9.8±2.5mA	p<0.001
No capture >10mA before RF	2	
No capture >10mA after RF	19	p<0.001
No of EGM measurements	28	
Bipolar voltage before RF	2.7±2.7mV	
Bipolar voltage after RF	0.7±0.4mV	p<0.001
Bipolar voltage reduction	100%	

Table 3. Ablation data

	Conventional RF	Needle RF	
No of RF applications	60	60	p=NS
RF duration (s)	55±13	58±10	p=0.33
Mean power delivery (W)	30±1.8	29±5.8	p=0.39
No of lesions found	45 (75%)	54 (90%)	p<0.05
Lesion depth (mm)	5.2±2.4	9.9±2.7	p<0.001
Lesion width (mm)	5.2±1.7	8.5±2.5	p<0.001
Lesion length (mm)	7.9±2.4	8.5±2.5	p=0.33
Lesion volume (mm3)	488±384	1030±362	p<0.001
Transmural lesion (%)	17%	62.5%	p<0.01
T0s and T30s impedance (Ohms)	134±31 and 116±21	109±13 and 94±8	p<0.01

Abbreviations: RF, radiofrequency; No, number; kg, kilograms; yrs, years; s, seconds; ml, milliliters; min, minutes; mm, millimeters; T_{0s}, after zero seconds; T_{30s}, after thirty seconds; p, p-value.

Figure legends.

Fig.1 Fluoroscopic image and EGM recording of a needle ablation procedure.

A. Irrigated needle catheter with extracted needle (white circle) inside the myocardium using retrograde aortic access. Another bipolar diagnostic catheter is positioned in the IVC for unipolar needle tip recording. **B.** Intramyocardial contrast staining (white outline) after injection of 1cc Omnipaque contrast trough the needle tip. No contrast perfusion into the pericardial space. **C.** BARD EP recordings: the first 3 lines are three different ECG derivations, the second 2 lines are bipolar recordings between the needle tip and ring electrode and the last 2 lines are unipolar recordings of the needle tip and the ring electrode. **Upper panel**: Sinus rhythm. Before ablation, a bipolar voltage of 3.16mV was measured. An R wave was observed on the unipolar recording before the application. **Middle panel**: An ST elevation was seen on the unipolar recordings during contrast injection. Often, PVC are seen, when the needle enters the myocardium. **Lower panel**: Sinus rhythm with multiple PVC. After ablation, 1.5mV bipolar voltage was measured. A QS pattern on the unipolar recording was seen after the application.

Fig.2 Comparison between conventional and needle lesions.

Left panel -Conventional RF. *Top.* Example of an endocardial transmural lesion at the LV apex. *Bottom.* Conventional lesions were only transmural at the apical sites. Other endocardial lesions are not transmural and smaller than the needle equivalent. **Right panel -**Needle RF. *Top.* A large and transmural lesion is observed. *Bottom.* Other endocardial lesions created with the needle catheter.

Fig.3 Macroscopic, histological and MRI comparison of the same needle RF lesion.

A. Histological analysis with a visible needle trajectory (arrow). No fibrosis is observed in the acute phase. **B.** Macroscopic evaluation of the same needle RF lesion with a 2mm gap towards the epicardium. These gaps (1-2mm) are often seen on purpose, to avoid complications of needle perforation, without information on local wall thickness. The needle trajectory is also macroscopically visible (arrow) **C.** High density ex vivo (9.4T) MRI image -short axis plane- of the same needle lesion with visualisation of the needle trajectory (arrow).

Fig.4 Comparison of acute needle RF lesions using in vivo and ex vivo MRI.

Visualization of acute lesions induced by the needle catheter on in vivo late gadolinium enhanced MRI at 1.5T and ex vivo high resolution MRI at 9.4T. A first animal is shown on the top row, a second on the bottom row. In vivo MRI data are shown on the left column, ex vivo MRI data on the right column. 2 lesions are visible in each animal. On in vivo MRI (inversion-recovery prepared 3DFLASH sequence with 1.25x1.25x2.5mm voxel size), lesions appear as bright peripheral enhancement surrounding a dark core, consistent with coagulative necrosis. On ex vivo MRI (3D FLASH sequence with 80x80x235µm voxel size), lesions appear as dark peripheral halo consistent with haemorrhagic tissue, surrounding a heterogeneous core.

Fig.5 Examples of needle RF lesions visualized by high density ex-vivo MRI.

The needle lesions are clearly visible (arrows) as a dark sphere, surrounded by a halo. In some lesions, we can appreciate the needle trajectory. All lesions are performed in the endocardium of the left ventricle.

Fig.6 Two examples of needle RF lesions visualized by histological analysis (Masson's Thrichrome staining). *From left to right.* **Upper panel:** The needle trajectory is sometimes visible on the coupes (arrow) with "boiled" appearance of the fibers. *Center of the lesion.* Hyper contracted muscle fibers (arrow) with fragmented sarcoplasm's. *Lesion borderzone.* Laquer coloured sarcoplasms (arrow) of less contracted muscle fibers. **Lower panel:** *Center of the lesion.* Degenerated Purkinje fibers (arrow). *Lesion borderzone.* Less contracted and degenerated muscle fibers (arrow).

Figure 1. Fluoroscopic and EGM image of a needle RF application.

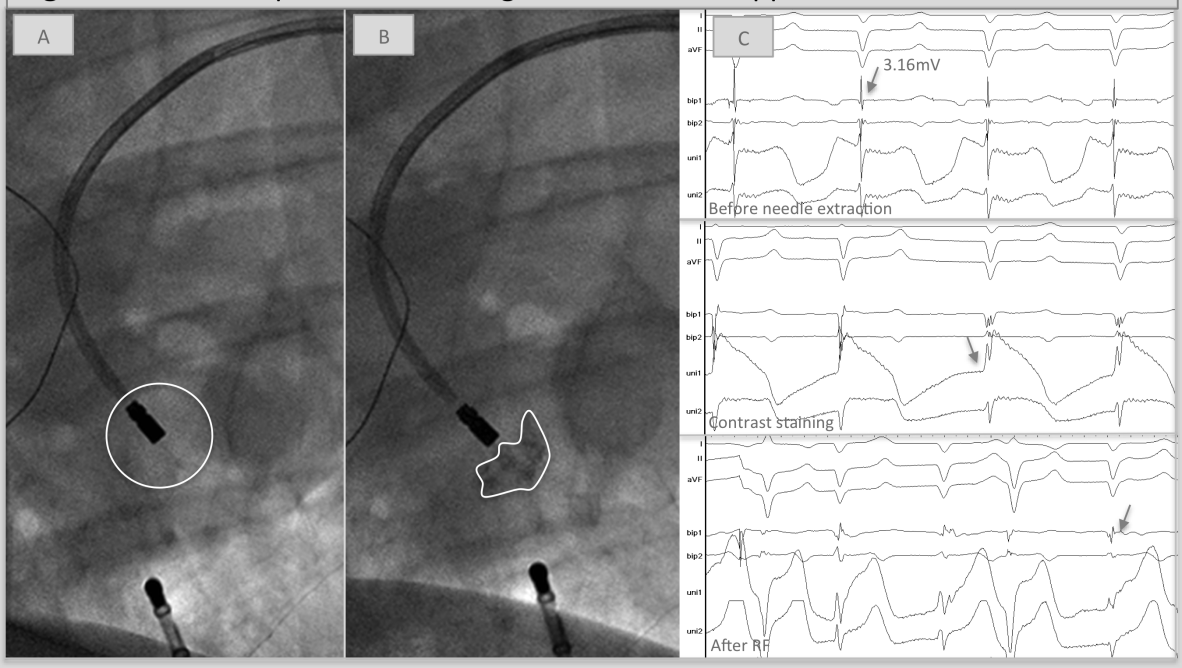

Figure 2. Macroscopic lesion comparison

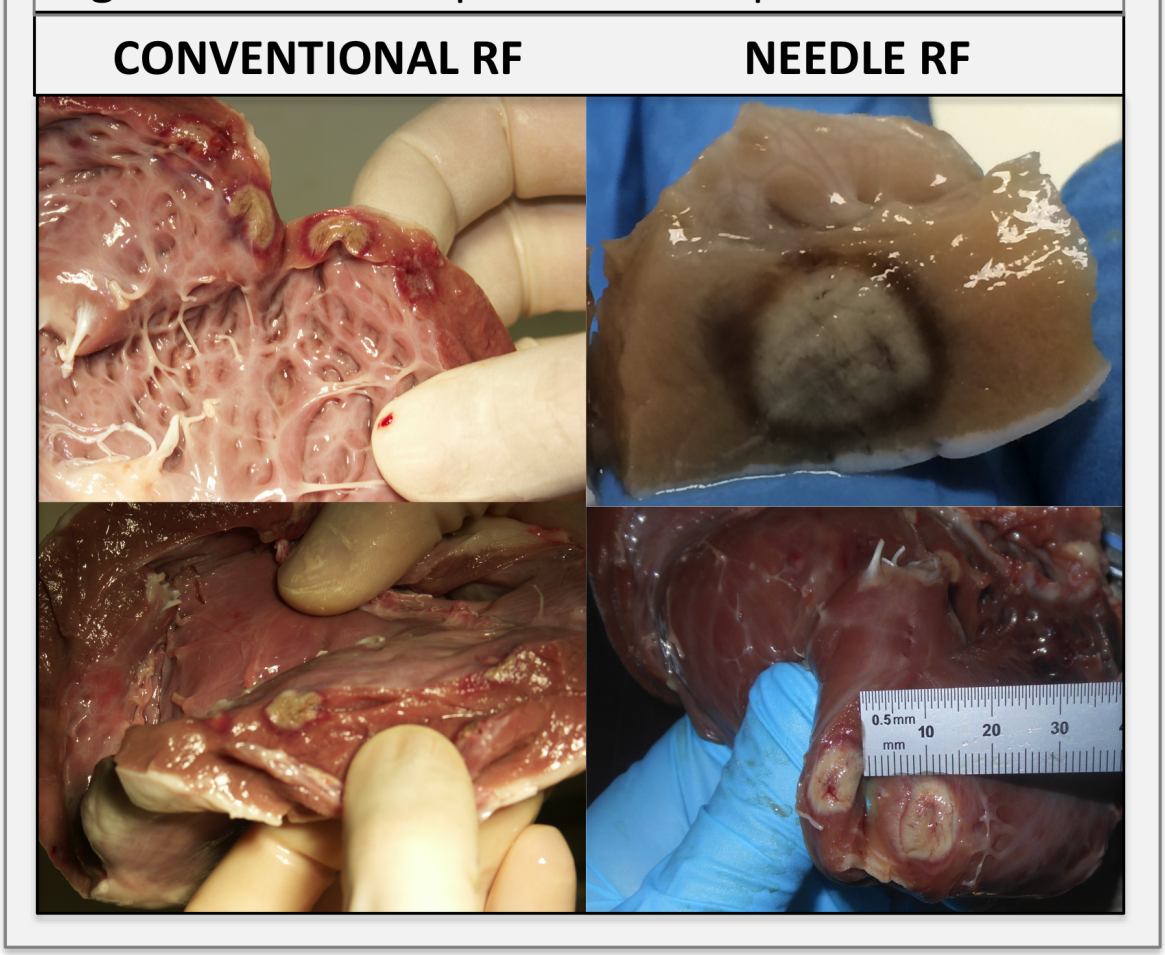

Figure 3. Acute results of needle RF lesions comparing in vivo and ex vivo MRI

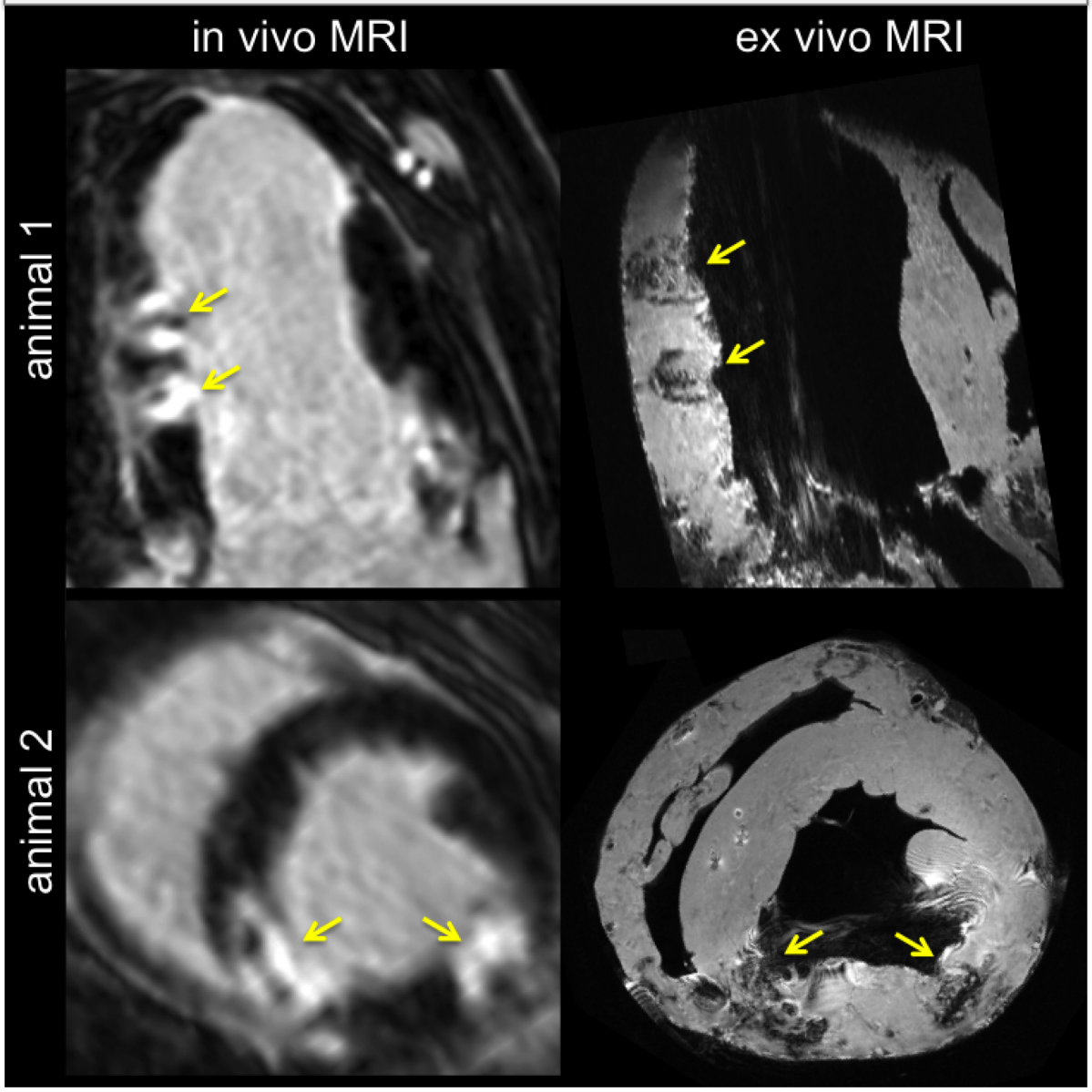

Figure 4. Different examples of needle RF lesions using ex vivo MRI.

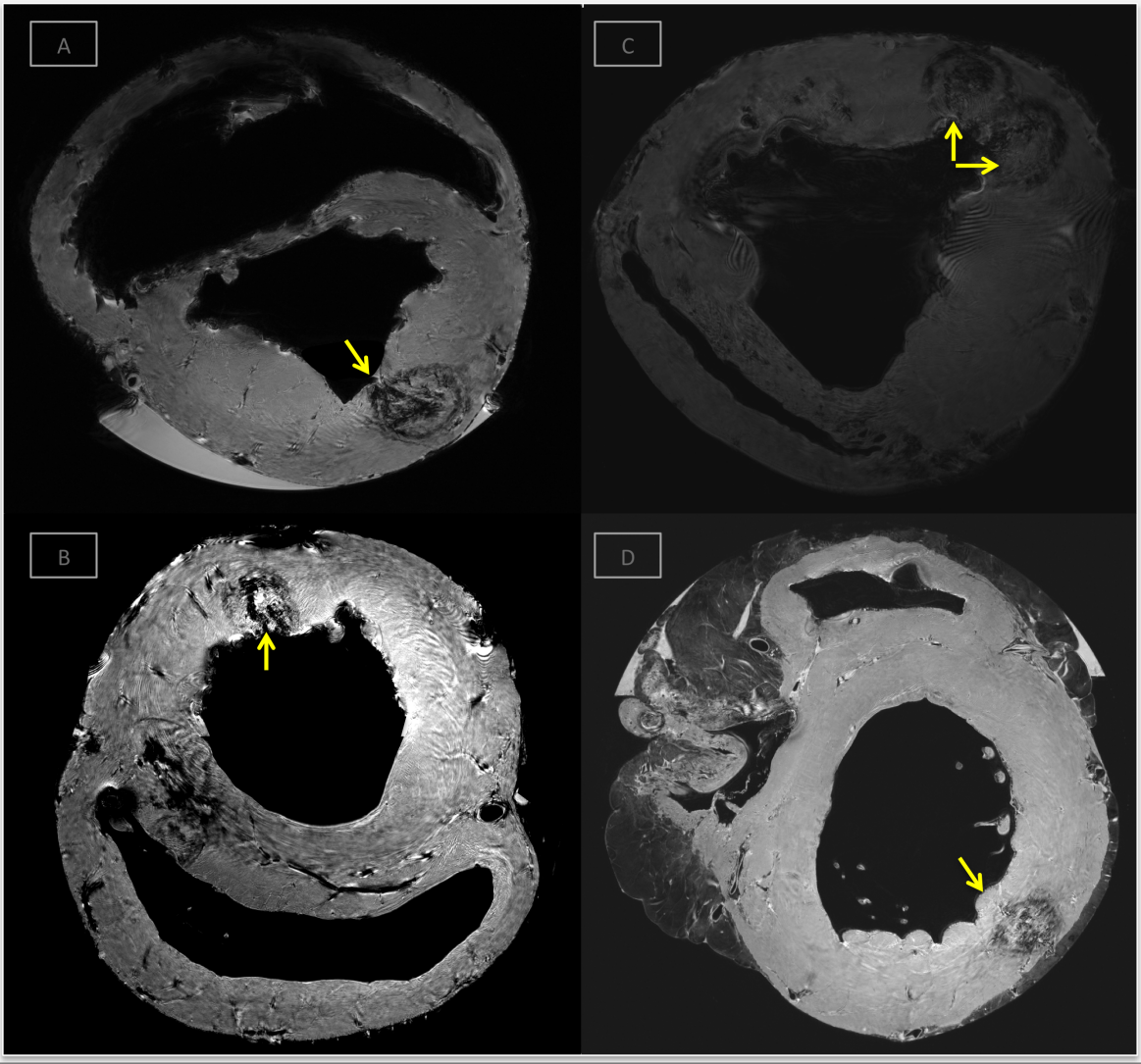

Figure 5. Histologic, macroscopic and MRI comparison of the same needle RF lesion

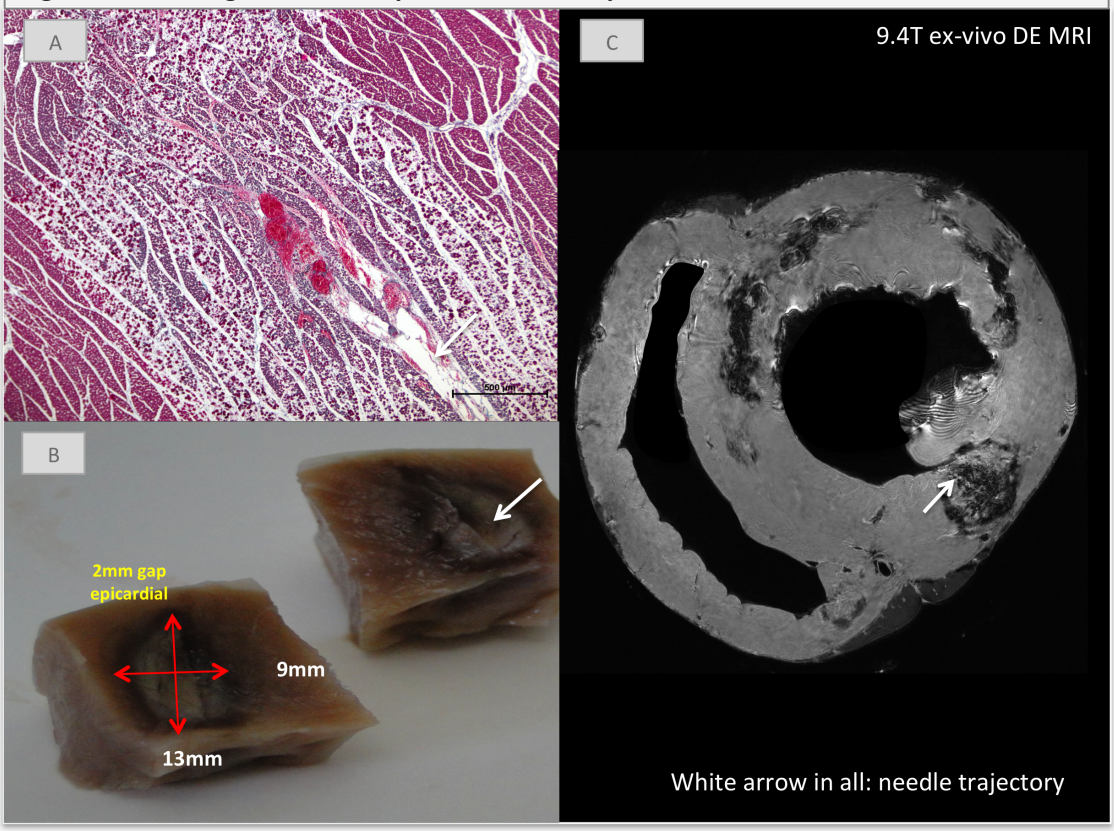

Figure. 6 Examples of histological analysis of needle RF lesions (Thrichrome Masson staining)

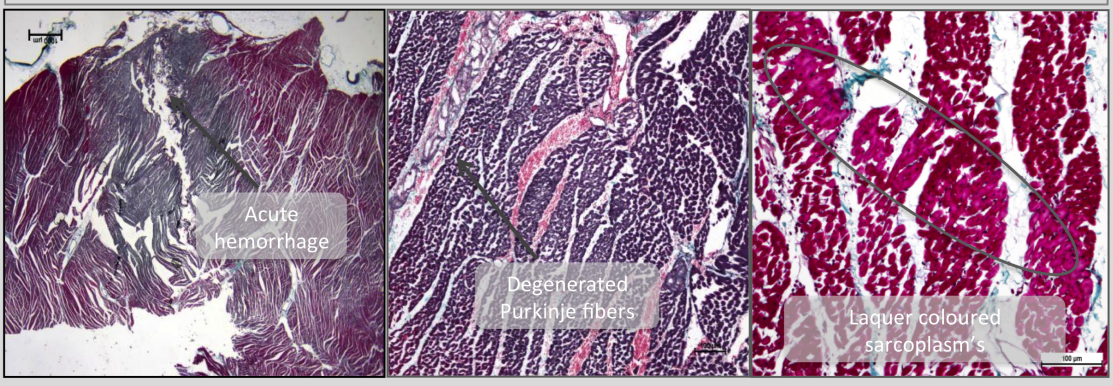

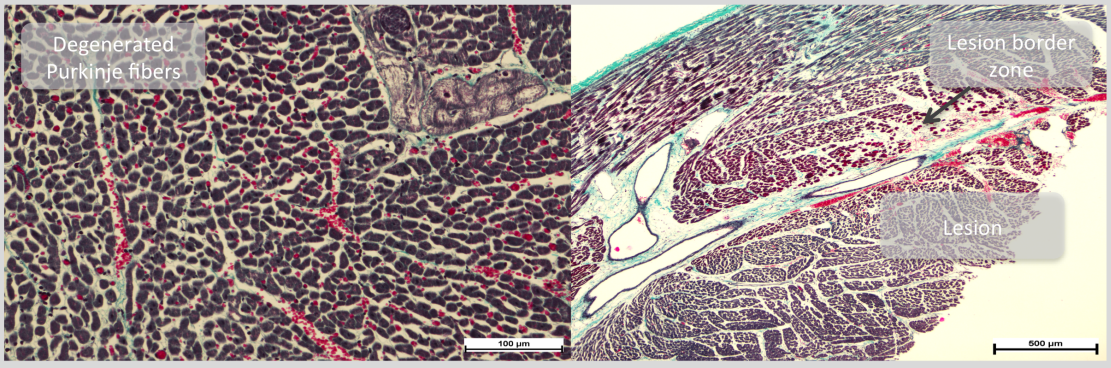

SUPPLEMENTARY MATERIALS

Figure legend

Supplementary Figure 1: Two examples of epicardial needle ablations using an open-chest approach.

Two ex-vivo freshly explanted sheep hearts after epicardial needle ablation (4 lesions in Figure A and 4 lesions in Figure B). Access was obtained by a surgical sternotomy. Saline infusion into the pericardial sac was performed (under hemodynamic monitoring) to ensure constant covering by saline of the needle tip during ablation.

A. The results of 4 needle ablation lesions are shown here. Power was increased in steps of 5 Watts (20-25-30-35 Watts) from left to right (yellow arrow) during 60sec ablation duration and fixed gap and needle irrigation rate at 2ml/min. Lesion size increased from left to right from 6mm depth and 5mm width to 10mm depth and 9mm width.

B. The results of 4 needle ablation lesions are shown here. Power was delivered at 35 Watts and fixed needle irrigation rate at 2ml/min. Ablation duration and gap flow rate was increased from left to right (yellow arrow). RF energy for the first two lesions was delivered during 30 seconds and RF energy was delivered during 60 seconds for the last two lesions. Gap flow rate was 1ml/min for lesion 1 and 3 and 2ml/min for lesion 2 and 4. Lesion depth for all lesions was constant at 10±1mm but lesion width increased from 4mm to 8mm.

Supplementary Figure 1. Two examples of epicardial needle ablations using an open-chest approach.

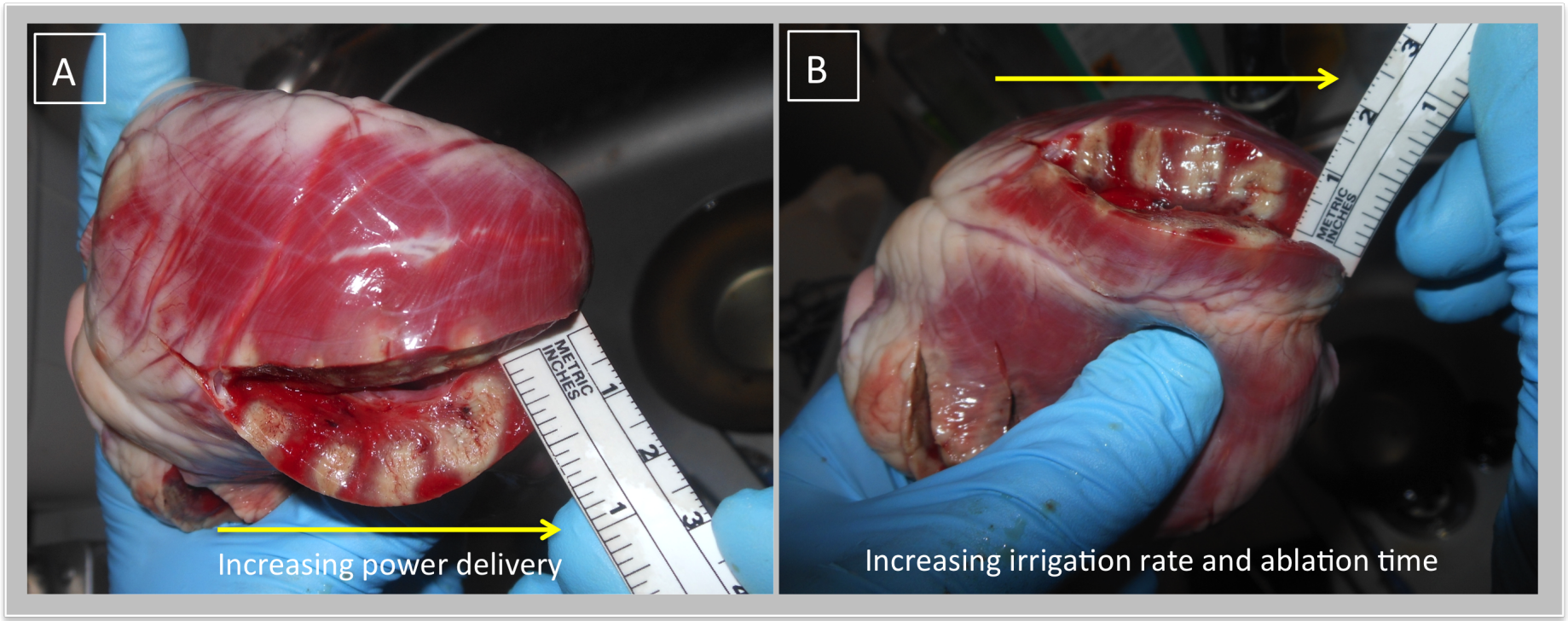

C. *Bipolar ablation:* Impact of septal radiofrequency ventricular tachycardia ablation: insights from magnetic resonance imaging.

Berte B, Sacher F, Mahida S, Yamashita S, Lim HS, Denis A, Derval N, Hocini M, Haïssaguerre M, Cochet H, Jaïs P. Circulation. 2014 Aug 19;130(8):716-8.

1. Study outline

In this case report, we discuss the case of a young female patient with an intraseptal VT focus. She was referred to our insitution following five failed VT ablation attempts. It was then decided to perform bipolar RF ablation from both sides of the ventricular septum, using steerable sheaths (Agilis, St Jude Medical) and 2 conventional non-NAV irrigated ablation catheters (Thermocool, Biosense Webster). After this procedure, the patient did not have any recurrence of VT, is free of AAD and regained her quality of life. DE-MRI imaging was performed initially before any ablation, after the five procedures, a day after the steam pop, one month later (dissapearance of the results of the steam pop) and finally after the bipolar ablation.

2. Implications

Bipolar ablation is promising and effective for the treatment of intramural VT but limited data is available for bipolar ablation. Human studies are mostly restricted to small case series: data of bipolar ablation performed for RVOT VT, septal VT and free wall VT are found with short term success ratios varying from 50 to 75%.[59, 100, 101]

This case report with multiple state-of-the art MRI images, provides a unique insight into the utility of imaging to evaluate results, complications and transmurality.

3. Manuscript

Impact of Septal Radiofrequency Ventricular Tachycardia Ablation

Insights From Magnetic Resonance Imaging

Benjamin Berte, MD; Frederic Sacher, MD, PhD; Saagar Mahida, MD, PhD; Seigo Yamashita, MD, PhD; Han S. Lim, MBBS; Arnaud Denis, MD; Nicolas Derval, MD; Mélèze Hocini, MD; Michel Haïssaguerre, MD, PhD; Hubert Cochet, MD, PhD; Pierre Jaïs, MD, PhD

We present the case of a 38-year-old woman with no past medical history and structurally normal heart with recurrent drug-refractory septal ventricular tachycardia (VT). Despite treatment with flecainide, celiprolol, and sotalol, she experienced breakthrough episodes of VT (Figure 1B). She had undergone 5 failed attempts at VT ablation. She was therefore referred for a further attempt at ablation. Cardiac multidetector computed tomography and late gadolinium enhancement (LGE) MRI were performed before VT ablation. MRI demonstrated nontransmural subendocardial LGE on either side of the septum, which corresponded to previous ablation sites (Figure 2A, Movie I in the online-only Data Supplement).

Consecutive Unipolar Ablation Procedures

Given the multiple failed attempts of endocardial ablation, we used a simultaneous endocardial and epicardial approach. VT was not inducible despite the use of isoproterenol and atropine. The ablation site was then targeted based on substrate mapping and pacemapping. Epicardial mapping did not show any abnormal voltage areas, and pacemap did not match the VT morphology. Endocardial mapping was then performed and radiofrequency energy was delivered at sites with good pacemaps (40 W, Thermocool Smarttouch, Biosense Webster) on the left and right ventricular midseptum. Radiofrequency delivery (40 W, 15*g* of contact force) at the right ventricular septum resulted in a steam pop after 34 seconds. A postprocedural MRI demonstrated the presence of a septal intramural hematoma without transmural scar (Figure 2B).

Bipolar Ablation Procedure

Because of VT recurrence, she was referred for a seventh attempt at ablation. Preprocedural MRI demonstrated resolution of the intramural hematoma and persistence of the nontransmural lesions (Figure 2C). During the procedure, VT was not inducible. Bipolar ablation was then performed at the optimal pacemap site, between left and right ventricular septum (Figure 3). The 2 catheters (Thermocool) were connected to the dual-catheter ablation box (Stockert, not CE marked). We delivered up to 60 W between both distal tips with close monitoring of temperature and impedance for 120 seconds. On day 1 postablation, MRI demonstrated myocardial swelling and transmural heterogeneous midseptal LGE (Figure 4A). Three months later, she was free of VT without any antiarrhythmic therapy. MRI demonstrated septal wall thinning and transmural LGE (Figure 4B).

Discussion

This case illustrates how MRI can offer new insights into scar formation after unipolar ablation, steam pop, and bipolar ablation. In the present case, before the first ablation, the transmurality of scar was minimal, despite repeated procedures. After steam pop, MRI demonstrated an intramural hematoma that disappeared at 3 months, with no significant impact on scar transmurality. After bipolar ablation, the acute LGE observed could also be related to an edematous response to ablation. However, MRI at 3 months clearly indicated a permanent septal lesion. First, LGE appears homogeneous and intense and is associated with wall thinning and akinesia (Movie II in the online-only Data Supplement), which indicates the absence of myocyte viability. Second, myocardial perfusion appears severely compromised, indicating microvascular necrosis (Figure 4B). Finally, a quantitative approach was applied by using T1 mapping before and after gadolinium administration. In the present case, the calculated extracellular volume fraction was 85% in the midseptum, indicating an extremely dense scar (Figure 4B). Further studies are desirable to better define the prognostic value of these structural and functional MRI measurements after VT ablation.

Sources of Funding

Dr Berte is supported by an educational European Heart Rhythm Association grant. The study is funded by an Equipex MUSIC ANR-11-EQPX-0030 and an IHU LIRYC ANR-10-IAHU-04 grant.

Disclosures

Drs Jaïs, Haïssaguerre, Hocini, and Sacher have received lecture fees from Biosense Webster and St. Jude Medical. The other authors report no conflicts.

From the Hôpital Cardiologique du Haut-L'évêque, l'Université Victor Segalen Bordeaux II, Institut LYRIC, Bordeaux, France.

The online-only Data Supplement is available with this article at http://circ.ahajournals.org/lookup/suppl/doi:10.1161/CIRCULATIONAHA.114.010175/-/DC1.

Correspondence to Benjamin Berte, MD, Hôpital Cardiologique du Haut L'évêque, Avenue de Magellan, 33604 Bordeaux-Pessac, France. E-mail Bertebenjamin@hotmail.com

(*Circulation*. 2014;130:716-718.)

***Circulation* is available at http://circ.ahajournals.org** **DOI: 10.1161/CIRCULATIONAHA.114.010175**

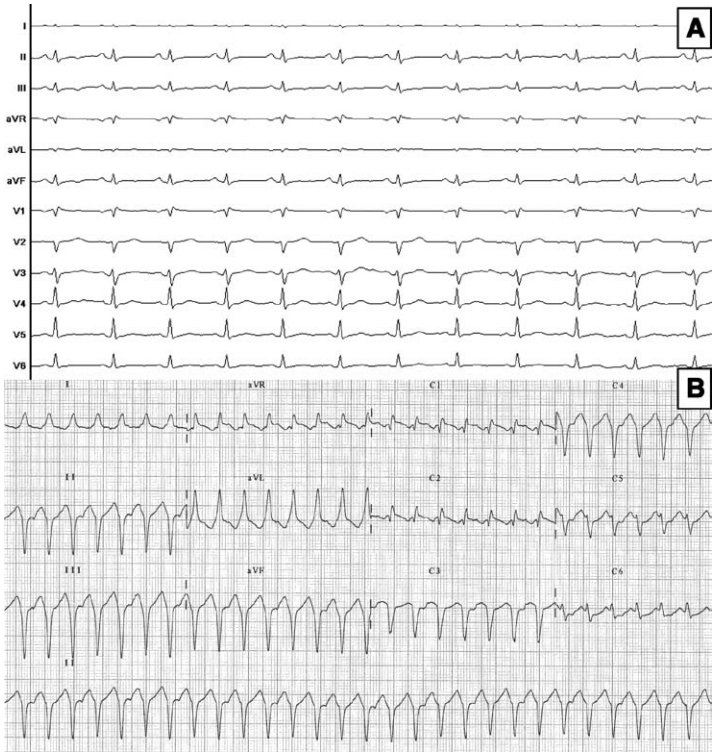

Figure 1. Twelve-lead ECG of sinus rhythm and clinical tachycardia. **A,** Sinus rhythm. **B,** Ventricular tachycardia with left superior axis, relatively small QRS, and a transition around V3.

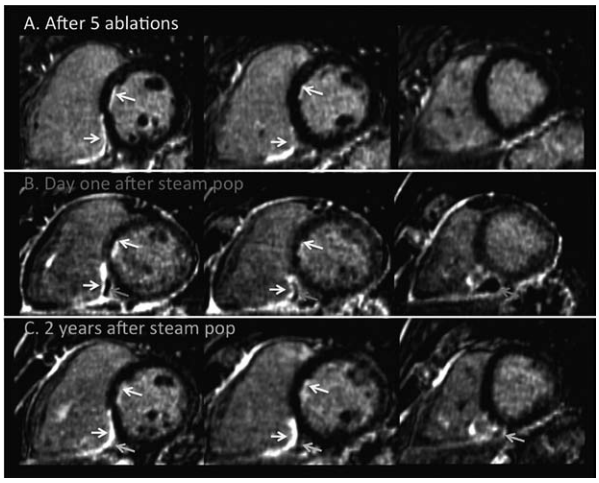

Figure 2. MRI data before and after sixth ablation procedure. **A,** LGE images acquired on the day before the procedure show subendocardial enhancement related to a nontransmural scar from previous ablations, on both sides of the interventricular septum and on the inferior RV wall (yellow arrows). **B,** LGE images acquired on day 1 after the procedure show an intramural hematoma in the septum at the site of steam pop (pink arrows). Images also show pericardial enhancement related to an inflammatory response to pericardial access during the procedure, but no pericardial bleeding. **C,** LGE images 2 years after the procedure show a complete resolution of the hematoma (blue arrows), and the persistence of a nontransmural scar on both sides of the septum. LGE indicates late gadolinium enhancement; and RV, right ventricular.

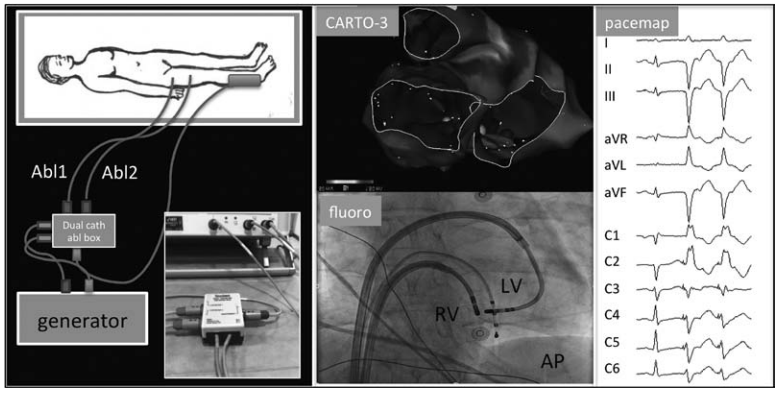

Figure 3. Bipolar ablation. **Left,** illustration of the procedure setup. Two ablation catheters are connected to a dual-catheter ablation box to deliver radiofrequency on both sides of the septum at the power of 30 to 60 watts over 120 seconds, with close monitoring of the temperature and impedance. **Middle,** superior view of the EAM substrate map without bipolar low-voltage area and fluoroscopic AP view showing catheter tips on both sides of the interventricular septum. **Right,** Pacemap from the tip of the LV ablation catheter on the ablation site: 12-lead ECG of a sinus beat and 2 paced beats with a good pacemap. AP indicates anteroposterior; EAM, epicardial electroanatomical mapping; and LV, left ventricular.

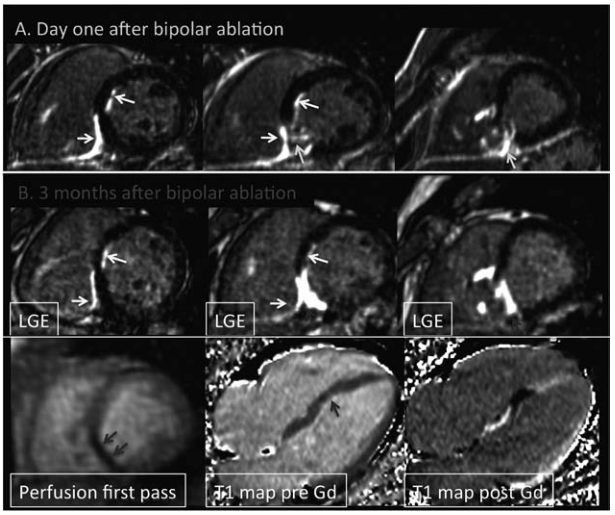

Figure 4. MRI data after bipolar ablation (seventh procedure). **A,** LGE images on day 1 after bipolar ablation show myocardial swelling and transmural heterogeneous enhancement on the interventricular septum at the midventricular and apical levels (green arrows). **B,** LGE images 3 months after bipolar ablation show myocardial thinning and intense transmural enhancement on the interventricular septum (**top,** blue arrows). First-pass perfusion imaging demonstrates severe microvascular dysfunction in the same area (**bottom left,** blue arrows). Myocardial T1 mapping before and after gadolinium administration indicates very dense scarring, with a calculated extracellular volume fraction of 85% (**bottom center** and **bottom right,** blue arrows). LGE indicates late gadolinium enhancement.

D. Ethanol ablation: A case of incessant VT from an intramural septal focus: ethanol or bipolar ablation?

Accepted for publication in Heart Rhythm Case Reports.

1. Study outline

This is another example of an intraseptal focus in an 81-year old patient. The patient had prior CABG and presented with an incessant monomorphic VT (408ms) with septal LVOT morphology. Mapping from all adjacent sites was performed and an intramural focus was suspected. Conventional RF delivery had a very late effect on the arrhythmia. These findings were indicative of a deeper arrhythmogenic focus. This case report highlights the value of an individually selected technique in case of an intramural focus. The patients' left main was protected by his prior CABG, the focus was quite close to the main conduction system and both led to the choice for ethanol over bipolar ablation.

2. Implications

Ethanol ablation is a well-known effective treatment strategy after failed RF attempt demonstrated. Long term VT free survival following ethanol ablation has been reported to be 67% at 24 months follow-up.[60, 61] In case of an intramural or septal focus, it is important to choose the appropriate strategy for the individual patient: ethanol, or bipolar ablation and probably needle ablation in the near future, based on specific advantages and disadvantages of each individual technique.

3. Manuscript

A case of incessant VT from an intramural septal focus: Ethanol or bipolar ablation?

Benjamin Berte, MD, Nicolas Derval, MD, Frederic Sacher, MD, PhD, Seigo Yamashita, MD, PhD, Michel Haïssaguerre, MD, PhD, Pïerre Jaïs, MD, PhD

From the Hôpital Cardiologique du Haut-Lévêque, Université de Bordeaux, LIRYC Institute, Bordeaux, France.

Introduction

Substrate-based radiofrequency (RF) ablation of scar-related ventricular tachycardia (VT) has become standard practice, often in addition to an intracardiac cardioverter-defibrillator.[1,2] VT procedures without identified substrate are particularly challenging cases, especially when VT is non-inducible.[3–6]

An intramural focus is often challenging to ablate using conventional RF ablation,[7] and different options are or will be possible such as high-power unipolar ablation, bipolar ablation, irrigated needle ablation, or selective coronary ethanol injection.[8–11]

The following case is used to illustrate a patient-tailored approach to choose between bipolar and ethanol ablation after a failed RF attempt, since needle ablation is not approved yet for human use.

Case report

We present the case of an 81-year-old man with an ischemic cardiomyopathy (decreased left ventricular ejection fraction of 30%) with 3-vessel disease, treated with coronary bypass surgery in 2004, and carrier of a dual-chamber pacemaker since 2002. The patient was in permanent atrial fibrillation with slow ventricular response. He entered the laboratory in incessant monomorphic VT (tachycardia cycle of 408 ms) for a procedure planned under local anesthesia and sedation. According to the baseline electrocardiographic characteristics, the ablation site was expected in the left ventricular outflow tract (LVOT) (compare the morphology of the VT with an inferior axis and a QS pattern in lead V_1 in Figure 1). The procedure was performed using a 4-mm irrigated catheter (ThermoCool SF, Biosense Webster, Inc, Diamond Bar, CA) with a 3-dimensional electroanatomic mapping system (CARTO3, Biosense Webster, Inc), based on the earliest local activation, a 12/12 pace map, a QS pattern on the unipolar recording, and a presystolic electrogram signal before the initiating premature ventricular contraction (PVC) (Figure 2). Since the monomorphic tachycardia was well tolerated, entrainment attempts were performed but each attempt stopped the tachycardia. Ablation till 40 W in the septal LVOT region was only partially successful after a prolonged ablation time of 137 seconds with only transient suppression of the VT episodes during ablation, indicating a deep intramyocardial focus. Further activation mapping was performed: The great cardiac vein showed late activation, compared with the onset of the triggering PVC. Then, the aortic cusps were mapped and finally the right ventricular outflow tract (RVOT) was mapped. Ablation was performed on the opposing site of the LVOT at 40 W, and VT episodes shortened and disappeared during RF delivery, but quickly came back after ablation. Since an intramural septal focus was expected as a result of deductive extensive mapping in all surrounding chambers (left ventricle, right ventricle, and great cardiac vein; Figure 3), the question was—after 13 minutes of LVOT ablation and 3 minutes of RVOT ablation—whether to selectively inject ethanol into a distal coronary branch or to perform bipolar ablation.

In this particular patient, we chose to use ethanol ablation because of the reversible effect and the possibility to evaluate the effect of iced saline in incessant VT. A coronary angiogram was made, and a distal branch of the second septal perforator was selected for cannulation. The local unipolar recording of the guidewire shows an early activation (−24 ms) at this site with a QS pattern (Figure 3, point 5, lower panel). A reversible challenge with 1.5-cm^3 sterile cold saline was performed after intracoronary balloon inflation and clearly affected VT episodes: directly after the injection, VT accelerated to finally terminate after 30 seconds (Figure 4). Ethanol (1.5 cm^3) was injected, and the patient was monitored. Directly after the injection,

KEYWORDS Ventricular tachycardia; Intramural focus; Ethanol ablation; Bipolar ablation

ABBREVIATIONS LVOT = left ventricular outflow tract; **PVC** = premature ventricular contraction; **RF** = radiofrequency; **RVOT** = right ventricular outflow tract; **VT** = ventricular tachycardia

(Heart Rhythm Case Reports 2015;1:89–94)

Dr Berte has received an educational European Heart Rhythm Association grant. Dr Jaïs, Dr Haïssaguerre, Dr Derval, and Dr Sacher have received lecture fees from Biosense Webster and St Jude Medical. **Address reprint requests and correspondence:** Dr Pierre Jaïs, Hôpital Cardiologique du Haut-Lévêque, Université de Bordeaux, LIRYC Institute, Bordeaux-Pessac 33604, France. E-mail address: pierre.jais@chu-bordeaux.fr.

http://dx.doi.org/10.1016/j.hrcr.2015.01.010

KEY TEACHING POINTS

- An intramural focus is often challenging to ablate using conventional radiofrequency ablation—since conventional ablation strategies often fail to obtain transmural lesion formation—and different options are or will be possible such as high-power unipolar ablation, bipolar ablation, irrigated needle ablation, or selective coronary ethanol injection.
- A patient-tailored approach between bipolar ablation and ethanol ablation after a previous failed radiofrequency attempt should be used on the basis of (dis)advantages of both strategies.
- Bipolar ablation is powerful, but it lacks the ability to identify the intramural activation time of the local electrogram and is irreversible, which is more dangerous close to the main conduction system.
- Intracoronary ethanol ablation preceded by injection of iced saline can be used as a reversible challenge and for the evaluation of the effect when applied during ventricular tachycardia. Ethanol ablation is limited by the anatomy of the coronary artery system and can be guided by the QS morphology and precocity of the unipolar local electrogram to choose the best distal branch.

shortening of the episodes to triplets and single PVCs occurred before the complete disappearance of VT episodes. Afterward, no PVC or VT was observed and no VT was inducible. After the procedure, the patient was informed about future possible therapeutic options and the patient renounced a possible upgrade to intracardiac cardioverter-defibrillator therapy. Troponine I levels raised to a peak value of 3.26 ng/mL 24 hours after the ethanol injection and declined rapidly. At 9-month follow-up, no new episodes of sustained or nonsustained VT were detected on his dual-chamber pacemaker.

Discussion

VT ablation of an intramural septal focus is particularly challenging, since conventional ablation strategies often fail to obtain transmural lesion formation. Different ablation techniques to create possible larger and (more) transmural lesions are shown in Figure 5.

In this case, we could clearly influence the exit site with conventional ablation (VT morphology), but we encountered an inability to penetrate in the true intramural focus. This explains why ablation was partially successful at the septal LVOT site (pace-map match of exit site) since episodes shortened, and shortly disappeared, but recurrence was quickly seen after the termination of RF.

In the case series of Sacher et al[10] and the update of Tokuda et al,[12] the transcoronary ethanol VT ablation technique performed after a failed RF attempt was demonstrated to be effective with a long-term VT-free survival in 67% at 24-month follow-up. Less data are available for bipolar ablation in human use and mostly small case series or case reports: data of bipolar ablation performed for RVOT, septal VT, and free-wall VT are found with short-term success ratios varying from 50% to 75%.[9,11,13] In addition, the bipolar ablation technique was found to be more effective than unipolar ablation in a computational model, except in the situation of the epicardial catheter tip surrounded by air or placed over a fat tissue layer.[14]

The aim of this case report was not to present ethanol ablation as a novel technique—since this technique exists since 1987, and already became a validated method—but to explain how to take a patient-tailored approach between bipolar ablation and ethanol ablation after a previous failed RF attempt on the basis of the (dis)advantages of both strategies that are listed in Table 1.

In this case, the focus was expected to be quite basal, close to the main conduction system. Bipolar ablation is powerful, but it lacks the ability to identify the intramural activation time of the local electrogram and is irreversible, which is more dangerous close to the main conduction system. The main disadvantage of bipolar ablation is the lack of catheter tip visualization with current mapping systems and the irreversibility of the effect. Accurate position of both catheters at the correct opposing sites based on different fluoroscopic angles alone can be challenging. Nowadays, one has to change the NAV catheter (magnetic visualization on CARTO3, Biosense Webster, Inc) version for 2 standard ablation catheters, which significantly increases the cost of the procedure and suppresses the contact force and vector orientation of the tip, both often valuable to evaluate septal contact. Since this leads to loss of all information of the mapping system, no distance measurement between the 2 catheter tips is possible. Ideally, the smallest distance between both tips would be looked for.

Ethanol ablation—initially used as a chemical method to perform septal myectomy in hypertrophic cardiomyopathy—is limited by the anatomy of the coronary artery system and most often used in septal perforators of the left anterior descending and distal branches of the left circumflex artery.[10] It can be guided by the QS morphology and precocity of the unipolar local electrogram to choose the best distal coronary branch, and injection of iced saline can be used as a reversible challenge and for the evaluation of the effect (possible effect on the conduction system and termination of the VT when applied during VT) before ethanol injection.[15] Probably, the history of coronary artery bypass graft and having a left main trunk protected by a functional bypass is also important since there is always the risk of having an ethanol leak and thrombosis of the left main trunk. These arguments led to the decision to perform ethanol ablation in this patient.

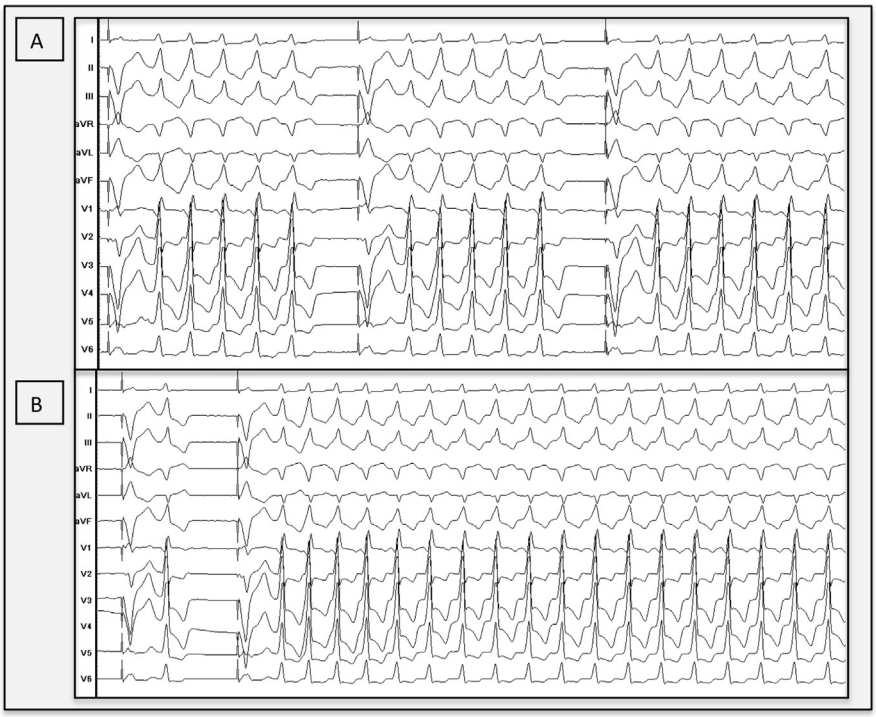

Figure 1 Clinical ventricular tachycardia. **A:** Monomorphic clinical ventricular tachycardia (tachycardia cycle length 408 ms) with inferior axis and QS morphology in lead V_1, suggesting an exit site at the aortomitral continuity. The patient is in permanent atrial fibrillation. **B:** In the electrophysiology laboratory, we observed poorly tolerated sustained ventricular tachycardia episodes.

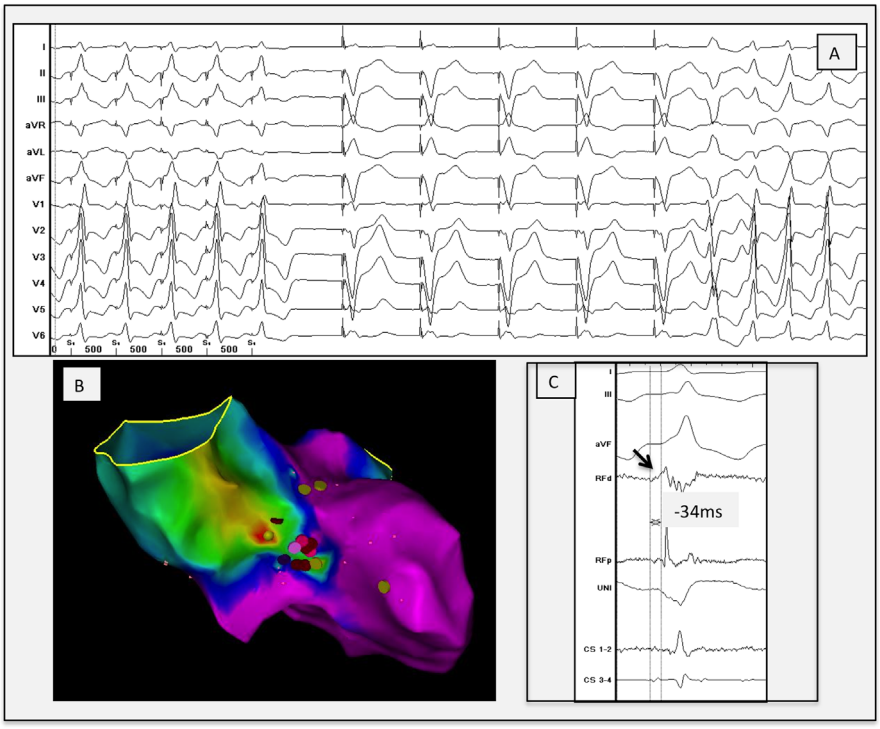

Figure 2 **A** Perfect local pace map (first 5 paced beats) at the septal left ventricular outflow tract site illustrating a 12/12 pace-map match with the initiating premature ventricular contraction, followed by 5 paced beats from the right ventricular apex (device) followed by the initiating premature ventricular contraction and the clinical ventricular tachycardia. **B:** Anteroposterior view of the local activation map made by the CARTO3, demonstrating earliest activation (focal red spot) at the aortomitral continuity. **C:** Local electrogram at the ablation site, showing a low-voltage sharp electrogram 34 ms before QRS onset of the clinical ventricular tachycardia and an isoelectric phase followed by a QS morphology on the unipolar. CS = coronary sinus; d = distal; p = proximal; RF = radiofrequency; UNI = unipolar recording.

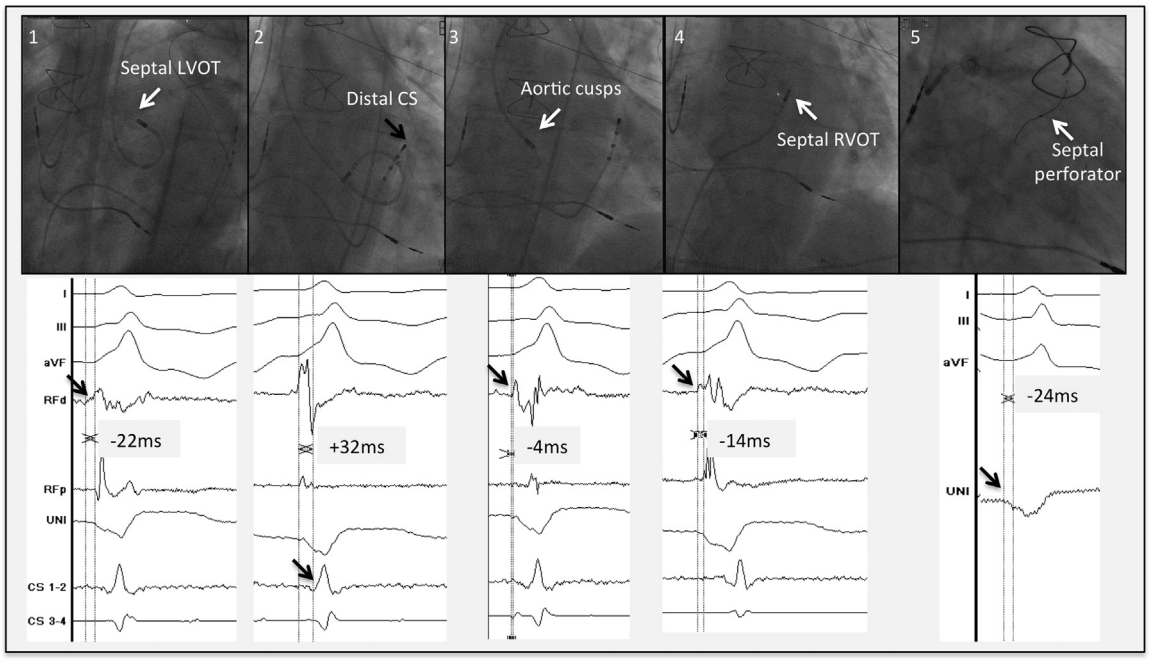

Figure 3 Different regions are mapped in the outflow tract region: 1. Septal LVOT: small presystolic sharp signal at −22 ms from the onset of the QRS. 2. Great cardiac vein: local signal at +32 ms from the onset of the QRS. 3. Aortic cusps: presystolic local signal −4 ms from the onset of the QRS. 4. RVOT: local electrogram at −14 ms compared with the onset of the QRS. 5. Intraseptal: the unipolar signal of the guidewire shows a QS signal slightly before (±24 ms) the onset of the QRS. The exact onset of the unipolar signal was not easy to define in this case. CS = coronary sinus; d = distal; LVOT = left ventricular outflow tract; p = proximal; RF = radiofrequency; RVOT = right ventricular outflow tract.

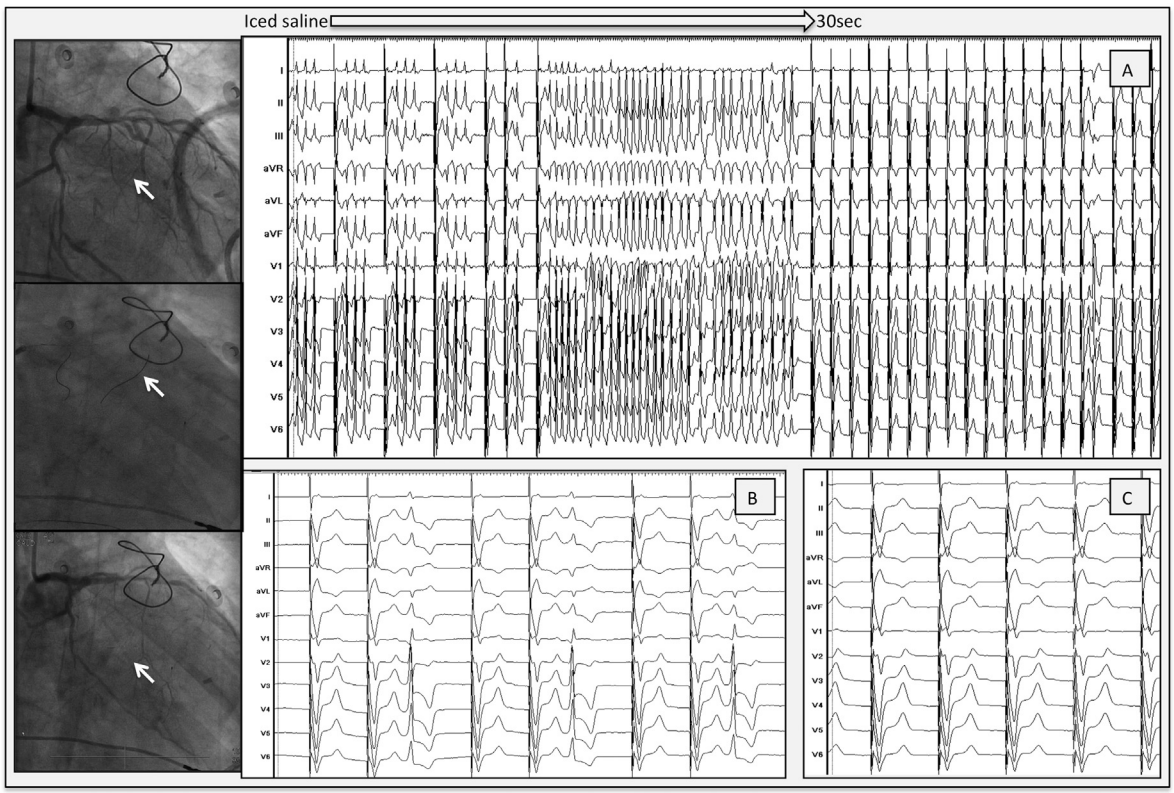

Figure 4 Selective ethanol injection into a septal perforator. Left panel with fluoroscopic views: Upper panel: left coronary angiography before injection. Distal branch of septal perforator is the target to cannulate (arrow). Middle panel: left coronary angiography with 1 guidewire inside the first and 1 guidewire inside the second perforator (arrow). Lower panel: angiography after ethanol injection. A distal branch (arrow) of the second perforator is occluded. **A:** Injection of iced saline. Fast VT with disappearance of VT, after 30 seconds. **B:** Injection of ethanol. Single premature ventricular contraction, with no VT afterward. **C:** Final result. Complete eradication of VT and premature ventricular contraction after a couple of minutes. VT = ventricular tachycardia.

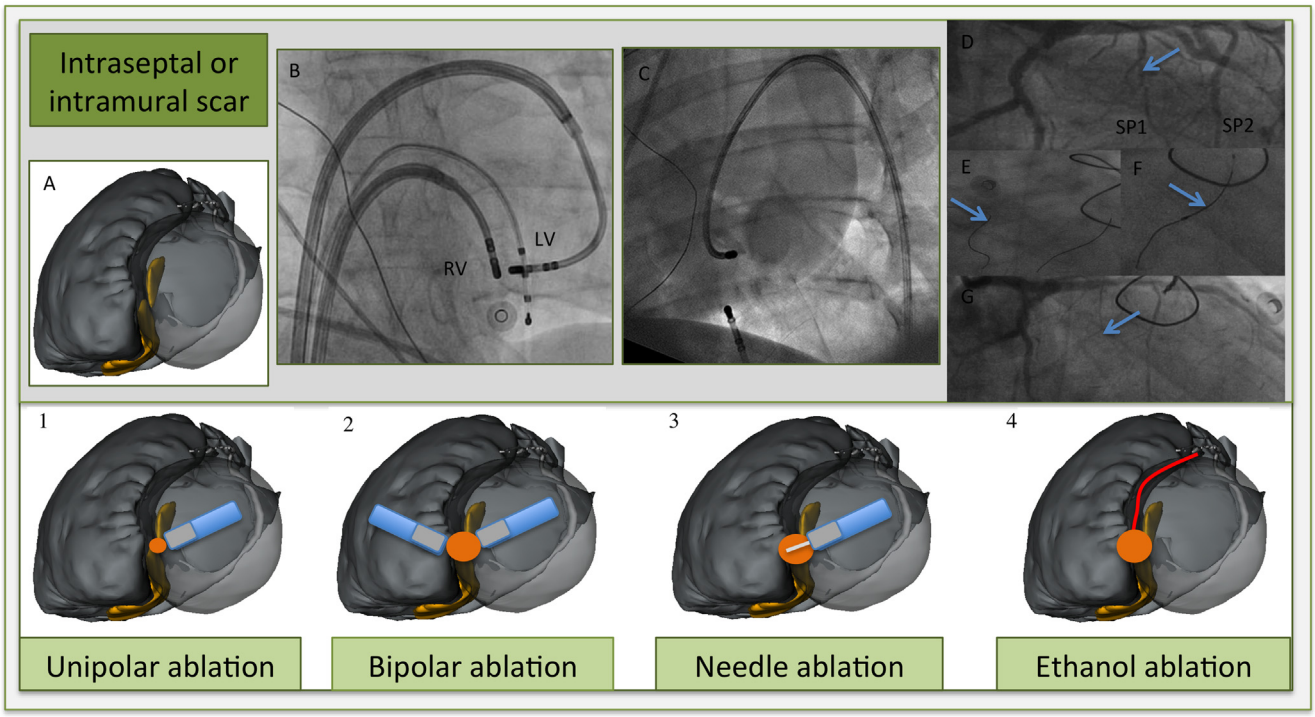

Figure 5 Different ablation techniques for intraseptal or intramural scar. **A:** Illustration of merged multidetector computed tomography/magnetic resonance imaging segmentation with postablation nontransmural scar regions (in yellow) on both sites of the septum (left anterior oblique view). Blue, ablation catheters; gray, tip; white, needle; read dot, ablation target; orange dot, expected ablation lesion; red, first septal perforator. 1. *High output ablation* (till 70 W) gives a slightly larger lesion; however, often not transmural and the risk of steam pop or catheter perforation increases. 2. *Bipolar ablation.* Two ablation catheters at opposing septum sites. (**B:** Anteroposterior view, 2 ablation catheters in steerable sheaths and an RV apex catheter for pacing purposes). 3. *Irrigated needle catheter at LV septum*. Needle extended (7–9 mm) inside the septum with staining of contrast. (**C:** fluoroscopic image with contrast staining at another basolateral site. Needle catheter in steerable sheath, and quadripolar catheter in coronary sinus and RV apex. Dual-chamber implantable cardioverter-defibrillator leads image). **4.** *Selective coronary ethanol injection* (cf fluoroscopic sequence). **D:** Coronary angiogram shows septal perforators, with the first septal perforator as target (arrow). **E:** Guidewire cannulation of first (arrow) and second septal perforator. **F:** Balloon occlusion (arrow) with iced saline injection and later with 1.5-mL ethanol injection because of ventricular tachycardia termination. **G:** Occlusion of the first septal perforator (arrow). LV = left ventricular; RV = right ventricular.

Table 1 (Dis)advantages of bipolar and ethanol ablation

Ablation strategy	Advantages	Disadvantages
Bipolar ablation	• Possibility of creating a transmural/intramural lesion • Lesion size more predictable • Transseptal approach preferred in ischemic cardiomyopathy	• Risk of conduction damage for basal intramural septal focus • No electro-anatomical mapping (EAM) system visualization, contact force, and vector information of catheter tips • Difficult to interpret good position on fluoroscopy only • No local intramural information • Irreversible effect • Special setup needed[11] • High cost of 2 new ablation catheters
Ethanol ablation	• More published data describing techniques and results[10,12] • Possibility of creating a transmural/intramural lesion • Reversible evaluation of the effect using iced saline • Local unipolar recording of guidewire possible • Low cost (no extra catheters or steerable sheath needed) • Available in case of failed epicardial access	• Limited by coronary anatomy • Retrograde approach needed in ischemic cardiomyopathy (possible silent emboli) • Iatrogenic final infarct size not always predictable • Risk of irreversible conduction block if not preceded by saline • Risk of ethanol leak in the nontargeted artery

In the future, irrigated needle ablation could be a valuable and apparently safe alternative since unipolar intramural recording from the needle tip is also feasible and larger intramural lesions can be created, without the anatomical restriction of the coronary artery system. However, this ablation technique is not reversible. More data for human use are still needed.[8]

Conclusion

This case illustrates the patient-tailored approach for an intramural VT focus based on the choice between bipolar and ethanol ablation.

References

1. Aliot EM, Stevenson WG, Almendral-Garrote JM, et al. European Heart Rhythm Association (EHRA); Registered Branch of the European Society of Cardiology (ESC); Heart Rhythm Society (HRS); American College of Cardiology (ACC); American Heart Association (AHA). EHRA/HRS Expert Consensus on Catheter Ablation of Ventricular Arrhythmias: developed in a partnership with the European Heart Rhythm Association (EHRA), a Registered Branch of the European Society of Cardiology (ESC), and the Heart Rhythm Society (HRS); in collaboration with the American College of Cardiology (ACC) and the American Heart Association (AHA). Europace 2009;11:771–817.
2. Jais P, Maury P, Khairy P, et al. Elimination of local abnormal ventricular activities: a new end point for substrate modification in patients with scar-related ventricular tachycardia. Circulation 2012;125:2184–2196.
3. Desjardins B, Yokokawa M, Good E, Crawford T, Latchamsetty R, Jongnarangsin K, Ghanbari H, Oral H, Pelosi F, Chugh A, Morady F, Bogun F. Characteristics of intramural scar in patients with non-ischemic cardiomyopathy and relation to intramural ventricular arrhythmias. Circ Arrhythm Electrophysiol 2013;6:891–897.
4. Tokuda M, Kojodjojo P, Tung S, Tedrow UB, Nof E, Inada K, Koplan BA, Michaud GF, John RM, Epstein LM, Stevenson WG. Acute failure of catheter ablation for ventricular tachycardia due to structural heart disease: causes and significance. J Am Heart Assoc 2013;2:e000072.
5. Yoshida K, Yokokawa M, Desjardins B, Good E, Oral H, Chugh A, Pelosi F, Morady F, Bogun F. Septal involvement in patients with post-infarction ventricular tachycardia: implications for mapping and radiofrequency ablation. J Am Coll Cardiol 2011;58:2491–2500.
6. Haqqani HM, Tschabrunn CM, Tzou WS, et al. Isolated septal substrate for ventricular tachycardia in nonischemic dilated cardiomyopathy: incidence, characterization, and implications. Heart Rhythm 2011;8:1169–1176.
7. Sapp JL, Cooper JM, Zei P, Stevenson WG. Large radiofrequency ablation lesions can be created with a retractable infusion-needle catheter. J Cardiovasc Electrophysiol 2006;17:657–661.
8. Sapp JL, Beeckler C, Pike R, Parkash R, Gray CJ, Zeppenfeld K, Kuriachan V, Stevenson WG. Initial human feasibility of infusion needle catheter ablation for refractory ventricular tachycardia. Circulation 2013;128:2289–2295.
9. Koruth JS, Dukkipati S, Miller Ma, Neuzil P, d'Avila A, Reddy VY. Bipolar irrigated radiofrequency ablation: a therapeutic option for refractory intramural atrial and ventricular tachycardia circuits. Heart Rhythm 2012;9:1932–1941.
10. Sacher F, Sobieszczyk P, Tedrow U, Eisenhauer AC, Field ME, Selwyn A, Raymond JM, Koplan B, Epstein LM, Stevenson WG. Transcoronary ethanol ventricular tachycardia ablation in the modern electrophysiology era. Heart Rhythm 2008;5:62–68.
11. Berte B, Sacher F, Mahida S, Yamashita S, Lim HS, Denis A, Derval N, Hocini M, Haissaguerre M, Cochet H, Jais P. Impact of septal radiofrequency ventricular tachycardia ablation: insights from magnetic resonance imaging. Circulation 2014;130:716–718.
12. Tokuda M, Sobieszczyk P, Eisenhauer AC, Kojodjojo P, Inada K, Koplan BA, Michaud GF, John RM, Epstein LM, Sacher F, Stevenson WG, Tedrow UB. Transcoronary ethanol ablation for recurrent ventricular tachycardia after failed catheter ablation: an update. Circ Arrhythm Electrophysiol 2011;4:889–896.
13. Teh AW, Reddy VY, Koruth JS, Miller MA, Choudry S, D'Avila A, Dukkipati SR. Bipolar radiofrequency catheter ablation for refractory ventricular outflow tract arrhythmias. J Cardiovasc Electrophysiol 2014;25:1093–1099.
14. Gonzalez-Suarez A, Trujillo M, Koruth J, d'Avila A, Berjano E. Radiofrequency cardiac ablation with catheters placed on opposing sides of the ventricular wall: computer modelling comparing bipolar and unipolar modes. Int J Hyperthermia 2014;30:372–384.
15. Roten L, Derval N, Pascale P, Jais P, Sacher F. What next after failed septal ventricular tachycardia ablation? Indian Pacing Electrophysiol J 2012;12:180–185.

References

1. Arenal A, Glez-Torrecilla E, Ortiz M, et al. Ablation of electrograms with an isolated, delayed component as treatment of unmappable monomorphic ventricular tachycardias in patients with structural heart disease. Journal of the American College of Cardiology 2003;41:81-92.
2. Nogami A, Sugiyasu A, Tada H, et al. Changes in the isolated delayed component as an endpoint of catheter ablation in arrhythmogenic right ventricular cardiomyopathy: predictor for long-term success. Journal of cardiovascular electrophysiology 2008;19:681-8.
3. Bogun F, Good E, Reich S, et al. Isolated potentials during sinus rhythm and pace-mapping within scars as guides for ablation of post-infarction ventricular tachycardia. Journal of the American College of Cardiology 2006;47:2013-9.
4. Jais P, Maury P, Khairy P, et al. Elimination of local abnormal ventricular activities: a new end point for substrate modification in patients with scar-related ventricular tachycardia. Circulation 2012;125:2184-96.
5. Teh AW, Reddy VY, Koruth JS, et al. Bipolar radiofrequency catheter ablation for refractory ventricular outflow tract arrhythmias. Journal of cardiovascular electrophysiology 2014;25:1093-9.
6. Koruth JS, Dukkipati S, Miller MA, Neuzil P, d'Avila A, Reddy VY. Bipolar irrigated radiofrequency ablation: a therapeutic option for refractory intramural atrial and ventricular tachycardia circuits. Heart rhythm : the official journal of the Heart Rhythm Society 2012;9:1932-41.
7. Berte B, Sacher F, Mahida S, et al. Impact of septal radiofrequency ventricular tachycardia ablation: insights from magnetic resonance imaging. Circulation 2014;130:716-8.
8. Sacher F, Sobieszczyk P, Tedrow U, et al. Transcoronary ethanol ventricular tachycardia ablation in the modern electrophysiology era. Heart rhythm : the official journal of the Heart Rhythm Society 2008;5:62-8.
9. Tokuda M, Sobieszczyk P, Eisenhauer AC, et al. Transcoronary ethanol ablation for recurrent ventricular tachycardia after failed catheter ablation: an update. Circulation Arrhythmia and electrophysiology 2011;4:889-96.

VI. FUTURE PERSPECTIVES

Significant progress has been made in delineating the arrhythmogenic substrate in VT patients. Improved substrate imaging and mapping is predicted to have a significant impact on outcome. However challenges persist and failures to eliminate VT either acutely or on long term outcome remain a problem in a significant proportion of patients. There is therefore a need for further improvements in current ablation techniques that may improve efficacy. The following section outlines potential areas of future research.

Improving risk stratification for VT and timing for VT ablation

Thus far, two randomized trials have investigated the role of early VT ablation on mortality. In the SMASH-VT study a trend towards a mortality benefit was reported when using early VT ablation in secondary prevention ICM.[102] The VTACH study on the other hand demonstrated no difference, although a trend towards benefit was reported in patients with LV EF > 30%.

There is growing evidence that ICD shocks are associated with increased mortality. Therefore, it seems reasonable to expect a mortality benefit with VT ablation which is consistently resulting in the disappearance of shocks in 80% of treated patients. A more recent study from Maury *et al* suggested that in a subset of patients with well tolerated VT, VT ablation may obviate the need for ICD implantation.[103]

Improving mapping techniques

Substrate-based mapping has several limitations. Unlike in the atria, the wall thickness of ventricles, particularly the LV, makes endocardial mapping only too limited. It has been demonstrated that endocardial voltage mapping (using an ablation catheter) may appear normal if a rim of surviving tissue as thin as 2-3 mm persists in between the catheter and the scar. Even when epicardial mapping is possible and performed, intramural substrates that maybe critical to the arrhythmia, may not be mapped. Mapping density and resolution are key factors that strongly impact mapping quality. Better diagnostic catheters are certainly required but we lack studies to determine the optimal electrode size and inter-electrode distance.

Activation mapping

Current activation mapping techniques can be improved by using a number of novel technologies including the multipolar mapping [PentaRay® catheter[22] (Biosense Webster), the Constellation® basket catheter[104], the Orion™ catheter[105] (Boston Scientific), and the Livewire™ catheter (St Jude Medical)] increase mapping density and decrease mapping time. However, there is only limited experience in human ventricles with the Constellation® and the Orion™ catheters.

Non-contact mapping and non-invasive mapping

Non-contact single beat mapping (endocardial balloon, Endocardial Solutions and Ensite™ Array™ ,St Jude Medical) and non-invasive electrocardiographic mapping (ecVUE™, CardioInsight) can be used in non-sustained, unmappable VT and can visualize the VT circuit or PVC exit site. Another non-contact multipolar mapping

system with real-time 3D imaging based on high-density dipole density mapping (Acutus Medical) is still under investigation.

New localisation and mapping systems

The CARTO® 3 system and Ensite™ Velocity™ system are discussed in the introduction section. Mediguide™ is a novel localisation system with accurate real-time tracking of specifically designed catheters (with a small magnetic coil within the tip) using a magnetic field. The additional value (over and above the Ensite™ Velocity™ system) of the Mediguide™ system has yet to be evaluated. At the present time the magnetic localization is not directly used in the Velocity platform but only to increase field scaling perfomance. This should be corrected in the next version. The newest mapping system is the Rhythmia™ mapping system, with both magnetic and impedance-based location of the catheters. There is currently no data from large studies regarding to clinical accuracy of the Rhythmia™ mapping system.

One of the areas where all EAM systems could be improved is registration monitoring and automatic shift corrections. The combination of cardiac and respiratory motion makes the display of a static 3D reconstruction inaccurate. Dynamic 3D visualisation of the left ventricle could potentially increase beat-to-beat accuracy.[106] An additional limitation is that patients' body movements are not always well identified by the system, and when identified often require re-mapping.

Improving imaging techniques, image integration and image merge

As discussed previously, the use of pre-procedural imaging has several advantages and it is our opinion that in the future, image-based VT ablation will be the standard of care. However, there are currently no prospective studies demonstrating prognostic benefit conferred by using these imaging modalities. Peri-procedural 3D rotational angiography could also be helpful to improve the image merge. A novel wideband LGE-MRI technique seems promising for device artifact removal in ICD patients with its efficacy depending on device to LV distance.[107]

New insights from MRI

DE-MRI can reduce procedure time by focussing more rapidly on the zone of interest. MRI defined scar is more accurate than voltage defined scar with EAM mapping, because of different parameters as catheter contact and angulation, epicardial fat and intramural scar. In addition, it has been demonstrated that a rim of healthy tissue of only 2mm thickness between the scar and the mapping catheter is enough to result in a normal bipolar voltage measurement of > 1.5mV.[108] DE-MRI is able to improve understanding of the three dimensional structure of conducting channels. Scar data of MRI can also result in better outcome since this information can be used to assess whether the whole scar has been delineated and/or ablated. The prognostic benefit of DE-MRI guided VT ablation has yet to be confirmed. The use of novel free breathing sequences for MRI can increase resolution from 5mm slice thickness to 2.5mm slice thickness resulting in superior image quality.[109] A fused MDCT/MRI image model combines the high spatial resolution of CT for accurate

assessment of the cardiac chambers with the ability of DE-MRI to image myocardial scar at high contrast. This multimodality approach is useful to improve both safety[34] and efficacy[110]. However, if accurate visualization of surviving bundles inside the scar is desired, an increase in spatial resolution is needed, at least to a 1mm cubic voxel. This should be available very soon on Siemens scanners and is under evaluation in CHU Bordeaux.

A new non-invasive imaging technique

Electrocardiographic mapping (e.g. ECVUE vest, CardioInsight) is another novel promising technique to acquire non-invasive unipolar maps of a 252 electrode vest and to project them on the epicardial surface of a prior acquired MDCT segmentation of the heart. This allows reconstruction of non-invasive maps during SR and VT.[111] Preliminary results with non-invasive mapping are promising in an elegant study from Rudy *and colleagues*.[112]

Improving safety

An endocardial approach for VT ablation is relatively safe with a reported 7% major complication risk.[113] Major complications include vascular access related problems, third degree AV block, cardiac tamponade, major bleeding and procedure related mortality. An epicardial approach is associated with additional complications. The epicardial complication rate varies from 5% to 14%.[114,115] Specific complications include cardiac tamponade, coronary stenosis, pericarditis, major bleeding, phrenic nerve paralysis and some atypical complications.[116] An important area of future research is the the development of novel techniques that reduce complications. A

large clinical use of the needle ablation catheter may result in fewer epicardial approaches and thereby reduced complications.

Improved epicardial puncture methods

3D anatomy of all adjacent organs with visualisation of the pericardial Tuohy needle tip into the EAM system or pericardial endoscopy can help to avoid potential organ damage.[117] Accurate image integration and merge with phrenic nerve segmentation and coronary segmentation can help to prevent these complications.[34, 118] Improvement of our techniques and knowledge to prevent steam pop and coronary lesions and to reduce complications of epicardial access is needed.

Improving efficacy

Incessant or frequent VT is controlled acutely in 90% of patients. All inducible VT are ablated in 50% of patients and at least one VT is eliminated in 80%. Recurrence of any VT/VF occurs in 50% of patients during follow-up, however a reduction of >75% of shocks is achieved in >70% of patients.[88, 119-121] VT ablation in ICM with ICD implantation for secondary prevention has been reported to reduce the risk of recurrence of VT with 65% at two-years follow up.[102,120] Complete LAVA elimination is feasible in 60-70% of VT patients.[22] New VT circuits in the vicinity of earlier ablated sites could potentially result in recurrent VT.[122] ICM patients have less recurrence of VT after VT ablation than NICM.[121] Disease progression and incomplete ablation are responsible for recurrent VT in NICM.[92] Intraseptal and intramural scar, large scar and fast VT are predictors for recurrence.[90, 113]

Conclusion

Scar related VT ablation is an established technique which is rapidly evolving with an emerging indication because of early revascularisation and increasing ICD implantations. Long-term outcome results and results of mortality benefit are needed. New mapping techniques, imaging modalities and ablation devices have to increase the 60% success burden and help to obtain better transmural lesions.

References

[1] Zipes DP, Camm AJ, Borggrefe M, Buxton AE, Chaitman B, Fromer M, Gregoratos G, Klein G, Moss AJ, Myerburg RJ, Priori SG, Quinones MA, Roden DM, Silka MJ, Tracy C, Blanc JJ, Budaj A, Dean V, Deckers JW, Despres C, Dickstein K, Lekakis J, McGregor K, Metra M, Morais J, Osterspey A, Tamargo JL, Zamorano JL, Smith SC, Jr., Jacobs AK, Adams CD, Antman EM, Anderson JL, Hunt SA, Halperin JL, Nishimura R, Ornato JP, Page RL, Riegel B, American College of Cardiology/American Heart Association Task F, European Society of Cardiology Committee for Practice G, European Heart Rhythm A, the Heart Rhythm S: ACC/AHA/ESC 2006 guidelines for management of patients with ventricular arrhythmias and the prevention of sudden cardiac death--executive summary: A report of the American College of Cardiology/American Heart Association Task Force and the European Society of Cardiology Committee for Practice Guidelines (Writing Committee to Develop Guidelines for Management of Patients with Ventricular Arrhythmias and the Prevention of Sudden Cardiac Death) Developed in collaboration with the European Heart Rhythm Association and the Heart Rhythm Society. European heart journal 2006; 27:2099-2140.

[2] Aliot EM, Stevenson WG, Almendral-Garrote JM, Bogun F, Calkins CH, Delacretaz E, Della Bella P, Hindricks G, Jais P, Josephson ME, Kautzner J, Kay GN, Kuck KH, Lerman BB, Marchlinski F, Reddy V, Schalij MJ, Schilling R, Soejima K, Wilber D, European Heart Rhythm A, Registered Branch of the European Society of C, Heart Rhythm S, American College of C, American Heart A: EHRA/HRS Expert Consensus on Catheter Ablation of Ventricular Arrhythmias: developed in a partnership with the European Heart Rhythm Association (EHRA), a Registered Branch of the European Society of Cardiology (ESC), and the Heart Rhythm Society (HRS); in collaboration with the American College of Cardiology (ACC) and the American Heart Association (AHA). Heart rhythm : the official journal of the Heart Rhythm Society 2009; 6:886-933.

[3] Ellison KE, Friedman PL, Ganz LI, Stevenson WG: Entrainment mapping and radiofrequency catheter ablation of ventricular tachycardia in right ventricular dysplasia. Journal of the American College of Cardiology 1998; 32:724-728.

[4] de Bakker JM, van Capelle FJ, Janse MJ, Tasseron S, Vermeulen JT, de Jonge N, Lahpor JR: Slow conduction in the infarcted human heart. 'Zigzag' course of activation. Circulation 1993; 88:915-926.

[5] Sosa E, Scanavacca M, d'Avila A, Pilleggi F: A new technique to perform epicardial mapping in the electrophysiology laboratory. Journal of cardiovascular electrophysiology 1996; 7:531-536.

[6] de Bakker JM, van Capelle FJ, Janse MJ, Wilde aa, Coronel R, Becker aE, Dingemans KP, van Hemel NM, Hauer RN: Reentry as a cause of ventricular tachycardia in patients with chronic ischemic heart disease: electrophysiologic and anatomic correlation. Circulation 1988; 77:589-606.

[7] Chen PS, Chen LS, Cao JM, Sharifi B, Karagueuzian HS, Fishbein MC: Sympathetic nerve sprouting, electrical remodeling and the mechanisms of sudden cardiac death. Cardiovascular research 2001; 50:409-416.

[8] Cao JM, Fishbein MC, Han JB, Lai WW, Lai AC, Wu TJ, Czer L, Wolf PL, Denton TA, Shintaku IP, Chen PS, Chen LS: Relationship between regional cardiac hyperinnervation and ventricular arrhythmia. Circulation 2000; 101:1960-1969.
[9] Sacher F, Tedrow UB, Field ME, Raymond JM, Koplan BA, Epstein LM, Stevenson WG: Ventricular tachycardia ablation: evolution of patients and procedures over 8 years. Circulation Arrhythmia and electrophysiology 2008; 1:153-161.
[10] Nademanee K, Taylor R, Bailey WE, Rieders DE, Kosar EM: Treating electrical storm : sympathetic blockade versus advanced cardiac life support-guided therapy. Circulation 2000; 102:742-747.
[11] Bujak M, Frangogiannis NG: The role of TGF-beta signaling in myocardial infarction and cardiac remodeling. Cardiovascular research 2007; 74:184-195.
[12] Wiener I, Mindich B, Pitchon R: Determinants of ventricular tachycardia in patients with ventricular aneurysms: results of intraoperative epicardial and endocardial mapping. Circulation 1982; 65:856-861.
[13] Miller JM, Tyson GS, Hargrove WC, 3rd, Vassallo JA, Rosenthal ME, Josephson ME: Effect of subendocardial resection on sinus rhythm endocardial electrogram abnormalities. Circulation 1995; 91:2385-2391.
[14] Harada T, Stevenson WG, Kocovic DZ, Friedman PL: Catheter ablation of ventricular tachycardia after myocardial infarction: relation of endocardial sinus rhythm late potentials to the reentry circuit. Journal of the American College of Cardiology 1997; 30:1015-1023.
[15] Arenal A, Glez-Torrecilla E, Ortiz M, Villacastin J, Fdez-Portales J, Sousa E, del Castillo S, Perez de Isla L, Jimenez J, Almendral J: Ablation of electrograms with an isolated, delayed component as treatment of unmappable monomorphic ventricular tachycardias in patients with structural heart disease. Journal of the American College of Cardiology 2003; 41:81-92.
[16] Marchlinski FE, Callans DJ, Gottlieb CD, Zado E: Linear ablation lesions for control of unmappable ventricular tachycardia in patients with ischemic and nonischemic cardiomyopathy. Circulation 2000; 101:1288-1296.
[17] Cano O, Hutchinson M, Lin D, Garcia F, Zado E, Bala R, Riley M, Cooper J, Dixit S, Gerstenfeld E, Callans D, Marchlinski FE: Electroanatomic substrate and ablation outcome for suspected epicardial ventricular tachycardia in left ventricular nonischemic cardiomyopathy. Journal of the American College of Cardiology 2009; 54:799-808.
[18] Piers SRD, Tao Q, van Huls van Taxis CFB, Schalij MJ, van der Geest RJ, Zeppenfeld K: Contrast-Enhanced MRI-Derived Scar Patterns and Associated Ventricular Tachycardias in Nonischemic Cardiomyopathy: Implications for the Ablation Strategy. Circulation Arrhythmia and electrophysiology 2013.
[19] Piers SR, van Huls van Taxis CF, Tao Q, van der Geest RJ, Askar SF, Siebelink HM, Schalij MJ, Zeppenfeld K: Epicardial substrate mapping for ventricular tachycardia ablation in patients with non-ischaemic cardiomyopathy: a new algorithm to differentiate between scar and viable myocardium developed by simultaneous integration of computed tomography and contrast-enhanced magnetic resonance imaging. European heart journal 2013; 34:586-596.
[20] Callans DJ, Ren JF, Michele J, Marchlinski FE, Dillon SM: Electroanatomic left ventricular mapping in the porcine model of healed anterior myocardial

infarction. Correlation with intracardiac echocardiography and pathological analysis. Circulation 1999; 100:1744-1750.
[21] Gardner PI, Ursell PC, Fenoglio JJ, Jr., Wit AL: Electrophysiologic and anatomic basis for fractionated electrograms recorded from healed myocardial infarcts. Circulation 1985; 72:596-611.
[22] Jais P, Maury P, Khairy P, Sacher F, Nault I, Komatsu Y, Hocini M, Forclaz A, Jadidi AS, Weerasooryia R, Shah A, Derval N, Cochet H, Knecht S, Miyazaki S, Linton N, Rivard L, Wright M, Wilton SB, Scherr D, Pascale P, Roten L, Pederson M, Bordachar P, Laurent F, Kim SJ, Ritter P, Clementy J, Haissaguerre M: Elimination of local abnormal ventricular activities: a new end point for substrate modification in patients with scar-related ventricular tachycardia. Circulation 2012; 125:2184-2196.
[23] de Chillou C, Lacroix D, Klug D, Magnin-Poull I, Marquie C, Messier M, Andronache M, Kouakam C, Sadoul N, Chen J, Aliot E, Kacet S: Isthmus characteristics of reentrant ventricular tachycardia after myocardial infarction. Circulation 2002; 105:726-731.
[24] Nogami A, Sugiyasu A, Tada H, Kurosaki K, Sakamaki M, Kowase S, Oginosawa Y, Kubota S, Usui T, Naito S: Changes in the isolated delayed component as an endpoint of catheter ablation in arrhythmogenic right ventricular cardiomyopathy: predictor for long-term success. Journal of cardiovascular electrophysiology 2008; 19:681-688.
[25] Bogun F, Bender B, Li YG, Groenefeld G, Hohnloser SH, Pelosi F, Knight B, Strickberger SA, Morady F: Analysis during sinus rhythm of critical sites in reentry circuits of postinfarction ventricular tachycardia. Journal of interventional cardiac electrophysiology : an international journal of arrhythmias and pacing 2002; 7:95-103.
[26] Vergara P, Trevisi N, Ricco A, Petracca F, Baratto F, Cireddu M, Bisceglia C, Maccabelli G, Della Bella P: Late potentials abolition as an additional technique for reduction of arrhythmia recurrence in scar related ventricular tachycardia ablation. Journal of cardiovascular electrophysiology 2012; 23:621-627.
[27] Kim RJ, Wu E, Rafael A, Chen EL, Parker MA, Simonetti O, Klocke FJ, Bonow RO, Judd RM: The use of contrast-enhanced magnetic resonance imaging to identify reversible myocardial dysfunction. The New England journal of medicine 2000; 343:1445-1453.
[28] Wijnmaalen AP, van der Geest RJ, van Huls van Taxis CF, Siebelink HM, Kroft LJ, Bax JJ, Reiber JH, Schalij MJ, Zeppenfeld K: Head-to-head comparison of contrast-enhanced magnetic resonance imaging and electroanatomical voltage mapping to assess post-infarct scar characteristics in patients with ventricular tachycardias: real-time image integration and reversed registration. European heart journal 2011; 32:104-114.
[29] Ranjan R, McGann CJ, Jeong EK, Hong K, Kholmovski EG, Blauer J, Wilson BD, Marrouche NF, Kim D: Wideband late gadolinium enhanced magnetic resonance imaging for imaging myocardial scar without image artefacts induced by implantable cardioverter-defibrillator: a feasibility study at 3 T. Europace : European pacing, arrhythmias, and cardiac electrophysiology : journal of the working groups on cardiac pacing, arrhythmias, and cardiac cellular electrophysiology of the European Society of Cardiology 2014.

[30] Desjardins B, Crawford T, Good E, Oral H, Chugh A, Pelosi F, Morady F, Bogun F: Infarct architecture and characteristics on delayed enhanced magnetic resonance imaging and electroanatomic mapping in patients with postinfarction ventricular arrhythmia. Heart rhythm : the official journal of the Heart Rhythm Society 2009; 6:644-651.
[31] Andreu D, Ortiz-Perez JT, Boussy T, Fernandez-Armenta J, de Caralt TM, Perea RJ, Prat-Gonzalez S, Mont L, Brugada J, Berruezo A: Usefulness of contrast-enhanced cardiac magnetic resonance in identifying the ventricular arrhythmia substrate and the approach needed for ablation. European heart journal 2014; 35:1316-1326.
[32] Komatsu Y, Cochet H, Jadidi A, Sacher F, Shah A, Derval N, Scherr D, Pascale P, Roten L, Denis A, Ramoul K, Miyazaki S, Daly M, Riffaud M, Sermesant M, Relan J, Ayache N, Kim S, Montaudon M, Laurent F, Hocini M, Haïssaguerre M, Jaïs P: Regional myocardial wall thinning at multidetector computed tomography correlates to arrhythmogenic substrate in postinfarction ventricular tachycardia: assessment of structural and electrical substrate. Circulation Arrhythmia and electrophysiology 2013; 6:342-350.
[33] Tian J, Jeudy J, Smith MF, Jimenez A, Yin X, Bruce PA, Lei P, Turgeman A, Abbo A, Shekhar R, Saba M, Shorofsky S, Dickfeld T: Three-dimensional contrast-enhanced multidetector CT for anatomic, dynamic, and perfusion characterization of abnormal myocardium to guide ventricular tachycardia ablations. Circulation Arrhythmia and electrophysiology 2010; 3:496-504.
[34] Komatsu Y, Sacher F, Cochet H, Jais P: Multimodality imaging to improve the safety and efficacy of epicardial ablation of scar-related ventricular tachycardia. Journal of cardiovascular electrophysiology 2013; 24:1426-1427.
[35] Bala R, Ren JF, Hutchinson MD, Desjardins B, Tschabrunn C, Gerstenfeld EP, Deo R, Dixit S, Garcia FC, Cooper J, Lin D, Riley MP, Tzou WS, Verdino R, Epstein AE, Callans DJ, Marchlinski FE: Assessing epicardial substrate using intracardiac echocardiography during VT ablation. Circulation Arrhythmia and electrophysiology 2011; 4:667-673.
[36] Bunch TJ, Weiss JP, Crandall BG, Day JD, DiMarco JP, Ferguson JD, Mason PK, McDaniel G, Osborn JS, Wiggins D, Mahapatra S: Image integration using intracardiac ultrasound and 3D reconstruction for scar mapping and ablation of ventricular tachycardia. Journal of cardiovascular electrophysiology 2010; 21:678-684.
[37] Yokoyama K, Nakagawa H, Shah DC, Lambert H, Leo G, Aeby N, Ikeda A, Pitha JV, Sharma T, Lazzara R, Jackman WM: Novel contact force sensor incorporated in irrigated radiofrequency ablation catheter predicts lesion size and incidence of steam pop and thrombus. Circulation Arrhythmia and electrophysiology 2008; 1:354-362.
[38] Bourier F, Fahrig R, Wang P, Santangeli P, Kurzidim K, Strobel N, Moore T, Hinkel C, Al-Ahmad A: Accuracy assessment of catheter guidance technology in electrophysiology procedures: a comparison of a new 3D-based fluoroscopy navigation system to current electroanatomic mapping systems. Journal of cardiovascular electrophysiology 2014; 25:74-83.
[39] Kapa S, Asirvatham SJ: You can't know where you're going until you know where you've been: the clinical relevance of differences in accurate assessment of

catheter location with mapping technologies. Journal of cardiovascular electrophysiology 2014; 25:84-86.
[40] Brunckhorst CB, Stevenson WG, Soejima K, Maisel WH, Delacretaz E, Friedman PL, Ben-Haim SA: Relationship of slow conduction detected by pace-mapping to ventricular tachycardia re-entry circuit sites after infarction. Journal of the American College of Cardiology 2003; 41:802-809.
[41] de Chillou C, Groben L, Magnin-Poull I, Andronache M, Magdi Abbas M, Zhang N, Abdelaal A, Ammar S, Sellal JM, Schwartz J, Brembilla-Perrot B, Aliot E, Marchlinski FE: Localizing the Critical Isthmus of Post-Infarct Ventricular Tachycardia: The Value of Pace Mapping during Sinus Rhythm. Heart rhythm : the official journal of the Heart Rhythm Society 2013.
[42] Brunckhorst CB, Delacretaz E, Soejima K, Maisel WH, Friedman PL, Stevenson WG: Identification of the ventricular tachycardia isthmus after infarction by pace mapping. Circulation 2004; 110:652-659.
[43] Soejima K, Stevenson WG, Maisel WH, Sapp JL, Epstein LM: Electrically unexcitable scar mapping based on pacing threshold for identification of the reentry circuit isthmus: feasibility for guiding ventricular tachycardia ablation. Circulation 2002; 106:1678-1683.
[44] Tung R, Mathuria N, Michowitz Y, Yu R, Buch E, Bradfield J, Mandapati R, Wiener I, Boyle N, Shivkumar K: Functional pace-mapping responses for identification of targets for catheter ablation of scar-mediated ventricular tachycardia. Circulation Arrhythmia and electrophysiology 2012; 5:264-272.
[45] Frankel DS, Mountantonakis SE, Zado ES, Anter E, Bala R, Cooper JM, Deo R, Dixit S, Epstein AE, Garcia FC, Gerstenfeld EP, Hutchinson MD, Lin D, Patel VV, Riley MP, Robinson MR, Tzou WS, Verdino RJ, Callans DJ, Marchlinski FE: Noninvasive programmed ventricular stimulation early after ventricular tachycardia ablation to predict risk of late recurrence. Journal of the American College of Cardiology 2012; 59:1529-1535.
[46] Carbucicchio C, Ahmad Raja N, Di Biase L, Volpe V, Dello Russo A, Trivedi C, Bartoletti S, Zucchetti M, Casella M, Russo E, Santangeli P, Moltrasio M, Tundo F, Fassini G, Natale A, Tondo C: High-density substrate-guided ventricular tachycardia ablation: role of activation mapping in an attempt to improve procedural effectiveness. Heart rhythm : the official journal of the Heart Rhythm Society 2013; 10:1850-1858.
[47] Stevenson WG, Khan H, Sager P, Saxon LA, Middlekauff HR, Natterson PD, Wiener I: Identification of reentry circuit sites during catheter mapping and radiofrequency ablation of ventricular tachycardia late after myocardial infarction. Circulation 1993; 88:1647-1670.
[48] Cano O, Hutchinson M, Lin D, Garcia F, Zado E, Bala R, Riley M, Cooper J, Dixit S, Gerstenfeld E, Callans D, Marchlinski FE: Electroanatomic Substrate and Ablation Outcome for Suspected Epicardial Ventricular Tachycardia in Left Ventricular Nonischemic Cardiomyopathy. JAC 2009; 54:799-808.
[49] Liuba I, Marchlinski FE: The Substrate and Ablation of Ventricular Tachycardia in Patients With Nonischemic Cardiomyopathy. Circulation Journal 2013; 77:1957-1966.
[50] Casella M, Perna F, Dello Russo A, Pelargonio G, Bartoletti S, Ricco A, Sanna T, Pieroni M, Forleo G, Pappalardo A, Di Biase L, Natale L, Bellocci F,

Zecchi P, Natale A, Tondo C: Right ventricular substrate mapping using the Ensite Navx system: Accuracy of high-density voltage map obtained by automatic point acquisition during geometry reconstruction. Heart rhythm : the official journal of the Heart Rhythm Society 2009; 6:1598-1605.
[51] Hutchinson MD, Gerstenfeld EP, Desjardins B, Bala R, Riley MP, Garcia FC, Dixit S, Lin D, Tzou WS, Cooper JM, Verdino RJ, Callans DJ, Marchlinski FE: Endocardial unipolar voltage mapping to detect epicardial ventricular tachycardia substrate in patients with nonischemic left ventricular cardiomyopathy. Circulation Arrhythmia and electrophysiology 2011; 4:49-55.
[52] Haqqani HM, Tschabrunn CM, Tzou WS, Dixit S, Cooper JM, Riley MP, Lin D, Hutchinson MD, Garcia FC, Bala R, Verdino RJ, Callans DJ, Gerstenfeld EP, Zado ES, Marchlinski FE: Isolated septal substrate for ventricular tachycardia in nonischemic dilated cardiomyopathy: incidence, characterization, and implications. Heart rhythm : the official journal of the Heart Rhythm Society 2011; 8:1169-1176.
[53] Yoshida K, Yokokawa M, Desjardins B, Good E, Oral H, Chugh A, Pelosi F, Morady F, Bogun F: Septal involvement in patients with post-infarction ventricular tachycardia: implications for mapping and radiofrequency ablation. Journal of the American College of Cardiology 2011; 58:2491-2500.
[54] Betensky BP, Kapa S, Desjardins B, Garcia FC, Callans DJ, Dixit S, Frankel DS, Hutchinson MD, Supple GE, Zado ES, Marchlinski FE: Characterization of trans-septal activation during septal pacing: criteria for identification of intramural ventricular tachycardia substrate in nonischemic cardiomyopathy. Circulation Arrhythmia and electrophysiology 2013; 6:1123-1130.
[55] Polin GM, Haqqani H, Tzou W, Hutchinson MD, Garcia FC, Callans DJ, Zado ES, Marchlinski FE: Endocardial unipolar voltage mapping to identify epicardial substrate in arrhythmogenic right ventricular cardiomyopathy / dysplasia. HRTHM 2011; 8:76-83.
[56] Tokuda M, Tedrow UB, Inada K, Reichlin T, Michaud GF, John RM, Epstein LM, Stevenson WG: Direct comparison of adjacent endocardial and epicardial electrograms: implications for substrate mapping. Journal of the American Heart Association 2013; 2:e000215.
[57] Sacher F, Wright M, Derval N, Denis A, Ramoul K, Roten L, Pascale P, Bordachar P, Ritter P, Hocini M, Dos Santos P, Haissaguerre M, Jais P: Endocardial versus epicardial ventricular radiofrequency ablation: utility of in vivo contact force assessment. Circulation Arrhythmia and electrophysiology 2013; 6:144-150.
[58] Sapp JL, Beeckler C, Pike R, Parkash R, Gray CJ, Zeppenfeld K, Kuriachan V, Stevenson WG: Initial human feasibility of infusion needle catheter ablation for refractory ventricular tachycardia. Circulation 2013; 128:2289-2295.
[59] Koruth JS, Dukkipati S, Miller MA, Neuzil P, d'Avila A, Reddy VY: Bipolar irrigated radiofrequency ablation: a therapeutic option for refractory intramural atrial and ventricular tachycardia circuits. Heart rhythm : the official journal of the Heart Rhythm Society 2012; 9:1932-1941.
[60] Sacher F, Sobieszczyk P, Tedrow U, Eisenhauer AC, Field ME, Selwyn A, Raymond JM, Koplan B, Epstein LM, Stevenson WG: Transcoronary ethanol ventricular tachycardia ablation in the modern electrophysiology era. Heart rhythm : the official journal of the Heart Rhythm Society 2008; 5:62-68.

[61] Tokuda M, Sobieszczyk P, Eisenhauer AC, Kojodjojo P, Inada K, Koplan BA, Michaud GF, John RM, Epstein LM, Sacher F, Stevenson WG, Tedrow UB: Transcoronary ethanol ablation for recurrent ventricular tachycardia after failed catheter ablation: an update. Circulation Arrhythmia and electrophysiology 2011; 4:889-896.
[62] Yagishita D, Ajijola OA, Vaseghi M, Nsair A, Zhou W, Yamakawa K, Tung R, Mahajan A, Shivkumar K: Electrical homogenization of ventricular scar by application of collagenase: a novel strategy for arrhythmia therapy. Circulation Arrhythmia and electrophysiology 2013; 6:776-783.
[63] Arruda M, Fahmy T, Armaganijan L, Di Biase L, Patel D, Natale A: Endocardial and epicardial mapping and catheter ablation of post myocardial infarction ventricular tachycardia: A substrate modification approach. Journal of interventional cardiac electrophysiology : an international journal of arrhythmias and pacing 2010; 28:137-145.
[64] Di Biase L, Santangeli P, Burkhardt DJ, Bai R, Mohanty P, Carbucicchio C, Dello Russo A, Casella M, Mohanty S, Pump A, Hongo R, Beheiry S, Pelargonio G, Santarelli P, Zucchetti M, Horton R, Sanchez JE, Elayi CS, Lakkireddy D, Tondo C, Natale A: Endo-epicardial homogenization of the scar versus limited substrate ablation for the treatment of electrical storms in patients with ischemic cardiomyopathy. Journal of the American College of Cardiology 2012; 60:132-141.
[65] Tilz RR, Makimoto H, Lin T, Rillig A, Deiss S, Wissner E, Mathew S, Metzner A, Rausch P, Kuck KH, Ouyang F: Electrical isolation of a substrate after myocardial infarction: a novel ablation strategy for unmappable ventricular tachycardias--feasibility and clinical outcome. Europace : European pacing, arrhythmias, and cardiac electrophysiology : journal of the working groups on cardiac pacing, arrhythmias, and cardiac cellular electrophysiology of the European Society of Cardiology 2014.
[66] Oza S, Wilber DJ: Substrate-based endocardial ablation of postinfarction ventricular tachycardia. Heart rhythm : the official journal of the Heart Rhythm Society 2006; 3:607-609.
[67] Komatsu Y, Daly M, Sacher F, Cochet H, Denis A, Derval N, Jesel L, Zellerhoff S, Lim HS, Jadidi A, Nault I, Shah A, Roten L, Pascale P, Scherr D, Aurillac-Lavignolle V, Hocini M, Haissaguerre M, Jais P: Endocardial Ablation to Eliminate Epicardial Arrhythmia Substrate in Scar-Related Ventricular Tachycardia. Journal of the American College of Cardiology 2014.
[68] Schweikert RA, Saliba WI, Tomassoni G, Marrouche NF, Cole CR, Dresing TJ, Tchou PJ, Bash D, Beheiry S, Lam C, Kanagaratnam L, Natale A: Percutaneous pericardial instrumentation for endo-epicardial mapping of previously failed ablations. Circulation 2003; 108:1329-1335.
[69] Schmidt B, Chun KR, Baensch D, Antz M, Koektuerk B, Tilz RR, Metzner A, Ouyang F, Kuck KH: Catheter ablation for ventricular tachycardia after failed endocardial ablation: epicardial substrate or inappropriate endocardial ablation? Heart rhythm : the official journal of the Heart Rhythm Society 2010; 7:1746-1752.
[70] Mountantonakis SE, Park RE, Frankel DS, Hutchinson MD, Dixit S, Cooper J, Callans D, Marchlinski FE, Gerstenfeld EP: Relationship between voltage map "channels" and the location of critical isthmus sites in patients with post-infarction

cardiomyopathy and ventricular tachycardia. Journal of the American College of Cardiology 2013; 61:2088-2095.
[71] Valles E, Bazan V, Marchlinski FE: ECG criteria to identify epicardial ventricular tachycardia in nonischemic cardiomyopathy. Circulation Arrhythmia and electrophysiology 2010; 3:63-71.
[72] Piers SR, Silva Mde R, Kapel GF, Trines SA, Schalij MJ, Zeppenfeld K: Endocardial or epicardial ventricular tachycardia in nonischemic cardiomyopathy? The role of 12-lead ECG criteria in clinical practice. Heart rhythm : the official journal of the Heart Rhythm Society 2014; 11:1031-1039.
[73] Tschabrunn CM, Haqqani HM, Cooper JM, Dixit S, Garcia FC, Gerstenfeld EP, Callans DJ, Zado ES, Marchlinski FE: Percutaneous epicardial ventricular tachycardia ablation after noncoronary cardiac surgery or pericarditis. Heart rhythm : the official journal of the Heart Rhythm Society 2013; 10:165-169.
[74] Soejima K, Couper G, Cooper JM, Sapp JL, Epstein LM, Stevenson WG: Subxiphoid surgical approach for epicardial catheter-based mapping and ablation in patients with prior cardiac surgery or difficult pericardial access. Circulation 2004; 110:1197-1201.
[75] D'Avila A, Thiagalingam A, Ruskin JN, Reddy VY: Combined ventricular endocardial and epicardial substrate mapping using a sonomicrometry-based electroanatomical mapping system. Pacing and clinical electrophysiology : PACE 2007; 30:781-786.
[76] Lachman N, Syed FF, Habib A, Kapa S, Bisco SE, Venkatachalam KL, Asirvatham SJ: Correlative anatomy for the electrophysiologist, Part I: the pericardial space, oblique sinus, transverse sinus. Journal of cardiovascular electrophysiology 2010; 21:1421-1426.
[77] Stavrakis S, Jackman WM, Nakagawa H, Sun Y, Xu Q, Beckman KJ, Lockwood D, Scherlag BJ, Lazzara R, Po SS: Risk of coronary artery injury with radiofrequency ablation and cryoablation of epicardial posteroseptal accessory pathways within the coronary venous system. Circulation Arrhythmia and electrophysiology 2014; 7:113-119.
[78] Roberts-Thomson KC, Steven D, Seiler J, Inada K, Koplan BA, Tedrow UB, Epstein LM, Stevenson WG: Coronary artery injury due to catheter ablation in adults: presentations and outcomes. Circulation 2009; 120:1465-1473.
[79] Buch E, Vaseghi M, Cesario DA, Shivkumar K: A novel method for preventing phrenic nerve injury during catheter ablation. Heart rhythm : the official journal of the Heart Rhythm Society 2007; 4:95-98.
[80] Di Biase L, Burkhardt JD, Pelargonio G, Dello Russo A, Casella M, Santarelli P, Horton R, Sanchez J, Gallinghouse JG, Al-Ahmad A, Wang P, Cummings JE, Schweikert RA, Natale A: Prevention of phrenic nerve injury during epicardial ablation: comparison of methods for separating the phrenic nerve from the epicardial surface. Heart rhythm : the official journal of the Heart Rhythm Society 2009; 6:957-961.
[81] Fan R, Cano O, Ho SY, Bala R, Callans DJ, Dixit S, Garcia F, Gerstenfeld EP, Hutchinson M, Lin D, Riley M, Marchlinski FE: Characterization of the phrenic nerve course within the epicardial substrate of patients with nonischemic cardiomyopathy and ventricular tachycardia. Heart rhythm : the official journal of the Heart Rhythm Society 2009; 6:59-64.

[82] d'Avila A, Neuzil P, Thiagalingam A, Gutierrez P, Aleong R, Ruskin JN, Reddy VY: Experimental efficacy of pericardial instillation of anti-inflammatory agents during percutaneous epicardial catheter ablation to prevent postprocedure pericarditis. Journal of cardiovascular electrophysiology 2007; 18:1178-1183.
[83] Bala R, Dhruvakumar S, Latif SA, Marchlinski FE: New endpoint for ablation of ventricular tachycardia: change in QRS morphology with pacing at protected isthmus as index of isthmus block. Journal of cardiovascular electrophysiology 2010; 21:320-324.
[84] de Chillou C, Groben L, Magnin-Poull I, Andronache M, MagdiAbbas M, Zhang N, Abdelaal A, Ammar S, Sellal JM, Schwartz J, Brembilla-Perrot B, Aliot E, Marchlinski FE: Localizing the critical isthmus of postinfarct ventricular tachycardia: the value of pace-mapping during sinus rhythm. Heart rhythm : the official journal of the Heart Rhythm Society 2014; 11:175-181.
[85] Piers SR, Leong DP, van Huls van Taxis CF, Tayyebi M, Trines SA, Pijnappels DA, Delgado V, Schalij MJ, Zeppenfeld K: Outcome of ventricular tachycardia ablation in patients with nonischemic cardiomyopathy: the impact of noninducibility. Circulation Arrhythmia and electrophysiology 2013; 6:513-521.
[86] Della Bella P, Baratto F, Tsiachris D, Trevisi N, Vergara P, Bisceglia C, Petracca F, Carbucicchio C, Benussi S, Maisano F, Alfieri O, Pappalardo F, Zangrillo A, Maccabelli G: Management of ventricular tachycardia in the setting of a dedicated unit for the treatment of complex ventricular arrhythmias: long-term outcome after ablation. Circulation 2013; 127:1359-1368.
[87] Stevenson WG, Tedrow UB: Ablation for ventricular tachycardia during stable sinus rhythm. Circulation 2012; 125:2175-2177.
[88] Tanner H, Hindricks G, Volkmer M, Furniss S, Kuhlkamp V, Lacroix D, C DEC, Almendral J, Caponi D, Kuck KH, Kottkamp H: Catheter ablation of recurrent scar-related ventricular tachycardia using electroanatomical mapping and irrigated ablation technology: results of the prospective multicenter Euro-VT-study. Journal of cardiovascular electrophysiology 2010; 21:47-53.
[89] Dinov B, Fiedler L, Schonbauer R, Bollmann A, Rolf S, Piorkowski C, Hindricks G, Arya A: Outcomes in Catheter Ablation of Ventricular Tachycardia in Dilated Non-Ischemic Cardiomyopathy in Comparison to Ischemic Cardiomyopathy: Results from the Prospective HEart Centre of LeiPzig VT (HELP - VT) Study. Circulation 2013.
[90] Tokuda M, Kojodjojo P, Tung S, Tedrow UB, Nof E, Inada K, Koplan BA, Michaud GF, John RM, Epstein LM, Stevenson WG: Acute failure of catheter ablation for ventricular tachycardia due to structural heart disease: causes and significance. Journal of the American Heart Association 2013; 2:e000072.
[91] Silberbauer J, Oloriz T, Maccabelli G, Tsiachris D, Baratto F, Vergara P, Mizuno H, Bisceglia C, Marzi A, Sora N, Guarracini F, Radinovic A, Cireddu M, Sala S, Gulletta S, Paglino G, Mazzone P, Trevisi N, Della Bella P: Non-Inducibility and Late Potential Abolition: A Novel Combined Prognostic Procedural Endpoint for Catheter Ablation of Post-infarction Ventricular Tachycardia. Circulation Arrhythmia and electrophysiology 2014.
[92] Liuba I, Frankel DS, Riley MP, Hutchinson MD, Lin D, Garcia FC, Callans DJ, Supple GE, Dixit S, Bala R, Squara F, Zado ES, Marchlinski FE: Scar Progression in Patients with Nonischemic Cardiomyopathy and Ventricular

Arrhythmias: Scar progression in NICM. Heart rhythm : the official journal of the Heart Rhythm Society 2014.
[93] Riley MP, Zado E, Bala R, Callans DJ, Cooper J, Dixit S, Garcia F, Gerstenfeld EP, Hutchinson MD, Lin D, Patel V, Verdino R, Marchlinski FE: Lack of uniform progression of endocardial scar in patients with arrhythmogenic right ventricular dysplasia/cardiomyopathy and ventricular tachycardia. Circulation Arrhythmia and electrophysiology 2010; 3:332-338.
[94] Komatsu Y, Daly M, Sacher F, Cochet H, Denis A, Derval N, Jesel L, Zellerhoff S, Lim HS, Jadidi A, Nault I, Shah A, Roten L, Pascale P, Scherr D, Aurillac-Lavignolle V, Hocini M, Haissaguerre M, Jais P: Endocardial ablation to eliminate epicardial arrhythmia substrate in scar-related ventricular tachycardia. Journal of the American College of Cardiology 2014; 63:1416-1426.
[95] Miani D, Pinamonti B, Bussani R, Silvestri F, Sinagra G, Camerini F: Right ventricular dysplasia: a clinical and pathological study of two families with left ventricular involvement. British heart journal 1993; 69:151-157.
[96] Horimoto M, Funayama N, Satoh M, Igarashi T, Sekiguchi M: Histological evidence of left ventricular involvement in arrhythmogenic right ventricular dysplasia. Japanese circulation journal 1989; 53:1530-1534.
[97] Sen-Chowdhry S, Syrris P, Ward D, Asimaki A, Sevdalis E, McKenna WJ: Clinical and genetic characterization of families with arrhythmogenic right ventricular dysplasia/cardiomyopathy provides novel insights into patterns of disease expression. Circulation 2007; 115:1710-1720.
[98] Berte B, Sacher F, Cochet H, Mahida S, Yamashita S, Lim H, Denis A, Derval N, Hocini M, Haissaguerre M, Jais P: Postmyocarditis ventricular tachycardia in patients with epicardial-only scar: a specific entity requiring a specific approach. Journal of cardiovascular electrophysiology 2015; 26:42-50.
[99] Bogun F, Good E, Reich S, Elmouchi D, Igic P, Lemola K, Tschopp D, Jongnarangsin K, Oral H, Chugh A, Pelosi F, Morady F: Isolated potentials during sinus rhythm and pace-mapping within scars as guides for ablation of post-infarction ventricular tachycardia. Journal of the American College of Cardiology 2006; 47:2013-2019.
[100] Teh AW, Reddy VY, Koruth JS, Miller MA, Choudry S, D'Avila A, Dukkipati SR: Bipolar radiofrequency catheter ablation for refractory ventricular outflow tract arrhythmias. Journal of cardiovascular electrophysiology 2014; 25:1093-1099.
[101] Berte B, Sacher F, Mahida S, Yamashita S, Lim HS, Denis A, Derval N, Hocini M, Haissaguerre M, Cochet H, Jais P: Impact of septal radiofrequency ventricular tachycardia ablation: insights from magnetic resonance imaging. Circulation 2014; 130:716-718.
[102] Reddy VY, Reynolds MR, Neuzil P, Richardson AW, Taborsky M, Jongnarangsin K, Kralovec S, Sediva L, Ruskin JN, Josephson ME: Prophylactic catheter ablation for the prevention of defibrillator therapy. The New England journal of medicine 2007; 357:2657-2665.
[103] Maury P, Baratto F, Zeppenfeld K, Klein G, Delacretaz E, Sacher F, Pruvot E, Brigadeau F, Rollin A, Andronache M, Maccabelli G, Gawrysiak M, Brenner R, Forclaz A, Schlaepfer J, Lacroix D, Duparc A, Mondoly P, Bouisset F, Delay M, Hocini M, Derval N, Sadoul N, Magnin-Poull I, Klug D, Haissaguerre M, Jais P,

Della Bella P, De Chillou C: Radio-frequency ablation as primary management of well-tolerated sustained monomorphic ventricular tachycardia in patients with structural heart disease and left ventricular ejection fraction over 30%. European heart journal 2014.
[104] Eldar M, Ohad DG, Goldberger JJ, Rotstein Z, Hsu S, Swanson DK, Greenspon AJ: Transcutaneous multielectrode basket catheter for endocardial mapping and ablation of ventricular tachycardia in the pig. Circulation 1997; 96:2430-2437.
[105] Ptaszek LM, Chalhoub F, Perna F, Beinart R, Barrett CD, Danik SB, Heist EK, Ruskin JN, Mansour M: Rapid acquisition of high-resolution electroanatomical maps using a novel multielectrode mapping system. Journal of interventional cardiac electrophysiology : an international journal of arrhythmias and pacing 2013; 36:233-242.
[106] Wielandts JY, De Buck S, Ector J, Nuyens D, Maes F, Heidbuchel H: Left ventricular four-dimensional rotational angiography with low radiation dose through interphase registration. Europace : European pacing, arrhythmias, and cardiac electrophysiology : journal of the working groups on cardiac pacing, arrhythmias, and cardiac cellular electrophysiology of the European Society of Cardiology 2014.
[107] Stevens SM, Tung R, Rashid S, Gima J, Cote S, Pavez G, Khan S, Ennis DB, Finn JP, Boyle N, Shivkumar K, Hu P: Device artifact reduction for magnetic resonance imaging of patients with implantable cardioverter-defibrillators and ventricular tachycardia: late gadolinium enhancement correlation with electroanatomic mapping. Heart rhythm : the official journal of the Heart Rhythm Society 2014; 11:289-298.
[108] Piers SR, Tao Q, van Huls van Taxis CF, Schalij MJ, van der Geest RJ, Zeppenfeld K: Contrast-enhanced MRI-derived scar patterns and associated ventricular tachycardias in nonischemic cardiomyopathy: implications for the ablation strategy. Circulation Arrhythmia and electrophysiology 2013; 6:875-883.
[109] McGann CJ, Kholmovski EG, Oakes RS, Blauer JJ, Daccarett M, Segerson N, Airey KJ, Akoum N, Fish E, Badger TJ, DiBella EV, Parker D, MacLeod RS, Marrouche NF: New magnetic resonance imaging-based method for defining the extent of left atrial wall injury after the ablation of atrial fibrillation. Journal of the American College of Cardiology 2008; 52:1263-1271.
[110] Cochet H, Komatsu Y, Sacher F, Jadidi AS, Scherr D, Riffaud M, Derval N, Shah A, Roten L, Pascale P, Relan J, Sermesant M, Ayache N, Montaudon M, Laurent F, Hocini M, Haissaguerre M, Jais P: Integration of merged delayed-enhanced magnetic resonance imaging and multidetector computed tomography for the guidance of ventricular tachycardia ablation: a pilot study. Journal of cardiovascular electrophysiology 2013; 24:419-426.
[111] Rudy Y: Noninvasive electrocardiographic imaging of arrhythmogenic substrates in humans. Circulation research 2013; 112:863-874.
[112] Rudy Y: Noninvasive imaging of cardiac electrophysiology and arrhythmia. Annals of the New York Academy of Sciences 2010; 1188:214-221.
[113] Arenal A, Hernandez J, Calvo D, Ceballos C, Atea L, Datino T, Atienza F, Gonzalez-Torrecilla E, Eidelman G, Miracle A, Avila P, Bermejo J, Fernandez-Aviles F: Safety, long-term results, and predictors of recurrence after complete

endocardial ventricular tachycardia substrate ablation in patients with previous myocardial infarction. The American journal of cardiology 2013; 111:499-505.
[114] Sacher F, Roberts-Thomson K, Maury P, Tedrow U, Nault I, Steven D, Hocini M, Koplan B, Leroux L, Derval N, Seiler J, Wright MJ, Epstein L, Haissaguerre M, Jais P, Stevenson WG: Epicardial ventricular tachycardia ablation a multicenter safety study. Journal of the American College of Cardiology 2010; 55:2366-2372.
[115] Sarkozy A, Tokuda M, Tedrow UB, Sieria J, Michaud GF, Couper GS, John R, Stevenson WG: Epicardial ablation of ventricular tachycardia in ischemic heart disease. Circulation Arrhythmia and electrophysiology 2013; 6:1115-1122.
[116] Killu AM, Friedman PA, Mulpuru SK, Munger TM, Packer DL, Asirvatham SJ: Atypical complications encountered with epicardial electrophysiological procedures. Heart rhythm : the official journal of the Heart Rhythm Society 2013; 10:1613-1621.
[117] Nagashima K, Watanabe I, Okumura Y, Ohkubo K, Kofune M, Ohya T, Kasamaki Y, Hirayama A: Efficacy and feasibility of pericardial endoscopy by a subcutaneous approach. Europace : European pacing, arrhythmias, and cardiac electrophysiology : journal of the working groups on cardiac pacing, arrhythmias, and cardiac cellular electrophysiology of the European Society of Cardiology 2011; 13:1501-1503.
[118] Zeppenfeld K, Tops LF, Bax JJ, Schalij MJ: Images in cardiovascular medicine. Epicardial radiofrequency catheter ablation of ventricular tachycardia in the vicinity of coronary arteries is facilitated by fusion of 3-dimensional electroanatomical mapping with multislice computed tomography. Circulation 2006; 114:e51-52.
[119] Calkins H, Epstein A, Packer D, Arria AM, Hummel J, Gilligan DM, Trusso J, Carlson M, Luceri R, Kopelman H, Wilber D, Wharton JM, Stevenson W: Catheter ablation of ventricular tachycardia in patients with structural heart disease using cooled radiofrequency energy: results of a prospective multicenter study. Cooled RF Multi Center Investigators Group. Journal of the American College of Cardiology 2000; 35:1905-1914.
[120] Stevenson WG, Wilber DJ, Natale A, Jackman WM, Marchlinski FE, Talbert T, Gonzalez MD, Worley SJ, Daoud EG, Hwang C, Schuger C, Bump TE, Jazayeri M, Tomassoni GF, Kopelman HA, Soejima K, Nakagawa H, Multicenter Thermocool VTATI: Irrigated radiofrequency catheter ablation guided by electroanatomic mapping for recurrent ventricular tachycardia after myocardial infarction: the multicenter thermocool ventricular tachycardia ablation trial. Circulation 2008; 118:2773-2782.
[121] Dinov B, Fiedler L, Schonbauer R, Bollmann A, Rolf S, Piorkowski C, Hindricks G, Arya A: Outcomes in catheter ablation of ventricular tachycardia in dilated nonischemic cardiomyopathy compared with ischemic cardiomyopathy: results from the Prospective Heart Centre of Leipzig VT (HELP-VT) Study. Circulation 2014; 129:728-736.
[122] Yokokawa M, Desjardins B, Crawford T, Good E, Morady F, Bogun F: Reasons for recurrent ventricular tachycardia after catheter ablation of post-infarction ventricular tachycardia. Journal of the American College of Cardiology 2013; 61:66-73.


liryc
L'INSTITUT DE RYTHMOLOGIE
ET MODÉLISATION CARDIAQUE


université
de BORDEAUX